

**DEVELOPMENT OF A RECREATIONAL-
PURPOSE TRANSIT VEHICLE,
*TRAMCAR***

**A technical Report Submitted to
Research Management Centre (RMC),
Universiti Teknologi Malaysia (UTM)**

AZHAR BIN ABDUL AZIZ

**Faculty of Mechanical Engineering
Universiti Teknologi Malaysia (UTM)**

May 2008

ACKNOWLEDGEMENT

In preparing for this project and subsequently this report, I was in constant contact with many parties, notably the fellow colleagues, academicians, technicians and a local platform developer. They have contributed tremendously towards the overall success of this challenging and daunting project. I am grateful to my colleague associate Professor Mustafa Yusof for his guidance and suggestion on different aspects of the vehicle analyses. I am also indebted to my research assistance i.e. Ahmad Kamal, Zaidi and Mazlan for their constant pursuance to have this project completed on time. Without their continued support and interest, this report would not have been produced as presented here. Last but not least, I would like to offer my sincere gratitude to the vice chancellor of Universiti Teknologi Malaysia (UTM) Y.Bhg Tan Sri Mohd Zulkifli bin Mohd Ghazali for his support and assistance enabling me to receive the prestigious institutional fund (RMC vote No 73206) in 2004- without which, this project would not have taken off and materialized.

ABSTRACT

Chassis and suspension system play an important role in the performance of a vehicle when it comes to safety and passenger comfort. The objectives of this project are to develop a “hop-in and hop-out” recreational vehicle with a capacity of eight-passenger, fitted with a dual-fuel system and to analyse the performance of its chassis and suspension system. This showcase vehicle is manufactured by a team of engineers from the Automotive Development Centre (ADC) in UTM. Both the chassis and suspension analyses are rigorously performed using industrial-standard computer software. The safety factor requirement for the vehicle chassis is set for over a factor of 2.0 and its torsional stiffness must in the range from 3000Nm/degree to 9000Nm/degree. The vehicle chassis is analyzed in several conditions, namely static, bumping and braking, while the comfort performance is largely speculated to depend on the demand of user. In this project, the comfortable performance for *tramcar* which is the performance of its suspension system is benchmarked with that of the performance for *Proton Waja 1.6*. The level of comfort for the *tramcar* suspension system is referred to the performance results with particular emphasis on bouncing, pitching and rolling. From the results of the analyses the *tramcar* has achieved satisfactory performance criteria. The safety factor is over the minimum requirement for a typical utility vehicle and the torsional stiffness is within the allowable range. In addition the suspension system shows the results are comparable to the performance of the *Proton Waja 1.6*.

ABSTRAK

Sistem gantungan (casis dan penyerap hentak) memainkan peranan penting dalam prestasi sesebuah kenderaan dimana ia memberikan keselamatan dan keselesaan kepada penumpang. Objective projek ini adalah untuk membina satu "hip-in and hip out" kenderaan rekreasi untuk kegunaan 8 orang penumpang dimana ianya dilengkapi dengan sistem dua bahan baker dan analisis prestasinya pada system casis dan gantungan. Produk ini telah dibangunkan oleh sekumpulan jurutera dari Pusat Pembangunan Automotif (ADC) di UTM. Analysis sistem gantungan dan casis telah dianalisis menggunakan perisian komputer standard industri dengan ditetapkan faktor selamat yang ditetapkan untuk casis melebihi 2.0 dan keupayaan kilasan di antara 3000Nm/darjah hingga 9000Nm/darjah. Casis kenderaan telah di analisis dengan beberapa keadaan yang berbeza seperti statik analisis, keadaan berbonggol dan memberek, sehingga keselesaan pengguna diambil kira sebelum rekabentuk diterima. Dalam projek ini keselesaan pemanduan Proton Waja 1.6 adalah menjadi bandingan. Tahap keselesaan bagi sisyem gantungan *Tramcar* dirujuk kepada keputusan prestasi oleh pemerhatian terhadap *bouncing*, *pitcing* dan *rolling*. Dari keputusan analisis tersebut, *tramcar* telah melapasi prestasi asa yang telah ditetapkan. Faktor selamat telah di rekabentuk melebihi tahap minimum yang diperlukan untuk kenderaan yang tipikal.

TABLE OF CONTENTS

CHAPTER	TITLE	PAGE
	TITLE	i
	ACKNOWLEDGEMENT	ii
	ABSTRACT	iii
	ABSTRAK	iv
	TABLE OF CONTENTS	v
	LIST OF TABLES	v
	LIST OF FIGURES	viii
	LIST OF SYMBOLS	ix
	LIST OF APPENDICES	x
1.	INTRODUCTION	
	1.1 Introduction	1
	1.2 <i>Tramcar</i> background	2
	1.3 Objectives	3
	1.4 Project Worksopce	4
	1.5 Methodology	5
2.	LITERATURE REVIEW	
	2.1 Brief Overview of Chassis	7
	2.1.1 Monocoque	8
	2.1.2 Twin Tube	9
	2.1.3 Multi Tube	10
	2.1.4 Space Frame	11
	2.1.5 Choice	12

2.2	Suspension Systems	12
2.2.1	Solid Axle	14
2.2.2	Four Link	14
2.2.3	De-Dion	15
2.2.4	Trailing Arm	16
2.2.5	McPherson Strut	17
2.2.6	Quadra Link	18
2.2.7	Double Wishbone	19

3. CHASSIS ANALYSIS

3.1	Introduction	20
3.2	Input Material Specification	21
3.3	Assumptions	23
3.4	Loadings applied	23
3.5	Static analysis	24
3.5.1	Boundary conditions	24
3.5.2	Results	24
3.6	Bumping analysis	25
3.6.1	Boundary conditions	25
3.6.2	Results	25
3.7	Braking analysis	26
3.7.1	Boundary conditions	26
3.7.2	Results	27
3.8	Chassis torsional stiffness analysis	28
3.8.1	Boundary conditions	28
3.8.2	Results	28

4.	SUSPENSION SYSTEM ANALYSIS	
4.1	Introduction	31
4.2	Quarter car model	31
4.3	Half car model	32
4.4	Full car model	33
4.5	Conditions of Analysis	43
4.6	The input of parameter	45
4.7	Assumptions	46
4.8	Results	47
5.	DISCUSSIONS	
5.1	Chassis analysis	49
5.1.1	Static analysis	49
5.1.2	Bumping analysis	51
5.1.3	Braking analysis	51
5.1.4	Chassis torsional stiffness analysis	52
5.2	Suspension system analysis	53
5.2.1	Bouncing performance	53
5.2.2	Pitching performance	54
5.2.3	Rolling performance	54
5.2.4	Comparison performance in different stiffness	55
6.	RETROFITTING OF CNG CONVERSION KIT	
6.1	Why is the Need for Retrofitting?	58
6.2	CNG Conversion Vehicle Requirements	58

6.2.1 Bi-fuel System and Dual-fuel System	59
6.2.2 Optimize System	60
6.2.3 CNG Operation System	60
6.2.4 Application of CNG in Vehicles	61
6.2.5 Sequential System (Multipoint Sequential Injection System)	65
6.2.6 Catalyst System (Natural Gas System with TN 1 Step Motor regulator and Lambda Control System/2)	65
6.2.7 Carburetor System	67
6.2.8 Economics of Vehicle Conversion to CNG	69
6.3 Retrofitting of the Conversion Kit	70
6.3.1 CNG Tank	71
6.3.2 Filling Valve	72
6.3.3 CNG Cut-off Valves	73
6.3.4 High Pressure Gas Piping	75
6.3.5 Pressure Regulator	76
6.3.6 Fuel Switch Injection	78
6.3.7 Gas Mixer	80
6.3.8 Injector Emulator	83
6.4 Vehicle Test with CNG Conversion Kit	87

7.

CONCLUSIONS AND RECOMMENDATIONS

7.1 Conclusions	88
7.2 Recommendations	90

BIBLIOGRAPHY	91
---------------------	----

APPENDICES A – G	93
-------------------------	----

LIST OF SYMBOLS

E	-	Young's Modulus
ρ	-	Mass density
ν	-	Poisson's ratio
n	-	Safety factor
g	-	Gravity (9.81m/s^2)
σ_{yield}	-	Yield stress
$\sigma_{ultimate}$	-	Ultimate tensile stress
$\sigma_{principal}$	-	Maximum principal stress
τ_{max}	-	Maximum shear stress
F, f	-	Force
a, b, w, r	-	Length
δ, z	-	Displacement
T	-	Torsion
θ, φ	-	Angle
M, m	-	Mass
K	-	Stiffness
C, B	-	Damping
$\dot{z}, \dot{\theta}, \dot{\varphi}$	-	Velocity
$\ddot{z}, \ddot{\theta}, \ddot{\varphi}$	-	Acceleration
I_{xx}, I_{yy}	-	Moment of inertia

LIST OF APPENDICES

APPENDIX	TITLE
A	<i>Tramcar</i> properties
B	The result for static analysis
C	The result for bumping analysis
D	The result for braking analysis
E	The result for chassis torsional stiffness analysis
F	The manufacturing drawing of <i>tramcar</i>
G	The picture of <i>tramcar</i>

UNIVERSITI TEKNOLOGI MALAYSIA

BORANG PENGESAHAN
LAPORAN AKHIR PENYELIDIKAN

TAJUK PROJEK : DEVELOPMENT OF A RECREATIONAL-PURPOSE
TRANSIT VEHICLE, TRAMCAR

Saya AZHAR BIN ABDUL AZIZ
(HURUF BESAR)

Mengaku membenarkan **Laporan Akhir Penyelidikan** ini disimpan di Perpustakaan Universiti Teknologi Malaysia dengan syarat-syarat kegunaan seperti berikut :

1. Laporan Akhir Penyelidikan ini adalah hakmilik Universiti Teknologi Malaysia.
2. Perpustakaan Universiti Teknologi Malaysia dibenarkan membuat salinan untuk tujuan rujukan sahaja.
3. Perpustakaan dibenarkan membuat penjualan salinan Laporan Akhir Penyelidikan ini bagi kategori TIDAK TERHAD.

Mandakan (/)

SULIT (Mengandungi maklumat yang berdarjah keselamatan atau Kepentingan Malaysia seperti yang termaktub di dalam AKTA RAHSIA RASMI 1972).

oleh TERHAD (Mengandungi maklumat TERHAD yang telah ditentukan Organisasi/badan di mana penyelidikan dijalankan).

TIDAK
TERHAD _____

PENYELIDIK

TANDATANGAN KETUA

CATATAN : * Jika Laporan Akhir Penyelidikan ini SULIT atau TERHAD, sila lampirkan surat daripada pihak berkuasa/organisasi berkenaan dengan menyatakan sekali sebab dan tempoh laporan ini perlu dikelaskan sebagai SULIT / TERHAD.

CHAPTER 1

INTRODUCTION

1.1 Introduction

Transportation systems have come to play a large part in the lives of a significant segment of the world's population. From daily trips to the place of employment, to occasional cross-country business or vacation trips, to once-in-a-lifetime intercontinental emigration, the human race has achieved a level of mobility, which would have been incomprehensible a short time ago.

For several years, the attention of the technical community has been attracted to the vibration environment of those making use of all types of transportation vehicles. For the passengers, discomfort and fatigue due to vibration are major considerations since this will determine their ability to perform tasks or enjoy recreation of their vehicle usages. The impact on safety of the trip, possible deterioration in efficiency and effectiveness in carrying out their duties are also the areas of concern for those who operate the vehicle.

Chassis play an important role in the performance of vehicle. The chassis is the framework of any vehicle. The suspension system, steering and drive train components are mounted into the chassis. Due to that, chassis analysis frequent done by manufacturer to ensure the vehicle stability. The chassis has to be a strong and rigid platform to support all the components. The connections between the chassis, the suspension system and the drive train must be made of rubber to dampen noise, vibration and hardness. The construction of today's vehicles required the use of many different materials. It must strong enough to protect the passenger.

One of the most important systems of the transportation vehicle, particularly when comfort is of interest, is the suspension system. The suspension system provides basic support, guidance, and in some cases propulsion of a vehicle. Suspensions also isolate passenger and freight compartments from disturbances due to roadway irregularities. When the 'softer' suspension, the effects of the irregularities on the vehicle vibration level (passenger comfort) is reduced and also the suspension stroke (rattle space requirement) is increased. When the suspension is harsh, vibration level will be increased while the suspension stroke is reduced. The requirement of achieving both low vibration magnitude and small suspension stroke will create conflicting factors in suspension design and to certain extent limit suspension performance capability.

1.2 *Tramcar* Background

Faculty mechanical of UTM has developed a non-commercial transport, better known as the *Tramcar*, whose sole purpose is to transport a group of people (visitors) from one point to another within its campus. This mobile platform ultimately can be used for other uses commercially i.e. to ferry people in recreational areas, large indoor exhibition centres, zoos, airports, hotels, and golf resort.

UTM's *Tramcar* is simple in design and construction, and is equipped with a dual-fuel capability. To achieve ease of operation, the concept of "hop-in, hop-out" is incorporated; thus it is not equipped with doors for easy access. It has eight seats in the configuration of two-three-three i.e. two for the front seat (inclusive the driver seat), three in the centre and three in the rear site. These are adjustable seats giving comfort and easy boarding for passengers.

The UTM's *Tramcar* uses a four-cylinder Ford engine equipped with 16 valves and having a displacement of 2000cc. The engine is mounted at the rear of the vehicle thus giving large intermediate volume for high-density

passenger capability. It uses the electronic control 2 way * OD attaching a 4-speed automatic ECT-S transmission system to the engine in the rear engine compartment.

The prototype uses Toyota ST 190 McPherson struts on its both sides of its suspension system. McPherson strut is an independent suspension system, which is small and lightweight yet with very little unsprung mass. It has fewer total components compared to conventional suspension systems and is fairly straightforward to assemble and repair.

The framework of this platform was built based on the twin tube (or common known as ladder frame) configuration. Even it is simple arrangement; it can carry a substantial amount of load. This is largely attributed to the ladder frame that use the welding method to joint the bar, as the stability of chassis is very much depends on the welding joints. Here oblique joints were used to joint all the bars. It is widely believe that the oblique joint can provide a good load arrangement and is able to prevent the abrupt failure of chassis.

1.3 Objectives

The main objective of this project is to produce a versatile people's mover platform within UTM campus, which is environmental-friendly and easy-operation.

The second objective is to analyse the *Tramcar's* chassis and suspension system towards further improvement from the aspect of safety and comfort factors.

The third objective is incorporation of the newly developed vehicle for dual fuel function with the augmentation of a typical CNG conversion kit for flexibility of fuel utilization.

1.4 Project Workscopes

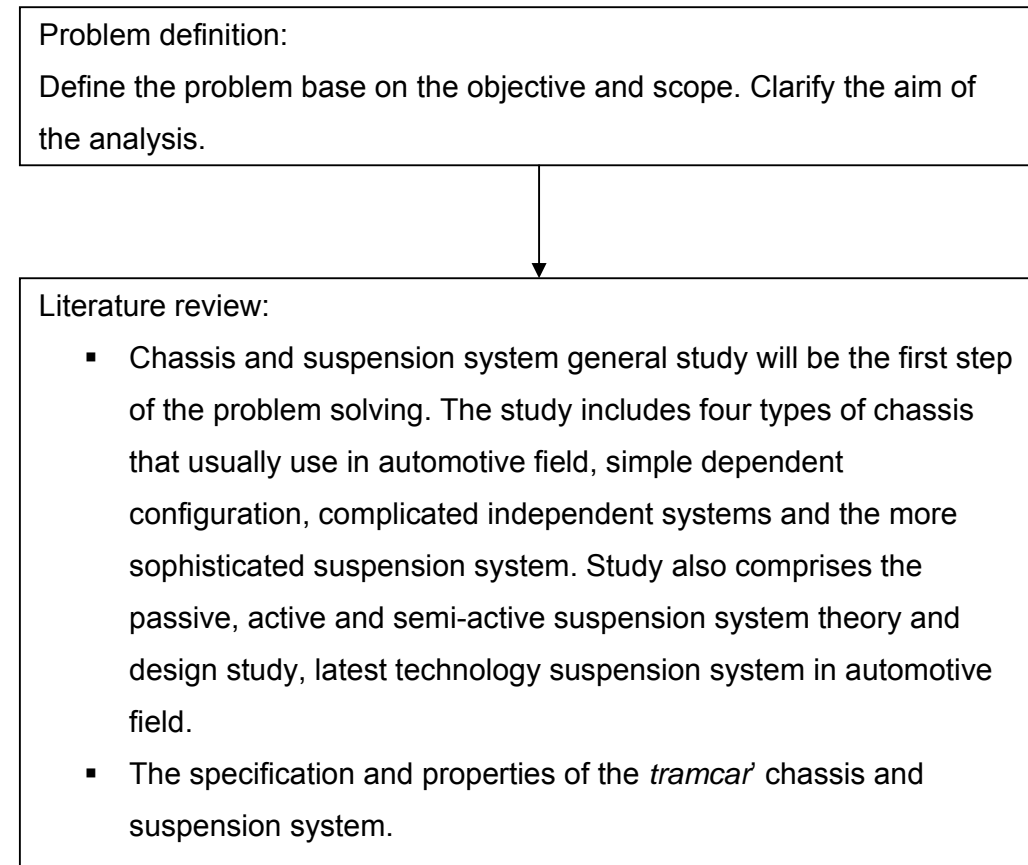
This project focuses on three major objectives mentioned earlier. However development and analysis work take up the bulk of the time allocated for the project.

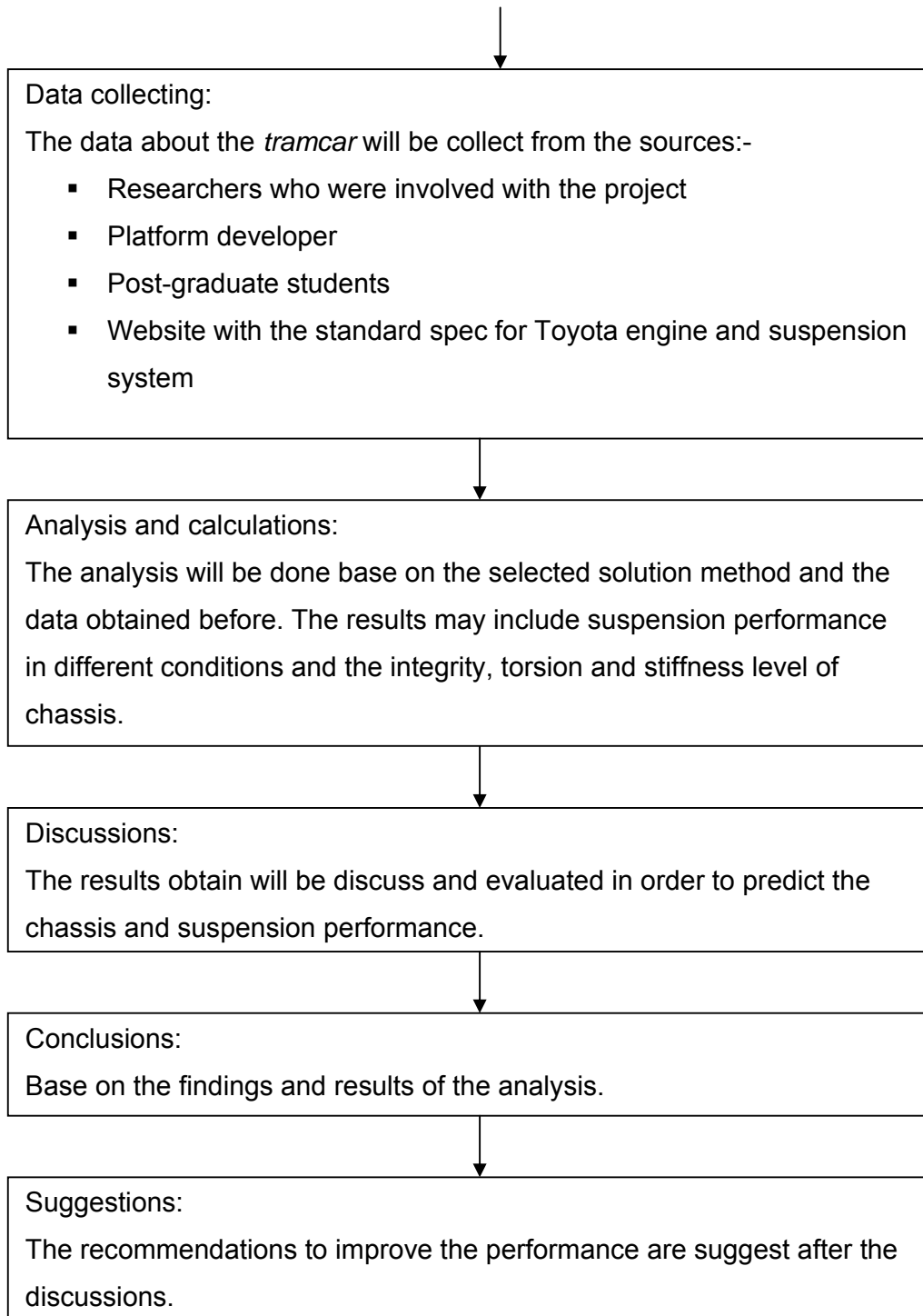
The specifications and properties on the chassis and suspension systems of the *Tramcar* are obtained from a series of discussions made with the group members. The scope in the work include: -

- i. Identify the displacements and stresses of the chassis due to static loadings.
- ii. Analyse the torsion of chassis when the *Tramcar* rides over a bump.
- iii. Analyse the chassis stability when the *Tramcar* undergoes a strenuous conditions such as braking and manoeuvring.
- iv. Obtain the maximum deformation of the structure, displacements and stresses contour.
- v. Dynamic analysis to the suspension system to obtain for: -
 - Bouncing characteristics
 - Pitching characteristics
 - Rolling characteristic

1.5 Methodology

In any analysis work, the general procedures that are usually included are: problem definition, literature review, data collecting, solution method selecting, analysis and calculations, evaluations and documentations. The methodology for the implementation of this project is shown in the flowchart below:-





CHAPTER 2

LITERATURE REVIEW

2.1 Brief Overview of Chassis

Chassis plays an important role in the performance of vehicle. A good chassis must be structurally sound in every way over the expected life of the vehicle and beyond. This means nothing will ever break under normal conditions. Chassis maintain the suspension mounting locations so that handling is safe and consistent under high cornering and bump loads. Besides of that, chassis support the body panels and other passenger components in vehicle so that everything feels solid and has a long and reliable life.

In the real world, few chassis designs will not meet the standard criteria. Major structural failures, even in kit cars are rare. Structural stiffness is the basis of what you feel at the seat of your pants. It defines how a car handles, body integrity and the overall feel of the car. Different basic chassis designs each have their own strengths and weaknesses. Every chassis is a compromise between weight, component size, vehicle intent, and ultimate cost. Even within a basic design method, strength and stiffness can vary significantly, depending on the details. There is no such thing as the ultimate method of construction for every car, because each car presents a different set of problems.

In this section, some types of chassis will be reviewed and one type will be selected for the proposed Tramcar. The types are i) monocoque, ii) twin tube, iii) multi-tube and iv) space frame respectively.

2.1.1 Monocoque

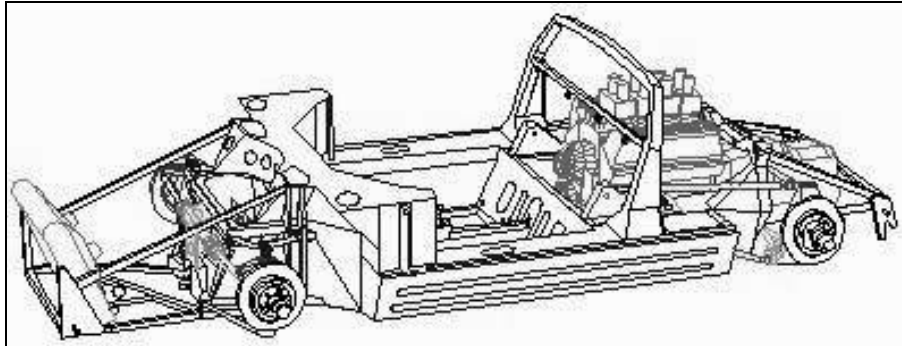


Figure 2.1: Monocoque [Source: *Automotive Engineering*, SAE].

Monocoque or in French "single shell" means unibody is a construction technique that utilizes the external skinning of an object to form most of the structure. This is as opposed to using an internal framework that is then covered with a non-structural skinning. Monocoque construction was first widely used in aircraft. The difference between monocoque with the other frame is monocoque built in unibody but the other frame is in joint form to build a unit of vehicle.

The monocoque skinning itself had significant structural properties of its own. With a sufficient thickness, one could do away with all of the internal structure. However this would be even heavier than the framing would have been. At thinner gauges the skinning could easily provide the structure for tension and shearing loads (metal resists being pulled apart quite well), and if it was bent into a curve or pipe, it became quite strong against bending loads as well. The only loading it could not handle on its own, at least in thin "skins" is compression. Combining this sort of structural skin with a greatly reduced internal framing to provide strength against compression led to what is known as "semi-monocoque".

In the post-war period the technique became more widely used in other areas. It is now used quite commonly in automobile construction as well. In this application it is common to see true monocoque frames, where the

structural members around the window and door frames are built by folding the skinning material several times. In these situations the main concern is spreading the load evenly, having no holes for corrosion to start, and reducing the overall workload. Compared to older techniques where a body would be bolted to a frame, monocoque cars are less expensive and stronger.

2.1.2 Twin Tube

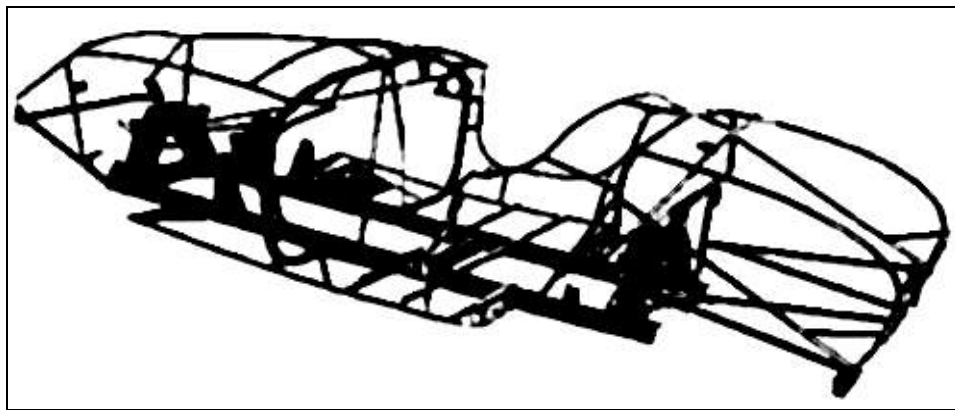


Figure 2.2: Ladder Frame [Source: *Automotive Engineering*, SAE].

Twin tube or known as ladder frame is the most simply frame among the others frame. The ladder frame is a shorthand description of a twin-rail chassis, typically made from round or rectangular tubing or channel. It can use straight or curved members, connected by two or more cross members. The cross member provide more strength to chassis and as a place to mount the seat. It is not necessary to use the same dimension for whole member in ladder frame.

Usually all members are joint by welding to build up a chassis and oblique joint use for the different dimension member. Oblique joint provides a good load arrangement and able to prevent the failure of chassis. Body mounts are usually integral outriggers from the main rails, and suspension points can be well or poorly integrated into the basic design.

Advantages of the ladder frame that are often overlooked are that the available space and ease of access to mechanical parts is often better and engine exhaust systems are less likely to be restricted by the need to route them around chassis tubes. Additional structures are often required with ladder frames to support bodywork but these can often be designed to brace the basic chassis structure. Ladder frame give a low performance in bending and torsional loads. However, it is the most easy and cheap for fabrication.

2.1.3 Multi Tube

Multi tube frame is described as a frame that has four side rails. It acts between the ladder frame and space frame. As ladder frame, multi tube frame also use cross member and diagonal member to improve its strength.

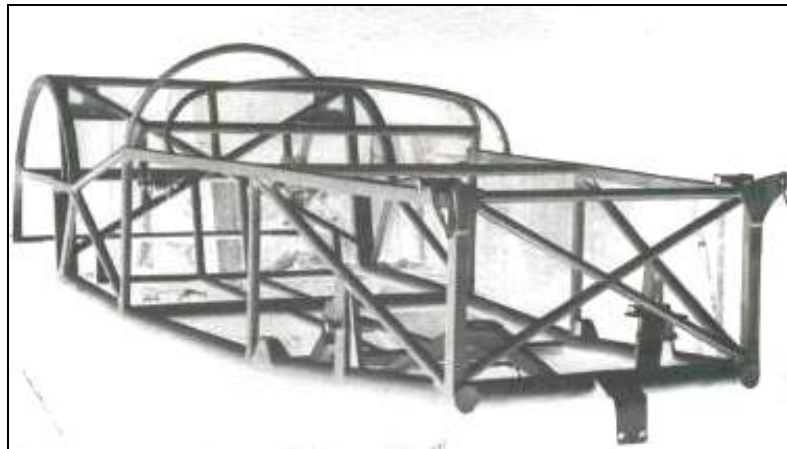


Figure 2.3: Multi Tube [Source: *Automotive Engineering*, SAE].

Multi tube chassis design is as much an art as a science. The art comes in deciding where to put the tubes so as best to connect and support all the hundreds of components, without using more than an absolute minimum number of tubes, and equally, an absolute minimum of sheet or plate in the brackets.

The bending performance for multi tube chassis is base on the diagonal member that used in the frame. The diagonal member will prevent whole chassis to occur deformation. The tube dimension and the total tube used in frame will influence the torsional performance. More the tubes used in the frame then better its torsion stiffness. Hence it will cause to increase the vehicle weight.

2.1.4 Space Frame

Space frame is a complexity frame. A true space frame has small tubes that are only in tension or compression with no bending or twisting loads. The chassis build from hundreds of separate tubes. It was difficult to build and a nightmare to fix. The space frame that is currently used for chassis simply uses smaller tubes, many carrying bending and torsional loads. If compare to ladder frame and multi tube frame, space frame able to provide a good performance in bending and torsional loads.

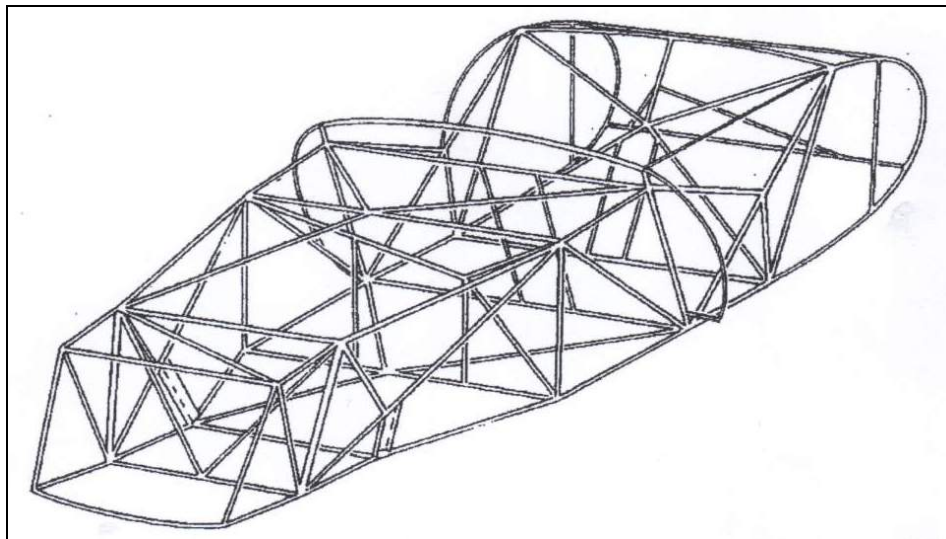


Figure 2.4: Space Frame [Source: *Automotive Engineering*, SAE].

Besides, space frame able to resist the impact forces. Space frame will absorb the momentum and arrange the momentum to whole body. Therefore, space frame can minimize the damage of passenger if the vehicles going to accident in high speed by reduce the load to passenger. Even through the space frame is the most efficient frame, but it is not effective in the cost. This is because it uses more tube and integrating work.

2.1.5 Choice

Having look and carefully examined the prospect of each of one of the possible concept. The multi-tube chassis was selected as it offers cost-effective for this project as the budget constrains heavily limits the choice available.

2.2 Suspension Systems

All dynamic vehicles have suspension systems. Commercial automobiles and trucks, motorcycles, road and mountain bikes and even shoes can be considered dynamic vehicles. By their nature, dynamic vehicles are concerned with motion and the generation of motion. With the motion, come forces, moments and accelerations that act on the vehicles, creating stresses, loads and moments on specific components and systems. The behaviour and response of the vehicle is dependent upon the forces imposed on that system from the external world. For wheeled and tired vehicles, the forces and moments generated by the tire's interaction with the ground are transmitted through the suspension system and create loads and moments at the chassis attachment points.

In the context of vibration theory, the suspension system is just a vibratory system with essential ingredients being inertial and elastic elements, and the central phenomenon is the cyclic interchange of kinetic and potential energies. Damping is essential for controlling the vibration. Damping is the

removal of energy from the oscillating system either by dissipating within the system or by transmission (radiation) away from the system. If the damping is light, the dynamical behaviour of the suspension system is principally determined by the relatively large elastic and inertial forces. The conventional suspension usually consists of springs as elastic elements, masses of various parts of the vehicle as inertial elements and shock absorber (dampers) as devices to provide damping. All of those elements are passive in the sense that no power is required from outside of the system. Such a suspension system is said to be a passive suspension system.

In the context of automatic control theory, the suspension system is a system that provides the desired control forces so that the vehicle body behaves in the desired manner. Optimal control theory has been used to determine the desired control forces of the suspension system. Unfortunately, the optimum suspension system cannot be implemented using only passive elements. The implementation of such a suspension system requires active force generators and thus power has to be supplied to the suspension system from an external source. For the reason that it requires an external power supply, it is called an active suspension system. Although, an active suspension shows better performance over a prescribed frequency band than that of the best possible passive system, or accomplishes a task that is not possible for a passive one, it must be admitted that active suspension, in general, are more costly, more complex and therefore, often less reliable than passive suspensions. To date, the use of the active suspension has been limited to cases of which performance gains outweigh the disadvantages of increased cost, complexity and weight.

A compromise between the active suspension and the passive one is called the 'semi-active' suspension system. In this type of suspension, some of the active suspension advantages are realized while using almost passive components in term of cost and complexity. Springs are still used as elastic elements as in the case of the passive suspension, but dampers are activated. The activated damper is a self-power, high-gain device which derives its control power from the disturbance of the roadway. In other words,

the damper force is generated totally passively as in a conventional damper. Only a small power source is required for instrumentation, signal-processing and low-power servos within the damper. For the fact that this suspension system uses only a small amount of externally supplied power, it is called a 'semi-active' suspension system. A significant advantage over fully active suspension is its fail-safe malfunction. Failure in the control circuitry cannot destabilize the system since the activated damper cannot supply power to the vehicle body. Most failures simply turn the semi-active damper back into a passive one which, however, may be stiffer or softer than desirable.

Several suspension systems will be discussed and outlined in this section, starting with a simple dependent configuration (solid axle, four link and De-Dion), progressing through more complicated independent systems (trailing arm suspensions) and finally discussing a more sophisticated suspension system like the McPherson Strut, multi link and double wishbone.

2.2.1 Solid Axle

In a solid axle configuration, the wheels are mounted on either side of a rigid beam. The motion of the wheels is therefore tied together and any motion experienced by one of the wheels is transmitted to the opposite wheel. The wheels act as like a coupled pair. It is a dependent suspension system, and consequently, the wheels must steer and track together. The advantage of a solid axle suspension is that the wheel camber is not affected by body roll. The disadvantages are that the sprung mass (mass of the axle, wheels and the suspension components) tends to be very high and that the volume required to package the suspension components (shock and leaf springs) tends to be significant.

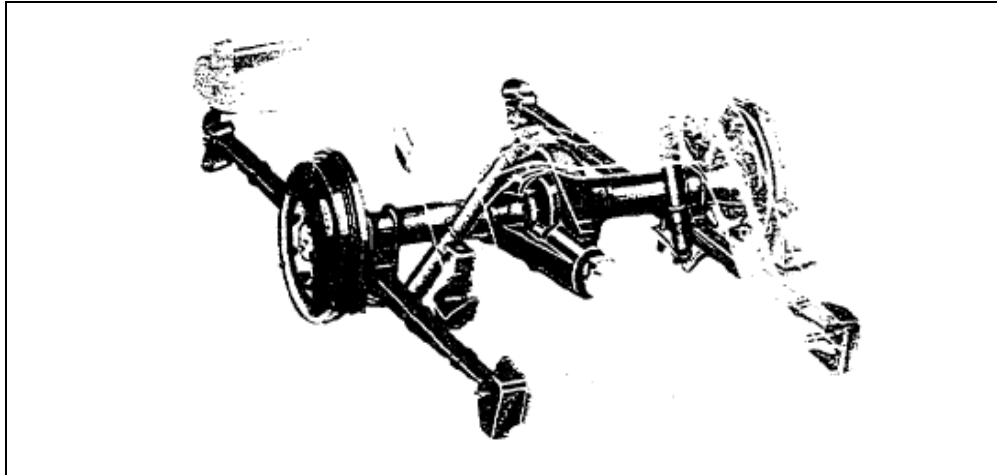


Figure 2.5: Solid Axle [Source: *Automotive Engineering*, SAE].

2.2.2 Four Link

Similar to the solid axle configuration, the wheels are mounted on either side of a rigid beam. The leaf springs are removed and replaced with coil springs and shocks absorbers. The rear differential is removed from the rear axle, thereby reducing the unsprung mass. The response of the axis is governed by the addition of linkages from the axle to the chassis. As is the case with the solid axle, the motions of the wheels are tied together.

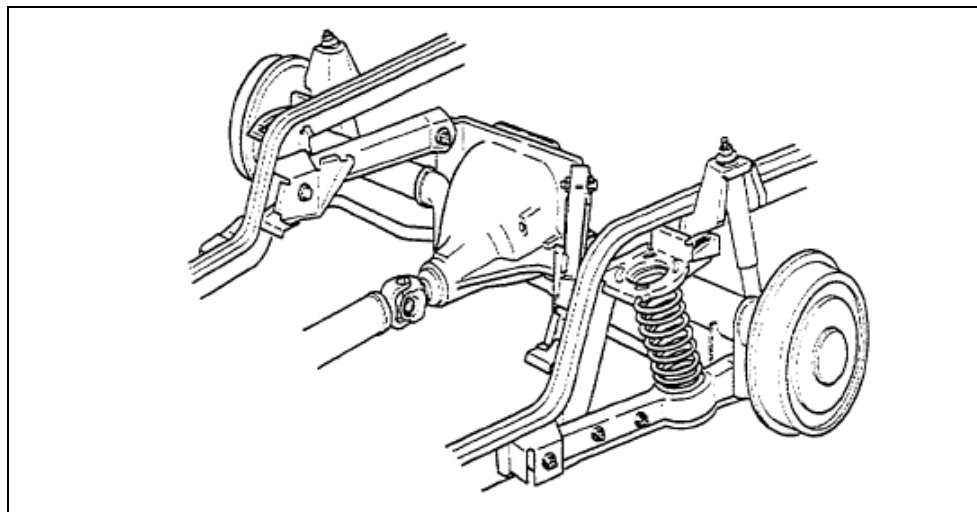


Figure 2.6: Four Link [Source: *Automotive Engineering*, SAE].

2.2.3 De-Dion

It consist of a cross tube between two driving wheels with a chassis mounted differential and half shaft. Trailing arm on each side supported the body by coil springs on it. The advantages are less interior space for rigid axle room and less differential weight for the gross vehicle weight. However, it needs sliding tube and half shaft as adding part of the suspension components. The main linkage components with its supporting axes are: trailing arm for x-axis; sliding tube and trailing arm for y-axis; leaf spring and damper for z-axis. The torque from acceleration and deceleration are by the semi elliptic leaf spring.

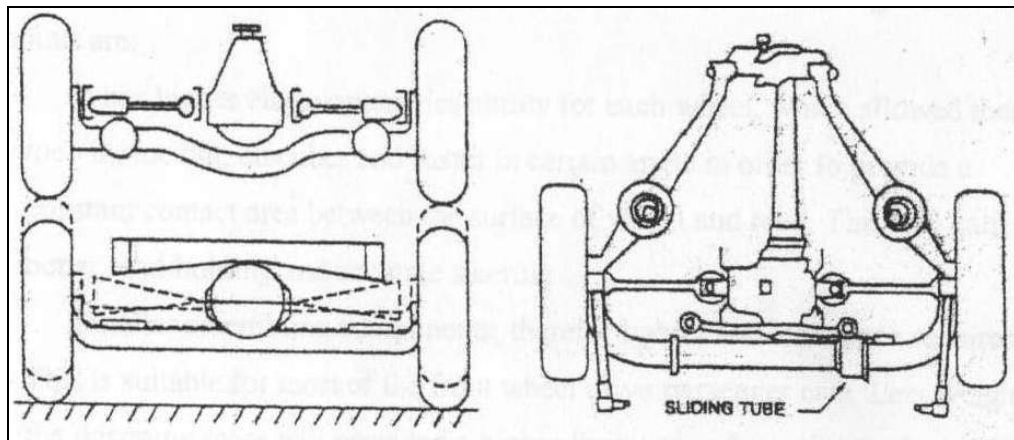


Figure 2.7: De-Dion [Source: *Automotive Engineering*, SAE].

2.2.4 Trailing Arm

The trailing arm suspension system is an independent suspension system. This suspension system allows for each wheel to move as a separate entity, without affecting the motion of the opposite wheel. By decoupling the wheels, the roll centre for each wheel is easier to control by geometrical design. Independent suspension systems allow for more efficient use of the packaging space restrictions of the automobile and provide a smoother passenger ride compared with the dependent suspension systems, with less overall vibration noise. Generally, independent suspension systems are less costly than alternative suspension systems.

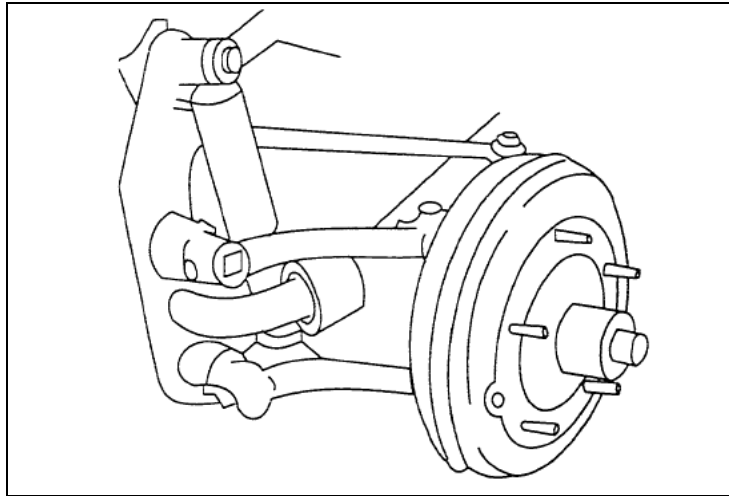


Figure 2.8: Trailing Arm [Source: *Automotive Engineering*, SAE]

The trailing arm suspension was developed as the first attempt at an independent suspension system. It uses parallel, equal length trailing arms connected to torsion bars. The torsion bars provide the springing action for the wheel. There is no coil spring or leaf spring.

2.2.5 McPherson Strut

The McPherson strut uses geometry with unequal arms. The primary advantage of the McPherson strut independent suspension system is that it is small and lightweight, with very little unsprung mass. It is also compact, but does tend to be large in the z-axis (tall). The McPherson strut suspension also has fewer total components compared to alternative rear suspension systems and is fairly straight forward to assemble and to repair. Another advantage of the McPherson suspension system is that the loads act as distributed loads over larger areas of the body structure.

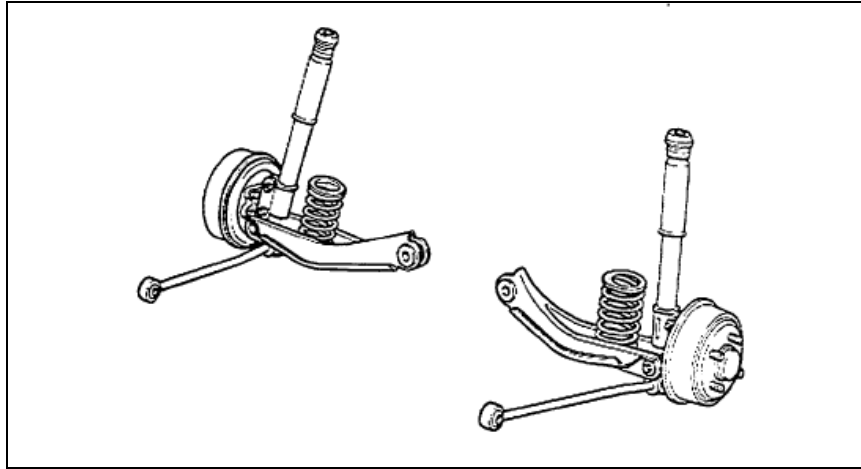


Figure 2.9: McPherson Strut [Source: *Automotive Engineering*, SAE]

2.2.6 Quadra Link

The Quadra link or multi link rear suspension utilizes the McPherson strut (shock absorber-coil spring) arrangement with three or four additional links. The suspension is positioned and controlled by use of the linkages. The multi-link rear suspension system is characterized by the use of radial bushings at the linkage ends, so that-plane bending moments are eliminated. The bushings are compliant, allowing for accurate control of the toe angle during cornering.



Figure 2.10: Quadra Link [Source: *Automotive Engineering*, SAE].

2.2.7 Double Wishbone

The double wishbone uses two 'A' shape lateral arms connected the wheel to the vehicle body. Usually the upper arm is shorter than the lower one. This unequal length characteristic will cause negative cambering during wheel vertical displacement. This suspension is suitable for front engine with rear wheel drives cars. There are few types recently for different suspension function design. The cambering effect will keep the outer turning wheel always straight to the road surface for good handling. Its geometry design required less space, able to assembly the rear differential and driving shafts. The disadvantages are requiring careful refinement and accurate geometry design because of its kinematics abilities. Besides, cambering will cause track changing then increase tire wearing. The lower and upper control arm will support all the forces except vertical forces, which acting on the coil spring and damper component.

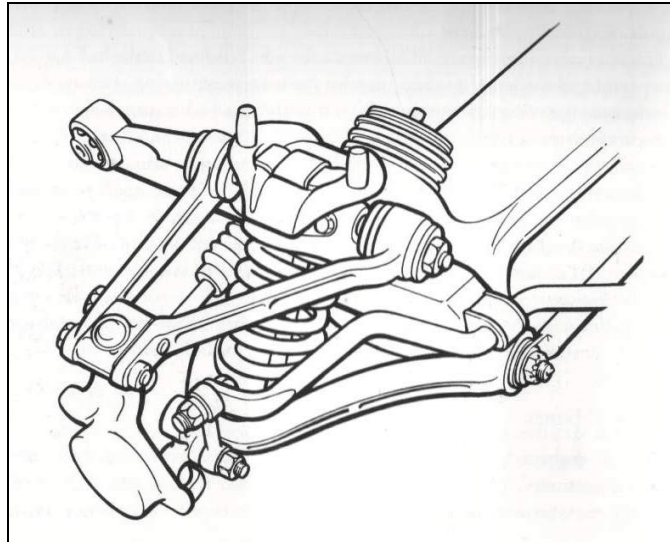


Figure 2.11: Double Wishbone [Source: *Automotive Engineering*, SAE].

CHAPTER 3

CHASSIS ANALYSIS

3.1 Introduction

Strength, rigidity and stiffness are the main concerns of constructing a supportive chassis for a vehicle. The chassis should be able to withstand the appropriate loads on and off the racetrack to ensure a high level of safety and performance. Chassis is frameworks that support the entire component in the car such as suspension system, seat, driver and engine. Even the framework of *Tramcar* is simple, but I need to know the maximum deformation of the chassis when all the loadings applied. Besides, I also need to know the torsional stiffness of the chassis when some cases occur, such as braking or one of the four wheels ride over a bump or into a hole.

In this thesis, all the deformation, stresses, contour and safety factor of the chassis analysed by using *visualNastran*. The drawing of chassis imported from *SolidWorks* into *VisualNastran* by ACIS file to make easier for analysis. Constraint fixed for each analysis. After the analysis in *VisualNastran*, we obtained the value of: -

- i. Maximum Von Mises stress/strain
- ii. Maximum shear stress/strain
- iii. Maximum principal stress/strain
- iv. Total displacement
- v. Safety Factor, n

3.2 Input Material Specifications

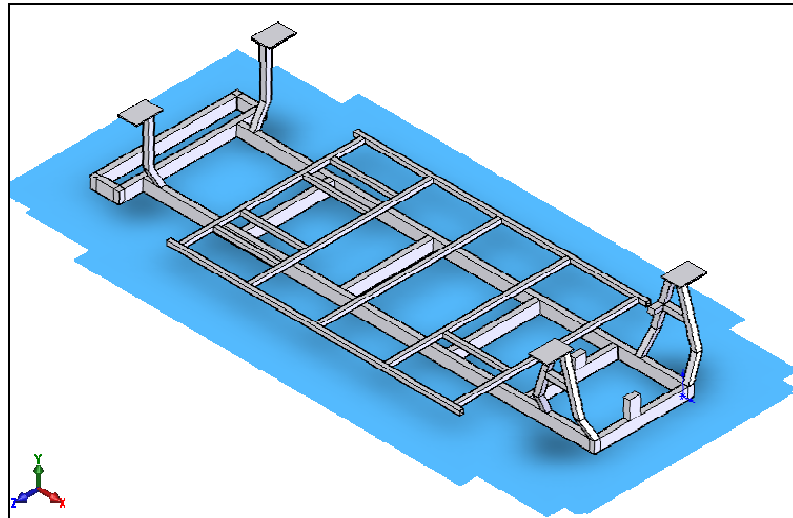
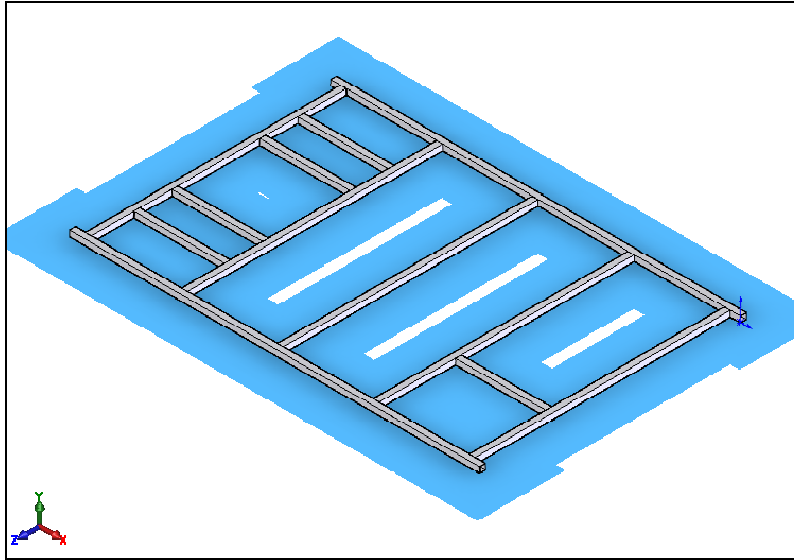


Figure 3.1: *Tramcar* chassis.

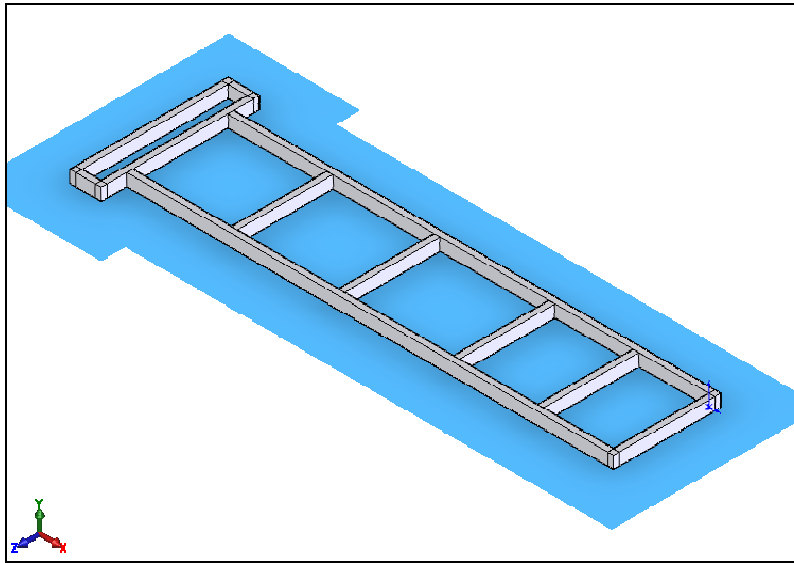
Figure 3.1 shows the isometric view of the *Tramcar* chassis design. Figure 3.2 and Figure 3.3 on the other hand show the upper and lower ladder frameworks associated with the chassis. The material selected is Structure Steel of ANSI i.e. the C1020 type. The material has the following properties: -

- Young's Modulus, E : 200GPa
- Yield stress, σ_{yield} : 331MPa
- Ultimate tensile stress, σ_{ultimate} : 448MPa
- Mass density, ρ : 7850kg/m³
- Poisson's ratio, ν : 0.29



Width : 38.10mm
Height : 38.10mm
Thickness: 2.50mm

Figure 3.2: The upper ladder frame



Width : 50.00mm
Height : 100.00mm
Thickness: 4.00mm

Figure 3.3: The lower ladder frame

3.3 Assumptions

The static and equivalent dynamic analyses were carried out with the assumption that material is of linear elastic. All joints were assumed to be perfectly welded or bonded. The structures were rested on a flat ground and fixed at the given bolting positions.

3.4 Loadings Applied

Before the analysis can be initiated, the boundary conditions were firstly set up. For this *Tramcar* chassis, the loads applied on it are estimated as given in the table below: -

Table 3.1: The loads applied on the chassis

Components	Estimated weight [kg]
Chassis	204.35
Seats and passengers	720.00
Engine	300.00
Tank with full petrol	30.80
Front cover body	23.00
Rear cover body	16.30
Cover roof	69.55
Others	300.00
Vehicle curb weight	984.00
Vehicle gross weight	1664.00

3.5 Static analysis

The static analysis was made to determine the safety factor of the chassis when the *Tramcar* was in a static condition. The loads due to passengers were taken in account in this analysis.

3.5.1 Boundary Conditions

For the static analysis, the boundary conditions were as follows: -

1. The entire load was applied to the chassis
2. Constraints are fixed onto the front and the rear suspension bars
3. 1g of force was applied on –y direction.

3.5.2 Results

All the results of the contours are shown in Appendix B. The values can be summarized as follows: -

- i. Maximum Von Mises stress (Figure B1): 101MPa
- ii. Maximum shear stress (Figure B2): 53.8MPa
- iii. Maximum principal stress (Figure B3): 113MPa
- iv. Maximum Von Mises strain (Figure B4): 0.000436
- v. Maximum shear strain (Figure B5): 0.000694
- vi. Maximum principal strain (Figure B6): 0.000531
- vii. Total displacement (Figure B7): 4.23mm
- viii. Safety Factor, n:

The safety factors are calculated as follows,

$$n = \frac{\sigma_{yield}}{\sigma_{principal}} = \frac{331 \times 10^6}{113 \times 10^6} = 2.93 \quad (\text{Normal stress}) \text{ --- (Eq 3.1)}$$

$$n = \frac{\sigma_{yield}}{2\tau_{max}} = \frac{331 \times 10^6}{2 \times 53.8 \times 10^6} = 3.08 \quad (\text{Shear stress}) \text{ --- (Eq 3.2)}$$

3.6 Bumping Analysis

The bumping analysis has been done to know the safety factor of chassis when the *Tramcar* rides over a bump.

3.6.1 Boundary Conditions

In bumping analysis, the boundary conditions were set as follows: -

1. The entire load was applied to the chassis.
2. Constraints fixed in front and rear suspension bar.
3. 2g of force was applied on the y -direction.

3.6.2 Results

All the results in the form of contour lines are shown in Appendix C. The values can conclude as below:-

- i. Maximum Von Mises stress (Figure C1): 114MPa

- ii. Maximum shear stress (Figure C2): 60.7MPa
- iii. Maximum principal stress (Figure C3): 128MPa
- iv. Maximum Von Mises strain (Figure C4): 0.000492
- v. Maximum shear strain (Figure C5): 0.000783
- vi. Maximum principal strain (Figure C6): 0.000599
- vii. Total displacement (Figure C7): 4.63mm
- viii. Safety Factor, n:

$$n = \frac{\sigma_{yield}}{\sigma_{principal}} = \frac{331 \times 10^6}{128 \times 10^6} = 2.59 \quad (\text{Normal stress})$$

$$n = \frac{\sigma_{yield}}{2\tau_{max}} = \frac{331 \times 10^6}{2 \times 60.7 \times 10^6} = 2.73 \quad (\text{Shear stress})$$

3.7 Braking Analyses

The braking analyses were made to identify the safety factor of the chassis when the *Tramcar* is subjected to a sudden braking.

3.7.1 Boundary Conditions

In undertaking the braking analyses, the boundary conditions were set with the following boundary conditions:-

1. The entire load was applied onto the chassis
2. Constraints fixed in front and rear suspension bars
3. 1g of force was applied in the x-direction

3.7.2 Results

All the results in the form of contours are shown in Appendix D. The values are summarised as below: -

- i. Maximum Von Mises stress (Figure D1): 76.5MPa
- ii. Maximum shear stress (Figure D2): 40.5MPa
- iii. Maximum principal stress (Figure D3): 85.4MPa
- iv. Maximum Von Mises strain (Figure D4): 0.000329
- v. Maximum shear strain (Figure D5): 0.000523
- vi. Maximum principal strain (Figure D6): 0.000400
- vii. Total displacement (Figure D7): 3.72mm
- viii. Safety Factor, n:

$$n = \frac{\sigma_{yield}}{\sigma_{principal}} = \frac{331 \times 10^6}{85.4 \times 10^6} = 3.88 \quad (\text{Normal stress})$$

$$n = \frac{\sigma_{yield}}{2\tau_{max}} = \frac{331 \times 10^6}{2 \times 40.5 \times 10^6} = 4.09 \quad (\text{Shear stress})$$

3.8 Chassis Torsional Stiffness Analysis

The torsional stiffness analysis was implemented to assess the chassis ability to withstand the torsional loading.

3.8.1 Boundary Conditions

In chassis torsional stiffness analysis, the boundary conditions set as follows:

1. Constraints fixed only in rear suspension bar.
2. 1.5kN, 3kN, 4.5kN, 6kN, 7.5kN and 9kN force applied in fore suspension bar on opposite direction.

3.8.2 Results

All the results in the form of contour lines are shown in Appendix E.

Examples of calculation to obtain the torsional stiffness are show as follows:

$$\begin{aligned} \text{Torsion, } T &= \text{Applied force x Distance (F x r)} && \text{--- (Eq. 3.3)} \\ &= 9000 \times 0.6275 \\ &= 5647.50 \text{ Nm} \end{aligned}$$

$$\begin{aligned} \text{Twisting Angle, } \theta &= \tan^{-1} \frac{\delta}{r} && \text{--- (Eq. 3.4)} \\ &= \tan^{-1} \frac{0.0121}{0.6275} \\ &= 1.1047^\circ \end{aligned}$$

Here the twist angle is rather low indicating the rigidity of the chassis frame in its totality.

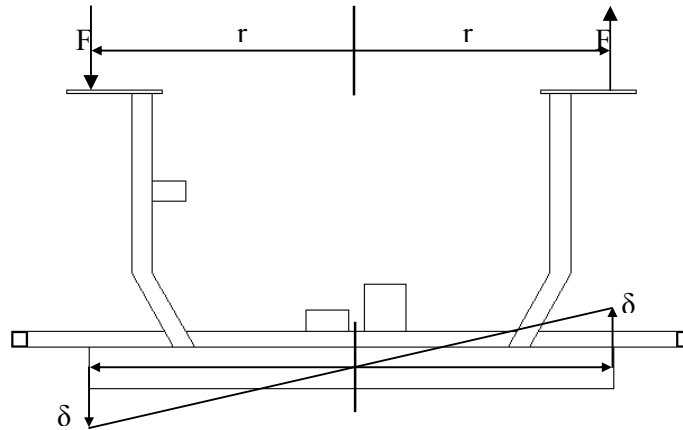


Figure 3.4: The chassis displacement

Table 3.2: Table of applied force, displacement, torsion and twisting angle during torsional stiffness analysis

Applied force, F [N]	Chassis displacement, δ [mm]	Torsion, T [Nm]	Twisting angle, θ [°]
0	0	0	0
1500	2.035	941.25	0.1858
3000	4.015	1882.50	0.3666
4500	6.050	2823.75	0.5524
6000	8.250	3765.00	0.7532
7500	9.900	4706.25	0.9039
9000	12.10	5647.50	1.1047

The values for torsion and twisting angle were used to plot a graph (Figure 3.5). The slope of the graph indicated the chassis torsional stiffness.

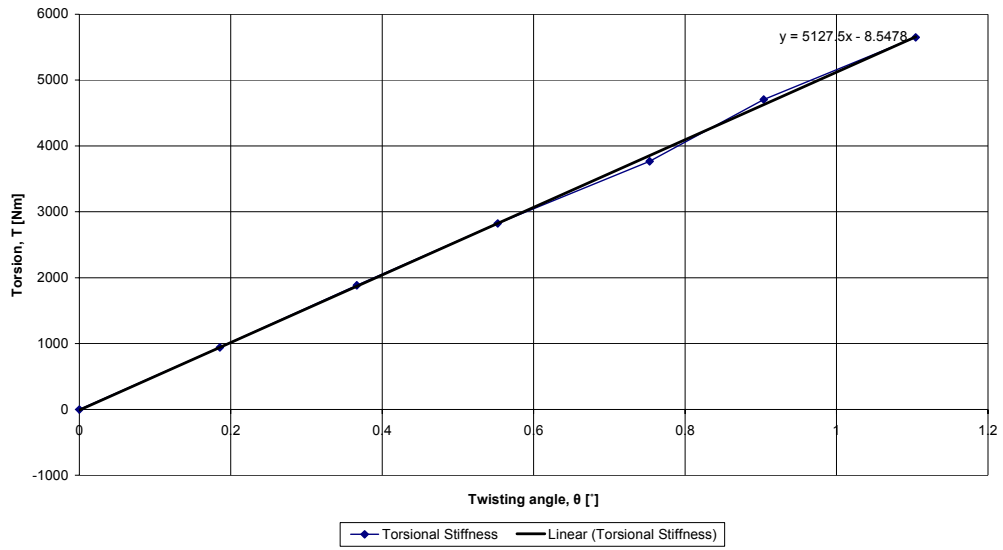


Figure 3.5: Graph torsion increasing against twisting angle.

CHAPTER 4

SUSPENSION SYSTEM ANALYSIS

4.1 Introduction

Quarter car, half car and full car model can be created to determine the different characteristics of a vehicle under study, to determine for its ride and handling performance respectively. As for the vehicle ride aspect, the important parameters will include i) vehicle displacement, ii) yaw, iii) roll and iv) pitch response.

4.2 Quarter Car Model

The Figure 4.1 shows below the quarter car model representation. The quarter car model is a two degree-of-freedom type that emulates the vehicle body and axle dynamics with a single time respectively.

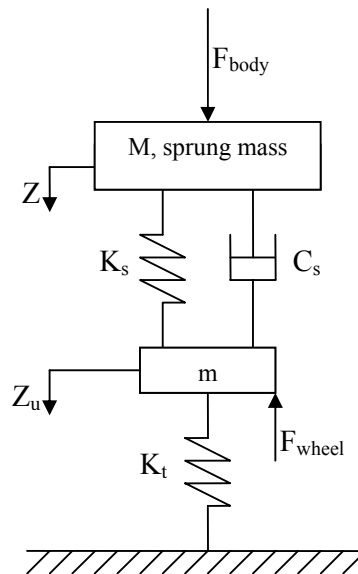


Figure 4.1: Quarter car model representation

For this model, the two degree-of-freedom that can be created is the heave displacement of the unsprung mass. However, model cannot be used to determine the roll and the pitching conditions. This study remains adequate and efficient to determine the many design issues but is not sufficient to warrant for the actual system design purposes.

As an example, the quarter car model is not able to study the influence of the wheelbase filtering mechanism on ride comfort. Half vehicle model is more convenient to design the passive as well as the active suspension systems and to study their influence on the interaction between the body bounce and pitch motions.

4.3 Half Car Model

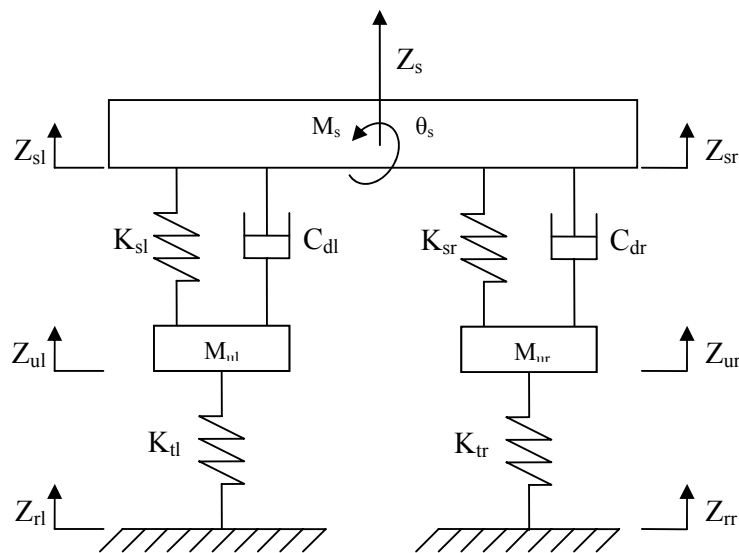


Figure 4.2: Half car model

The Figure 4.2 on the other hand illustrates a half car model of the Tramcar. The half car model is a four degree-of-freedom model that emulates the vehicle body and axle dynamics with a single time.

For a half car model, the four degree-of-freedom that can be created includes the roll or pitch model. The half-car model can either be the half car roll plane or the half car pitch plane.

An example for a half car pitch plane is whereby the vehicle is represented by a sprung mass supported by primary suspension system at each wheel. Here the lateral dynamics of the vehicle are ignored. As a result, only one front tire and one rear tire are considered in the model. The model consists of the sprung mass or car body supported on suspensions at the front and rear. The suspensions are connected to their respective tire axles, which are considered to be un-sprung masses. Additionally, the suspensions have stiffness and damping properties, the tire is represented as a simple spring.

As stated above, the half car model is convenience to determine either the passive susceptible system or active suspension system of their influence on the interaction the vehicle movement include the bounce, pitch or roll motion.

4.4 Full Car Model

Figure 4.3 shows a full car model. The full car model shown is a seven degree-of-freedom model that emulates the vehicle body and axle dynamics with a single time condition. Here the full car model was used to do the simulation since it was thought that the better overall result can be obtained through this technique.

The full vehicle suspension system is represented as a linearized seven degree-of-freedom system. It consists of a single sprung mass (car body) connected to four unsprung masses (front-left, front-right, rear left and rear-right wheels) at each corner.

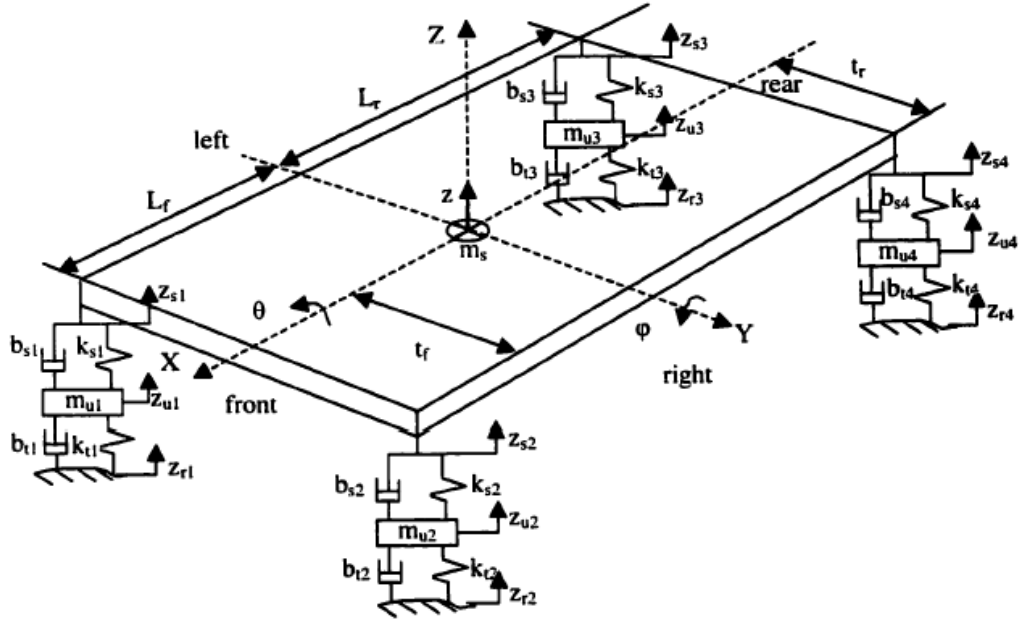


Figure 4.3: Full car model

The sprung mass is free to heave, pitch and roll while the unsprung masses are free to bounce vertically with respect to the sprung mass. The suspensions between the sprung mass and unsprung masses are modelled as linear viscous dampers and spring elements, while the tires are modelled as simple linear springs without damping. For simplicity, all pitch and roll angles are assumed to be small. The full car model can be used to predict more complexity of the vehicle ride and handling characteristic. The full car model can be used to determine the roll and pitch moment in one step compare to the half car model.

After applying a force-balance analysis to the model in Figure 4.3, the equations of motion are given as: -

$$\begin{aligned}
 m_s \ddot{z} = & -m_s g - (2K_{s_f} + 2K_{s_r})z - (2B_{s_f} + 2B_{s_r})\dot{z} + (2aK_{s_f} - 2bK_{s_r})\theta + (2aB_{s_f} - 2bB_{s_r})\dot{\theta} + \dots \\
 & + K_{s_f} z_{u_{fl}} + B_{s_f} \dot{z}_{u_{fl}} + K_{s_f} z_{u_{fr}} + B_{s_f} \dot{z}_{u_{fr}} + K_{s_r} z_{u_{rl}} + B_{s_r} \dot{z}_{u_{rl}} + K_{s_r} z_{u_{rr}} + B_{s_r} \dot{z}_{u_{rr}} + \dots \\
 & + f_{fl} + f_{fr} + f_{rl} + f_{rr}
 \end{aligned}
 \quad \text{--- (Eq. 4.1)}$$

$$\begin{aligned}
I_{xx}\ddot{\phi} = & -0.25w^2(2K_{s_f} + 2K_{s_r})\phi - 0.25w^2(2B_{s_f} + 2B_{s_r})\dot{\phi} + 0.5wK_{s_f}z_{u_{fl}} + 0.5wB_{s_f}\dot{z}_{u_{fl}} + \dots \\
& -0.5wK_{s_f}z_{u_{fr}} - 0.5wB_{s_f}\dot{z}_{u_{fr}} + 0.5wK_{s_r}z_{u_{rl}} + 0.5wB_{s_r}\dot{z}_{u_{rl}} - 0.5wK_{s_r}z_{u_{rr}} - 0.5wB_{s_r}\dot{z}_{u_{rr}} + \dots \\
& + 0.5wf_{fl} - 0.5wf_{fr} + 0.5wf_{rl} - 0.5wf_{rr}
\end{aligned}$$

--- (Eq. 4.2)

$$\begin{aligned}
m_u\ddot{z}_{u_{fl}} = & -m_u g + K_{s_f}z + B_{s_f}\dot{z} - aK_{s_f}\theta - aB_{s_f}\dot{\theta} + 0.5wK_{s_f}\phi + 0.5wB_{s_f}\dot{\phi} + \dots \\
& - (K_{s_f} + K_u)z_{u_{fl}} - B_{s_f}\dot{z}_{u_{fl}} + K_u z_{r_{fl}} - f_{fl}
\end{aligned}$$

--- (Eq. 4.3)

$$\begin{aligned}
m_u\ddot{z}_{u_{fr}} = & -m_u g + K_{s_f}z + B_{s_f}\dot{z} - aK_{s_f}\theta - aB_{s_f}\dot{\theta} - 0.5wK_{s_f}\phi - 0.5wB_{s_f}\dot{\phi} + \dots \\
& - (K_{s_f} + K_u)z_{u_{fr}} - B_{s_f}\dot{z}_{u_{fr}} + K_u z_{r_{fr}} - f_{fr}
\end{aligned}$$

--- (Eq. 4.4)

$$\begin{aligned}
m_u\ddot{z}_{u_{rl}} = & -m_u g + K_{s_r}z + B_{s_r}\dot{z} + bK_{s_r}\theta + bB_{s_r}\dot{\theta} + 0.5wK_{s_r}\phi + 0.5wB_{s_r}\dot{\phi} + \dots \\
& - (K_{s_r} + K_u)z_{u_{rl}} - B_{s_r}\dot{z}_{u_{rl}} + K_u z_{r_{rl}} - f_{rl}
\end{aligned}$$

--- (Eq. 4.5)

$$\begin{aligned}
m_u\ddot{z}_{u_{rr}} = & -m_u g + K_{s_r}z + B_{s_r}\dot{z} + bK_{s_r}\theta + bB_{s_r}\dot{\theta} - 0.5wK_{s_r}\phi - 0.5wB_{s_r}\dot{\phi} + \dots \\
& - (K_{s_r} + K_u)z_{u_{rr}} - B_{s_r}\dot{z}_{u_{rr}} + K_u z_{r_{rr}} - f_{rr}
\end{aligned}$$

--- (Eq. 4.6)

The system states are assigned as: -

- $x_1 = z$ heave position (ride height of sprung mass)
- $x_2 = \dot{z}$ heave velocity (payload velocity of sprung mass)
- $x_3 = \theta$ roll angle
- $x_4 = \dot{\theta}$ roll angular velocity
- $x_5 = \phi$ pitch angle
- $x_6 = \dot{\phi}$ pitch angular velocity
- $x_7 = z_{u_{fl}}$ front-left wheel unsprung mass height
- $x_8 = \dot{z}_{u_{fl}}$ front-left wheel unsprung mass velocity

$x_9 = z_{u_{fr}}$	front-right wheel unsprung mass height
$x_{10} = \dot{z}_{u_{fr}}$	front-right wheel unsprung mass velocity
$x_{11} = z_{u_{rl}}$	rear-left wheel unsprung mass height
$x_{12} = \dot{z}_{u_{rl}}$	rear-left wheel unsprung mass velocity
$x_{13} = z_{u_{rr}}$	rear-right wheel unsprung mass height
$x_{14} = \dot{z}_{u_{rr}}$	rear-right wheel unsprung mass velocity

The results of the system state equations analysis are as follows: -

$$\begin{aligned} \dot{x}_1 &= x_2 \\ \dot{x}_2 &= -\frac{(2K_{s_f} + 2K_{s_r})}{m_s} x_1 - \frac{(2B_{s_f} + 2B_{s_r})}{m_s} x_2 + \frac{(2aK_{s_f} + 2bK_{s_r})}{m_s} x_3 + \frac{(2aB_{s_f} + 2bB_{s_r})}{m_s} x_4 + \frac{K_{s_f}}{m_s} x_7 + \frac{B_{s_f}}{m_s} x_8 + \dots \\ &\quad + \frac{K_{s_f}}{m_s} x_9 + \frac{B_{s_f}}{m_s} x_{10} + \frac{K_{s_r}}{m_s} x_{11} + \frac{B_{s_r}}{m_s} x_{12} + \frac{K_{s_r}}{m_s} x_{13} + \frac{B_{s_r}}{m_s} x_{14} + \frac{1}{m_s} f_{fl} + \frac{1}{m_s} f_{rl} + \frac{1}{m_s} f_{rl} + \frac{1}{m_s} f_{rr} \end{aligned}$$

--- (Eq. 4.7)

$$\begin{aligned} \dot{x}_3 &= x_4 \\ \dot{x}_4 &= \frac{(2aK_{s_f} + 2bK_{s_r})}{I_{yy}} x_1 + \frac{(2aB_{s_f} + 2B_{s_r})}{I_{yy}} x_2 - \frac{(2a^2K_{s_f} + 2b^2K_{s_r})}{I_{yy}} x_3 - \frac{(2a^2B_{s_f} + 2b^2B_{s_r})}{I_{yy}} x_4 - \frac{aK_{s_f}}{I_{yy}} x_7 + \dots \\ &\quad - \frac{aB_{s_f}}{I_{yy}} x_8 - \frac{aK_{s_f}}{I_{yy}} x_9 - \frac{aB_{s_f}}{I_{yy}} x_{10} + \frac{bK_{s_f}}{I_{yy}} x_{11} + \frac{bB_{s_f}}{I_{yy}} x_{12} + \frac{bK_{s_f}}{I_{yy}} x_{13} + \frac{bB_{s_f}}{I_{yy}} x_{14} - \frac{a}{I_{yy}} f_{fl} - \frac{a}{I_{yy}} f_{fr} + \dots \\ &\quad + \frac{b}{I_{yy}} f_{rl} + \frac{b}{I_{yy}} f_{rr} \end{aligned}$$

--- (Eq. 4.8)

$$\begin{aligned} \dot{x}_5 &= x_6 \\ \dot{x}_6 &= -\frac{w^2(2K_{s_f} + 2K_{s_r})}{4I_{xx}} x_5 - \frac{w^2(2B_{s_f} + 2B_{s_r})}{4I_{xx}} x_6 + \frac{wK_{s_f}}{2I_{xx}} x_7 + \frac{wB_{s_f}}{2I_{xx}} x_8 - \frac{wK_{s_f}}{2I_{xx}} x_9 - \frac{wB_{s_f}}{2I_{xx}} x_{10} + \dots \\ &\quad + \frac{wK_{s_r}}{2I_{xx}} x_{11} + \frac{wB_{s_r}}{2I_{xx}} x_{12} - \frac{wK_{s_r}}{2I_{xx}} x_{13} - \frac{wB_{s_r}}{2I_{xx}} x_{14} + \frac{w}{2I_{xx}} f_{fl} - \frac{w}{2I_{xx}} f_{fr} + \frac{w}{2I_{xx}} f_{rl} - \frac{w}{2I_{xx}} f_{rr} \end{aligned}$$

--- (Eq. 4.9)

$$\begin{aligned}\dot{x}_7 &= x_8 \\ \dot{x}_8 &= \frac{K_{s_f}}{m_u} x_1 + \frac{B_{s_f}}{m_u} x_2 - \frac{aK_{s_f}}{m_u} x_3 - \frac{aB_{s_f}}{m_u} x_4 + \frac{wK_{s_f}}{2m_u} x_5 + \frac{wB_{s_f}}{2m_u} x_6 - \frac{(K_{s_f} + K_u)}{m_u} x_7 - \frac{B_{s_f}}{m_u} x_8 + \dots \\ &\quad - \frac{1}{m_u} f_{fl} - g + \frac{K_u}{m_u} z_{r_{fl}}\end{aligned}$$

--- (Eq. 4.10)

$$\begin{aligned}\dot{x}_9 &= x_{10} \\ \dot{x}_{10} &= \frac{K_{s_f}}{m_u} x_1 + \frac{B_{s_f}}{m_u} x_2 - \frac{aK_{s_f}}{m_u} x_3 - \frac{aB_{s_f}}{m_u} x_4 - \frac{wK_{s_f}}{2m_u} x_5 - \frac{wB_{s_f}}{2m_u} x_6 - \frac{(K_{s_f} + K_u)}{m_u} x_9 - \frac{B_{s_f}}{m_u} x_{10} + \dots \\ &\quad - \frac{1}{m_u} f_{fr} - g + \frac{K_u}{m_u} z_{r_{fr}}\end{aligned}$$

--- (Eq. 4.11)

$$\begin{aligned}\dot{x}_{11} &= x_{12} \\ \dot{x}_{12} &= \frac{K_{s_r}}{m_u} x_1 + \frac{B_{s_r}}{m_u} x_2 + \frac{bK_{s_r}}{m_u} x_3 + \frac{bB_{s_r}}{m_u} x_4 + \frac{wK_{s_r}}{2m_u} x_5 + \frac{wB_{s_r}}{2m_u} x_6 - \frac{(K_{s_r} + K_u)}{m_u} x_{11} - \frac{B_{s_r}}{m_u} x_{12} + \dots \\ &\quad - \frac{1}{m_u} f_{rl} - g + \frac{K_u}{m_u} z_{r_{rl}}\end{aligned}$$

--- (Eq. 4.12)

$$\begin{aligned}\dot{x}_{13} &= x_{14} \\ \dot{x}_{14} &= \frac{K_{s_r}}{m_u} x_1 + \frac{B_{s_r}}{m_u} x_2 + \frac{bK_{s_r}}{m_u} x_3 + \frac{bB_{s_r}}{m_u} x_4 + \frac{wK_{s_r}}{2m_u} x_5 - \frac{wB_{s_r}}{2m_u} x_6 - \frac{(K_{s_r} + K_u)}{m_u} x_{13} - \frac{B_{s_r}}{m_u} x_{14} + \dots \\ &\quad - \frac{1}{m_u} f_{rr} - g + \frac{K_u}{m_u} z_{r_{rr}}\end{aligned}$$

--- (Eq. 4.13)

All the equations stated above are then converted to simulate the performance using simulation tool i.e. *Matlab ver 6.5*. For easy reference the diagrams for models used are shown below.

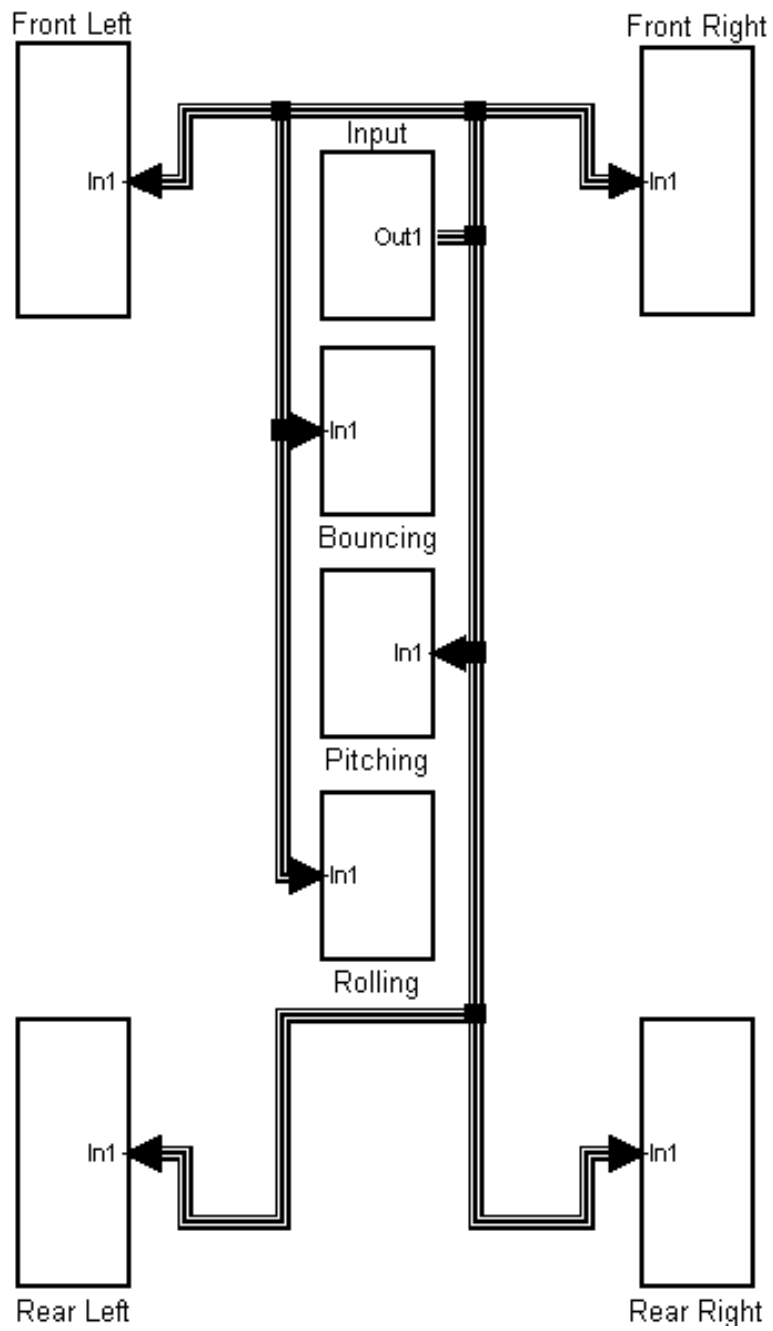


Figure 4.4: The full system of full car model

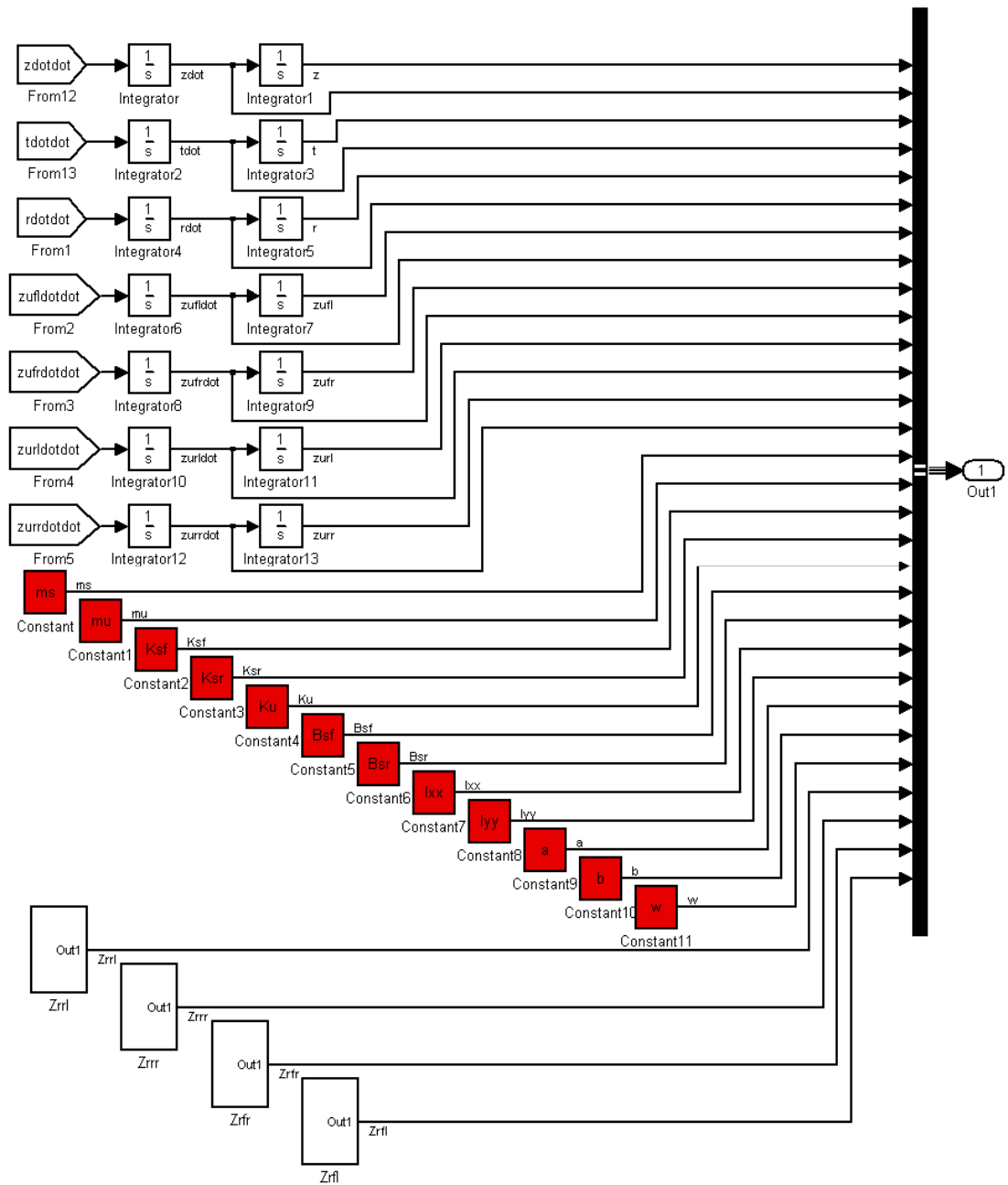


Figure 4.5: The inputs for the system

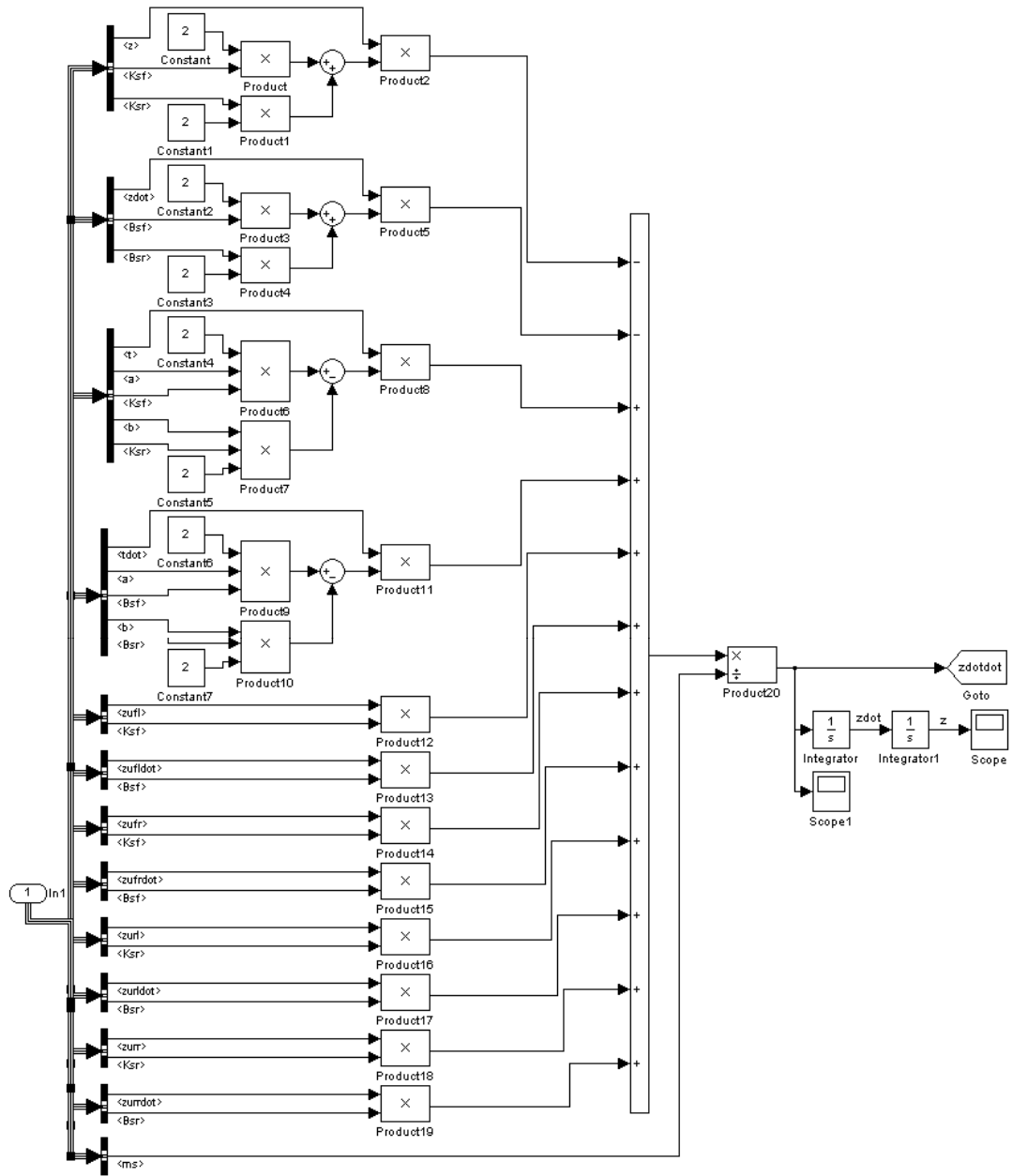


Figure 4.6: Subsystem for bouncing

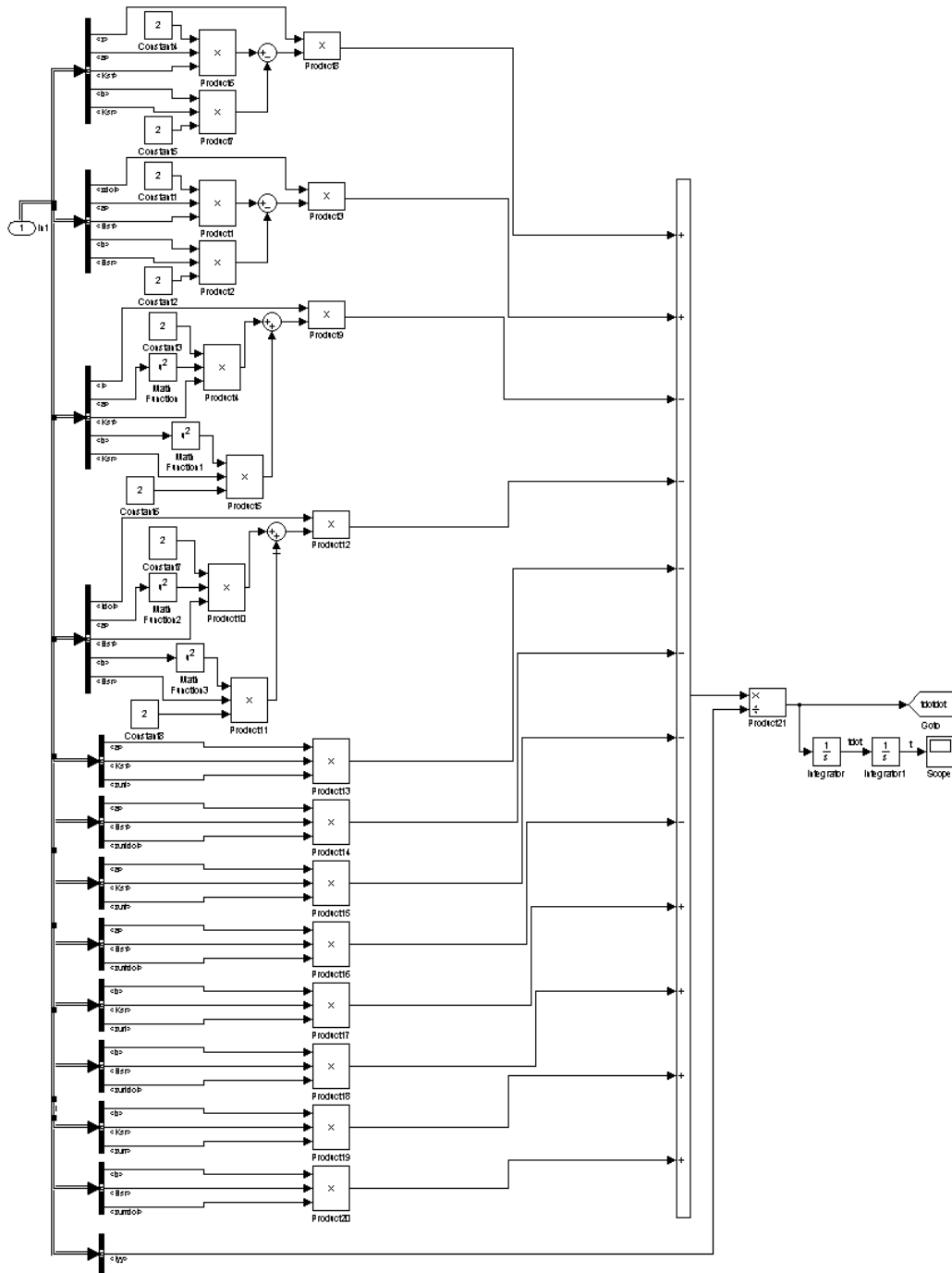


Figure 4.7: Subsystem for pitching

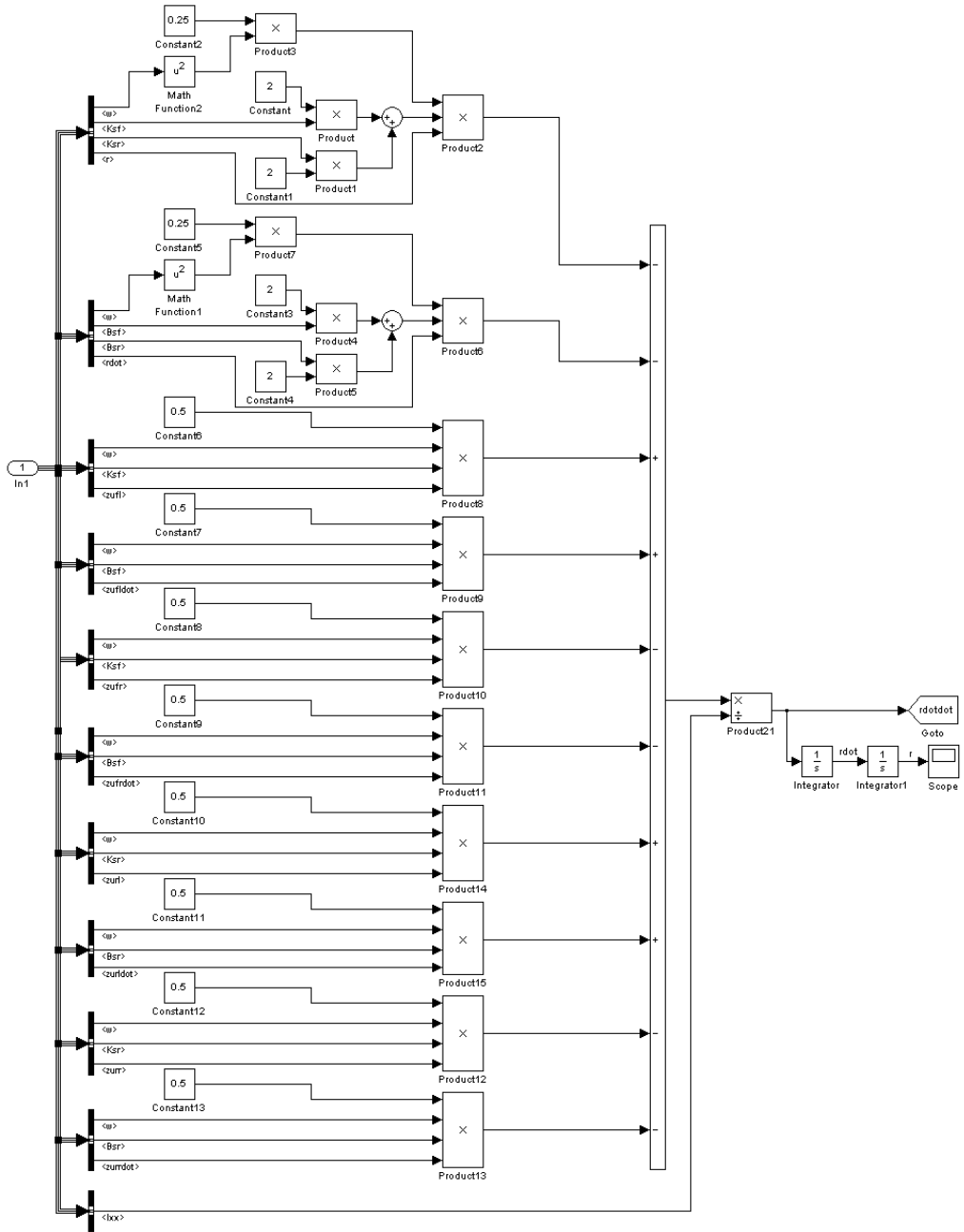


Figure 4.8: Subsystem for rolling

4.5 Conditions for Analysis

The conditions have been set up in the suspension analysis before we simulate in *Matlab 6.5*. There are: -

1. Vehicle driven over the bump at a constant speed of 20km/h.
2. The bump is 0.072m heights.
3. In bouncing and rolling analysis, only left hand side of vehicle driven over the bump (Figure 4.9) while both of the side driven over the bump in pitching analysis (Figure 4.10).
4. Two different suspensions stiffness are assumed to make a comparison suspension performance where the rest of input parameter remains constant.
5. To identify more clearly for the comfort of *Tramcar*, the result will compare with the result from *Proton Waja 1.6* which finish analyzed by ADC where the same analysis condition applied.

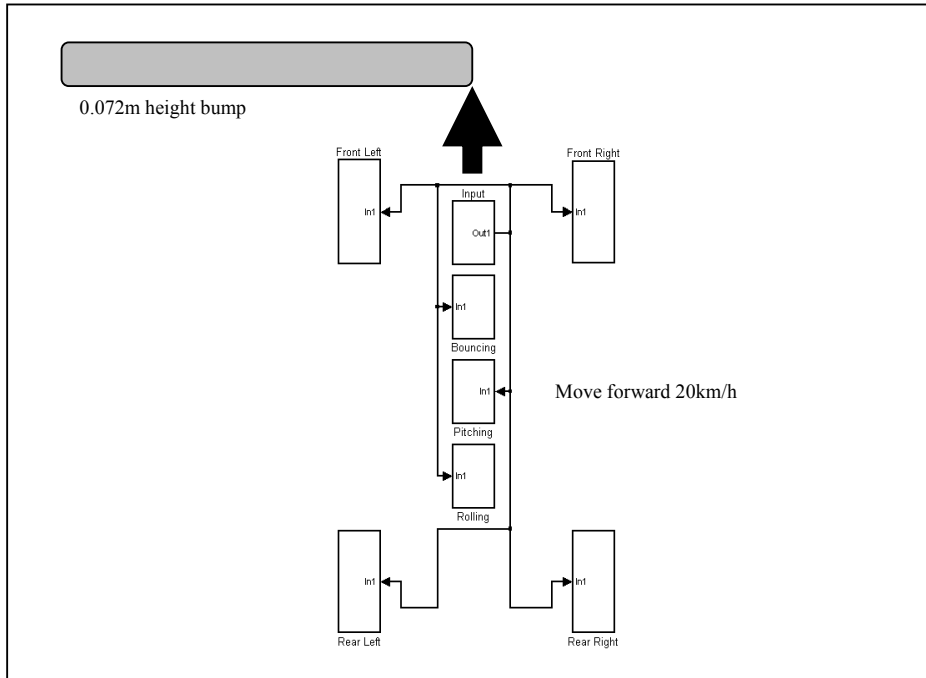


Figure 4.9: Condition for bouncing and rolling analysis

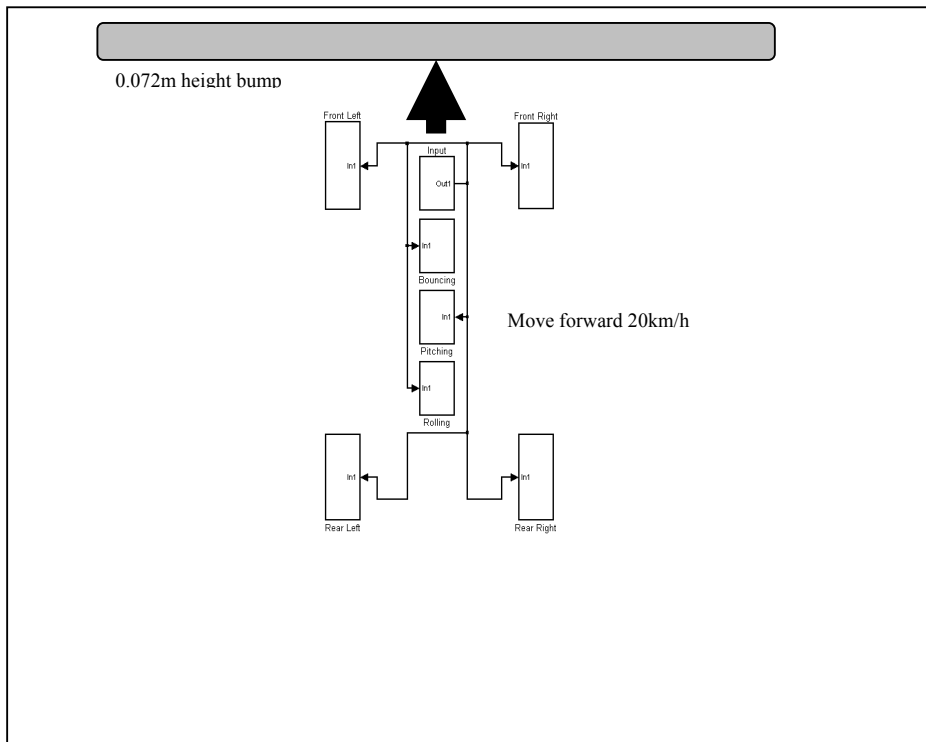


Figure 4.10: Condition for pitching analysis

4.6 The Input of Parameter

The following data are the input of parameter for *Tramcar* benchmarked to a reference i.e. *Proton Waja 1.6* using *Matlab* ver 6.5.

Table 4.1: Input parameters for *Tramcar* and *Proton Waja 1.6*.

Description [Units]	<i>Tramcar</i> parameter	<i>Proton Waja 1.6</i> parameter
Sprung mass [kg]	1664	1500
Unsprung mass [kg]	59*	59
Front suspension spring stiffness [N/m]	26500	35000
Rear suspension spring stiffness [N/m]	26500	38000
Tire spring stiffness [N/m]	190000*	190000
Front suspension damping [N/m/s]	1030.05	1000
Rear suspension damping [N/m/s]	1030.05	1100
Roll axis moment of inertia [kg-m ²]	729.67	460
Pitch axis moment of inertia [kg-m ²]	2813.79	2160
Length between front of vehicle and centre of gravity of sprung mass [m]	1.7085	1.4
Length between rear of vehicle and centre of gravity of sprung mass [m]	1.7085	1.7
Width of sprung mass [m]	3.417	3

* The value of unsprung mass and tire spring stiffness for *Tramcar* assumed same as the parameter with *Proton Waja 1.6*

4.7 Assumptions

The following are the assumptions made pertaining to the simulation outcomes:

1. The road profile has zero noise.
2. Air drag is neglected for a low speed (20km/hr).
3. The model is a passive suspension system where there is not control input.
4. The roll movement occurs around the vehicle's centre of mass but not around the roll centre.
5. All the chassis deformations were not taken into accounts as it was modelled as a rigid body.
6. Small angles for the slip angle of the tire, so the lateral forces always acts perpendicular to the vehicle axis.
7. The displacement of the suspension is only in the vertical direction, and geometry angles were not taken into account.
8. Small displacement for the masses so the displacement of the points where the forces applied was not needed to considerate.
9. The specified weight of the *Tramcar* is 984kg plus with 8 passengers' weight of 680kg includes the driver that gives a total of 1664kg of unsprung mass.
10. It is well known that motion of the sprung mass at the wheel frequency modes cannot be reduced if the only control input is a force applied between the sprung and unsprung masses.

11. The natural frequencies of heave, pitch and roll are determined from vehicle suspension dynamics and moments of inertia. Their damping is determined from the ride-dependent dynamics and moments.

4.8 Results

All the simulation results are shown in the form of graphical representations as follows: -

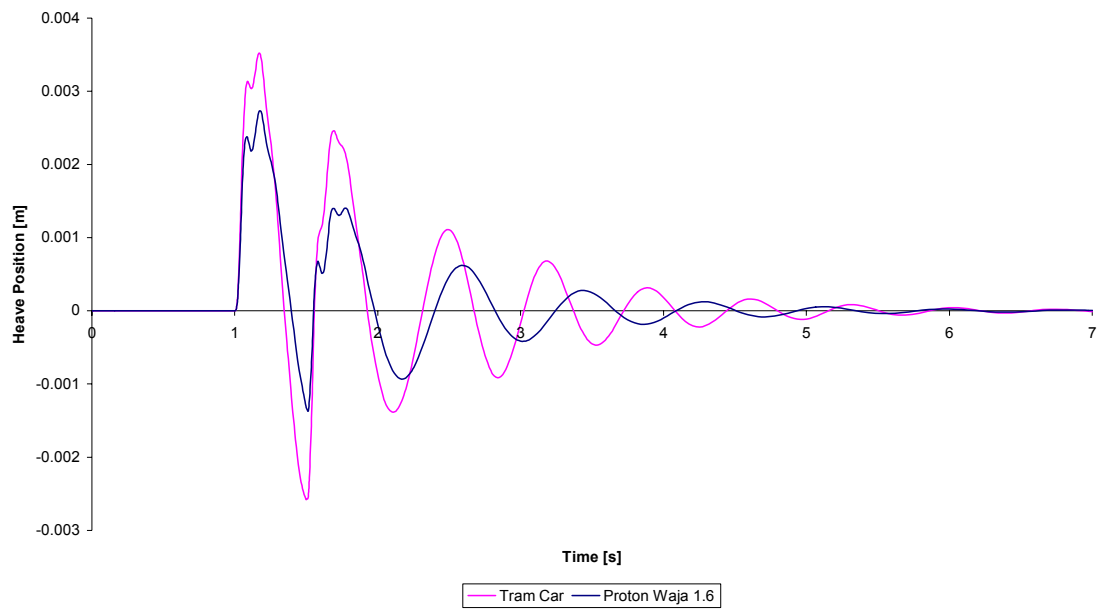


Figure 4.11: Bouncing Performance

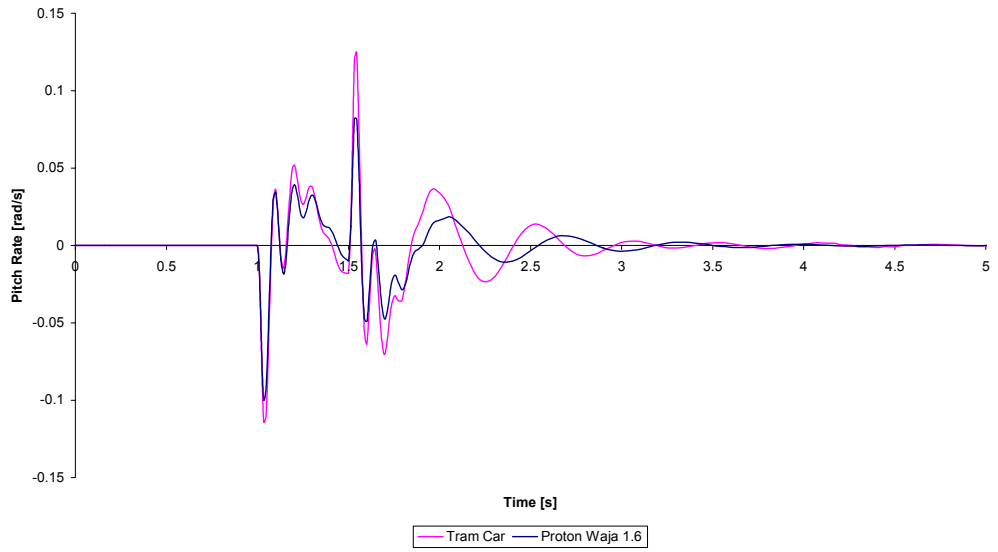


Figure 4.12: Pitching Performance

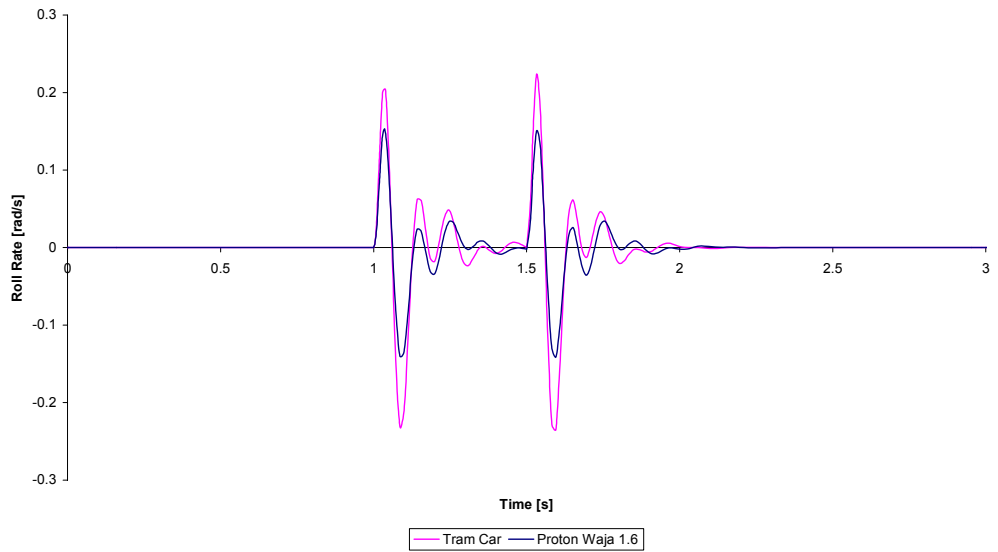


Figure 4.13: Rolling Performance

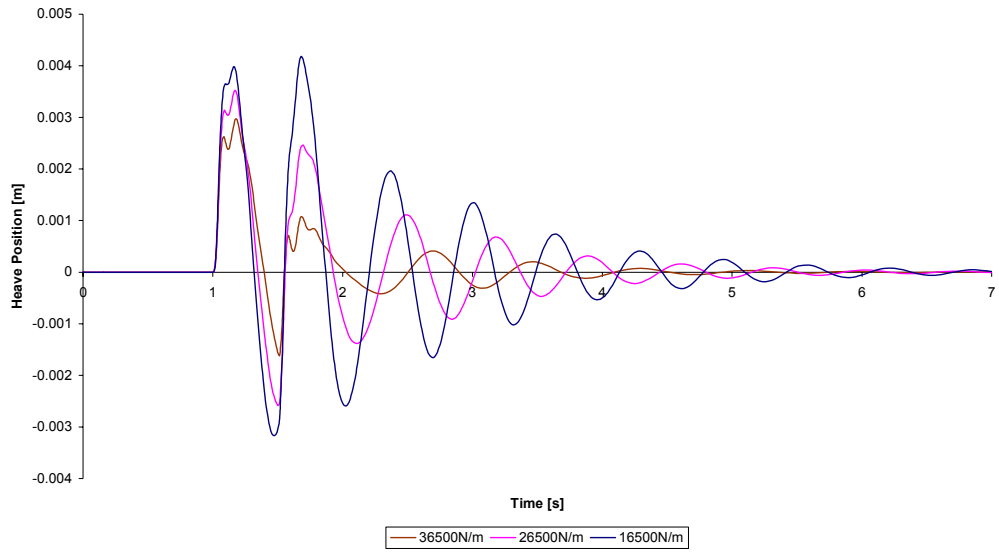


Figure 4.14: Comparison in bouncing performance for different stiffness

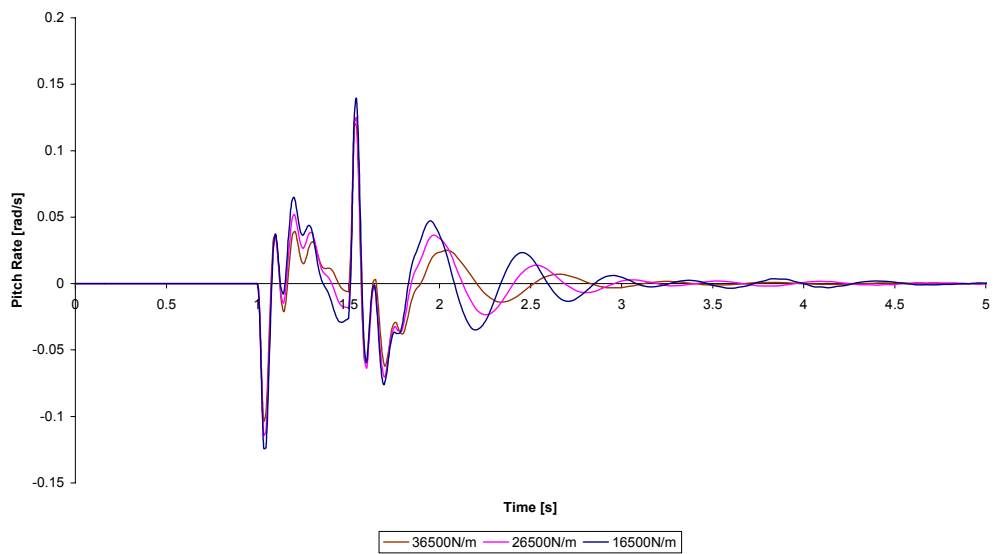


Figure 4.15: Comparison in pitching performance for different stiffness

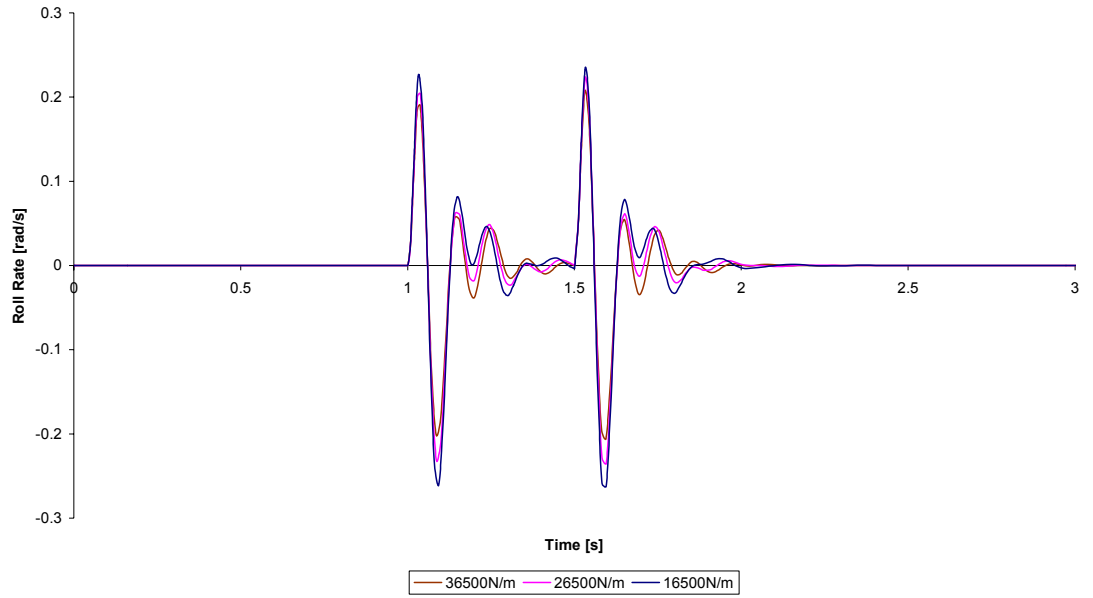


Figure 4.16: Comparison in rolling performance for different stiffness

CHAPTER 5

DISCUSSIONS

Chassis Analysis

From the chassis and suspension analyses of this project, the performance for both these parts in different situations can be obtained. Each of the results is discussed in the following sub-sections.

Static Analysis

In the first analysis, we got the maximum Von Mises Stress is 101MPa, the maximum shear stress is 53.8MPa, the maximum principal stress is 113MPa and the maximum displacement is 4.23mm. The safety factor for normal stress is 2.93 while in shear stress is 3.08.

From the safety factor, we can conclude that the framework is safe in static. The safety factor is satisfied for a vehicle. From literature review, we have known that a vehicle can be said 'safe' if the safety factor over 2.0. In the analysis we assumed all the joints are perfectly welded.

From the analysis, we obtained that the maximum stress occurred at the middle of chassis. The deformation is large here. The chassis will most probably fail at this place. Hence, we need to strengthen the cross bar. We can either use bigger diameter of steel bar or increase the thickness of the bar.

From the analysis, we can found out that the actual maximum stress occurred in the joint between the fore suspension bar and the lower ladder frame. In the contour of stress, we can see that the colour in orange-yellow. In this analysis, the fore suspension bar is assumed while the fore suspension bar is not appearing in the real *Tramcar*. This is because the entire fore of *Tramcar* is built from monoque. We can only analyze the chassis in this project. Although the maximum stress occurred in fore suspension bar, we did not take it as result.

The maximum Von Mises strain is 0.000436MPa, the maximum shear strain is 0.000694MPa and the maximum principal strain is 0.000531MPa. The value for strain is small which almost the zero, so we are neglected the effect of strain to the chassis.

In most vehicles applications, the static loading in normal condition would not create any problem or permanent distortion to the chassis. The torsion due to the unbalance support will bring more severe case.

Bumping Analysis

The second analysis is bumping analysis. In the analysis, we got the maximum Von Mises Stress is 114MPa, the maximum shear stress is 60.7MPa, the maximum principal stress is 128MPa and the maximum displacement is 4.63mm. The safety factor for normal stress is 2.59 while in shear stress is 2.73.

From the safety factor, we can conclude that the framework is safe when the *Tramcar* rode over a bump. The safety factor is satisfied for *Tramcar*. In the analysis we assume all the joints are perfectly welded.

From the result, we found out that the critical location for bumping analysis is almost the same for the static analysis. Referred to the contour, we obtained that the maximum displacement occurred at the middle of chassis. The chassis will most probably fail at this place. The maximum stress occurred at the fore suspension bar. As we mentioned before, we did not take it as result although the maximum stress occurred in fore suspension bar.

In bumping analysis, we assumed that 2g force applied to the whole chassis in $-y$ direction. This is equal to the force when *Tramcar* rode over a bump.

Braking Analysis

Based on the results of the bumping analysis, the chassis gives a better performance than the braking analysis. In the braking analysis, the maximum Von Mises Stress is 76.5MPa, the maximum shear stress is 40.5MPa, the maximum principal stress is 85.4MPa and the maximum displacement is 3.72mm respectively.

The chassis gives a more secure safety factor in braking analysis. The safety factor for normal stress has been determined as 3.88 while for shear stress is 4.09. From the safety factor, it can be concluded that the framework will safe when the *Tramcar* is subjected to sudden braking. Here, all the joints for the chassis are regarded as being perfectly welded.

As for the braking analysis, it was assumed that 1g force was applied to the whole chassis in $-x$ direction. This equals to the force when *Tramcar* brakes suddenly. This is the reason that caused for the maximum deformation to occur in y direction to be less than the maximum deformation due to bumping effect. When the *Tramcar* brakes suddenly, two directional forces will be applied to the chassis, i.e. the $-x$ direction and the $-y$ direction. In the bumping analysis, only $-y$ direction force was considered to be applied to the chassis.

Chassis Torsional Stiffness Analysis

It is apparent that torsion will be increase with the increase in the twisting angle. This was plotted for the purpose to getting the torsional stiffness value of the chassis, particularly so when there are extra forces applied on the fore suspension bar.

From the graph of torsion against the degree of torsion, it is found that the relationship is linear. As can be observed from the graph, the torsional stiffness of the chassis (from the slope of the graph), is 5127.5Nm/degree. This value is in range allowed for normal saloon car, which is from 3000Nm/degree to 9000Nm/degree.

When 10kN force is applied, the chassis lost its elasticity property. To maintain the elasticity property, the analysis only can be done until 9kN.

Suspension System Analysis

Base on the graph, the results for suspension system analysis are discussed as follows.

Bouncing Performance

Figure 4.11 shows the bouncing performance for the *Tramcar* and *Proton Waja 1.6* in 8 seconds simulation. We can clearly see that there were two different two curves plotted. The pink colour curve line indicated the simulation curve for *Tramcar*, we note that increment of the sprung mass heave position started at 1s which is the time when the front left wheel hit the bump. From the curve too, we note that there was a peak point around 3.522mm at 1.1711s. That means the *Tramcar* heaved the maximum value

3.522mm when the front wheel hit the bump. The second peak point occurred at 1.6943s where the rear wheel hit the bump. It is around 2.461mm heaved from the centre of gravity. Then the graph is damped off until more steady state. We noticed that the heave position was almost fully damped at around 7s.

On the other hand, the *Proton Waja 1.6* simulation curve was indicated in dark blue colour. The almost same orientation of behaviour as the *Tramcar* happened on the *Proton Waja 1.6* step up and down when compared to the simulation curve for *Tramcar*. What was different here, *Proton Waja 1.6* indicated the peak point around 2.727mm at 1.1706s. The second peak point occurred at 1.7712s where the rear wheel hit the bump. It is around 1.402mm heaved from the centre of gravity. Both the simulation graph shows that their heave position had a same pattern of length. They were being fully damped at almost the same time.

Pitching Performance

Graph 4.12 shows the pitching performance for the *Tramcar* and *Proton Waja 1.6* in 8 seconds simulation. Both of the graph indicated in much similarity started at 1s. The first negative slope shows that the vehicle pitched in the anti-clockwise direction. *Tramcar* shows the maximum pitch rate at 1.0358s about -0.11421rad/s . After the peak point, the curve was move to the positive value at 1.1001s about 0.036279rad/s and reached to 0.052034rad/s at 1.2040s. After that, the pitching motion is slowly damped before the rear wheel hit the bump. The curve was reach to the maximum positive value when the rear wheel hit the bump. The positive slope from the graph means that the *Tramcar* pitched in the clockwise direction. The *Tramcar* reached the maximum pitch rate at 1.5448s about 0.12485rad/s . The graph after that was almost the same with the performance for front wheel but in the negative value. All the pitching motion was being fully damped after 4s.

Meanwhile the fluctuation pattern was almost the same where the *Proton Waja 1.6* curve is a bit lower than the *Tramcar* curve. *Proton Waja 1.6* reached its maximum pitch rate at 1.0359s about -0.1002rad/s when the front wheel hit the bump and then reached the maximum value about 0.082056rad/s at 1.5327s after the rear wheels hit the bump.

Rolling Performance

Graph 4.13 shows the rolling performance for the *Tramcar* and *Proton Waja 1.6* for a period of 8 seconds simulation. Both of the cars set to hit the bump at 1 second. The first positive slope shows that the vehicle will roll in the clockwise direction. As for the *Tramcar*, the roll rate reached the maximum value at 1.0386s i.e. about 0.2038rad/s , which equals to $11.6769^\circ/\text{s}$. This happened when the car hit the bump and subsequently roll in the clockwise direction. It goes back to zero when it rode on the bump again. The roll rate then reached a negative value nearly i.e. -0.2320rad/s at 1.0871s. This occur when the front wheel slip down from the bump. The rolling effect then damped by the absorber slowly until it reached a more steady state at 1.5s before the rear wheel step on the bump. The graph then continued with the effect by the rear wheel when it step on the bump 0.5s after the front wheel. The almost same orientation of behaviour as the front wheel happened on the rear wheel step up and down. The roll rate reached the maximum at 1.5322s about 0.2234rad/s which equal to $12.7999^\circ/\text{s}$ for rear wheel. The rolling effect then damped by the absorber slowly as the front wheel until it reached a more steady state at 2 s.

For *Proton Waja 1.6*, the roll rate reached the first maximum at 1.0370s about 0.1527rad/s which equal to $8.7473^\circ/\text{s}$ while the negative value nearly -0.1399rad/s at 1.0857s for front wheel. The rolling effect then damped by the absorber slowly until it reached a more steady state at 1.5s before the rear wheel step on the bump. The graph then continued with the effect by the rear wheel when it step on the bump 0.5s after the front wheel. The almost same orientation of behaviour as the front wheel happened on the rear wheel step

up and down like the *Tramcar*. The roll rate reached the maximum at 1.5319s about 0.1505rad/s, which equals to 8.6230°/s for rear wheel. The rolling effect then damped by the absorber slowly as the front wheel until it reached a more steady state at 2 s.

Comparison Performance in Different Stiffness

The following graphs are the comparison for *Tramcar* suspension performance in different stiffness. Graph 4.14 shows the comparison in bouncing performance for different stiffness; graph 4.15 shows the comparison in pitching performance for different stiffness and graph 4.16 shows the comparison in rolling performance for different stiffness. From the graph, it is clearly indicated that the heave position, pitch rate and roll rate strongly dependent on the suspension stiffness when the other inputs are fix. If the softer suspension use on the *Tramcar*, then the heave position, pitch rate and roll rate is a bit higher if compared with the harder suspension. For example, in bouncing performance simulation, we can know that the heave position at 1.68s for 15600N/m stiffness is 4.18mm, for 25600N/m stiffness is 2.461mm and for 35600N/m stiffness is 1.074mm. The harder suspension gives the highest value of heave position. One more example we can look for the influenced of different stiffness at the rolling performance. If the 16500N/m stiffness use on the *Tramcar*, then the maximum roll rate is 0.23504rad/s while the 36500N/m stiffness give only the maximum roll rate at 0.20763rad/s. The same trend of results will be obtained when the pitching performance is examined for the *Tramcar* in different suspension stiffness.

CHAPTER 6

RETROFITTING OF CNG CONVERSION KIT

6.1 Why is the Need for Retrofitting?

This vehicle is not only to serve its purpose but also to showcase the ability of ADC in adapting new and relevant technologies pertaining to automotive engineering and able to demonstrate their applications in the creation of human wealth. With this in mind having to develop the vehicle is not enough but also to incorporate added value from the perspective of able to demonstrate its capability to use non conventional fuel.

In its early effort CNG in tandem with gasoline will be used. With the successful retrofitting of the tramcar with a commercially viable conversion kit, it is hope that this initiative can be expended to include hybrid and all-electric powertrain in the future.

6.2 CNG Conversion Vehicle Requirements

Suggested engine modifications are needed to assure engine reliability, optimized power, fuel consumption and emissions that include optimizing compression ratio, valve lift, valve timing, exhaust system and intake manifold. Special attention goes to the engine cooling, lubrication and the potential issue of excessive oil consumption. A properly modified and tuned engine can make the same power as the base engine.

Generally for gasoline conversion it calls for:

- i) improve cooling system
- ii) the need for engine oil cooler
- iii) the need for new valve seats
- iv) increase compression ratio

However, the key to the successful use of gaseous fuel is a sophisticated engine controller unit (ECU), i.e. the electronic engine management system which enables gasoline engines to operate on clean-burning CNG, LPG or Hydrogen.

ECU duty is to sense engine parameters in real time and instantly adjust to deliver the correct amount of fuel and the correct ignition timing. The system results in optimal engine performance, while always operating at the lowest emissions. The system and components can be installed in new vehicles, or retrofitted in existing fleets.

6.2.1 Bi-fuel System and Dual-fuel System

Bi-fuel systems use only one fuel at a time; they are particularly advantageous when alternative-fuel refueling stations are not always readily available. A switching system is added as part of the conversion so that the driver can switch from one fuel to the other.

Dual-fuel systems, on the other hand, run on a combination of an alternative fuel and diesel; they inject both fuels into the combustion chamber at the same time. Dual-fuel systems are used mostly in heavy-duty diesel engines, while bi-fuel systems are usually used in passenger cars or light- and medium-duty trucks.

Dedicated conversion systems run on only one fuel. These systems generally provide reduced emissions and better performance if they are tuned to optimize their operations on only one fuel, and they have no evaporative emissions because they use no gasoline. There are many types of pure CNG system vehicle in the market today and have been used quite successfully in many other countries such as Canada, Italy, New Zealand, India and the far east.

6.2.2 Optimize System

An optimize system is synonymous with a closed-loop system. A closed-loop system uses a feedback system to monitor and adjust engine performance continuously. An oxygen sensor in the exhaust system monitors the fuel/air mixture to the engine and compensates for changes, thereby optimizing emissions performance.

An open-loop system, in which carburetor is throttle-regulated does not provide optimum emission performance. This is because it does not compensate for changes in the fuel/air mixture. Such systems are generally used on older model vehicles that do not have computerized fuel control systems.

6.2.3 CNG Operation System

In CNG vehicles, the fuel is stored at a pressure range of 160 to 250 bar (2400-3600 psi) in one or more cylinders located under the body or in the trunk of the vehicle. The filling valve is placed near the tank or in the front grille. When the CNG leaves the cylinder tank, it travels through high-pressure fuel lines into one or more pressure regulators, where it is reduced to low atmospheric pressure prior entering the engine intake.

Unlike gasoline, which must be vaporized before ignition, CNG is already gaseous when it enters the combustion chamber. When the intake valve opens, the gas enters the combustion chamber, where it is ignited to power the vehicle.

6.2.4 Application of CNG in Vehicles

Natural gas is compressed to a high pressure and is stored on board the vehicle in cylinders installed in the rear, undercarriage, or atop the vehicle. When natural gas is required by the engine, it leaves the cylinders traveling through a high pressure pipe to a high pressure regulator (most often located in the engine compartment) where the pressure is reduced.

In carbureted engines, the fuel enters the carburetor (through a special fuel/air mixer) at close to atmospheric pressure through a specially designed natural gas mixer where it is properly mixed with air.

In fuel injected vehicles the natural gas enters the injectors at relatively low pressure (up to about 6 bars). In either case, natural gas then flows into the engine's combustion chamber and is ignited by spark, to create the power required to drive the vehicle. Special solenoid valves prevent the gas from entering the engine when it is shut off.

In bi-fuel vehicles, a fuel selector switch controls the flow of either natural gas or petrol. (In some systems the switchover is done automatically when the vehicle is out of natural gas). A fuel gauge is provided on the dashboard or it is incorporated into the normal fuel gauge so the driver can determine the amount of natural gas remaining in the fuel tanks.

The types of conversion kits are shown in Figure 6.1 and 6.2 respectively.

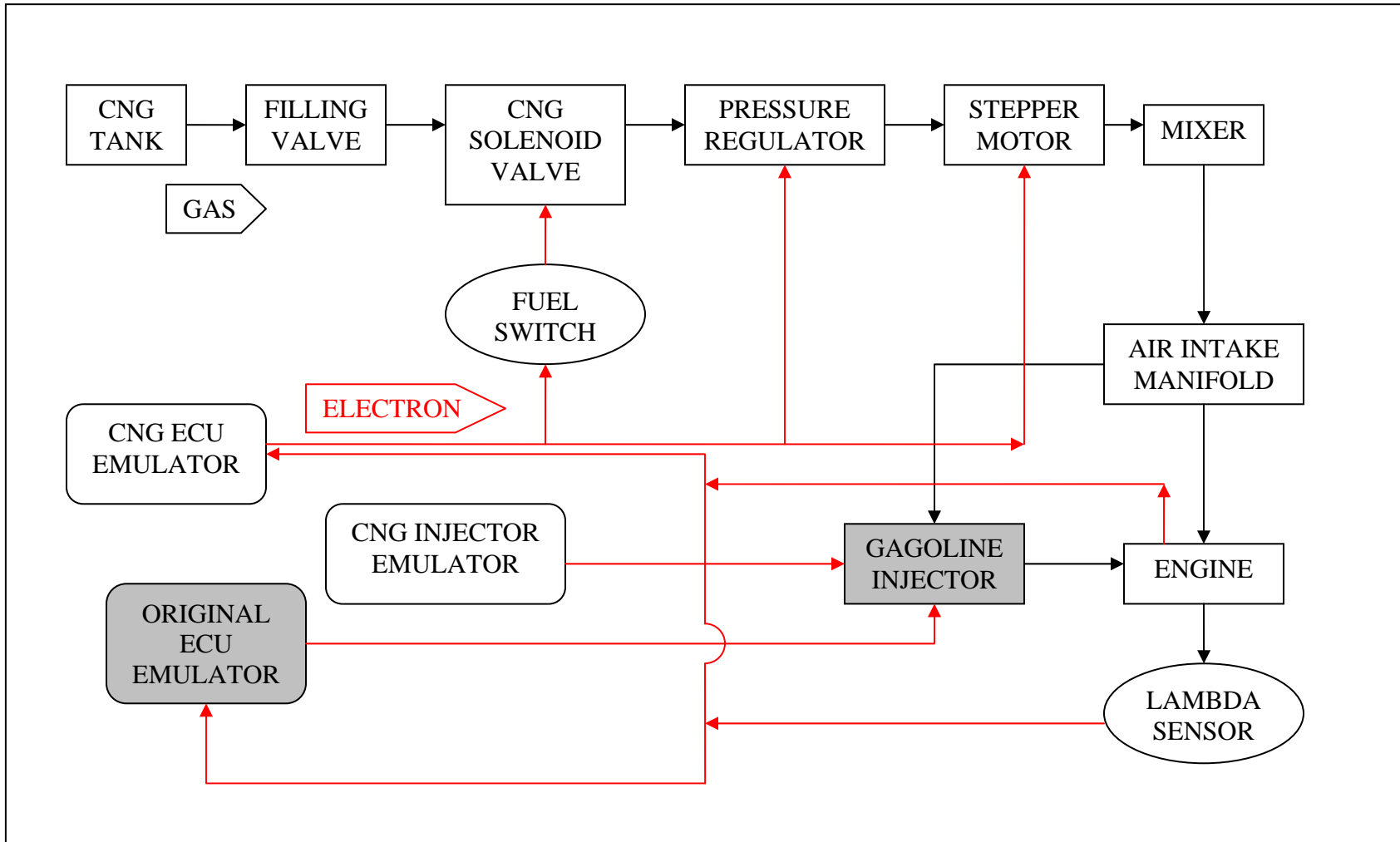


Figure 6.1: Catalyst System

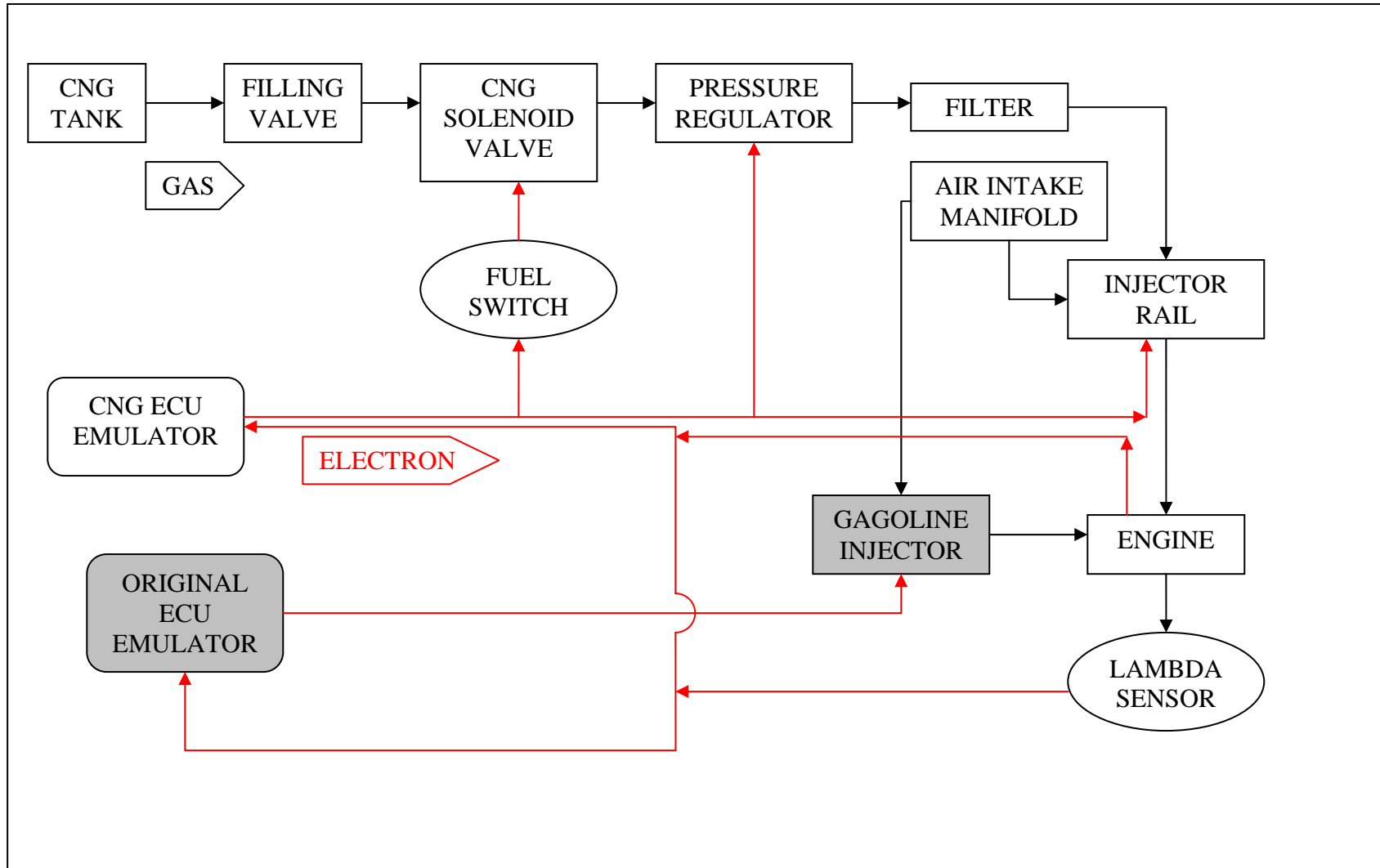


Figure 6.2: Sequential System

6.2.5 Sequential System (Multipoint Sequential Injection System)

One of the new technologies in natural gas vehicle, the multipoint sequential injection system, represents a new generation of bi-fuel CNG conversion system. The principle used by the CNG ECU to calculate the injection timing applied to the CNG injectors, is based on the acquisition of the gasoline injection timing by CNG ECU during CNG mode.

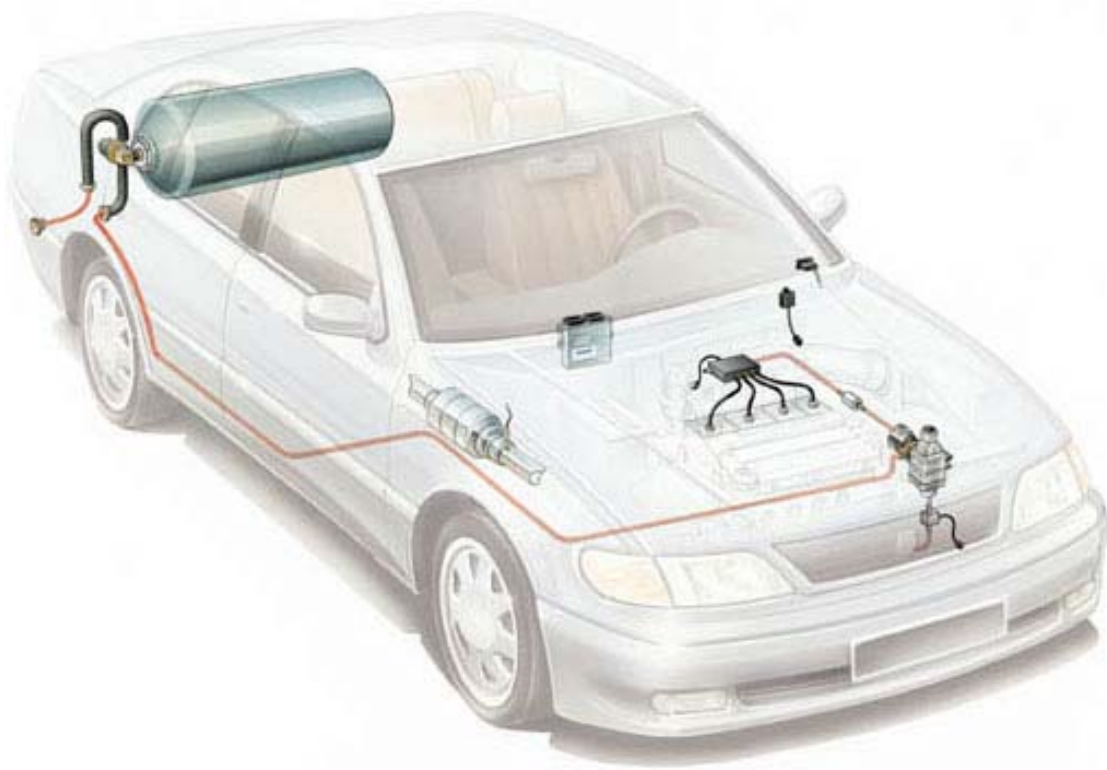


Figure 6.3: Sequential system illustrated

The engine management is, therefore, mainly left to the gasoline ECU whilst the CNG control unit translates gasoline actuations into an appropriate control for CNG injectors. In order to maintain the coherence with the gasoline system, the CNG ECU drives CNG injectors in the same sequence as gasoline injectors. Roughly, the CNG ECU converts an amount of energy that should be actuated

by the gasoline into an equivalent amount of energy that CNG has to release in order to compensate the differences between two fuels. This system can use different types of injectors according to the specifications of the application. In addition, it is minimally invasive with respect to the original gasoline engine management system. The CNG ECU is able to be easily integrated with the main engine management functions as mixture control, cut off, EGR, purge canister, etc and auxiliaries engine management functions as air-conditioning, power-steering, electric loads, etc.. The CNG ECU is able to calculate CNG injection timing using specific information as CNG injector rail pressure, CNG temperature, engine coolant temperature, and engine RPM and battery voltage, in addition to the inputs of the gasoline ECU [10].

6.2.6 Catalyst System (Natural Gas System with TN 1 Step Motor regulator and Lambda Control System/2)

Natural gas flows from the tank through the special valve and is conveyed to the engine compartment through high-pressure piping that is also connected to the refueling system.

The TN1/B step-motor reducer is installed in the engine compartment where the pressure of the incoming natural gas is reduced from 220 bars to the engine supply pressure. From the reducer, the natural gas flows to the air/fuel mixer (installed on the suction piping), which mixes the gas flow in proportion to engine demand represented by the vacuum generated in the mixing devices. The high-pressure solenoid valve allows the gas to flow only while the engine is running and with the switch in the gas position.

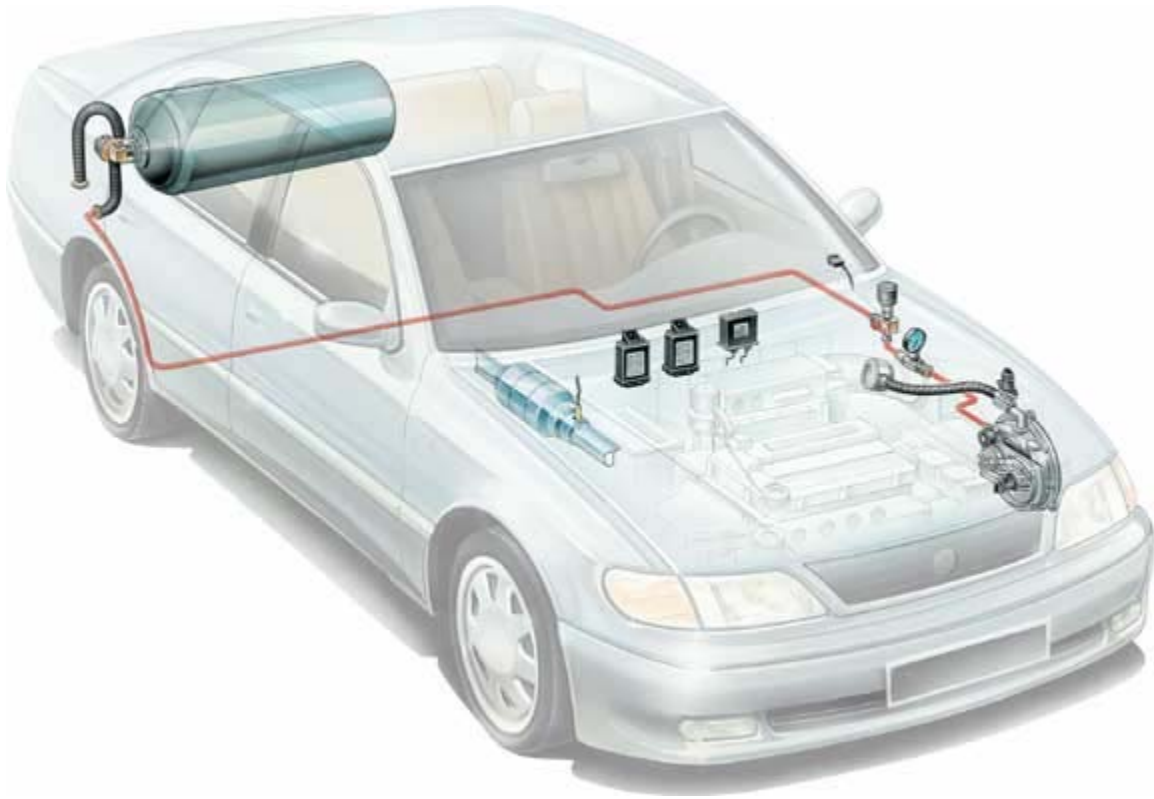


Figure 6.4: Catalyst System illustration

Lambda Control System/2 is a self-adjusting electronic system: no manual adjustments are required and it can adapt automatically to the different environmental and vehicle use conditions, ensuring efficient carburetion in terms of driving style, consumption and emissions. The Lambda Control System/2 computer electronically manages the gas flow adjustment, allowing the Lambda factor to reach the required value at all engine rpm thanks to 2 electromechanical actuators. One actuator is installed between the reducer and the mixer and doses the quantity of gas at medium and high rpm (maximum), while the second actuator of the pressure reducer adjusts the optimum gas flow for engine operation at idle (minimum), keeping it stable even when accessories such as an air conditioner or power steering system are operational.

Among its other functions, the LCS/2 computer can be used to start always with petrol, with automatic switchover to gas and, through the switch/indicator, allows the user, at any time, to select the fuel required, displaying the natural gas level in the tank. During gas operation, the electronic emulator (or the injector exclusion wiring) cuts off the petrol flow to the engine; while during petrol operation the natural gas flow to the engine is cut off by the high-pressure solenoid valve [10].

6.2.7 Carburetor System

The schematic arrangement of a simple gas assisted system is the carburetor system. This is shown in Figure 6.5 below.

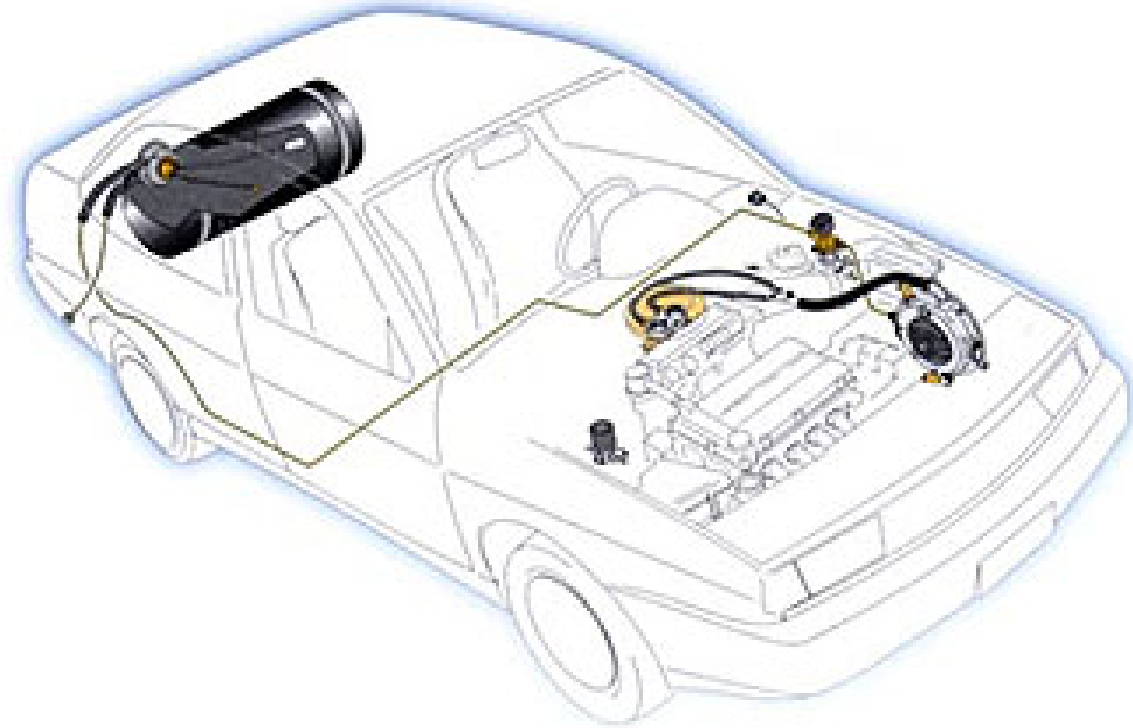


Figure 6.5: Carburetor system linking pressurized tank to engine

An example a CNG Minikit for retrofitting in a carburetor car is shown in Figure 6.6. This is suitable for use in engine from 20 to 90 kW.



Figure 6.6: Conversions kit for carburetor car

The above system includes the following main components:

- CNG electronic reducer RME090
- AMP super seal harness for pressure reducer
- petrol solenoid valve
- fuel switch with level indicator M198 C
- pressure gauge complete with electronic pick-up for level indication
- reducer installation bracket
- accessory package for minikit installation

6.2.8 Economics of Vehicle Conversion to CNG

Converting a vehicle to CNG involves installing a natural gas fuel system and storage tanks. Dual fuel systems will retain the original conventional fuel system. On a dedicated NGV, the original conventional fuel system can be removed. Generally, dedicated NGV demonstrate better vehicle performance and lower emissions than dual-fuel NGV because the fuel system can be set to take advantage of the characteristics of only one fuel.

Prior to 1985, most gasoline vehicles had carbureted engines and NGV conversion systems were open-loop type - all controls are pre-set with no feed back and re-adjustment of air/fuel ratios, etc. Consequently, first generation and open-loop conversion systems do not provide a mechanism to allow the conversion system to adjust for optimum engine and emissions performance. However, with the advent of fuel-injected engines, computerized electronic engine and emissions controls allow adjustment of the air/fuel ratio and spark timing (on spark-ignition engines) to optimize engine and emissions performance. Monitoring and adjusting engine and emissions performance by computerized controls is carried out by the closed-loop feed back system for optimum engine and emissions performance [10].

The costs to convert a vehicle to operate on natural gas vary and depend on several factors such as the followings:

- A. First generation system
- B. Open-loop or closed-loop
- C. The type of vehicle to be converted and the ease of installation
- D. The quantity of on-board fuel storage desired
- E. The type of on-board fuel storage tanks selected
- F. Labor rates for conversion

6.3 Retrofitting of the Conversion Kit

The catalyst conversion system selected for the Tramcar can best be illustrated in the following Figure 6.7.

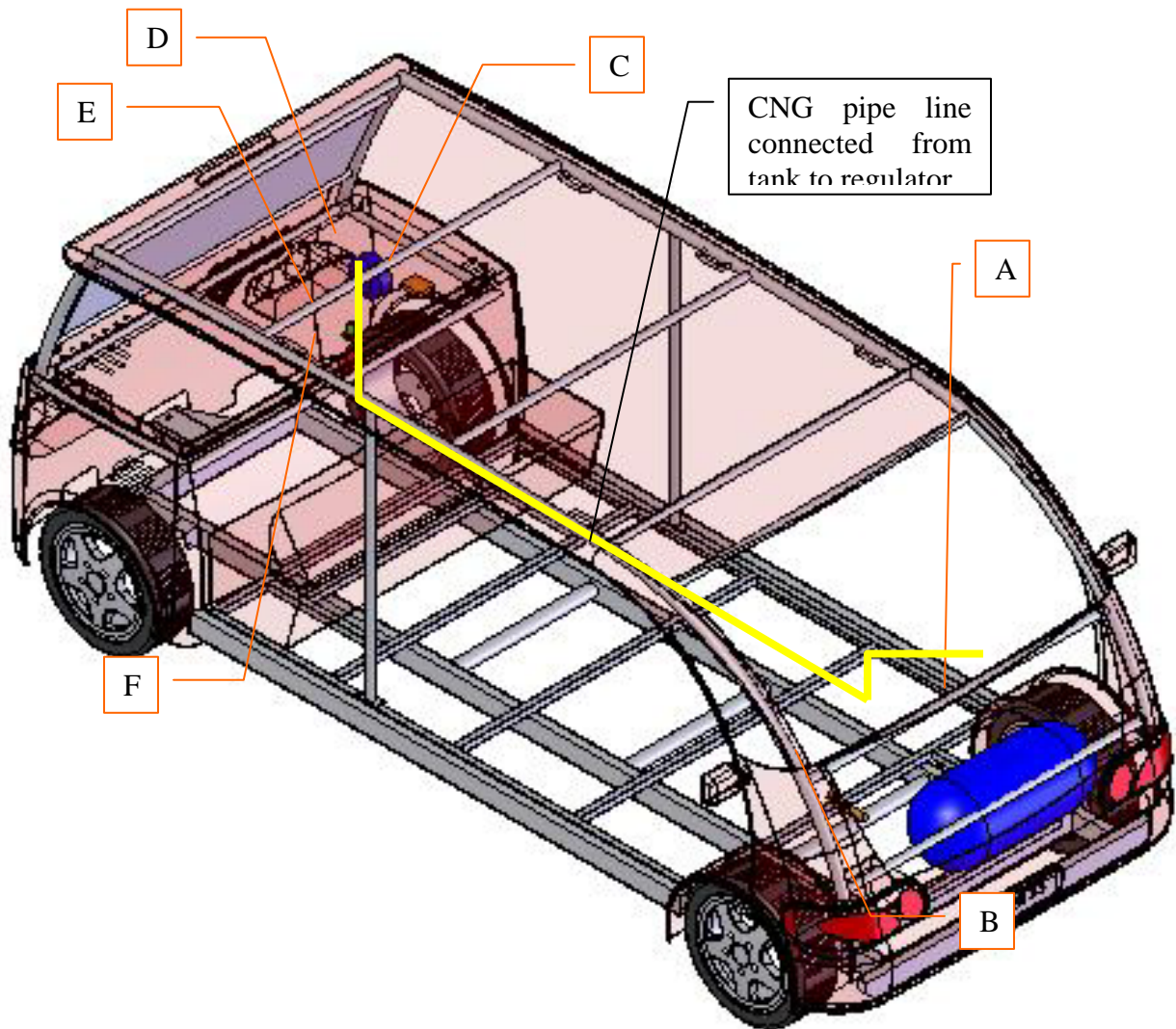


Figure 6.7: Schematic illustration about the Catalyst conversion system

The items labeled in the Figure are:

- A** - CNG tank
- B** - Filling valve
- C** - CNG ECU
- D** - Regulator
- E** - Stepper motor
- F** - Mixer

6.3.1 CNG Tank

The tank used is similar to the one shown here. It has a volume of 55 liter with a massive weight of 80 kg.



Figure 6.8: CNG steel tanks



Figure 6.9: Location of CNG tank in the front compartment the *Tramcar*

6.3.2 Filling Valve



CNG
cut-off
valve

Figure 6.10: Filling valve location

Filling valve is a quick-coupling valve that allows fast charging of the gas during refilling. Figure 6.10 shows its close feature while Figure 6.11 shows how gas is being charged.



Figure 6.11: Charging of the gaseous fuel into the tank using the filling valve

6.3.3 CNG Cut-off Valves

In the event of emergency the gas is required to be isolated from the engine and its sub-system. In a CNG conversion kit an isolated valve, better known as the cut-off valve is incorporated in the system. There are two types of the cut-off valve used - a manual-operated and automatic. Figure 6.12 and 6.13 illustrates its physical features.



Figure 6.12: CNG cut-off valve 200 Bar, completed with wiring 500 mm attached to filling valve.



Figure 6.13: The emergency manual shut-off valve at the cylinder head

6.3.4 High Pressure Gas Piping

A high pressure pipework is required in dealing with pressurized gas. This is a steel pipe with a typical external diameter of 8 mm.

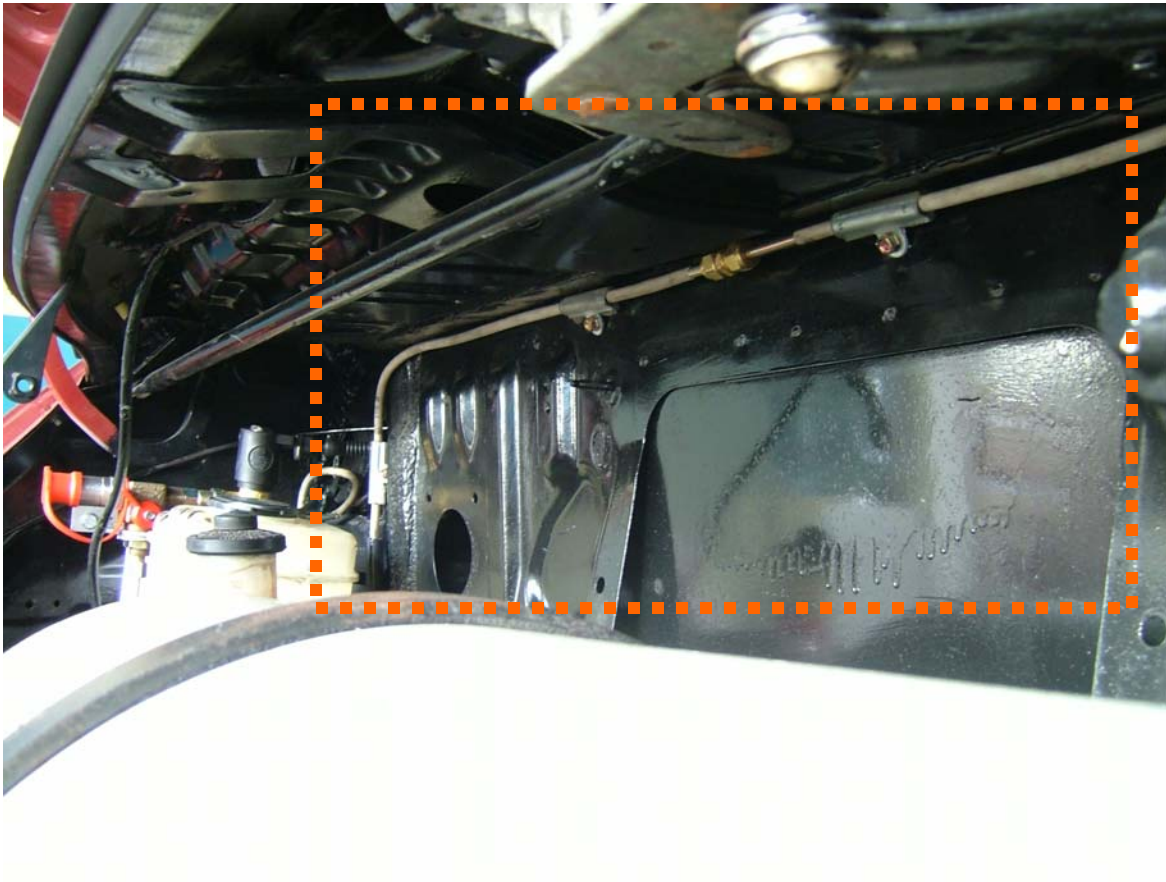


Figure 6.14: The gas pipe from CNG tank to the filling valve



The lowest chassis framework use as conduit and support for the gas pipe.

Figure 6.15: Connection of the gas pipe from the filling valve to the regulator

6.3.5 Pressure Regulator



Figure 5.16: Lovato pressure regulator (RME090)

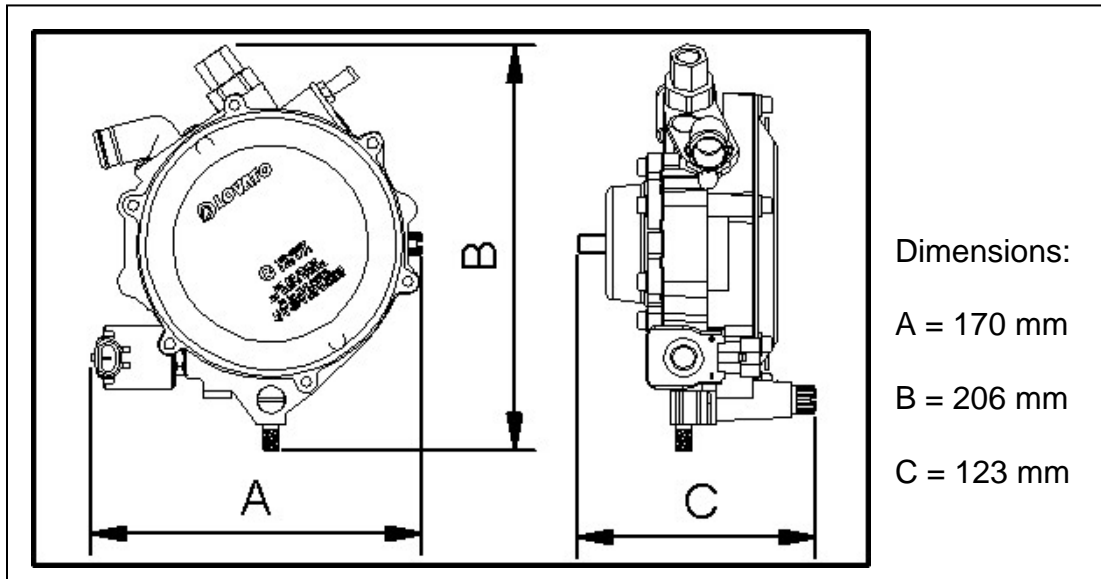


Figure 6.17: Dimension of the pressure regulator (RME090)

A CNG electronic reducer with dedicated fine idle tuning (for engine output of 20 to 90 kW) includes the following main components:

- 3-stage reducer with positive pressure idle device
- Vehicular application (suitable for vehicles with catalytic converter, fuel injection)
- Type of fluid: CNG (Compressed natural gas)
- Casing: GDALSI 13 UNI 5079
- Engine cooling circuit liquid heating
- Inlet pressure: 220 bar
- First stage adjustment pressure: 4 bar
- Second stage adjustment pressure: 1.5 bar
- Power supply: 12 V dc
- High-pressure solenoid valve coil power: 20 W
- Linear electromechanically actuator power: 2 W

The complete arrangement is shown in Figure 6.18.

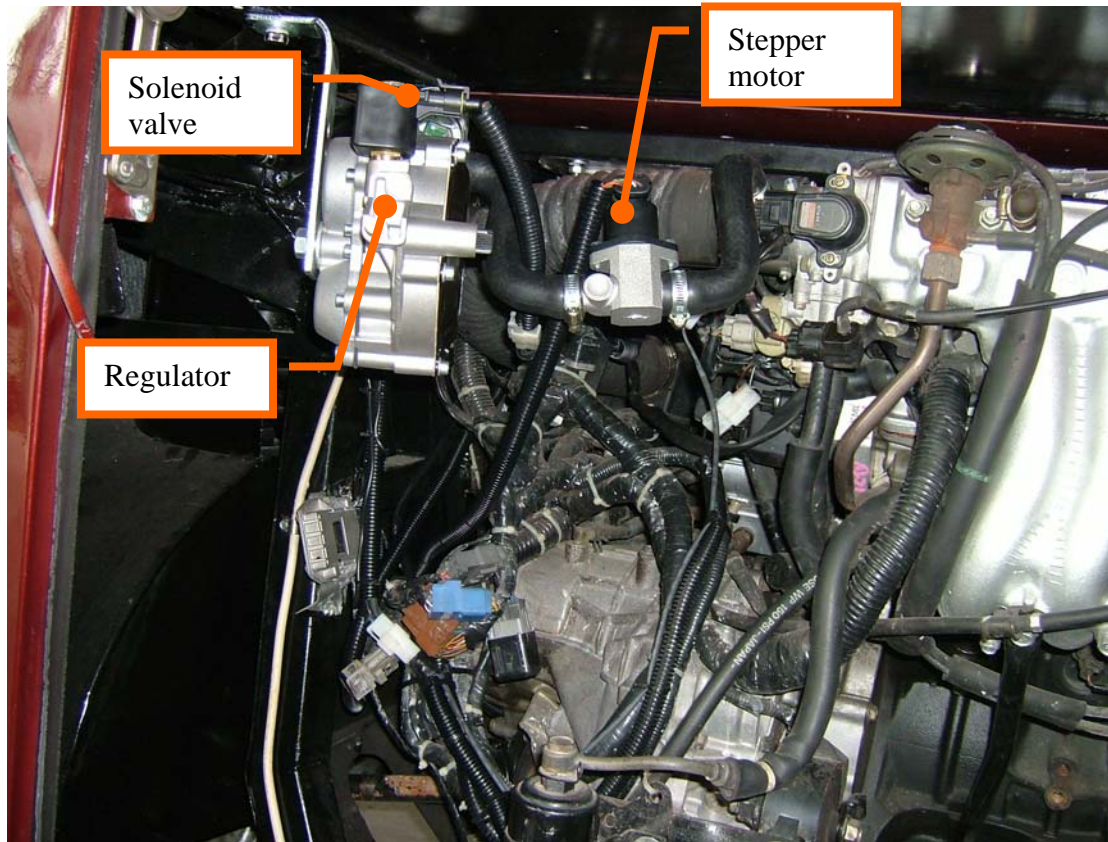


Figure 6.18: The regulator is installed in the engine compartment at the rear of *Tramcar*

The solenoid valve placed on the pressure regulator is switched on when the threshold of engine coolant temperature is reached. The system will switch to CNG mode when all the other conditions such as minimum RPM threshold and acceleration are reached.

6.3.6 Fuel Switch Injection

A fuel switch injection system allows the vehicle operator to switch fuel from gasoline to CNG and vice versa with ease. At a push of a button fuel switching is effortless and of fast response.



Figure 6.19: Fuel switch injection THERMOTRONIC M 198I with fuel level indicator, level indication is given by means of 4 green leds and 1 red led for reserve



Figure 6.20: Location of the fuel switches that is convenience for the driver to observe the running system.

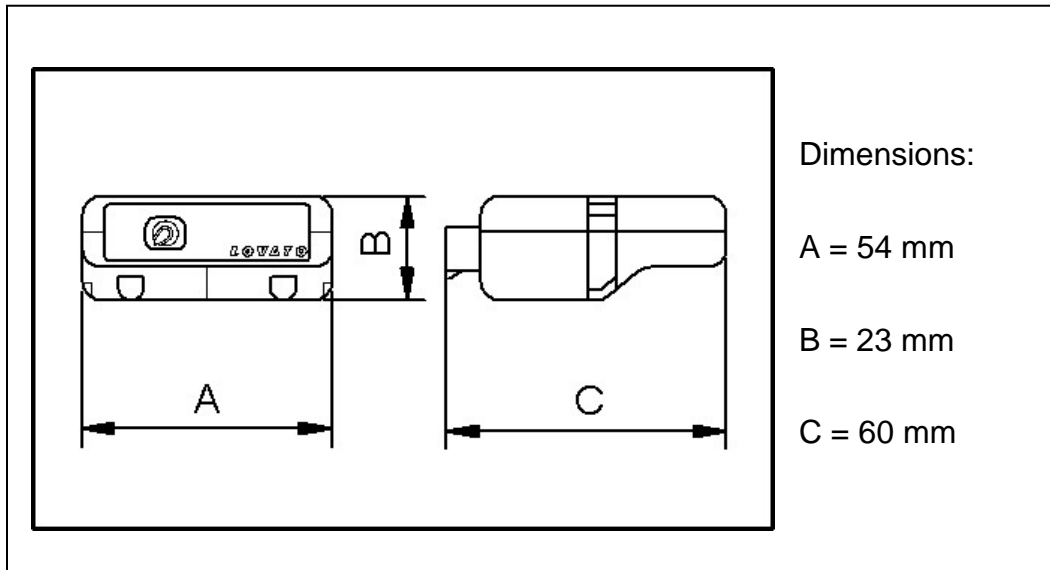


Figure 6.21: Dimension of the fuel switch

6.3.7 Gas Mixer

A gas mixer is a device that meters the proportionate amount of gas into the engine with the flow of air via the air filter assembly. Its internal geometrical structure resembles a venturi with fine holes embedded within the circumference of the venturi constriction. As the air flows through the constriction section, it will induce the gas thus allowing the more or less constant air-gas ratio to rush into the engine intake manifold at every engine cycle.



Figure 6.16: Prototype mixer use at the air intake manifold



Figure 6.17: Installation of the mixer to the air intake manifold and the CNG supply line



Figure 6.18: Pressure gauge completed with electronic pick-up for level indicator



Figure 5.19: The pressure gauge connect to the high pressure pipe to monitor the pressure in the CNG tank

6.3.8 Injector Emulators



Figure 6.20: Emulator type 2, 5 - 5 cylinders with Europe standard harness

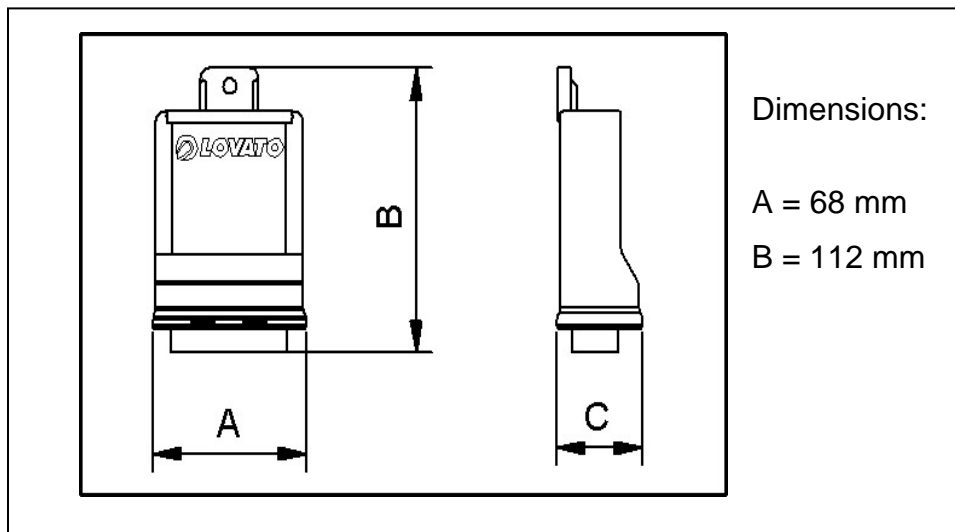


Figure 6.21: Dimension of the injector emulator

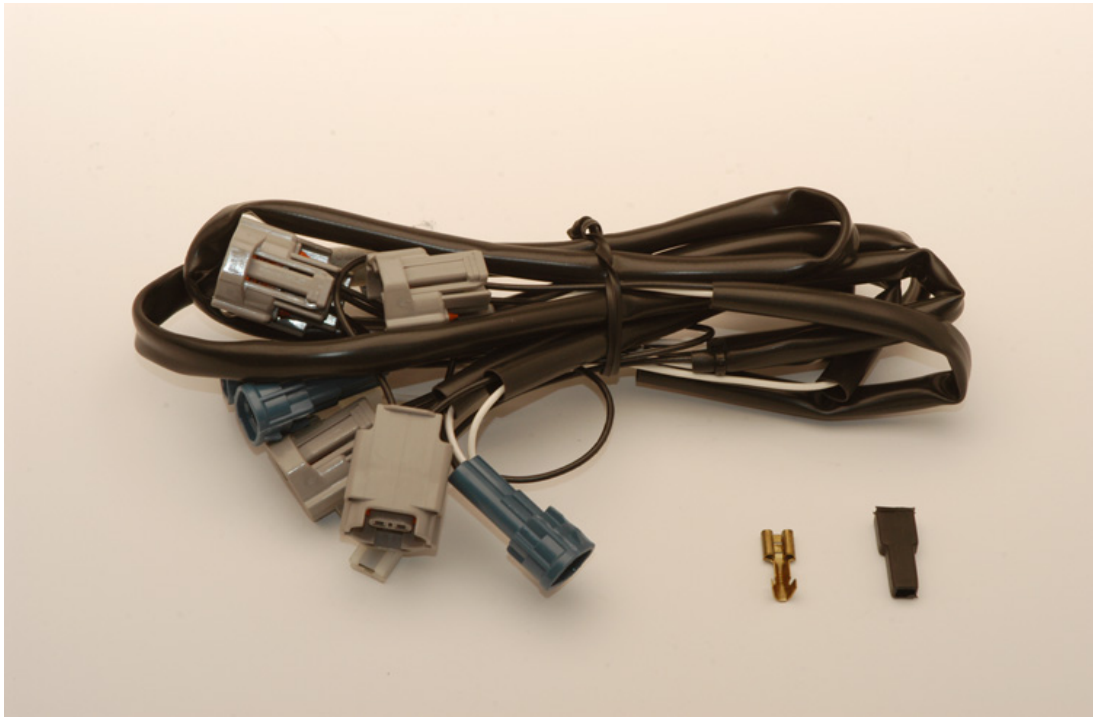


Figure 6.22: Injector cut-out Japan standard harness specified for Japanese engine

The LOVECO-PRO closed loop system is equipped with a level indicator fuel switch. It also includes the following main components:

- fuel switch MICRO LEVEL
- electronic ECU
- Flow actuator with step motor
- NTC temperature sensor
- wiring harness
- accessories package

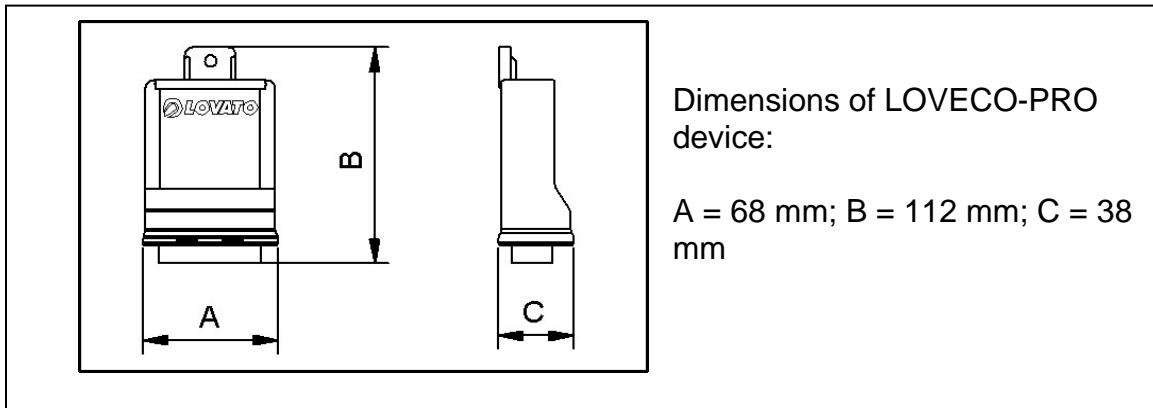


Figure 6.23: Photo and dimension of LOVECO-PRO.

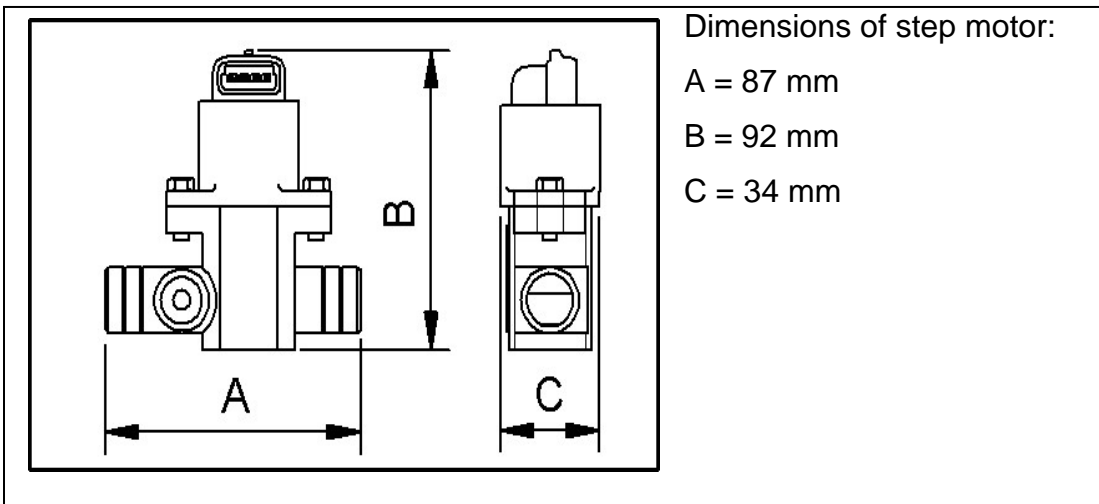


Figure 6.25: The photo of the stepper motor and its physical dimension

The gasoline injector during CNG mode is switched off with the control of injector emulator. The CNG ECU (LOVECO-PRO) starts to control the CNG system including the lambda sensor, throttle position sensor, RPM sensor, stepper motor and others relevant devices respectively.

6.4 Vehicle Test with CNG Conversion Kit

Having fitted the complete conversion kit with the assistance of the supplier, the *Tramcar* was tried extensively to assess its overall performance. It was noticed that after several trials and fine-tuning efforts, the vehicle now is fully a dual-fuel vehicle with a capability to demonstrate the gasoline-CNG operation.

CHAPTER 7

CONCLUSIONS AND RECOMMENDATIONS

7.1 Conclusions

The Tramcar was successfully designed, developed and tested for recreational purposes as part of the flagship project for ADC. To add an interesting feature to it is the incorporation of CNG conversion kit which has proven to be successful, in line with the theme of environmental-friendly people's mover within the UTM campus.

Proceeding all the analysis and computational results obtained on the *Tramcar*, the safety and comfort impart on the passengers due to its chassis and suspension system, subjected to various operating conditions were successfully identified.

The safety factor for a vehicle chassis has earlier been stressed to be beyond 2.0. The following table summarizes the safety factors for normal stress and shear stress and displacements of chassis for each of the analysis.

Table 7.1: Safety factors

	Safety factor		Displacement [mm]
	Normal stress	Shear stress	
Static analysis	2.93	3.08	4.23
Bumping analysis	2.59	2.73	4.63
Braking analysis	3.88	4.09	3.72

The maximum deformations in the three analyses have been proven to be less than 5mm. From the contour of deformation, it can be said that the maximum deformation will occur at the middle of chassis. However the deformation can be regarded as small and it can be concluded that the chassis is safe for use.

The magnitude of the chassis torsional stiffness was obtained from the slope of the graph of torsion against twisting angle. The value is 5127.5Nm/degree, which is in the range allowed for a normal saloon car i.e., 3000Nm/degree to 9000Nm/degree. As far as the torsional stiffness analysis is concern it has proven that the chassis is safe.

Also covered in the analysis was the comfort factor, which was only confined to the effect from the suspension system. Using the full car model and based on the response gain from the suspension design of *Proton Waja 1.6*, the *Tramcar* has performed badly in frequency isolation. For bouncing, pitching and rolling analysis, all the peak point in the graph for *Tramcar* were noted to be higher than the peak point for *Proton Waja 1.6*. This was due to *Tramcar's* suspension system was 'softer' than the *Proton Waja 1.6*. To support this argument, in rolling analysis, the *Tramcar* reached the maximum roll rate at 0.2234rad/s. However the *Proton Waja 1.6* reached the maximum roll rate at 0.1505rad/s. The different here is only 0.0719rad/s.

The results also indicate that both the suspension systems have almost taken the same time to damp their respective displacement. That clearly shows that the displacement absorption (for the suspension system) is almost the same with *Proton Waja 1.6*. Hence, it can be concluded that the *Tramcar* suspension performance does not differ much from *Proton Waja 1.6*.

7.2 Recommendations

Although the *Tramcar* can be classified as suitable for use, there are still some improvements to be made.

From the results of the contour of deformation analysis, the maximum stress will occur at the middle section of chassis. The maximum deformation is noted to occur at the same point. Since this is the weakest point, the chassis will most probably fail at this place. Hence, strengthening of the upper ladder frame cross bar must be made to avoid the failure occurrence. Two choices are available here, i.e. the use bigger diameter of steel bar or increase the thickness of bar.

For suspension system, the displacement is more on *Tramcar* than the reference vehicle, which is the *Proton Waja 1.6*. Here it is suggested that the *Tramcar* may consider the use of the higher suspension stiffness to mitigate the vibration level, and indirectly to increase the passengers' comfortable level. It is also suggested that to isolate the disturbance due to road irregularities, the increase the suspension damping rate must be made.

Below are some recommendations for future work with regard to safety and comfort factors: -

1. Analysis for other factor that influence the comfort level such as the position of seat, the view angle and the space for leg.
2. Design an external cover roof to protect passengers getting wet when raining.
3. The aerodynamic drag analysis.

BIBLIOGRAPHY

1. Gillespie, Thomas D. (1992). ***Fundamentals of Vehicle Dynamics***. Society of Automotive Engineers, Inc., Warrendale, Pennsylvania, USA.
2. Wild, R. (1978). ***A Practical Approach to Cab Suspension***. Society of Automotive Engineers, Warrendale, Pennsylvania, USA.
3. Brueck, Donald M. (1977). ***A Simplified Method for the Identification of Vehicle Suspension Parameters***, Society of Automotive Engineers (SAE), Warrendale, Pennsylvania, USA.
4. Ikenaga, S., Frank, L.L., Campos, J. and Leo, D. ***Active Suspension Control on Ground Vehicle Based on a Full Vehicle Model*** University of Texas, Arlington, USA.
5. Davis, L., Lewis, F.L., Scully, S. and Evans, M. ***Active Suspension Control of Ground Vehicle Heave and Pitch Motions***. University of Texas, Arlington, USA.
6. Zaid Hj. Mohd. Zin (1995). ***Pengenalan Kepada Pembuatan Kereta***. Kuala Lumpur: Dewan Bahasa dan Pustaka (DBP), Kementerian Pendidikan Malaysia.
7. Gibbs, H. G. and Richards, T. H. (1975). ***Stress, Vibration and Noise Analysis in Vehicles***, Applied Science Publication, London.
8. Fenton, John (1998). ***Handbook of Automotive Body and Systems Design***, Professional Engineering Publishing, London.
9. Howard, Geoffrey (1998). ***Chassis & Suspension Engineering***, Osprey Publication Ltd, London.
10. Campbell, Colin (1981). ***Automobile Suspensions***. London: Chapman and Hall Ltd., London, UK.
11. Bastow, Donald (1988). ***Car Suspension and Handling***, Pentech Press, London UK.
12. Reimpell, J. ***The Automotive Chassis***. Arnold Publisher.
13. L.Y. Chan, Doecke, M., Lalwani, H., H.W. Lau, T. Lau, C.C. Lee and C.C. Low. ***Design and Build of a Formula SAE Vehicle (Chassis, Shell and Instrumentation)***. Australia: Department of Mechanical Engineering, University of Adelaide, Adelaide, Australia.

14. Whitney, J.D. (1995). ***Experimental Characterize and Dynamic Simulation of a Quadra Link Independent Rear Automotive Suspension System***. University of Massachusetts, USA, M.Sc. Thesis.
15. Muhammad Hayat Bin Mohd Zamberi (2004). ***Relkabentuk Go-Kart***. Universiti Teknologi Malaysia (UTM), Final year project thesis.
16. Saiful Rahman Tarson (2003). ***Merekabentuk Cesis dan Pemilihan Roda untuk Go-Kart***. Universiti Teknologi Malaysia (UTM), Final-year project thesis.
17. Tam Wee Kong (2003). ***Study of Stress onto Car Body When Reached By Torsional and Bending Stiffness***. Universiti Teknologi Malaysia (UTM), Final-year project thesis.
18. Cheah Tat Wee (2001). ***Study and Analysis of a Passenger Car Suspension System***. Universiti Teknologi Malaysia (UTM), Final-year project thesis.
19. Kenneth J. Kelly (1998), ***The Effect of Fuels and Test Cycles on Light-Duty Vehicle Exhaust Emissions***, Ohio University Department of Mechanical Engineering.
20. Pulkrabek W.W. (1997), ***Engineering Fundamentals of the Internal Combustion Engines***. Prentice Hall International, inc.
21. www.lovatogas.com
22. www.iangv.org
23. www.angva2005.com
24. www.omnitekcorp.com
25. www.epa.gov
26. www.dieselgas.co.nz
27. www.mckenziecorp.com/dehydration.htm
28. www.brettandwolffllc.com/engines.html#Northport
29. www.baftechnologies.com/afs.htm
30. www.autogas.lv

APPENDIX A

OVERALL VEHICLE CHARACTERISTICS

Table A1: Engine characteristics

Engine type	Serial 4 Cylinder DOHC 16 Valve
Engine model	3S-FE
Displacement	1998 cc
Power density	8.71
Maximum power (net)	102.97 kW (140 PS)/6000 rpm
Maximum torque (net)	19.0 kgm (186.33 Nm)/4400 rpm
Fuel system	Electronic Fuel Injection
Fuel type	Unleaded Premium Gasoline
Compression ratio	9.5
Bore	86 mm
Stroke	86 mm

Table A2: Tramcar physical characteristics

Dimension [mm]	
Overall length	4700
Overall width	1851
Overall height	1763
Wheelbase	3417
Front track	1600
Rear track	1600
Unload ground clearance	190
Front overhang	970
Rear overhang	1090

Table A3: The vehicle estimation weight

Component	Estimated weight [kg]
Chassis	204.35
Seats and passengers	720.00
Engine	300.00
Full petrol tank	30.80
Front cover body	23.00
Rear cover body	16.30
Cover roof	69.55
Others	300.00
Vehicle curb weight	984.00
Vehicle gross weight	1664.00

Table A4: The suspension specifications

Suspension type	Independent McPherson Struts
Coil spring outer diameter	114 mm
Free length	351 mm
Fitted length	228 mm
Fitted load	5700 N
Spring constant	26.5 N/mm
Kingpin inclination	6°35' - 7°35'
Shock absorber type	Double Acting Tube
Stroke	120 mm
Damping forces (at 0.3 m/s):-	
Expansion	1030.05 N
-	353.16 N
Contraction	

APPENDIX B

RESULTS OF STATIC ANALYSES

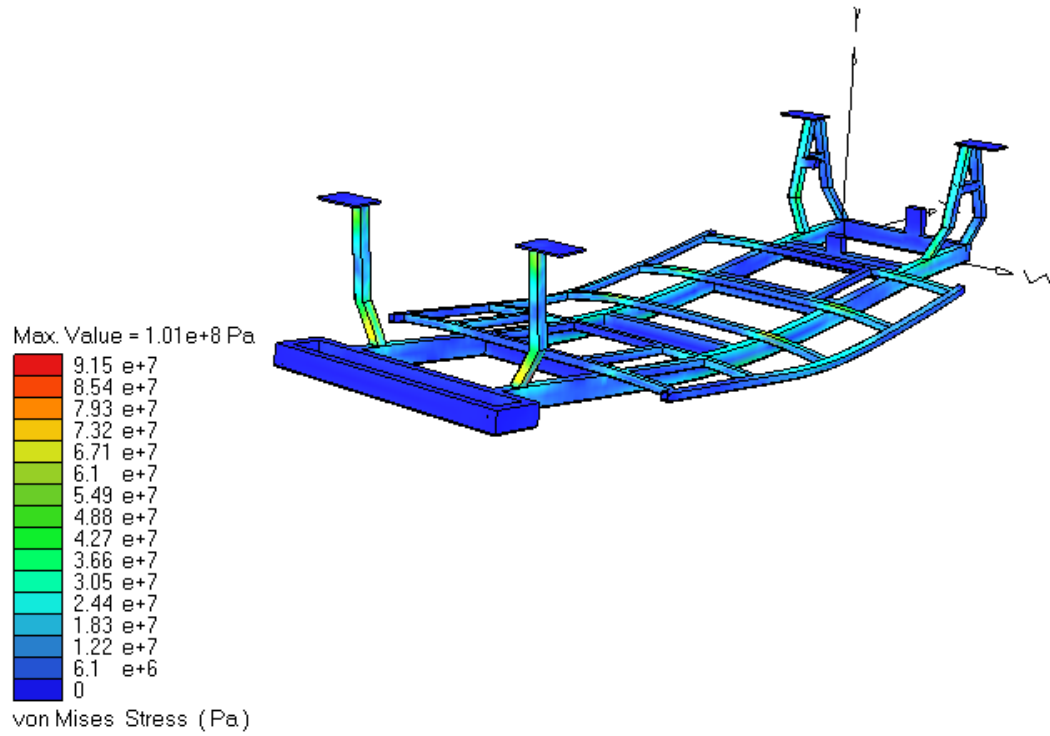


Figure B1: The contour of Von Mises stress

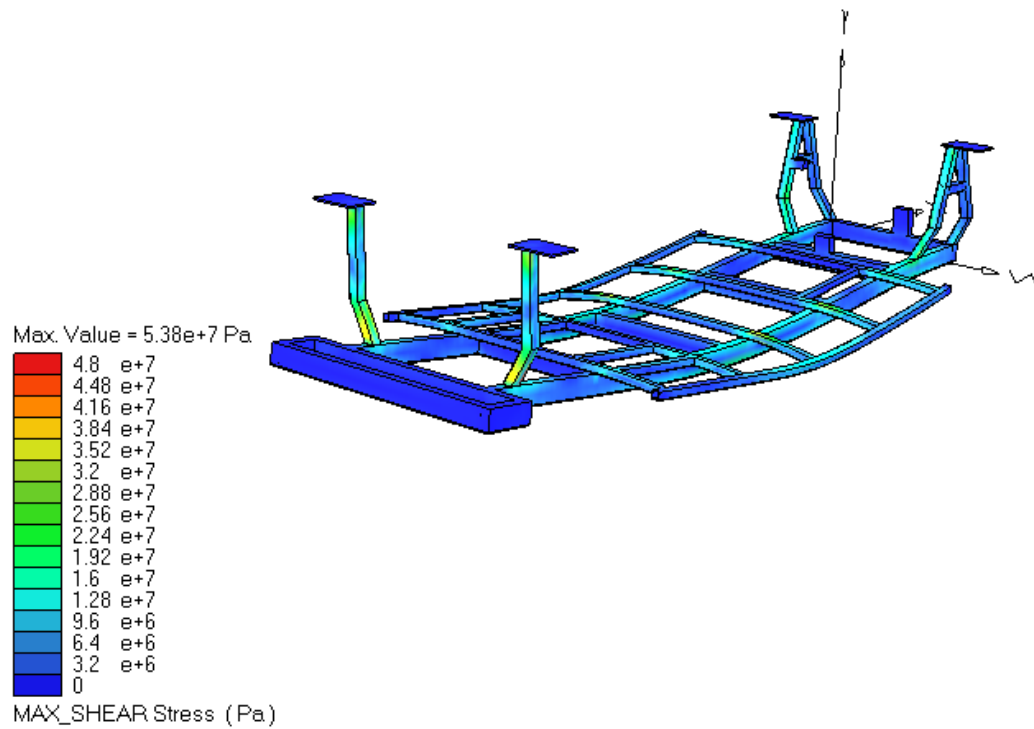


Figure B2: The contour of shear stress

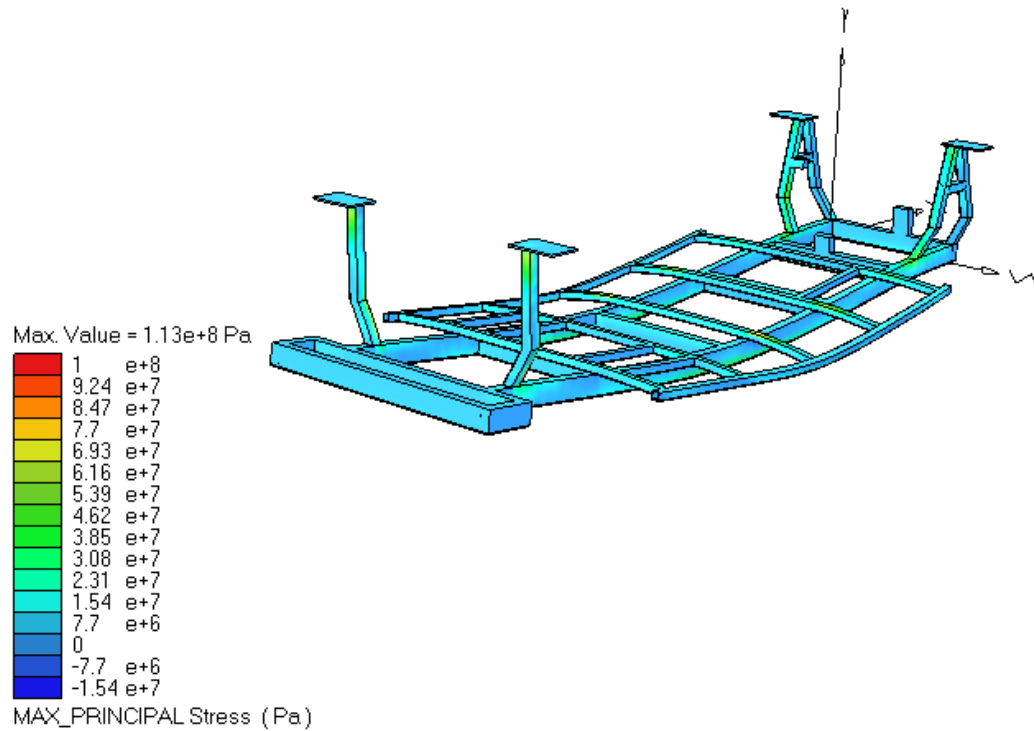


Figure B3: The contour of principal stress

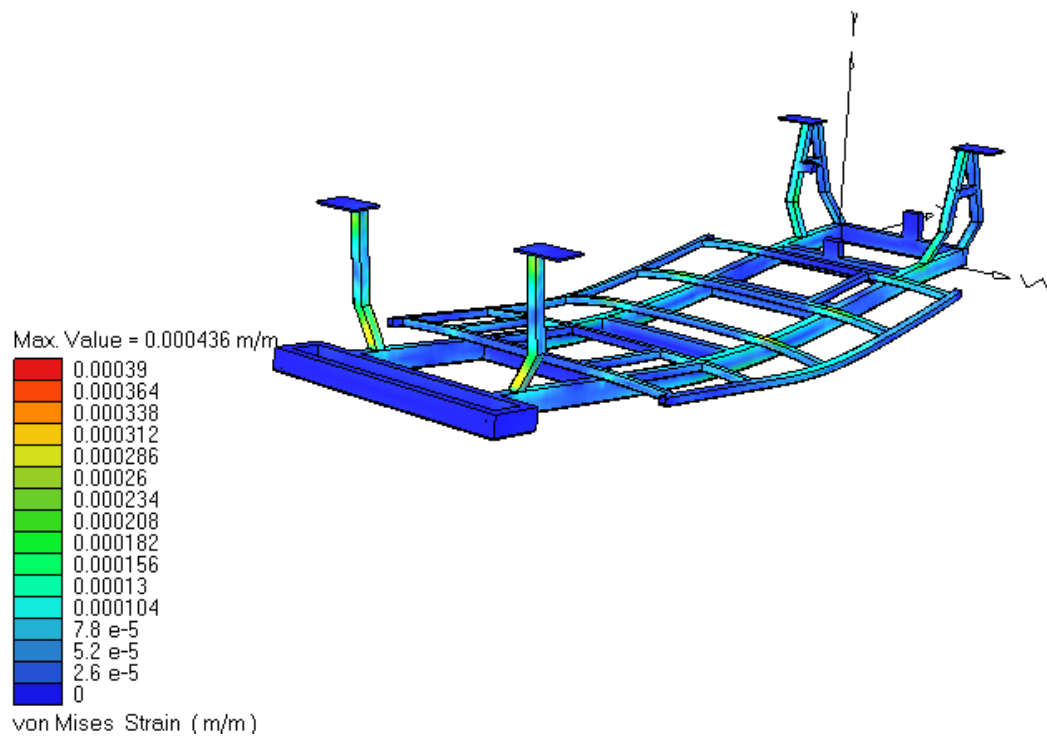


Figure B4: The contour of Von Mises strain

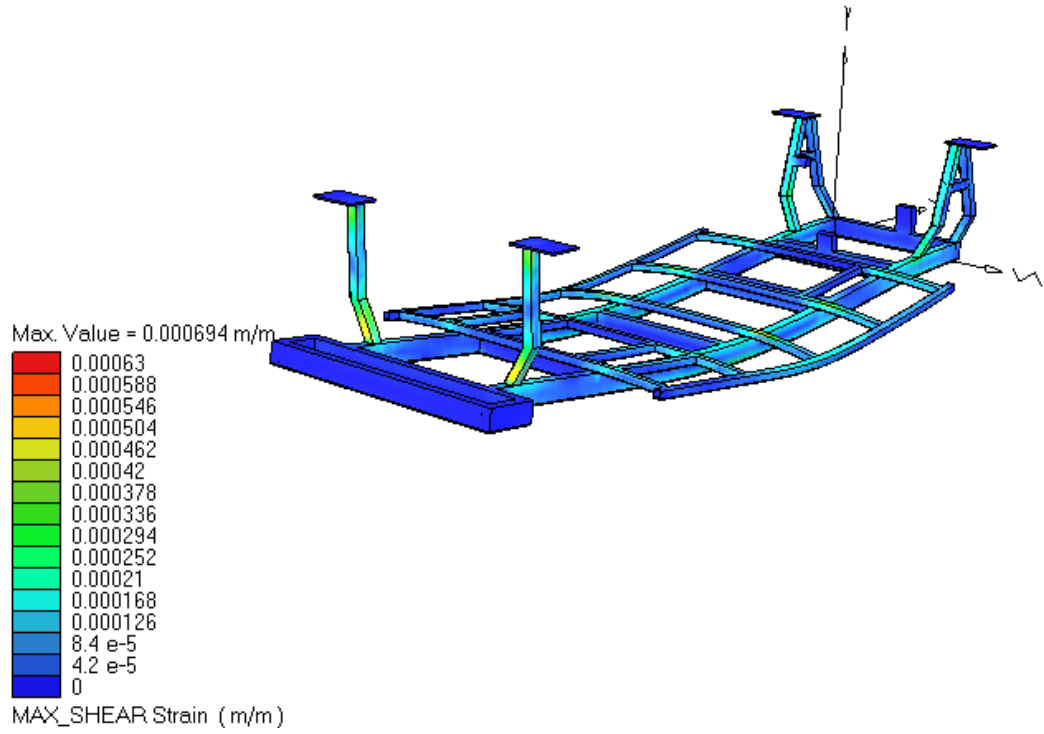


Figure B5: The contour of shear strain

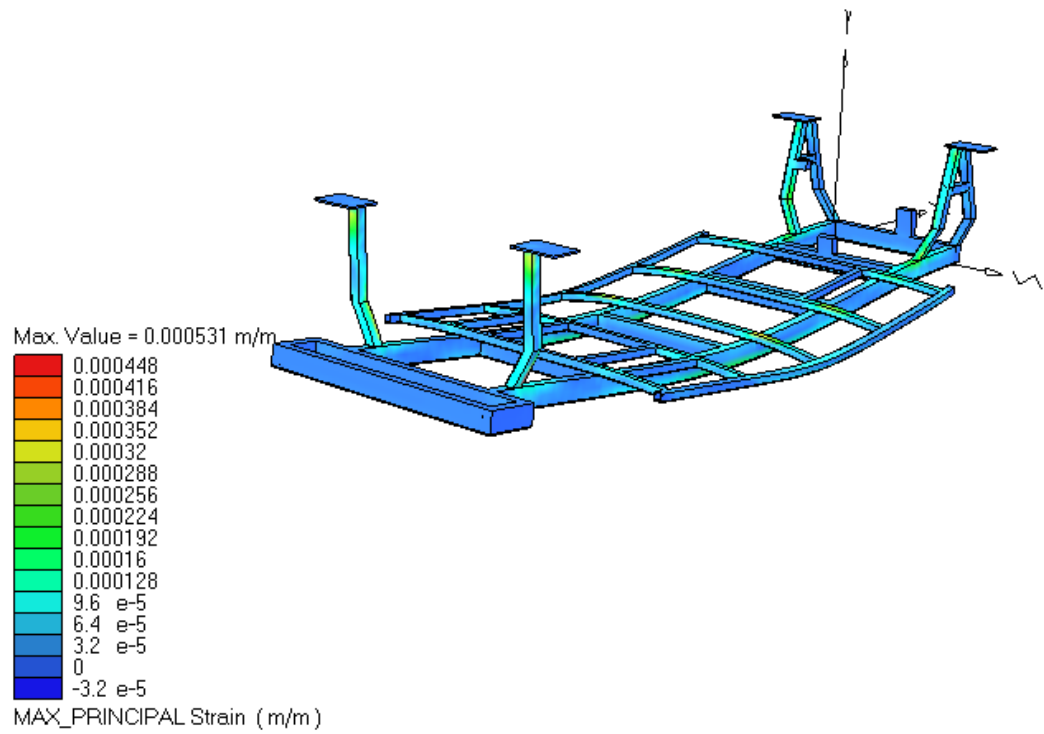


Figure B6: The contour of principal strain

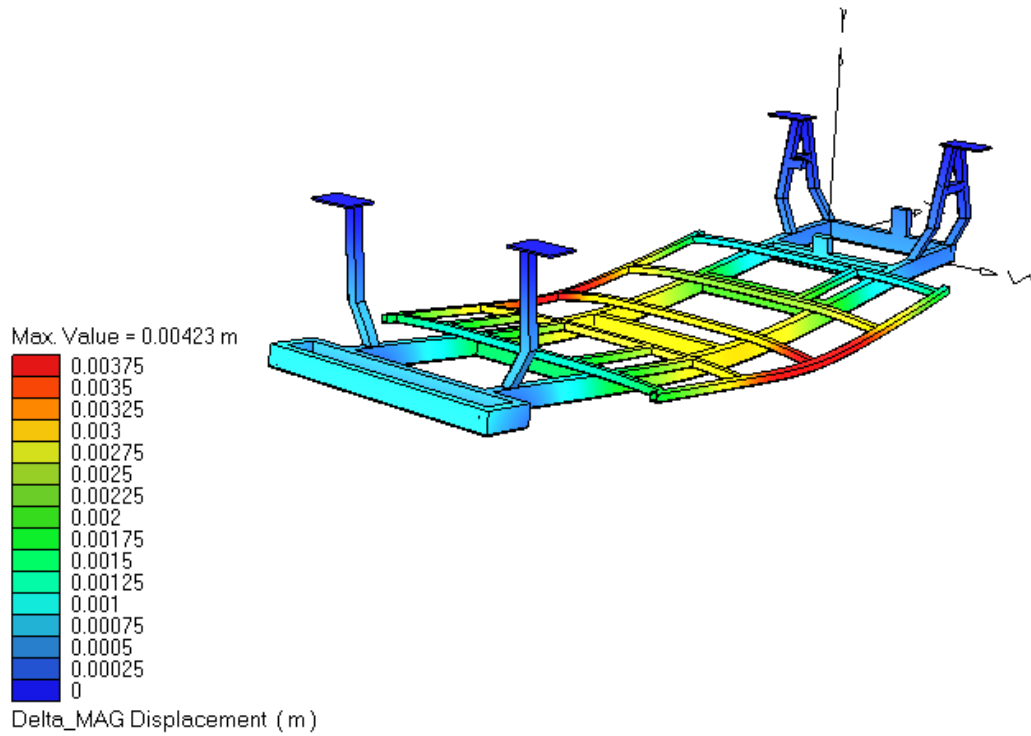


Figure B7: The contour of delta MAG displacement

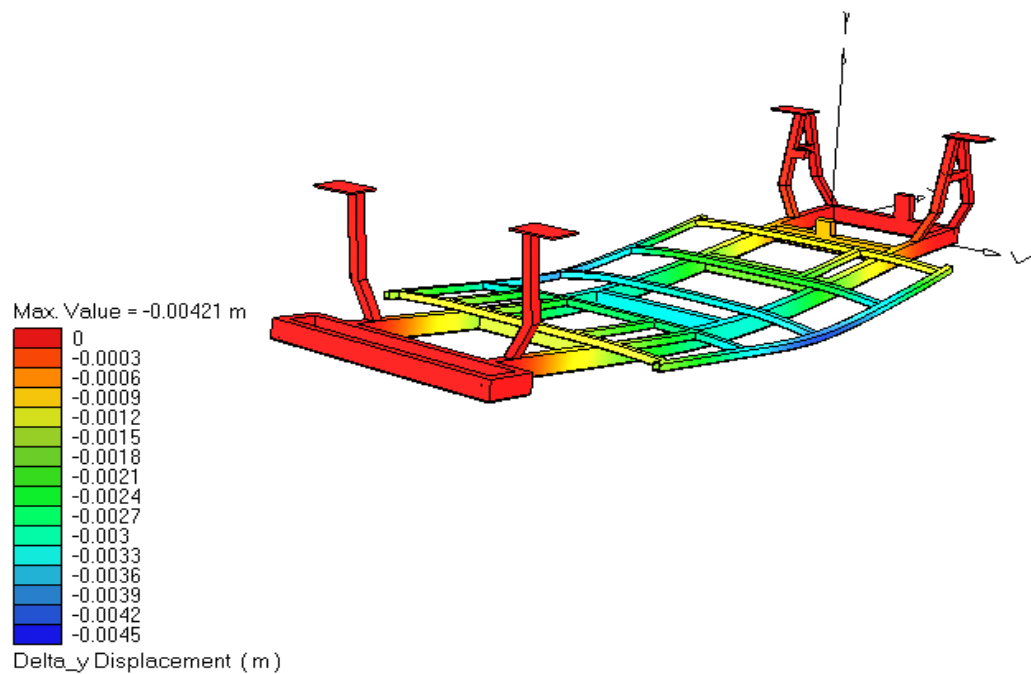


Figure B8: The contour of y-direction displacement

Note: All the deformation scaled by 48.5

APPENDIX C

RESULTS OF THE BUMPING ANALYSIS

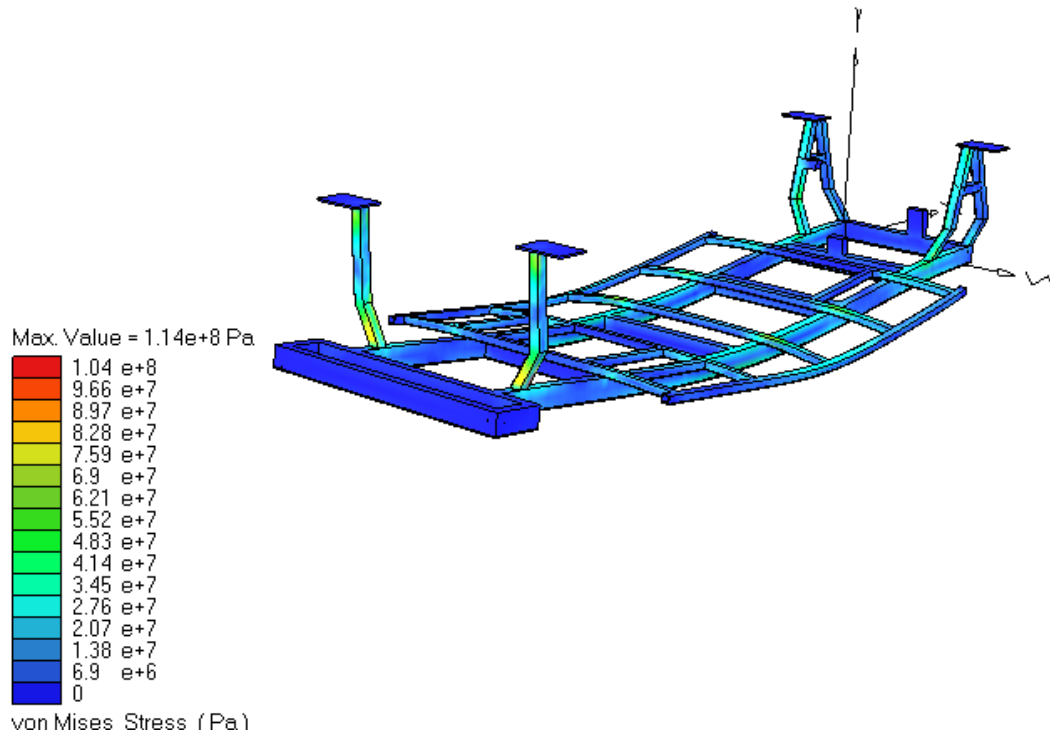


Figure C1: The contour of Von Mises stress

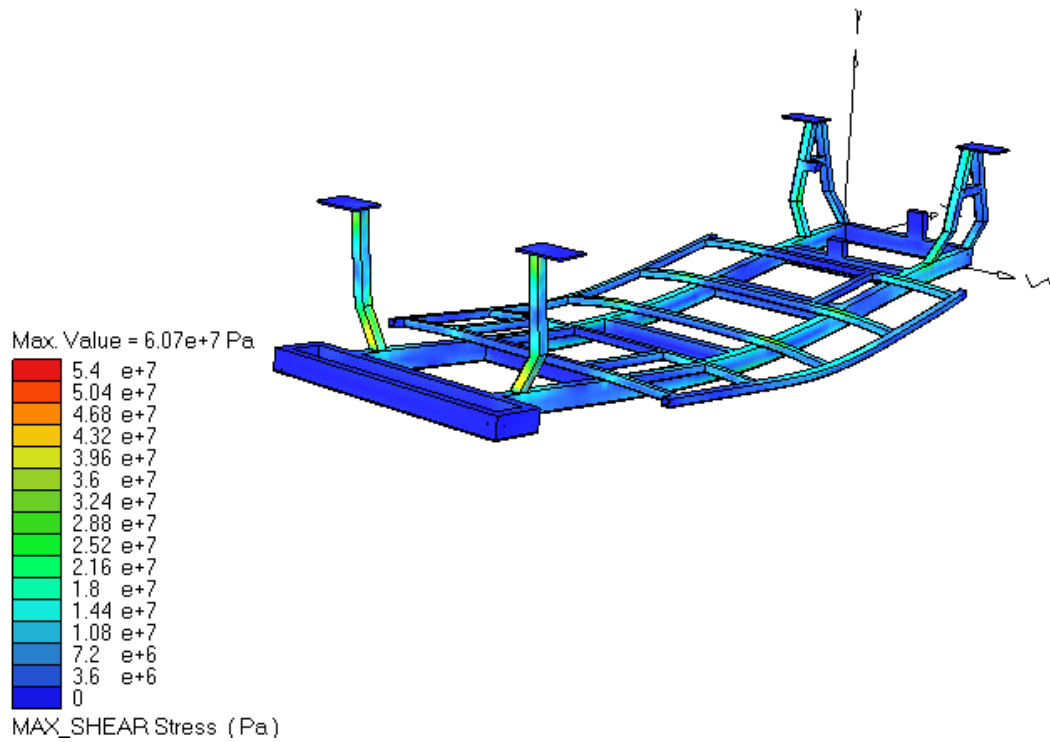


Figure C2: The contour of shear stress

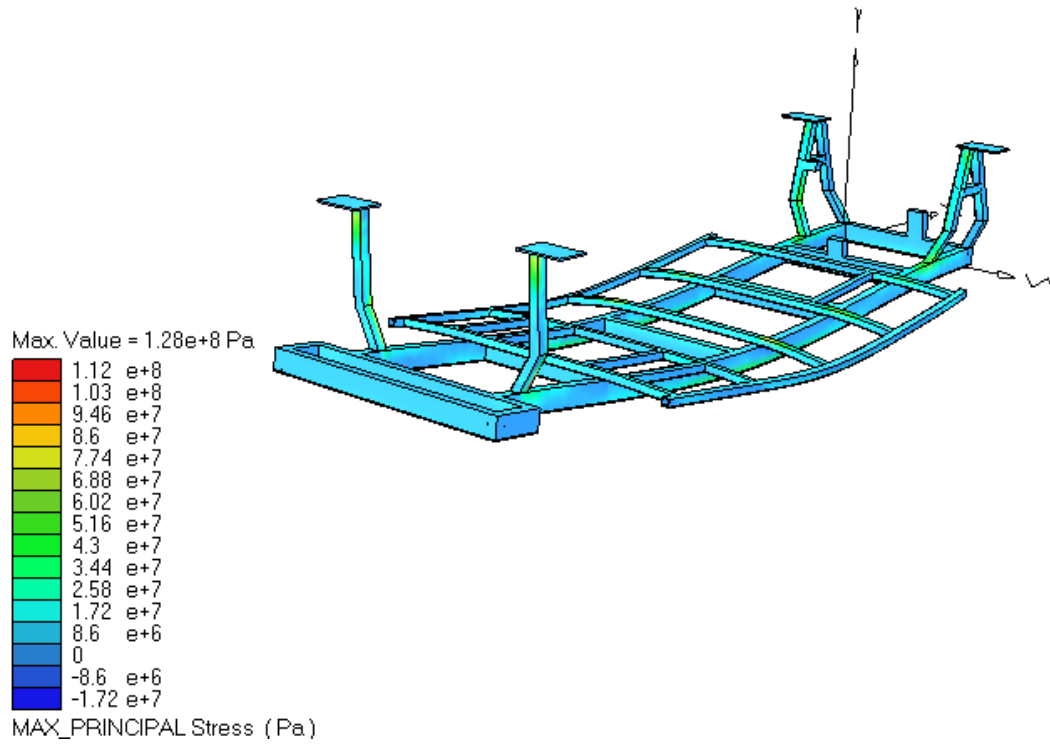


Figure C3: The contour of principal stress

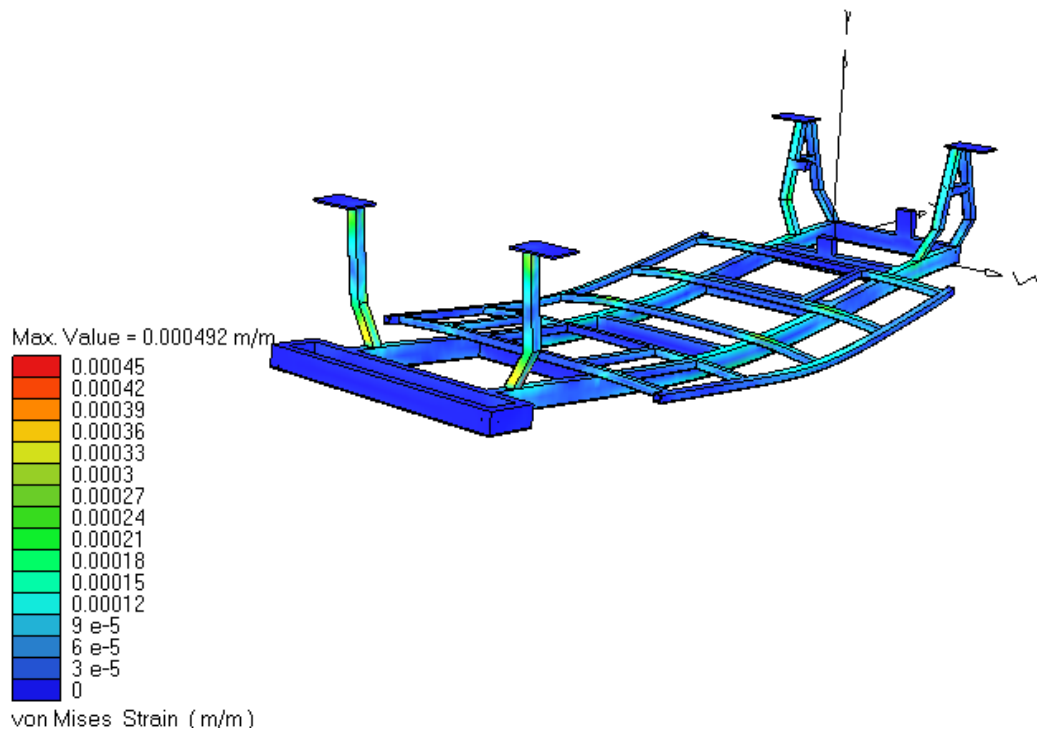


Figure C4: The contour of Von Mises strain

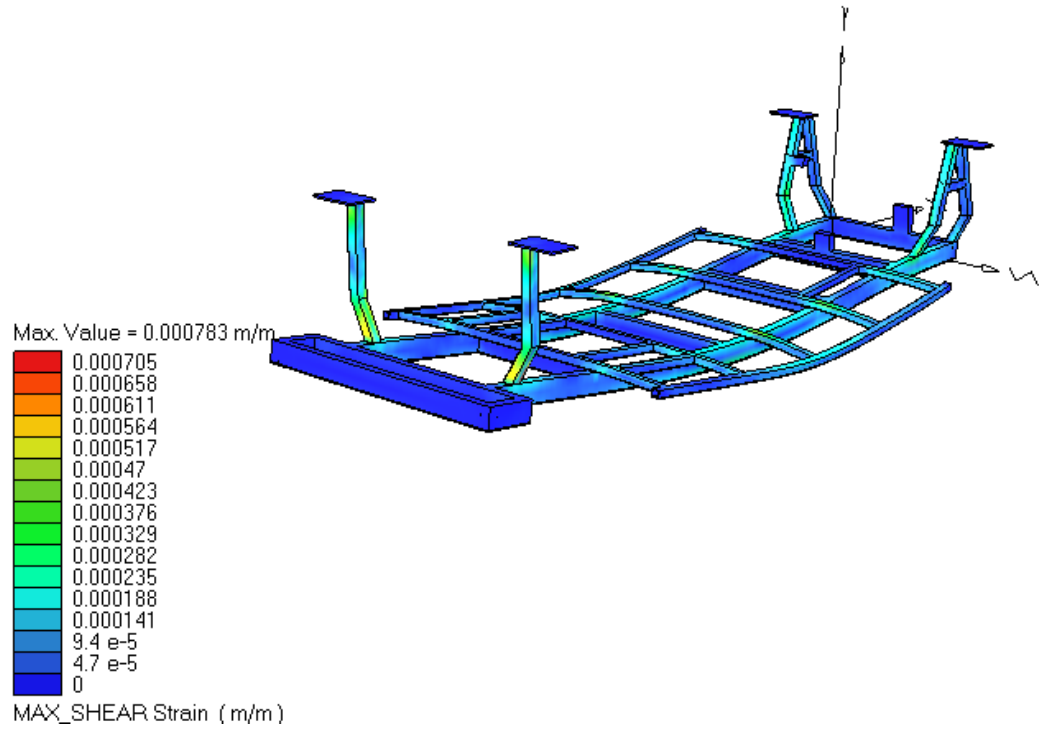


Figure C5: The contour of shear strain

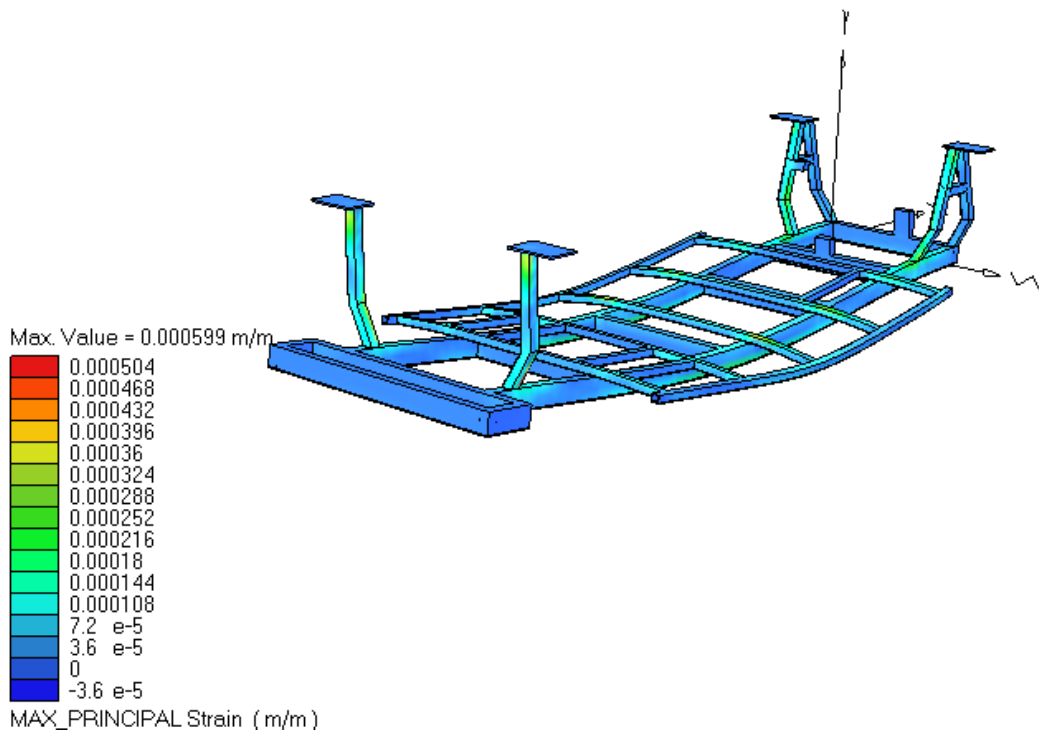


Figure C6: The contour of principal strain

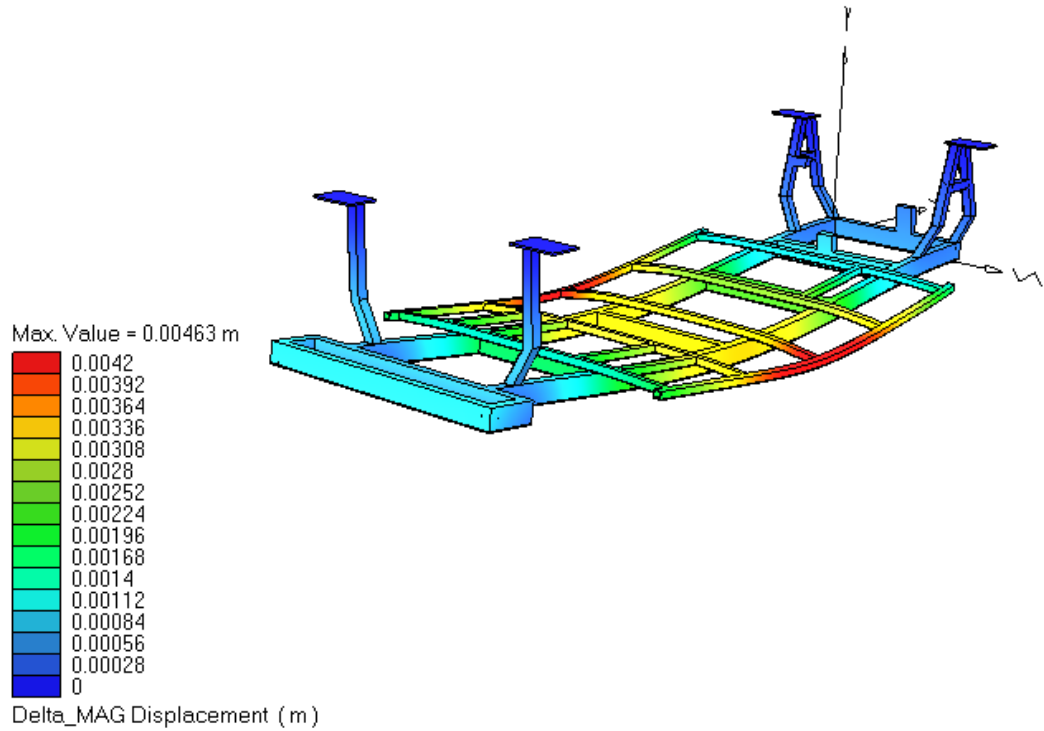


Figure C7: The contour of delta MAG displacement

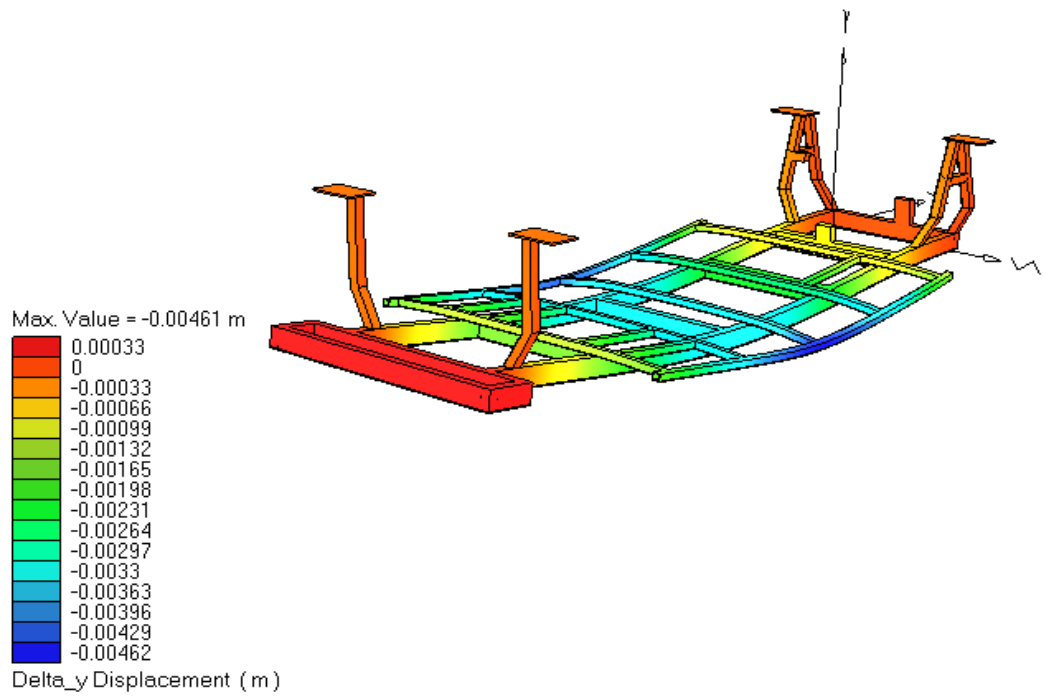


Figure C8: The contour of y-direction displacement

Note: All the deformation scaled by a factor of 44.3

APPENDIX D

RESULTS OF THE BRAKING ANALYSIS

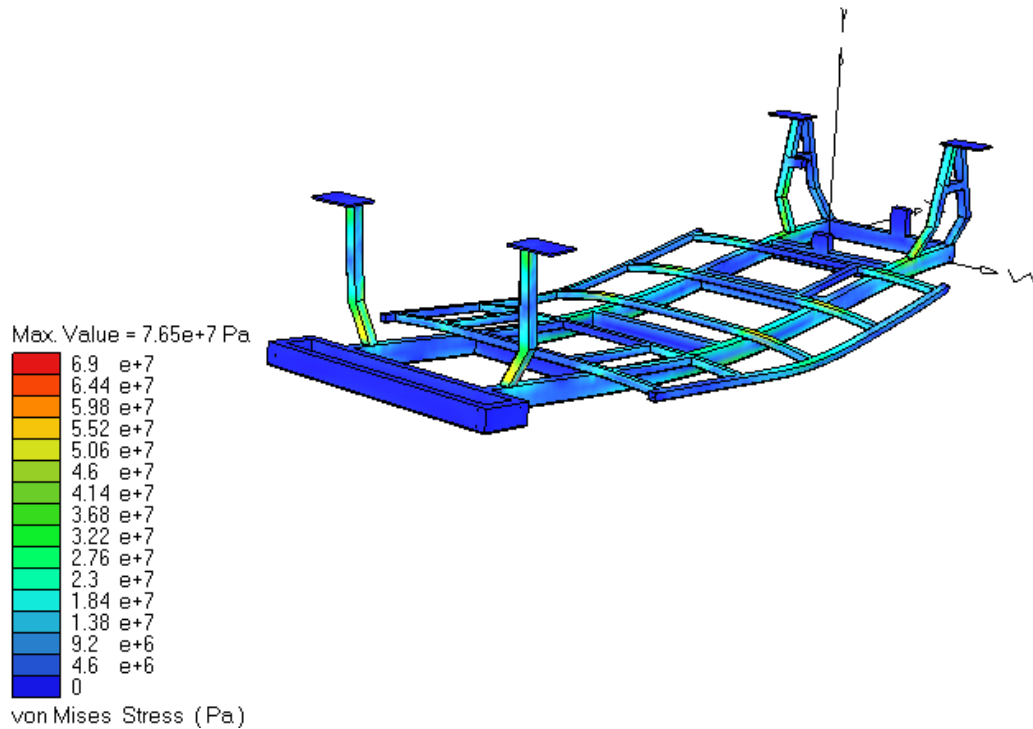


Figure D1: The contour of Von Mises stress

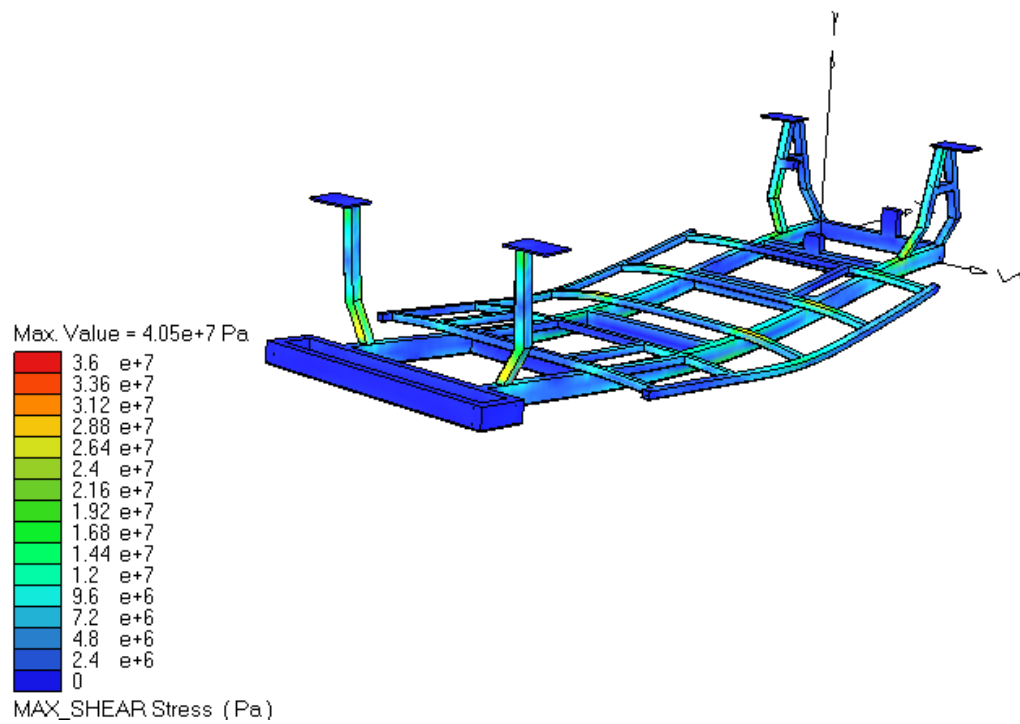


Figure D2: The contour of shear stress

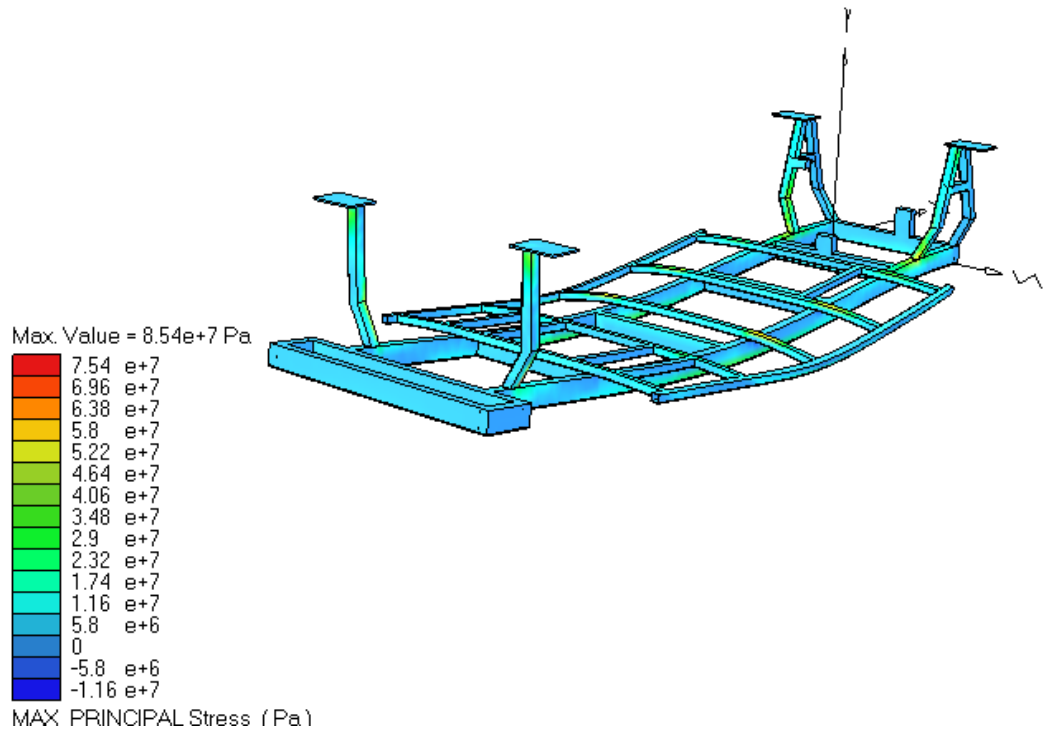


Figure D3: The contour of principal stress

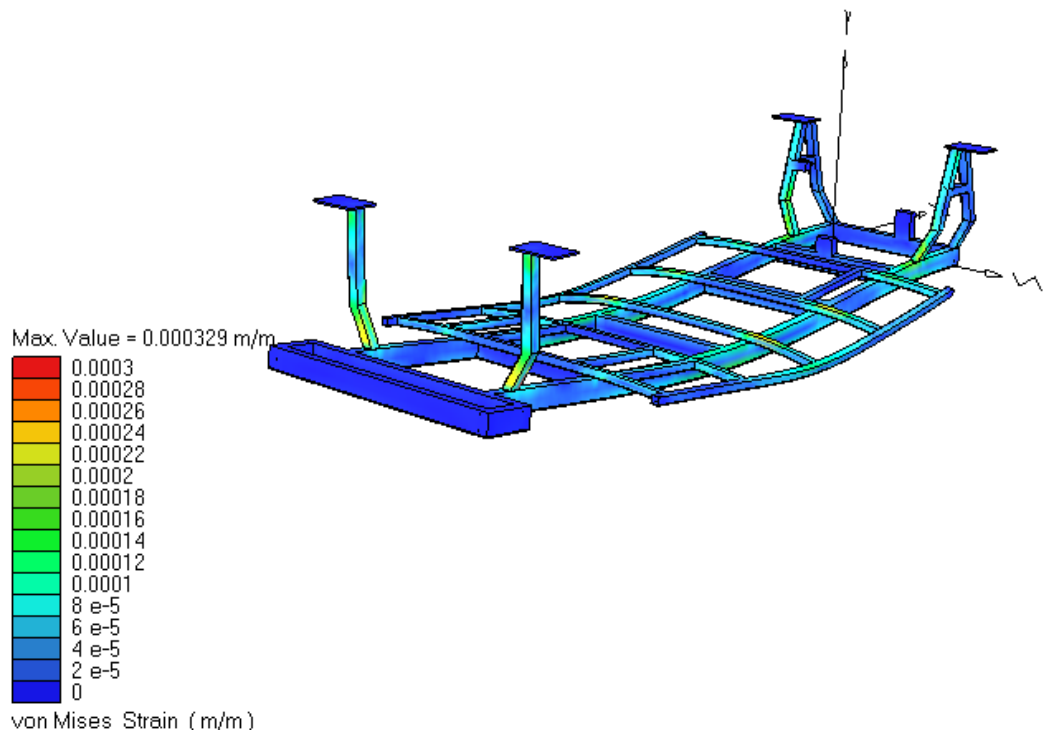


Figure D4: The contour of Von Mises strain

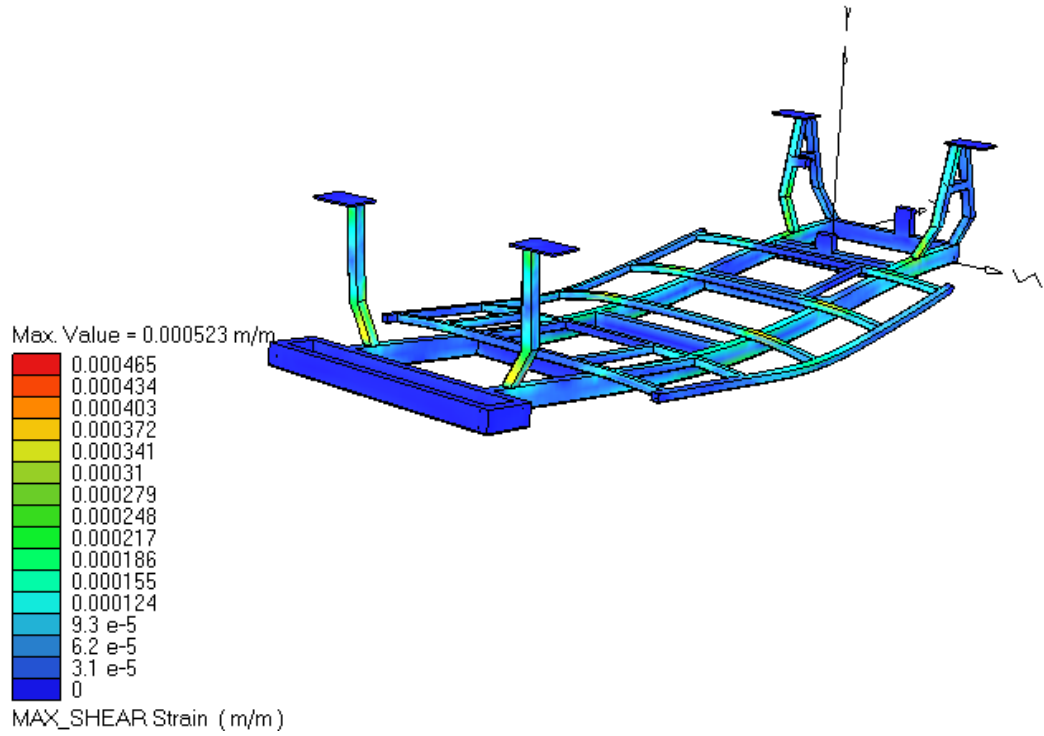


Figure D5: The contour of shear strain

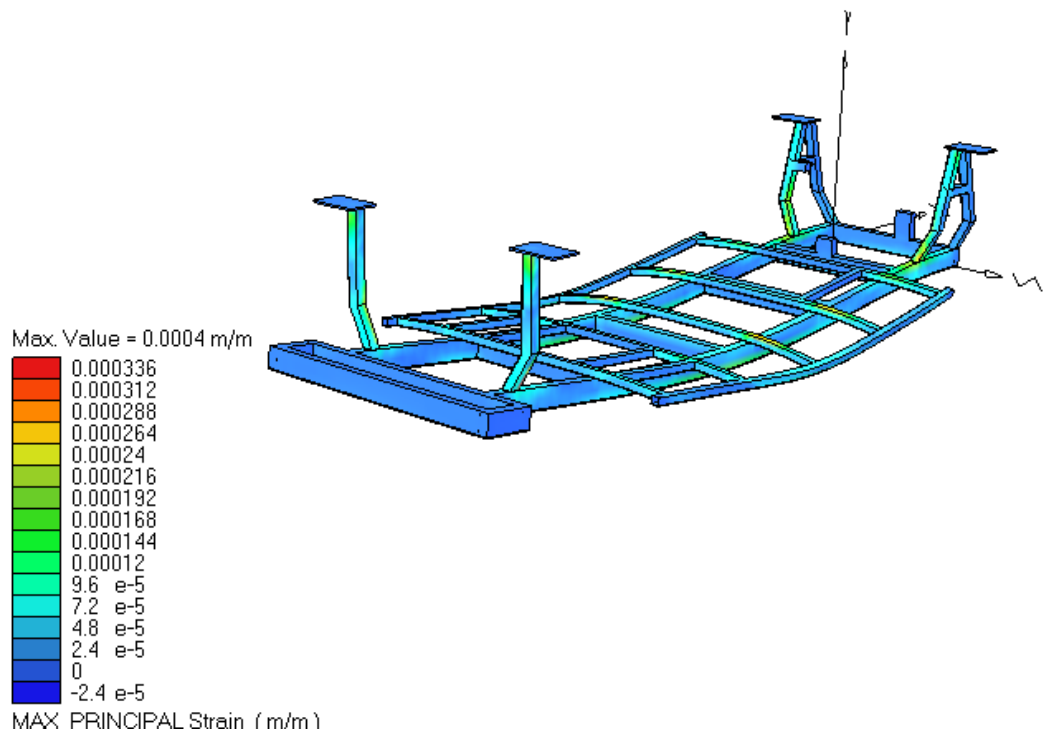


Figure D6: The contour of principal strain

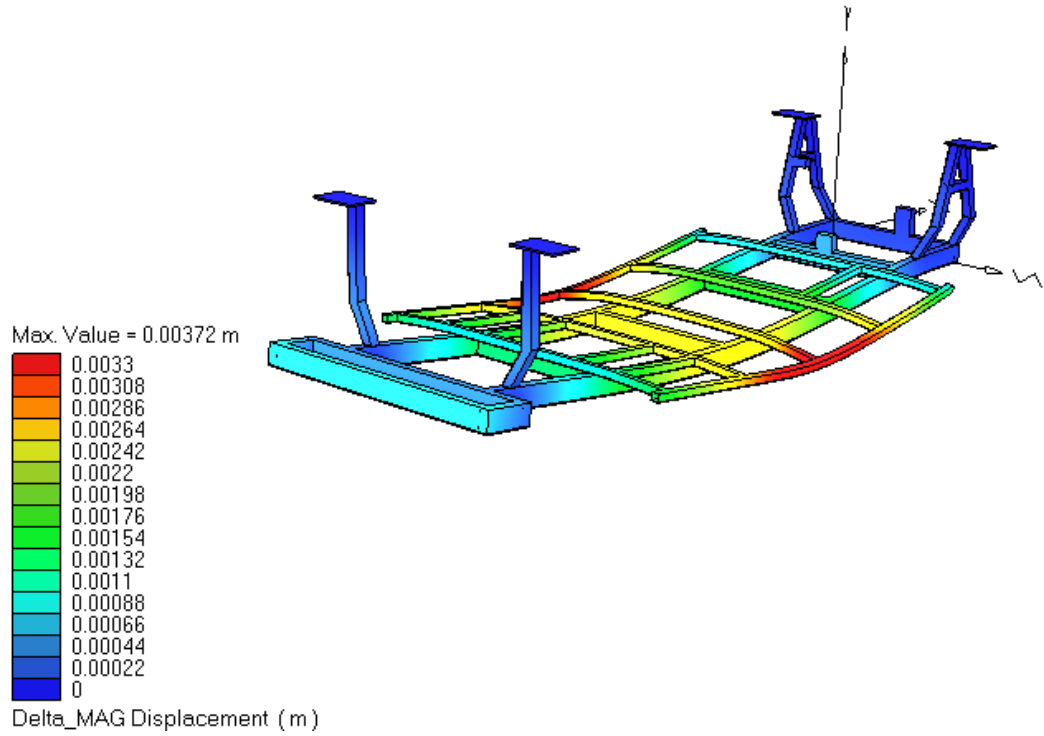


Figure D7: The contour of delta MAG displacement

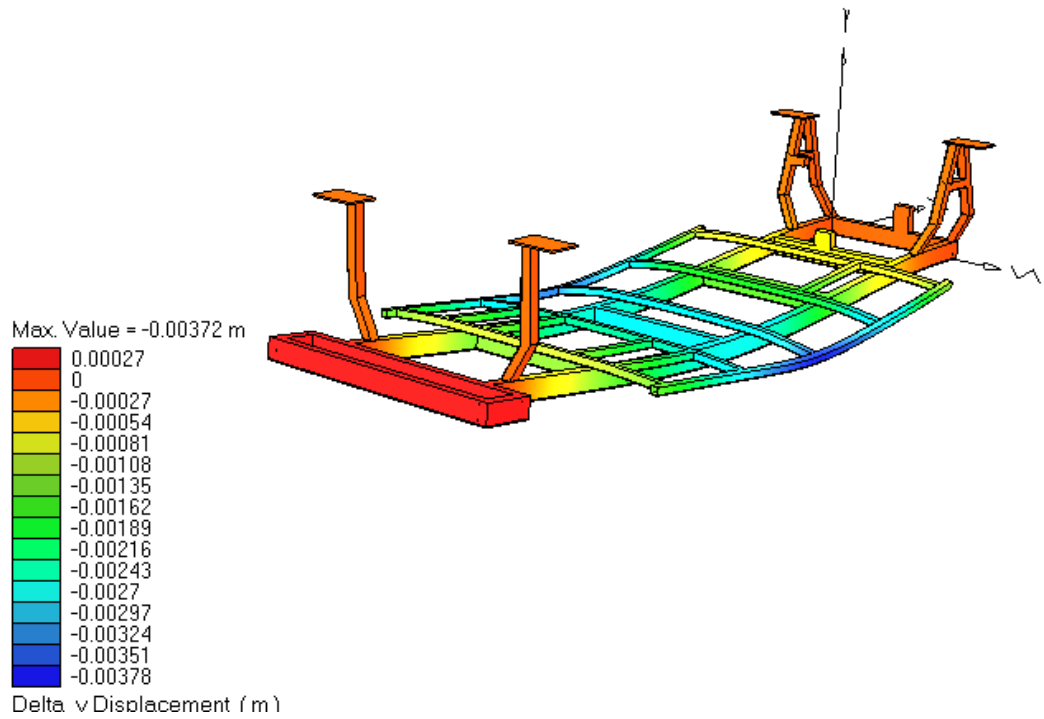


Figure D8: The contour of y-direction displacement

Note: All the deformation were scaled by a factor of 55.1

APPENDIX E

RESULTS OF THE CHASSIS TORSIONAL STIFFNESS ANALYSES

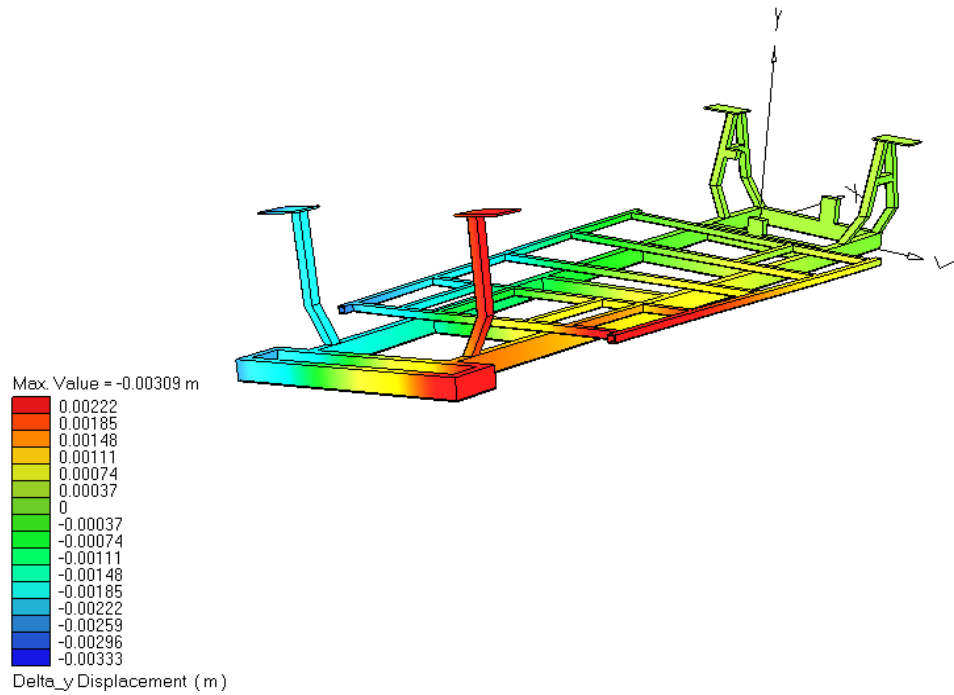


Figure E1: The contour and displacement due to 1500N
(The deformation scaled by 42.2)

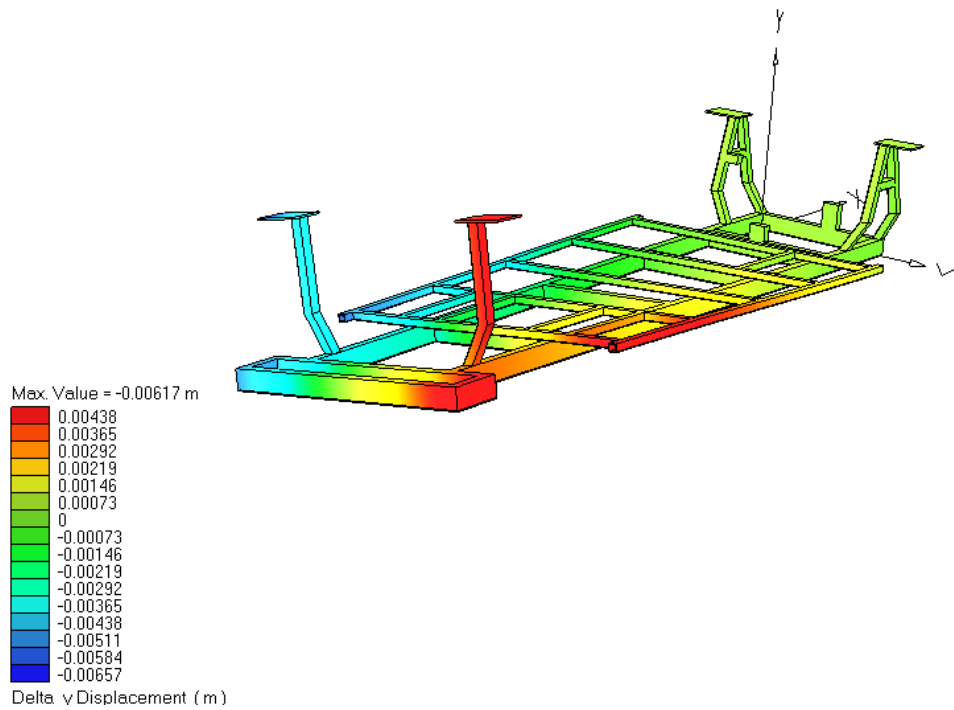


Figure E2: The contour and displacement due to 3000N
(The deformation scaled by a factor of 21.1)

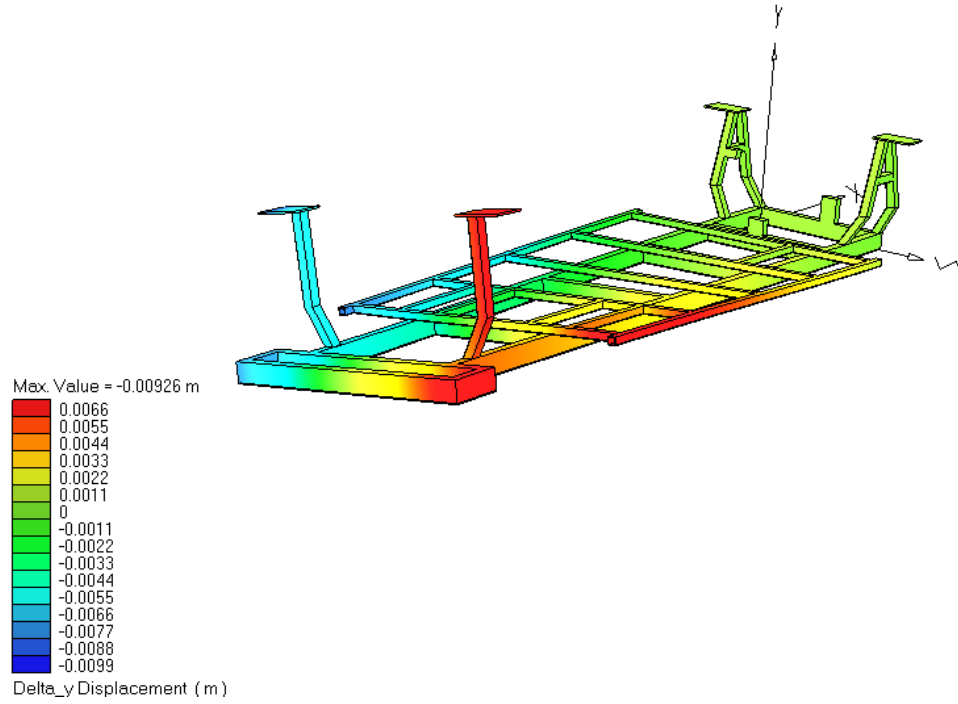


Figure E3: The contour and displacement due to 4500N
 (The deformation was scaled by a factor of 14.1)

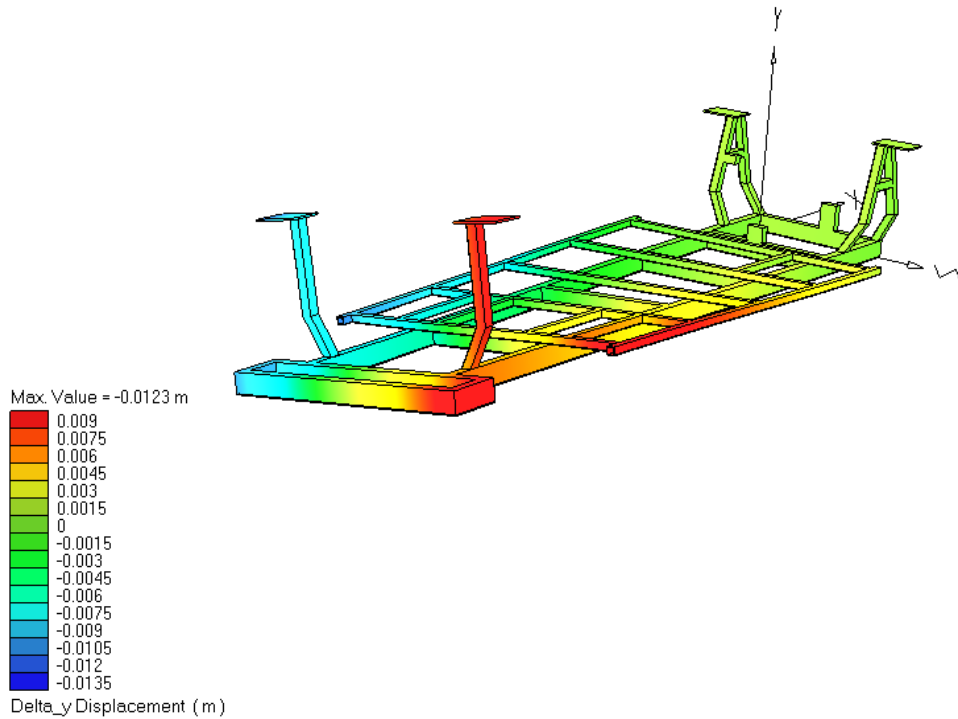


Figure E4: The contour and displacement due to 6000N
 (The deformation was scaled by a factor of 10.6)

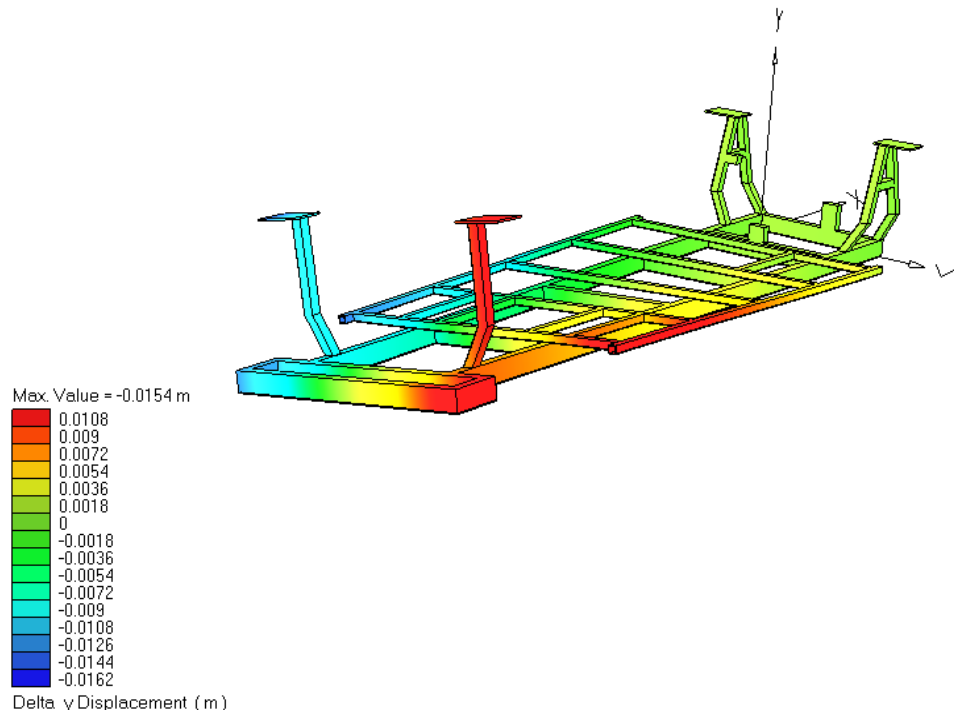


Figure E5: The contour and displacement due to 7500N
 (The deformation was scaled by a factor of 8.44)

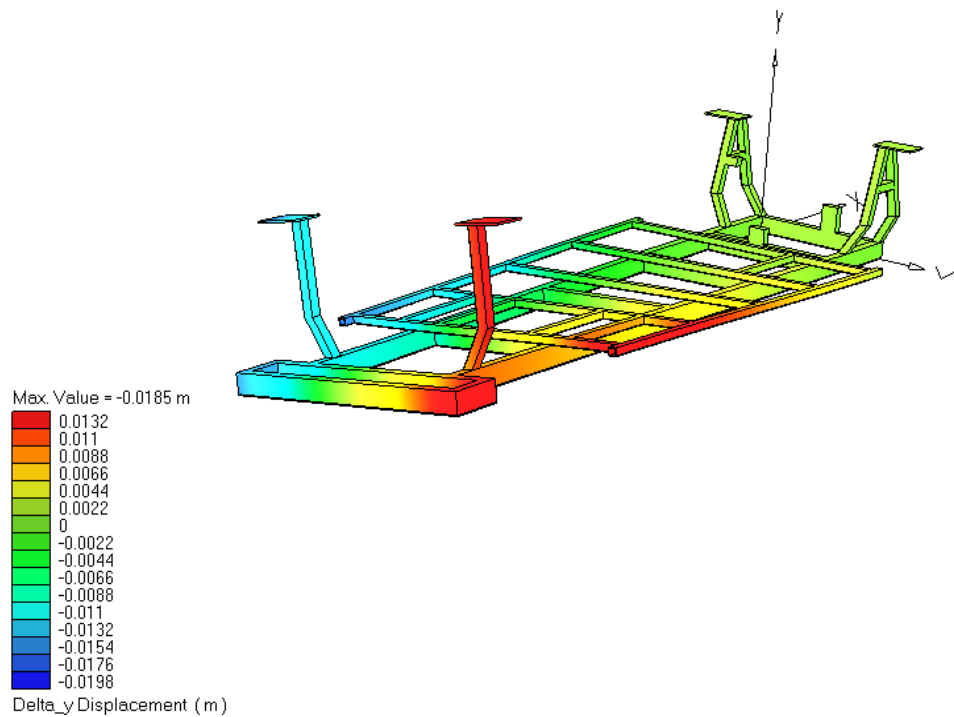
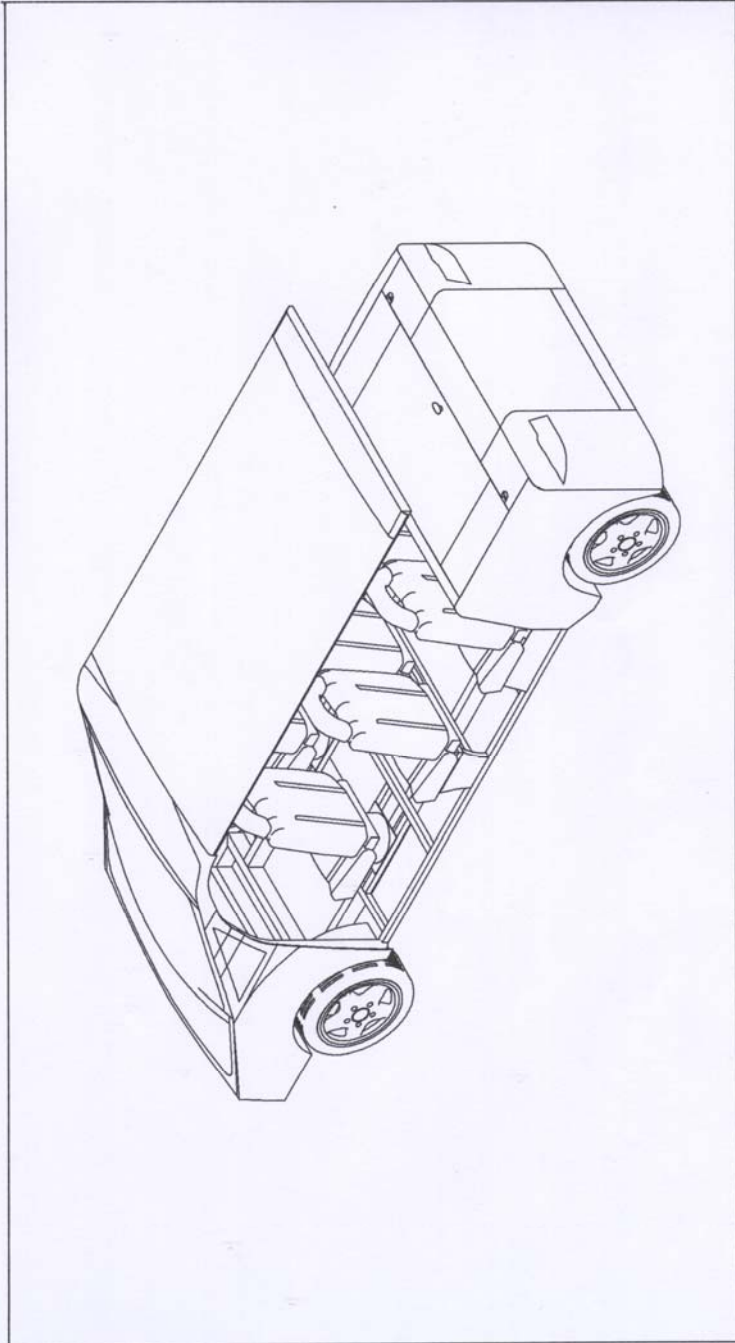


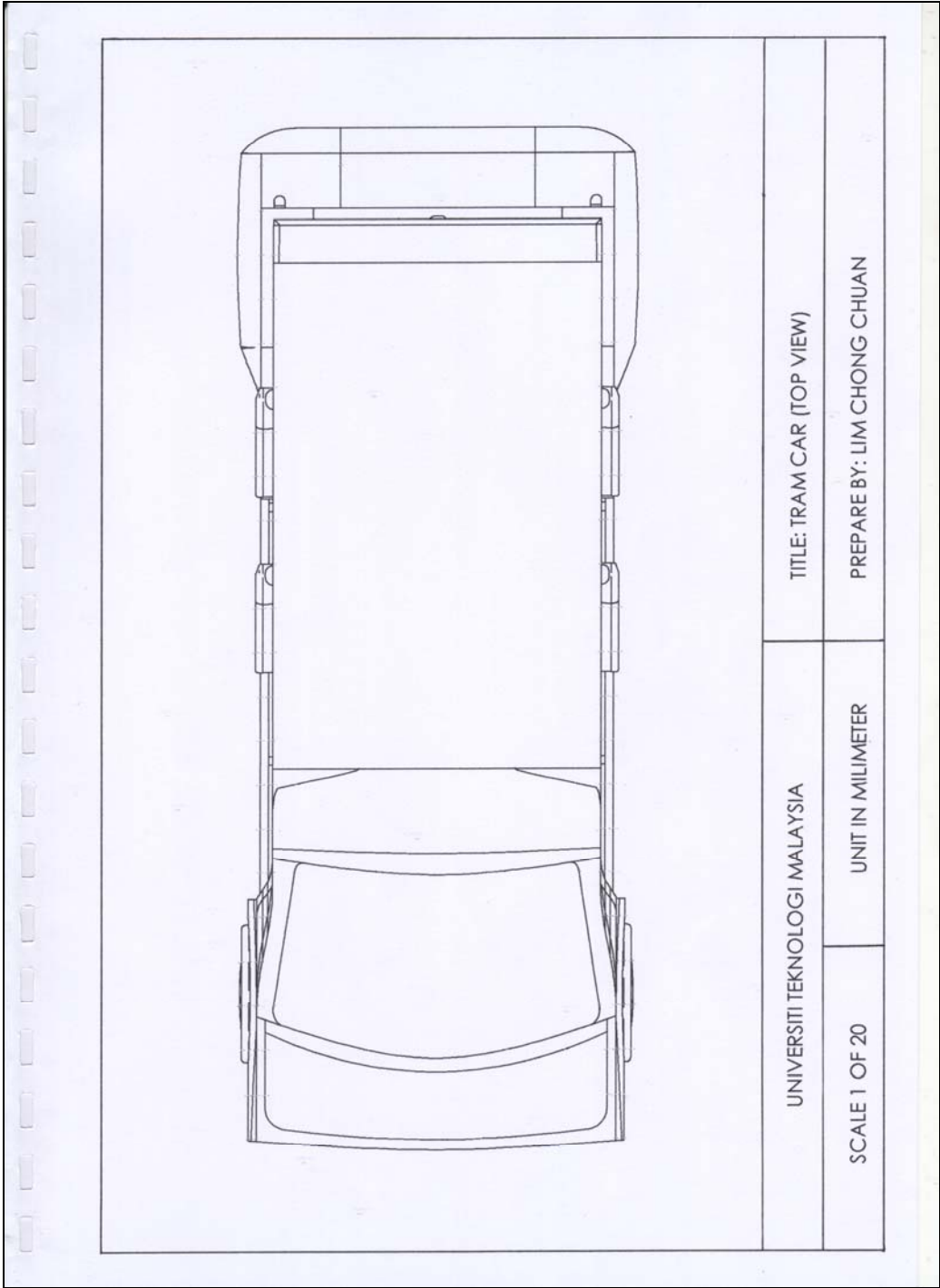
Figure E6: The contour and displacement due to 9000N
 (The deformation was scaled by a factor of 7.04)

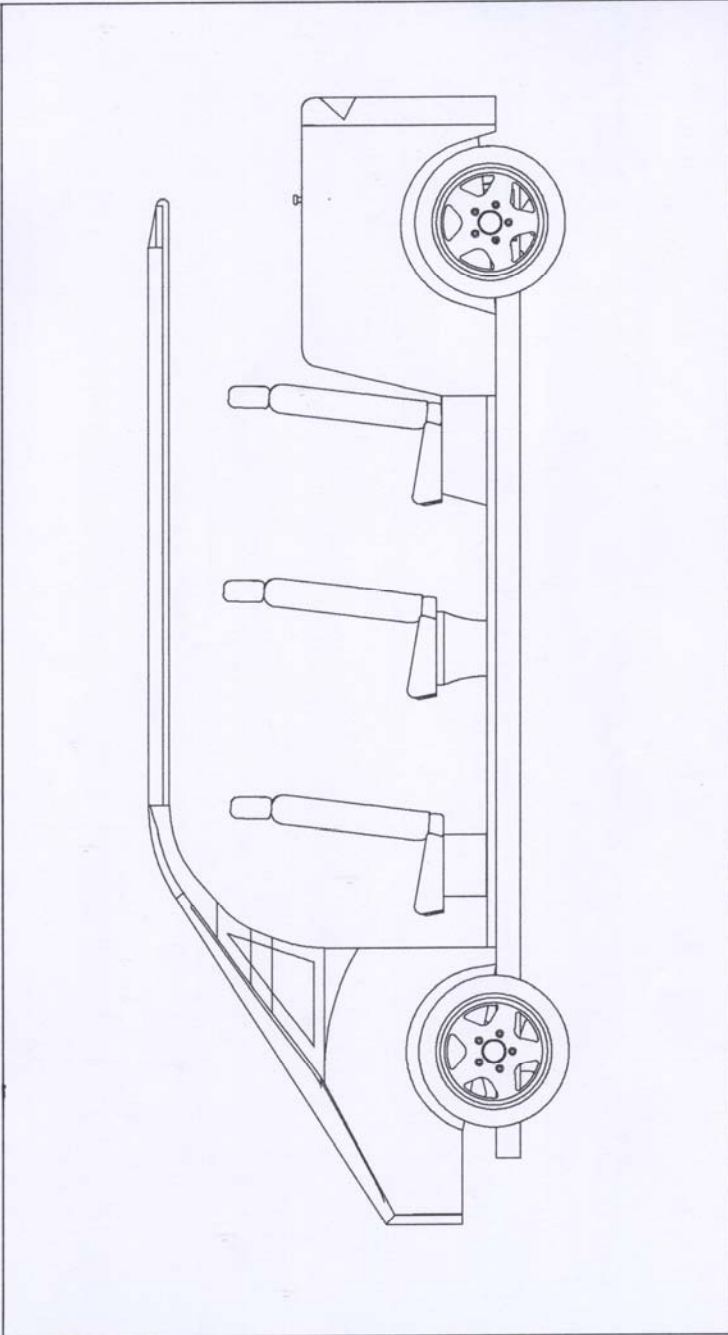
APPENDIX F

**MANUFACTURING DRAWINGS OF THE
*TRAMCAR***



UNIVERSITI TEKNOLOGI MALAYSIA	TITLE: TRAM CAR (ISOMETRIC)
SCALE 1 OF 25	PREPARE BY: LIM CHONG CHUAN
UNIT IN MILLIMETER	





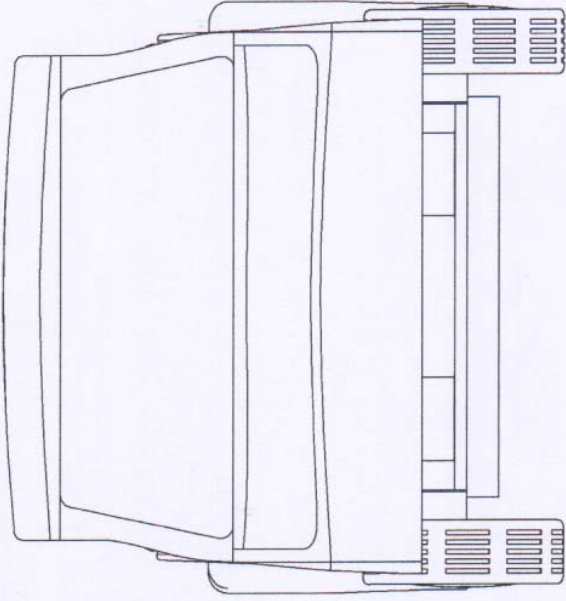
UNIVERSITI TEKNOLOGI MALAYSIA

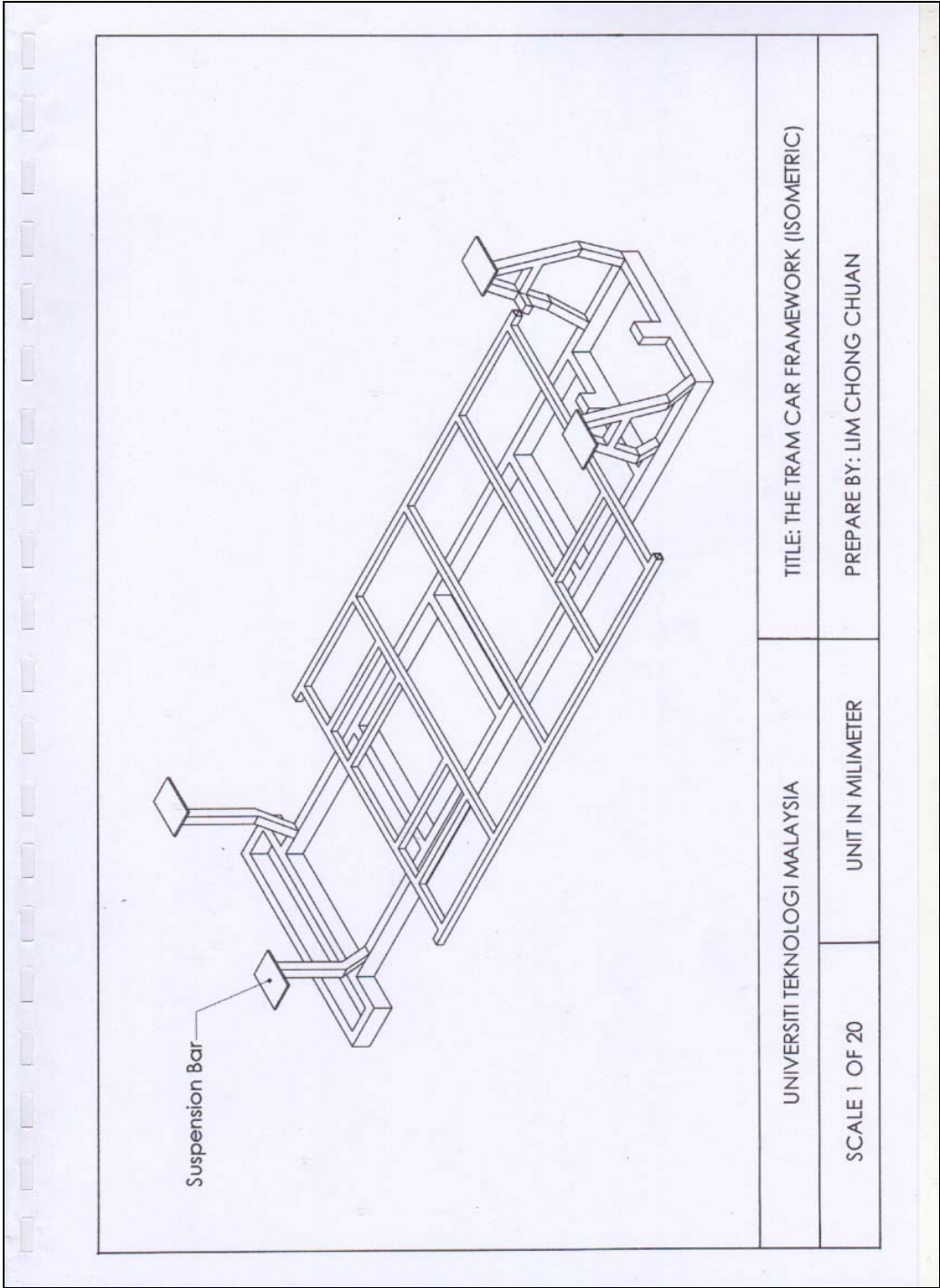
SCALE 1 OF 20

TITLE: TRAM CAR (SIDE VIEW)

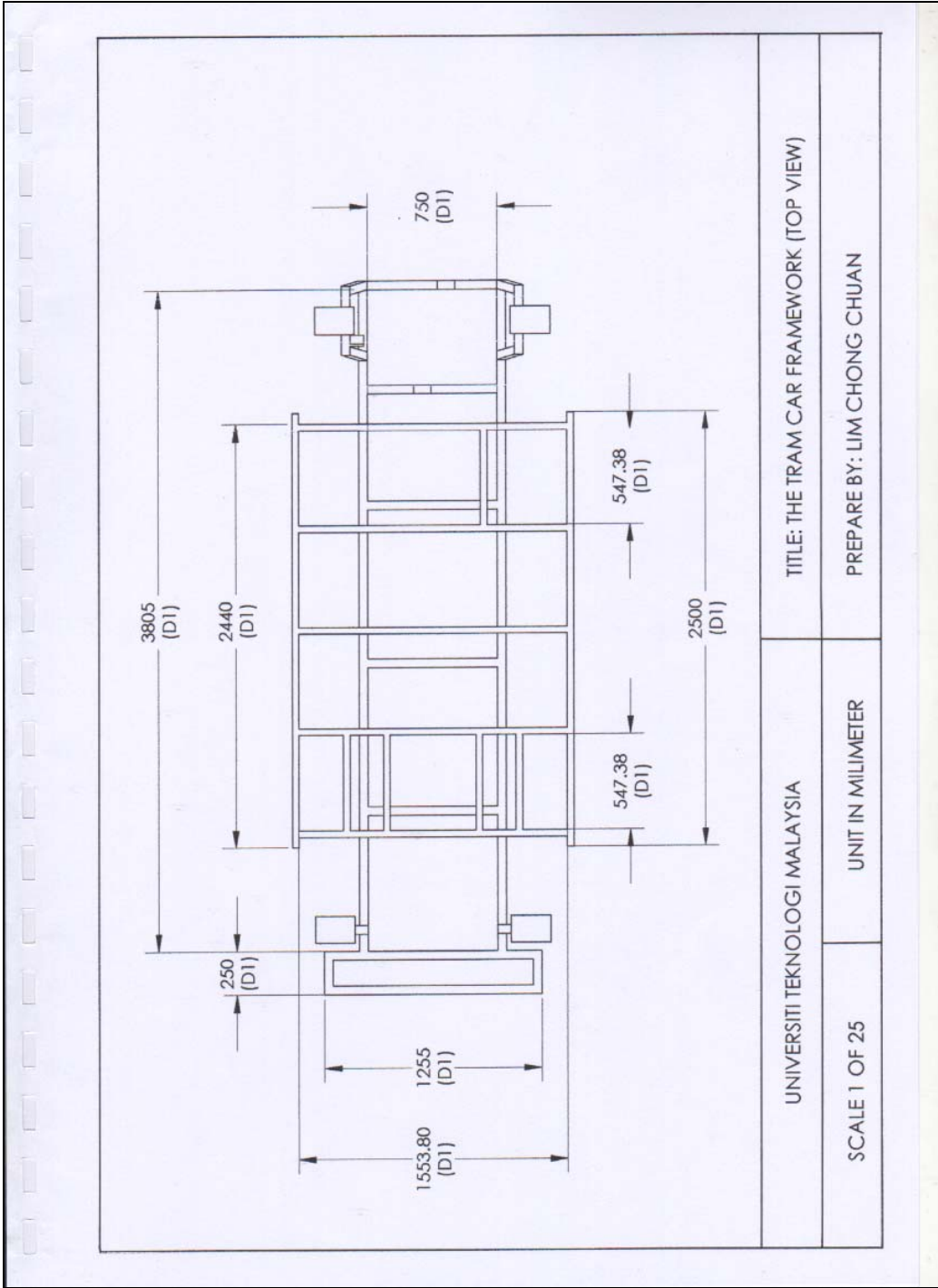
UNIT IN MILLIMETER

PREPARE BY: LIM CHONG CHUAN

		TITLE: TRAM CAR (FRONT VIEW)
UNIVERSITI TEKNOLOGI MALAYSIA	UNIT IN MILLIMETER	PREPARE BY: LIM CHONG CHUAN
SCALE 1 OF 15		



UNIVERSITI TEKNOLOGI MALAYSIA	TITLE: THE TRAM CAR FRAMEWORK (ISOMETRIC)
SCALE 1 OF 20	PREPARE BY: LIM CHONG CHUAN
UNIT IN MILLIMETER	



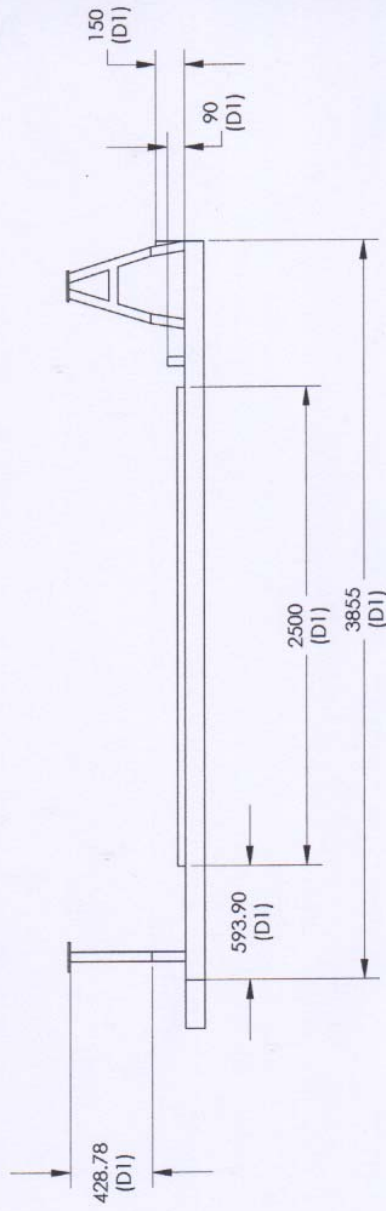
UNIVERSITI TEKNOLOGI MALAYSIA

TITLE: THE TRAM CAR FRAMEWORK (TOP VIEW)

SCALE 1 OF 25

UNIT IN MILLIMETER

PREPARE BY: LIM CHONG CHUAN



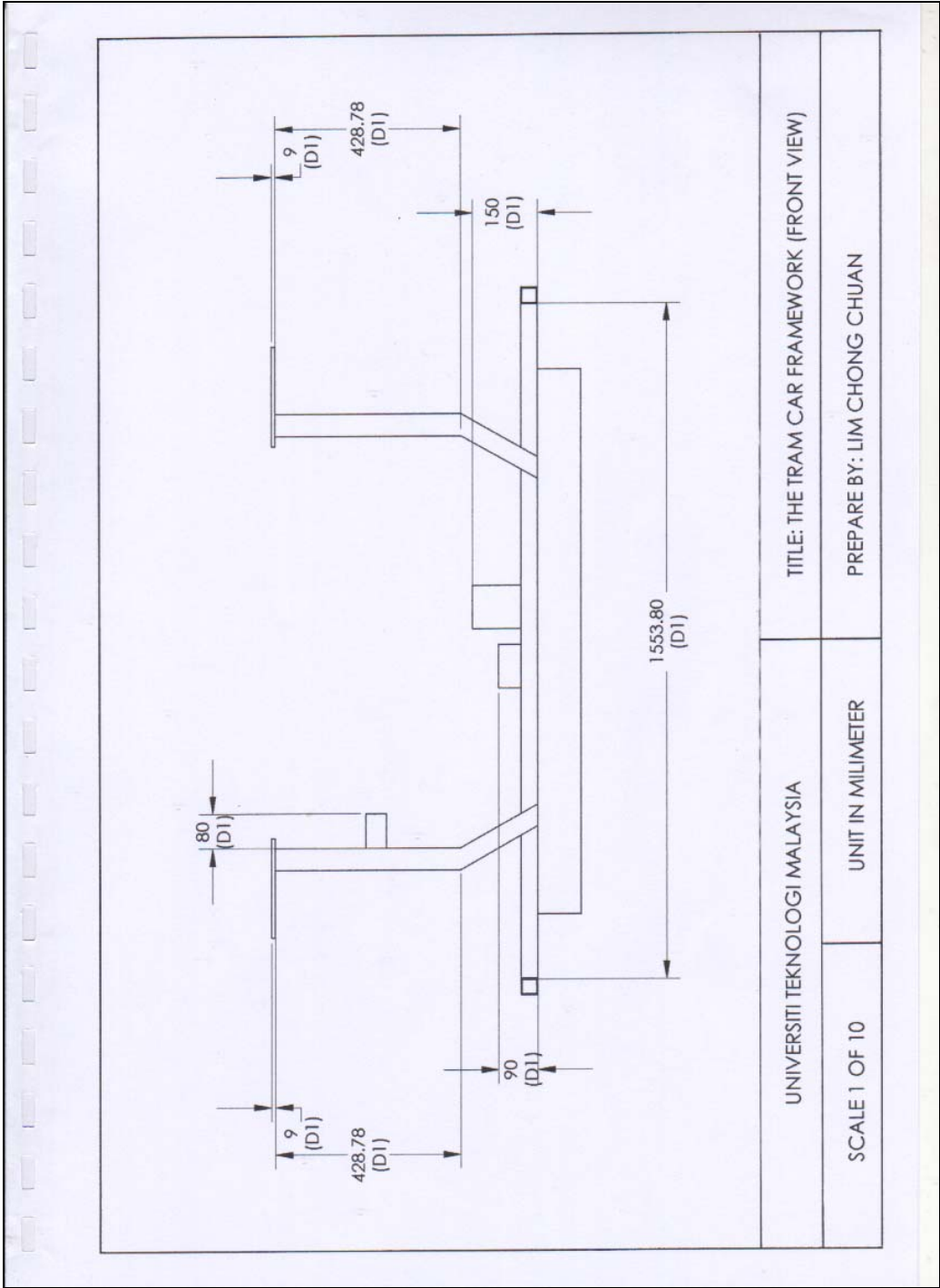
TITLE: THE TRAM CAR FRAMEWORK (SIDE VIEW)

PREPARE BY: LIM CHONG CHUAN

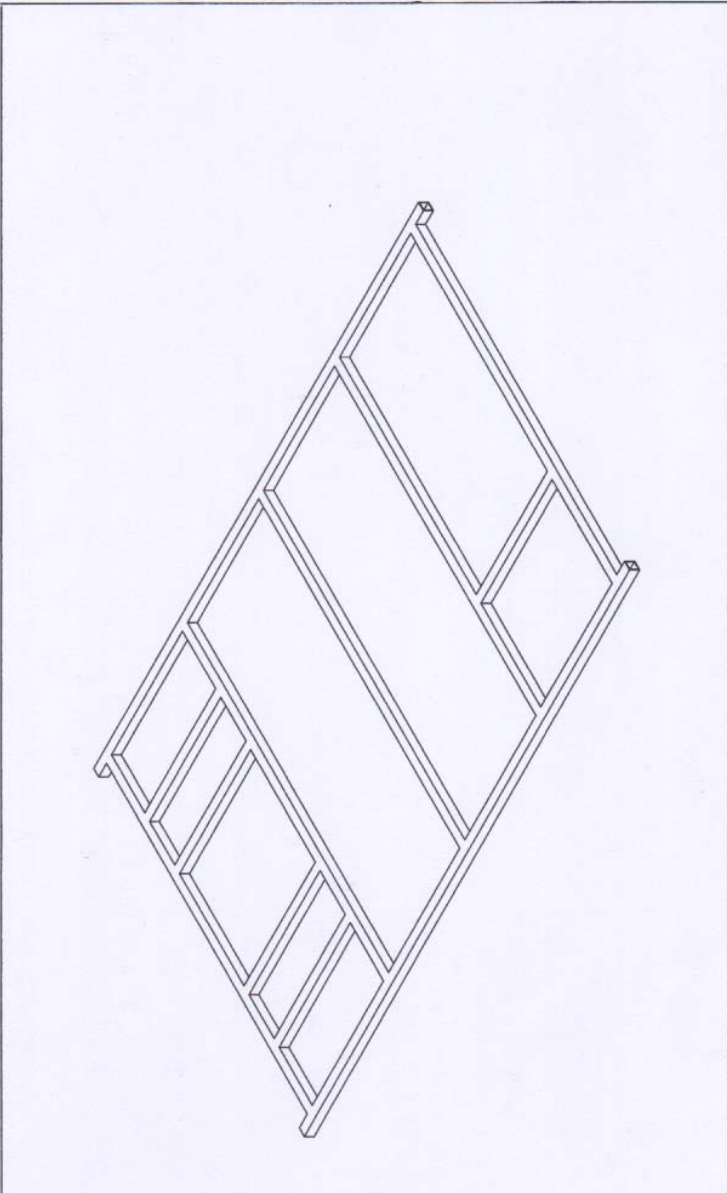
UNIVERSITI TEKNOLOGI MALAYSIA

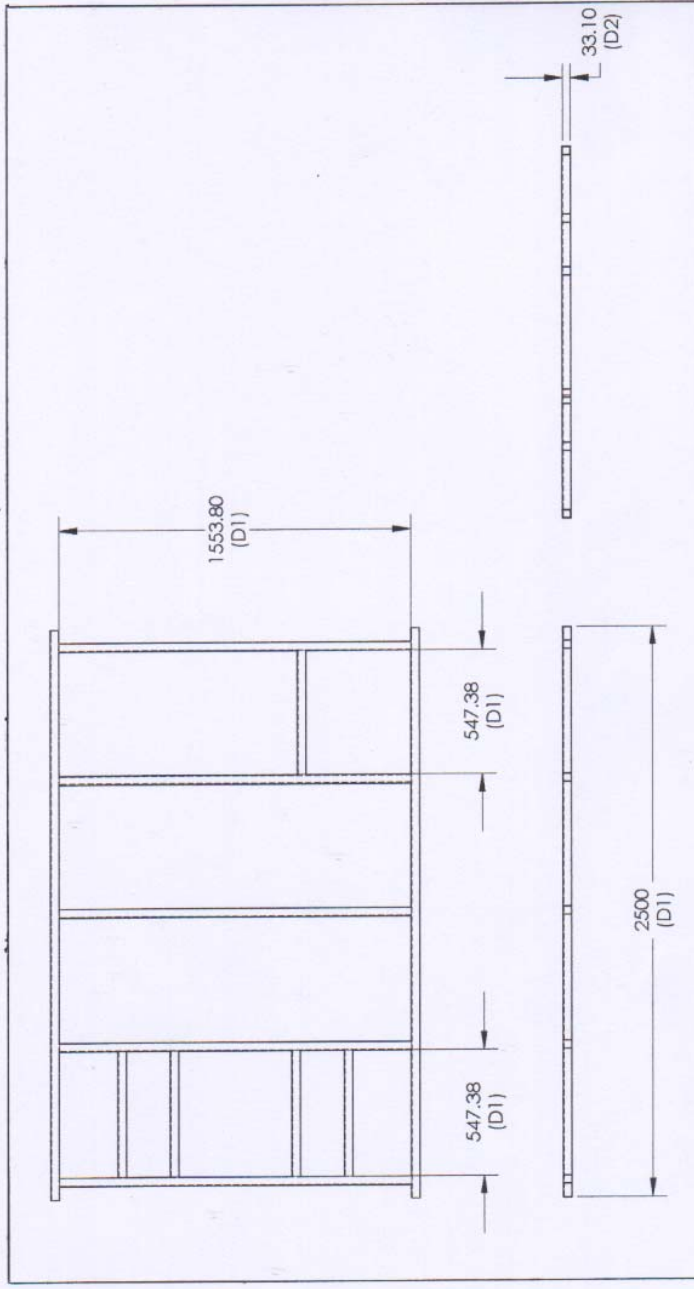
UNIT IN MILLIMETER

SCALE 1 OF 25

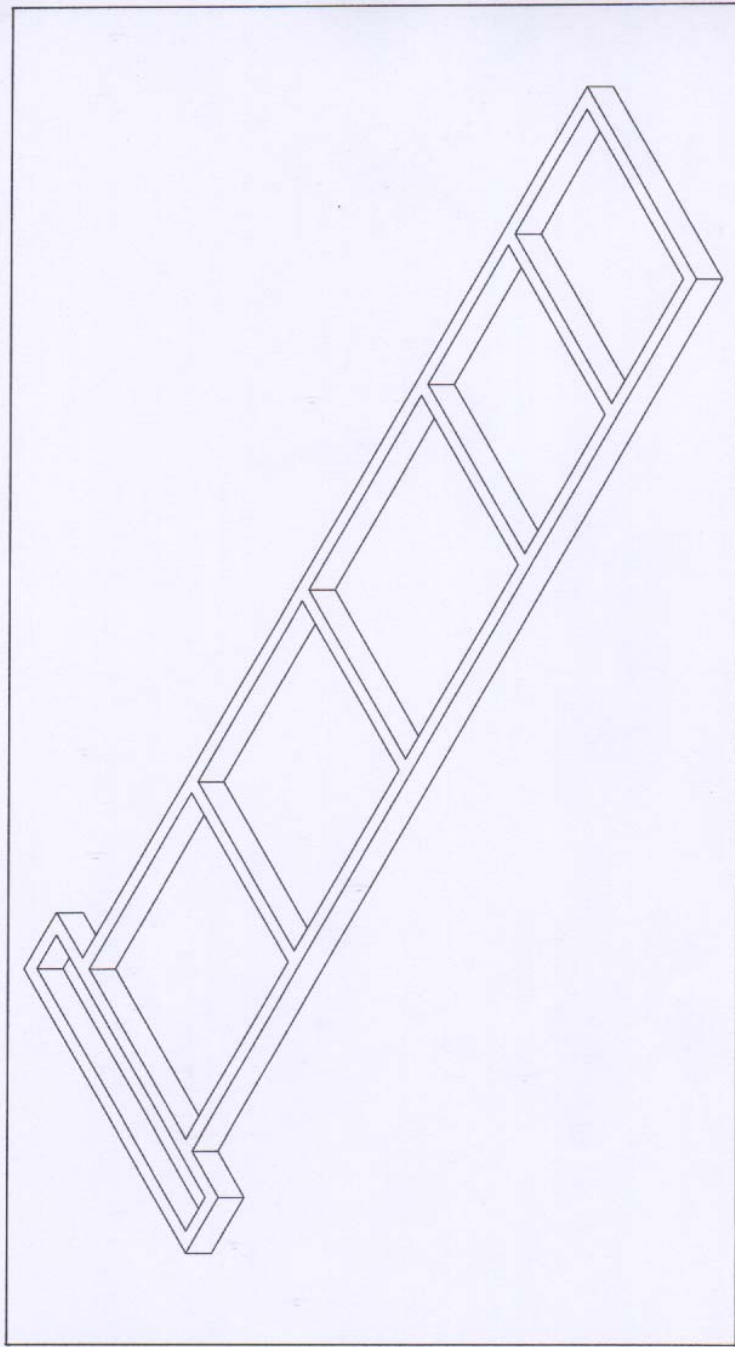


UNIVERSITI TEKNOLOGI MALAYSIA	TITLE: THE TRAM CAR FRAMEWORK (FRONT VIEW)
SCALE 1 OF 10	PREPARE BY: LIM CHONG CHUAN
UNIT IN MILLIMETER	

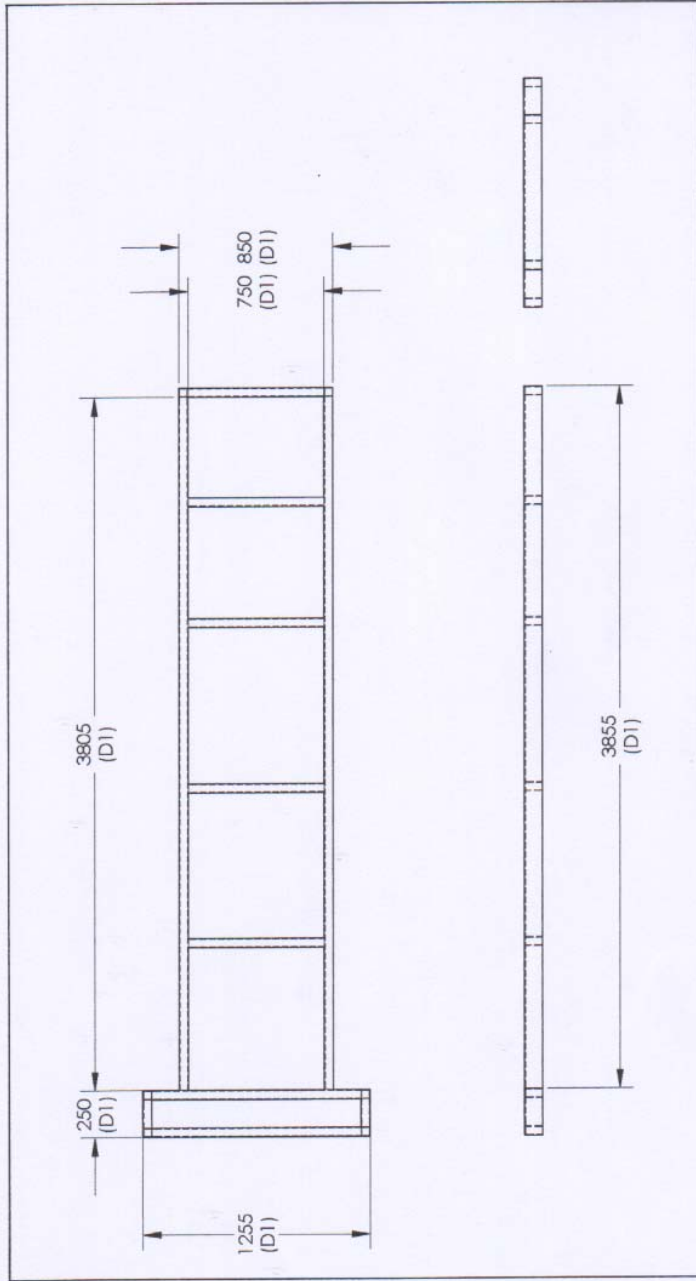
		UNIVERSITI TEKNOLOGI MALAYSIA		TITLE: THE UPPER LADDER FRAMEWORK (ISOMETRIC)	
		SCALE 1 OF 15	UNIT IN MILLIMETER	PREPARE BY: LIM CHONG CHUAN	



UNIVERSITI TEKNOLOGI MALAYSIA		TITLE: THE UPPER LADDER FRAMEWORK (ORTHOGRAPHIC)	
SCALE 1 OF 20	UNIT IN MILLIMETER	PREPARE BY: LIM CHONG CHUAN	



UNIVERSITI TEKNOLOGI MALAYSIA		TITLE: THE LOWER LADDER FRAMEWORK (ISOMETRIC)	
SCALE 1 OF 15	UNIT IN MILLIMETER	PREPARE BY: LIM CHONG CHUAN	



UNIVERSITI TEKNOLOGI MALAYSIA		TITLE: THE LOWER LADDER FRAMEWORK (ORTHOGRAPHIC)	
SCALE 1 OF 25	UNIT IN MILLIMETER	PREPARE BY: LIM CHONG CHUAN	

APPENDIX G

PICTURES OF THE *TRAMCAR*



Figure G1: The exterior view of *tramcar*.



Figure G2: The front view of *tramcar*.



Figure G3: The rear view of *tramcar*.



Figure G4: The engine location in *tramcar*.



Figure G5: The luxury seat in *tramcar*.



Figure G6: The interior view.



Figure G7: The Toyota Corona 16 valves engine.



Figure G8: The capacity of the engine used.

UNIVERSITI TEKNOLOGI MALAYSIA

BORANG PENGESAHAN
LAPORAN AKHIR PENYELIDIKAN

TAJUK PROJEK : DEVELOPMENT OF A RECREATIONAL-PURPOSE TRANSIT
VEHICLE, TRAMCAR

Saya AZHAR BIN ABDUL AZIZ
(HURUF BESAR)

Mengaku membenarkan **Laporan Akhir Penyelidikan** ini disimpan di Perpustakaan Universiti Teknologi Malaysia dengan syarat-syarat kegunaan seperti berikut :

1. Laporan Akhir Penyelidikan ini adalah hakmilik Universiti Teknologi Malaysia.
2. Perpustakaan Universiti Teknologi Malaysia dibenarkan membuat salinan untuk tujuan rujukan sahaja.
3. Perpustakaan dibenarkan membuat penjualan salinan Laporan Akhir Penyelidikan ini bagi kategori TIDAK TERHAD.
4. * Sila tandakan (/)

- | | | |
|-------------------------------------|--------------|---|
| <input type="checkbox"/> | SULIT | (Mengandungi maklumat yang berdarjah keselamatan atau Kepentingan Malaysia seperti yang termaktub di dalam AKTA RAHSIA RASMI 1972). |
| <input type="checkbox"/> | TERHAD | (Mengandungi maklumat TERHAD yang telah ditentukan oleh Organisasi/badan di mana penyelidikan dijalankan). |
| <input checked="" type="checkbox"/> | TIDAK TERHAD | |


TANDATANGAN KETUA PENYELIDIK

Nama & Cop Ketua Penyelidik
PROF. IR. DR. AZHAR BIN ABDUL AZIZ
Pengarah
Tarikh : **Pusat Pembangunan Automotif**
Fakulti Kejuruteraan Mekanikal
Universiti Teknologi Malaysia

CATATAN : *Jika Laporan Akhir Penyelidikan ini SULIT atau TERHAD, sila lampirkan surat daripada pihak berkuasa/organisasi berkenaan dengan menyatakan sekali sebab dan tempoh laporan ini perlu dikelaskan sebagai SULIT dan TERHAD.

FAKULTI KEJURUTERAAN MEKANIKAL
 Senarai Projek Penyelidikan Institusi 2004

BIL.	VOT	KETUA PENYELIDIK	TAJUK PROJEK	TARIKH MULA	TARIKH TAMAT	JUMLAH PERUNTUKAN
1	73206	Prof. Ir. Dr. Azhar Abdul Aziz	Cadangan Bagi Membangunkan Sistem Pengangkutan Ringan Halatuju Rendah Jenis "Articulating" Bagi Kegunaan Membawa Pelawat di UTM	15/4/2004	31/8/2004	RM100,000.00

**DEVELOPMENT OF A RECREATIONAL-
PURPOSE TRANSIT VEHICLE,
*TRAMCAR***

**A technical Report Submitted to
Research Management Centre (RMC),
Universiti Teknologi Malaysia (UTM)**

AZHAR BIN ABDUL AZIZ

**Faculty of Mechanical Engineering
Universiti Teknologi Malaysia (UTM)**

May 2008

ACKNOWLEDGEMENT

In preparing for this project and subsequently this report, I was in constant contact with many parties, notably the fellow colleagues, academicians, technicians and a local platform developer. They have contributed tremendously towards the overall success of this challenging and daunting project. I am grateful to my colleague associate Professor Mustafa Yusof for his guidance and suggestion on different aspects of the vehicle analyses. I am also indebted to my research assistance i.e. Ahmad Kamal, Zaidi and Mazlan for their constant pursuance to have this project completed on time. Without their continued support and interest, this report would not have been produced as presented here. Last but not least, I would like to offer my sincere gratitude to the vice chancellor of Universiti Teknologi Malaysia (UTM) Y.Bhg Tan Sri Mohd Zulkifli bin Mohd Ghazali for his support and assistance enabling me to receive the prestigious institutional fund (RMC vote No 73206) in 2004- without which, this project would not have taken off and materialized.

ABSTRACT

Chassis and suspension system play an important role in the performance of a vehicle when it comes to safety and passenger comfort. The objectives of this project are to develop a "hop-in and hop-out" recreational vehicle with a capacity of eight-passenger, fitted with a dual-fuel system and to analyse the performance of its chassis and suspension system. This showcase vehicle is manufactured by a team of engineers from the Automotive Development Centre (ADC) in UTM. Both the chassis and suspension analyses are rigorously performed using industrial-standard computer software. The safety factor requirement for the vehicle chassis is set for over a factor of 2.0 and its torsional stiffness must in the range from 3000Nm/degree to 9000Nm/degree. The vehicle chassis is analyzed in several conditions, namely static, bumping and braking, while the comfort performance is largely speculated to depend on the demand of user. In this project, the comfortable performance for *tramcar* which is the performance of its suspension system is benchmarked with that of the performance for *Proton Waja 1.6*. The level of comfort for the *tramcar* suspension system is referred to the performance results with particular emphasis on bouncing, pitching and rolling. From the results of the analyses the *tramcar* has achieved satisfactory performance criteria. The safety factor is over the minimum requirement for a typical utility vehicle and the torsional stiffness is within the allowable range. In addition the suspension system shows the results are comparable to the performance of the *Proton Waja 1.6*.

ABSTRAK

Sistem gantungan (casis dan penyerap hentak) memainkan peranan penting dalam prestasi sesebuah kenderaan dimana ia memberikan keselamatan dan keselesaan kepada penumpang. Objective projek ini adalah untuk membina satu "hip-in and hip out" kenderaan rekreasi untuk kegunaan 8 orang penumpang dimana ianya dilengkapi dengan sistem dua bahan baker dan analisis prestasinya pada system casis dan gantungan. Produk ini telah dibangunkan oleh sekumpulan jurutera dari Pusat Pembangunan Automotif (ADC) di UTM. Analisis sistem gantungan dan casis telah dianalisis menggunakan perisian komputer standard industri dengan ditetapkan faktor selamat yang ditetapkan untuk casis melebihi 2.0 dan keupayaan kilasan di antara 3000Nm/darjah hingga 9000Nm/darjah. Casis kenderaan telah di analisis dengan beberapa keadaan yang berbeza seperti statik analisis, keadaan berbonggol dan memberek, sehingga keselesaan pengguna diambil kira sebelum rekabentuk diterima. Dalam projek ini keselesaan pemanduan Proton Waja 1.6 adalah menjadi bandingan. Tahap keselesaan bagi sisyem gantungan *Tramcar* dirujuk kepada keputusan prestasi oleh pemerhatian terhadap *bouncing, pitcing* dan *rolling*. Dari keputusan analisis tersebut, *tramcar* telah melapasi prestasi asa yang telah ditetapkan. Faktor selamat telah di rekabentuk melebihi tahap minimum yang diperlukan untuk kenderaan yang tipikal.

TABLE OF CONTENTS

CHAPTER	TITLE	PAGE
	TITLE	i
	DECLARATION	ii
	DEDICATION	iii
	ACKNOWLEDGEMENT	iv
	ABSTRACT	v
	TABLE OF CONTENTS	vi
	LIST OF TABLES	vii
	LIST OF FIGURES	viii
	LIST OF SYMBOLS	ix
	LIST OF APPENDICES	x
1.	INTRODUCTION	
	1.1 Introduction	1
	1.2 <i>Tramcar</i> background	2
	1.3 Objectives	3
	1.4 Project Workscope	4
	1.5 Methodology	5

2. LITERATURE REVIEW

2.1	Brief Overview of Chassis	7
2.1.1	Monocoque	8
2.1.2	Twin Tube	9
2.1.3	Multi Tube	10
2.1.4	Space Frame	11
2.1.5	Choice	12
2.2	Suspension Systems	12
2.2.1	Solid Axle	14
2.2.2	Four Link	14
2.2.3	De-Dion	15
2.2.4	Trailing Arm	16
2.2.5	McPherson Strut	17
2.2.6	Quadra Link	18
2.2.7	Double Wishbone	19

3. CHASSIS ANALYSIS

3.1	Introduction	20
3.2	Input Material Specification	21
3.3	Assumptions	23
3.4	Loadings applied	23
3.5	Static analysis	24
3.5.1	Boundary conditions	24
3.5.2	Results	24
3.6	Bumping analysis	25
3.6.1	Boundary conditions	25
3.6.2	Results	25
3.7	Braking analysis	26
3.7.1	Boundary conditions	26

3.7.2	Results	27
3.8	Chassis torsional stiffness analysis	28
3.8.1	Boundary conditions	28
3.8.2	Results	28
4.	SUSPENSION SYSTEM ANALYSIS	
4.1	Introduction	31
4.2	Quarter car model	31
4.3	Half car model	32
4.4	Full car model	33
4.5	Conditions of Analysis	43
4.6	The input of parameter	45
4.7	Assumptions	46
4.8	Results	47
5.	DISCUSSIONS	
5.1	Chassis analysis	49
5.1.1	Static analysis	49
5.1.2	Bumping analysis	51
5.1.3	Braking analysis	51
5.1.4	Chassis torsional stiffness analysis	52
5.2	Suspension system analysis	53
5.2.1	Bouncing performance	53
5.2.2	Pitching performance	54
5.2.3	Rolling performance	54
5.2.4	Comparison performance in different stiffness	55

6.

RETROFITTING OF CNG CONVERSION KIT

6.1 Why is the Need for Retrofitting?	58
6.2 CNG Conversion Vehicle Requirements	58
6.2.1 Bi-fuel System and Dual-fuel System	59
6.2.2 Optimize System	60
6.2.3 CNG Operation System	60
6.2.4 Application of CNG in Vehicles	61
6.2.5 Sequential System (Multipoint Sequential Injection System)	65
6.2.6 Catalyst System (Natural Gas System with TN 1 Step Motor regulator and Lambda Control System/2)	65
6.2.7 Carburetor System	67
6.2.8 Economics of Vehicle Conversion to CNG	69
6.3 Retrofitting of the Conversion Kit	70
6.3.1 CNG Tank	71
6.3.2 Filling Valve	72
6.3.3 CNG Cut-off Valves	73
6.3.4 High Pressure Gas Piping	75
6.3.5 Pressure Regulator	76
6.3.6 Fuel Switch Injection	78
6.3.7 Gas Mixer	80
6.3.8 Injector Emulator	83
6.4 Vehicle Test with CNG Conversion Kit	87

7.	CONCLUSIONS AND RECOMMENDATIONS	
	7.1 Conclusions	88
	7.2 Recommendations	90
	BIBLIOGRAPHY	91
	APPENDICES A – G	93

LIST OF SYMBOLS

E	-	Young's Modulus
ρ	-	Mass density
ν	-	Poisson's ratio
n	-	Safety factor
g	-	Gravity (9.81m/s^2)
σ_{yield}	-	Yield stress
$\sigma_{ultimate}$	-	Ultimate tensile stress
$\sigma_{principal}$	-	Maximum principal stress
τ_{max}	-	Maximum shear stress
F, f	-	Force
a, b, w, r	-	Length
δ, z	-	Displacement
T	-	Torsion
θ, φ	-	Angle
M, m	-	Mass
K	-	Stiffness
C, B	-	Damping
$\dot{z}, \dot{\theta}, \dot{\varphi}$	-	Velocity
$\ddot{z}, \ddot{\theta}, \ddot{\varphi}$	-	Acceleration
I_{xx}, I_{yy}	-	Moment of inertia

LIST OF APPENDICES

APPENDIX	TITLE
A	<i>Tramcar</i> properties
B	The result for static analysis
C	The result for bumping analysis
D	The result for braking analysis
E	The result for chassis torsional stiffness analysis
F	The manufacturing drawing of <i>tramcar</i>
G	The picture of <i>tramcar</i>

CHAPTER 1

INTRODUCTION

1.1 Introduction

Transportation systems have come to play a large part in the lives of a significant segment of the world's population. From daily trips to the place of employment, to occasional cross-country business or vacation trips, to once-in-a-lifetime intercontinental emigration, the human race has achieved a level of mobility, which would have been incomprehensible a short time ago.

For several years, the attention of the technical community has been attracted to the vibration environment of those making use of all types of transportation vehicles. For the passengers, discomfort and fatigue due to vibration are major considerations since this will determine their ability to perform tasks or enjoy recreation of their vehicle usages. The impact on safety of the trip, possible deterioration in efficiency and effectiveness in carrying out their duties are also the areas of concern for those who operate the vehicle.

Chassis play an important role in the performance of vehicle. The chassis is the framework of any vehicle. The suspension system, steering and drive train components are mounted into the chassis. Due to that, chassis analysis frequent done by manufacturer to ensure the vehicle stability. The chassis has to be a strong and rigid platform to support all the components. The connections between the chassis, the suspension system and the drive train must be made of rubber to dampen noise, vibration and hardness. The construction of today's vehicles required the use of many different materials. It must strong enough to protect the passenger.

One of the most important systems of the transportation vehicle, particularly when comfort is of interest, is the suspension system. The suspension system provides basic support, guidance, and in some cases propulsion of a vehicle. Suspensions also isolate passenger and freight compartments from disturbances due to roadway irregularities. When the 'softer' suspension, the effects of the irregularities on the vehicle vibration level (passenger comfort) is reduced and also the suspension stroke (rattle space requirement) is increased. When the suspension is harsh, vibration level will be increased while the suspension stroke is reduced. The requirement of achieving both low vibration magnitude and small suspension stroke will create conflicting factors in suspension design and to certain extent limit suspension performance capability.

1.2 Tramcar Background

Faculty mechanical of UTM has developed a non-commercial transport, better known as the *Tramcar*, whose sole purpose is to transport a group of people (visitors) from one point to another within its campus. This mobile platform ultimately can be used for other uses commercially i.e. to ferry people in recreational areas, large indoor exhibition centres, zoos, airports, hotels, and golf resort.

UTM's *Tramcar* is simple in design and construction, and is equipped with a dual-fuel capability. To achieve ease of operation, the concept of "hop-in, hop-out" is incorporated; thus it is not equipped with doors for easy access. It has eight seats in the configuration of two-three-three i.e. two for the front seat (inclusive the driver seat), three in the centre and three in the rear site. These are adjustable seats giving comfort and easy boarding for passengers.

The UTM's *Tramcar* uses a four-cylinder Ford engine equipped with 16 valves and having a displacement of 2000cc. The engine is mounted at the rear of the vehicle thus giving large intermediate volume for high-density

passenger capability. It uses the electronic control 2 way * OD attaching a 4-speed automatic ECT-S transmission system to the engine in the rear engine compartment.

The prototype uses Toyota ST 190 McPherson struts on its both sides of its suspension system. McPherson strut is an independent suspension system, which is small and lightweight yet with very little unsprung mass. It has fewer total components compared to conventional suspension systems and is fairly straightforward to assemble and repair.

The framework of this platform was built based on the twin tube (or common known as ladder frame) configuration. Even it is simple arrangement; it can carry a substantial amount of load. This is largely attributed to the ladder frame that use the welding method to joint the bar, as the stability of chassis is very much depends on the welding joints. Here oblique joints were used to joint all the bars. It is widely believe that the oblique joint can provide a good load arrangement and is able to prevent the abrupt failure of chassis.

1.3 Objectives

The main objective of this project is to produce a versatile people's mover platform within UTM campus, which is environmental-friendly and easy-operation.

The second objective is to analyse the *Tramcar's* chassis and suspension system towards further improvement from the aspect of safety and comfort factors.

The third objective is incorporation of the newly developed vehicle for dual fuel function with the augmentation of a typical CNG conversion kit for flexibility of fuel utilization.

1.4 Project Workscopes

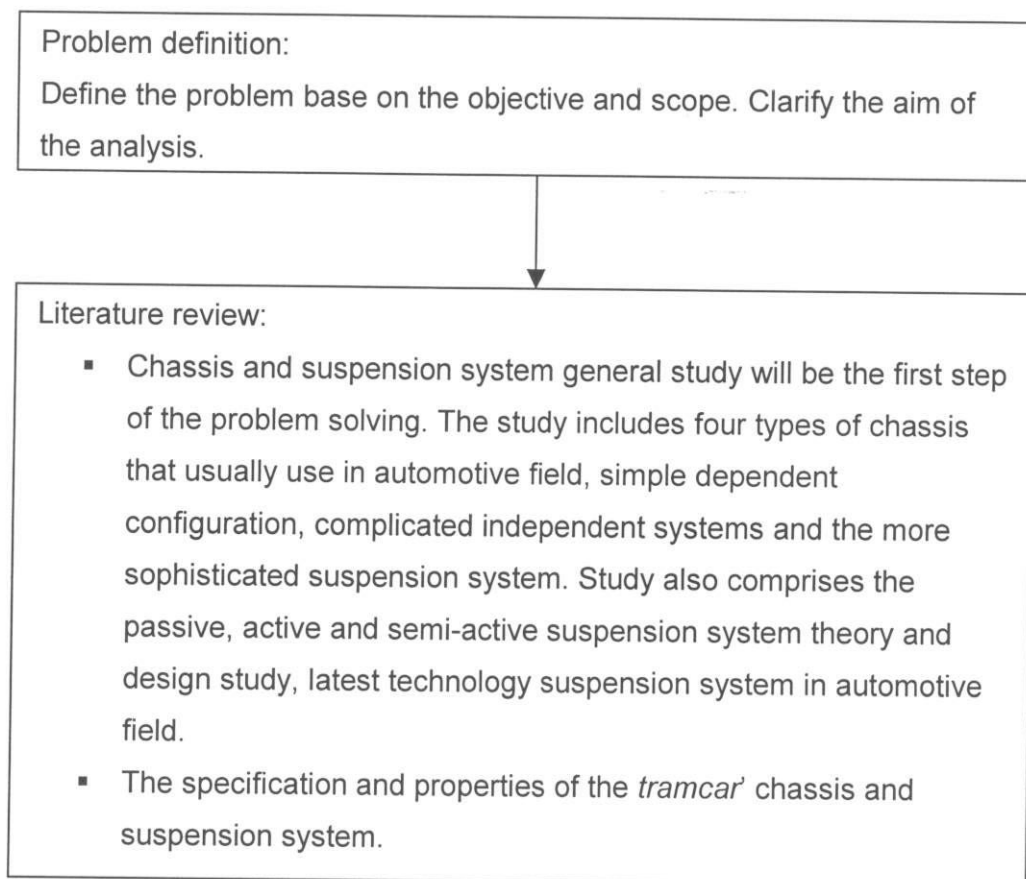
This project focuses on three major objectives mentioned earlier. However development and analysis work take up the bulk of the time allocated for the project.

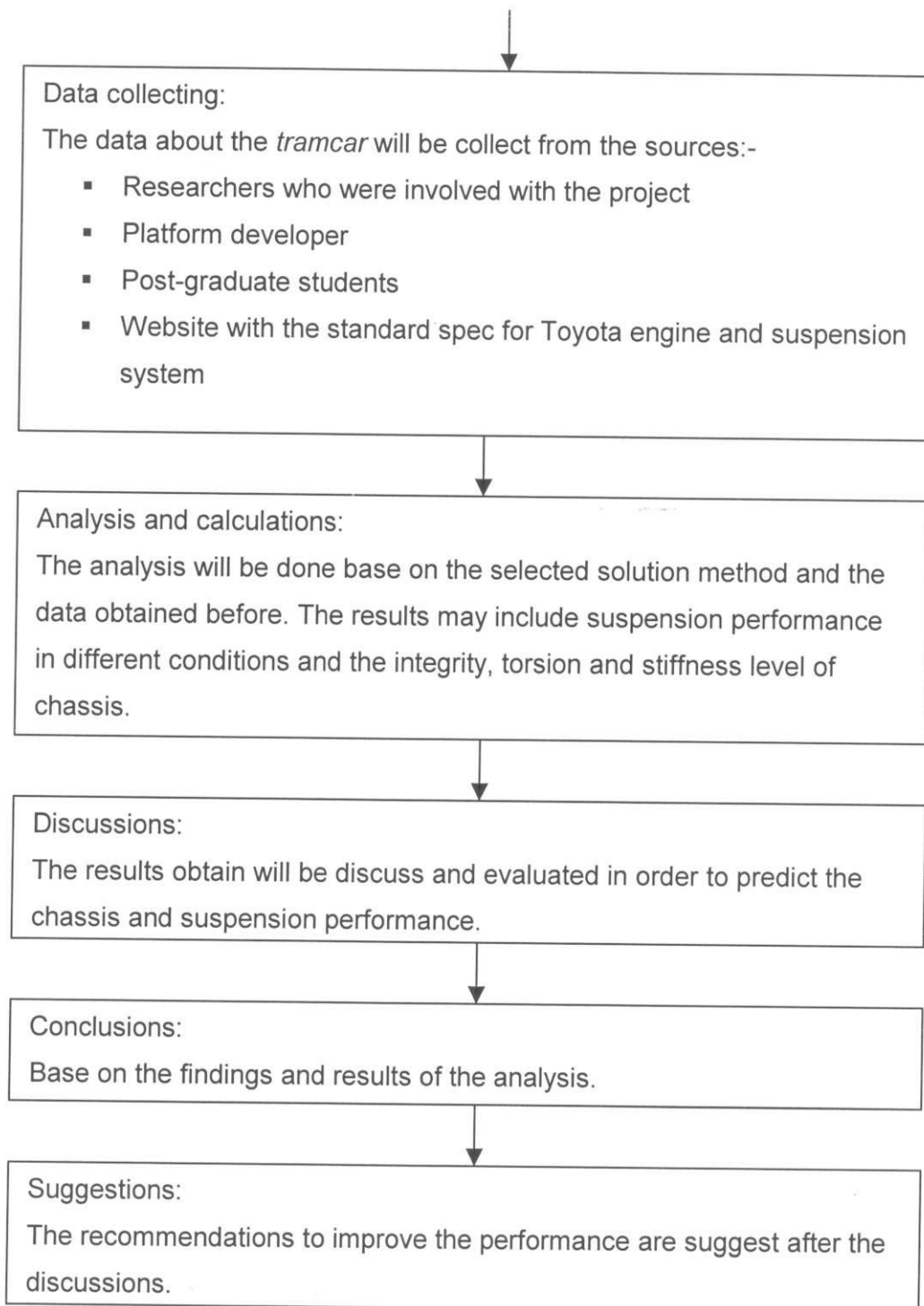
The specifications and properties on the chassis and suspension systems of the *Tramcar* are obtained from a series of discussions made with the group members. The scope in the work include: -

- i. Identify the displacements and stresses of the chassis due to static loadings.
- ii. Analyse the torsion of chassis when the *Tramcar* rides over a bump.
- iii. Analyse the chassis stability when the *Tramcar* undergoes a strenuous conditions such as braking and manoeuvring.
- iv. Obtain the maximum deformation of the structure, displacements and stresses contour.
- v. Dynamic analysis to the suspension system to obtain for: -
 - Bouncing characteristics
 - Pitching characteristics
 - Rolling characteristic

1.5 Methodology

In any analysis work, the general procedures that are usually included are: problem definition, literature review, data collecting, solution method selecting, analysis and calculations, evaluations and documentations. The methodology for the implementation of this project is shown in the flowchart below:-





CHAPTER 2

LITERATURE REVIEW

2.1 Brief Overview of Chassis

Chassis plays an important role in the performance of vehicle. A good chassis must be structurally sound in every way over the expected life of the vehicle and beyond. This means nothing will ever break under normal conditions. Chassis maintain the suspension mounting locations so that handling is safe and consistent under high cornering and bump loads. Besides of that, chassis support the body panels and other passenger components in vehicle so that everything feels solid and has a long and reliable life.

In the real world, few chassis designs will not meet the standard criteria. Major structural failures, even in kit cars are rare. Structural stiffness is the basis of what you feel at the seat of your pants. It defines how a car handles, body integrity and the overall feel of the car. Different basic chassis designs each have their own strengths and weaknesses. Every chassis is a compromise between weight, component size, vehicle intent, and ultimate cost. Even within a basic design method, strength and stiffness can vary significantly, depending on the details. There is no such thing as the ultimate method of construction for every car, because each car presents a different set of problems.

In this section, some types of chassis will be reviewed and one type will be selected for the proposed Tramcar. The types are i) monocoque, ii) twin tube, iii) multi-tube and iv) space frame respectively.

2.1.1 Monocoque

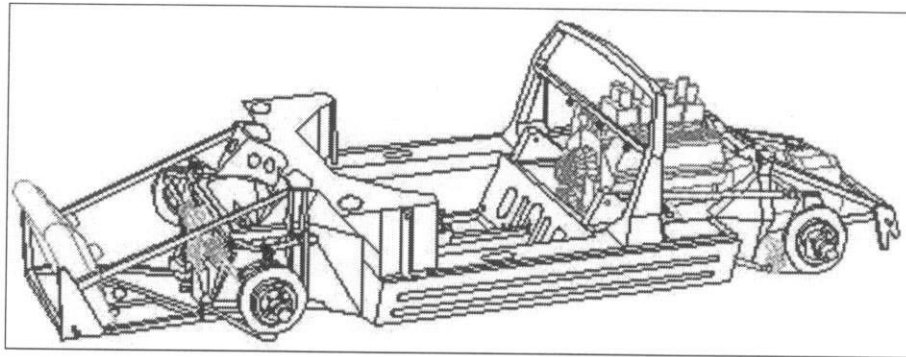


Figure 2.1: Monocoque [Source: *Automotive Engineering*, SAE].

Monocoque or in French "single shell" means unibody is a construction technique that utilizes the external skinning of an object to form most of the structure. This is as opposed to using an internal framework that is then covered with a non-structural skinning. Monocoque construction was first widely used in aircraft. The difference between monocoque with the other frame is monocoque built in unibody but the other frame is in joint form to build a unit of vehicle.

The monocoque skinning itself had significant structural properties of its own. With a sufficient thickness, one could do away with all of the internal structure. However this would be even heavier than the framing would have been. At thinner gauges the skinning could easily provide the structure for tension and shearing loads (metal resists being pulled apart quite well), and if it was bent into a curve or pipe, it became quite strong against bending loads as well. The only loading it could not handle on its own, at least in thin "skins" is compression. Combining this sort of structural skin with a greatly reduced internal framing to provide strength against compression led to what is known as "semi-monocoque".

In the post-war period the technique became more widely used in other areas. It is now used quite commonly in automobile construction as well. In this application it is common to see true monocoque frames, where the

structural members around the window and door frames are built by folding the skinning material several times. In these situations the main concern is spreading the load evenly, having no holes for corrosion to start, and reducing the overall workload. Compared to older techniques where a body would be bolted to a frame, monocoque cars are less expensive and stronger.

2.1.2 Twin Tube

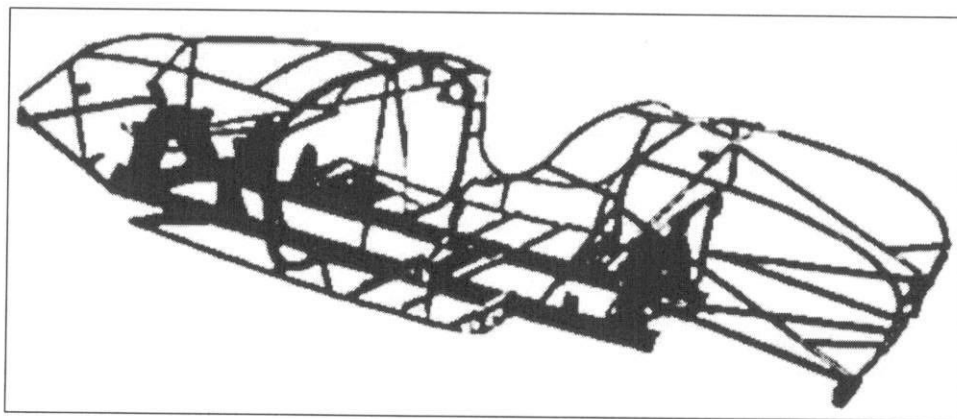


Figure 2.2: Ladder Frame [Source: *Automotive Engineering*, SAE].

Twin tube or known as ladder frame is the most simply frame among the others frame. The ladder frame is a shorthand description of a twin-rail chassis, typically made from round or rectangular tubing or channel. It can use straight or curved members, connected by two or more cross members. The cross member provide more strength to chassis and as a place to mount the seat. It is not necessary to use the same dimension for whole member in ladder frame.

Usually all members are joint by welding to build up a chassis and oblique joint use for the different dimension member. Oblique joint provides a good load arrangement and able to prevent the failure of chassis. Body mounts are usually integral outriggers from the main rails, and suspension points can be well or poorly integrated into the basic design.

Advantages of the ladder frame that are often overlooked are that the available space and ease of access to mechanical parts is often better and engine exhaust systems are less likely to be restricted by the need to route them around chassis tubes. Additional structures are often required with ladder frames to support bodywork but these can often be designed to brace the basic chassis structure. Ladder frame give a low performance in bending and torsional loads. However, it is the most easy and cheap for fabrication.

2.1.3 Multi Tube

Multi tube frame is described as a frame that has four side rails. It acts between the ladder frame and space frame. As ladder frame, multi tube frame also use cross member and diagonal member to improve its strength.

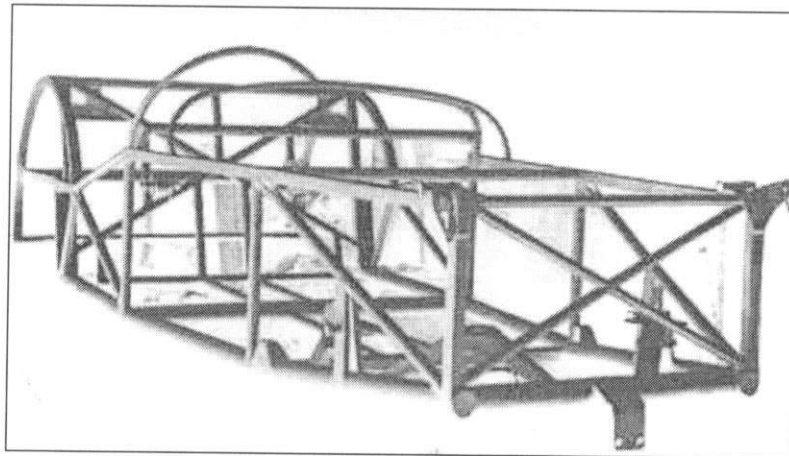


Figure 2.3: Multi Tube [Source: *Automotive Engineering*, SAE].

Multi tube chassis design is as much an art as a science. The art comes in deciding where to put the tubes so as best to connect and support all the hundreds of components, without using more than an absolute minimum number of tubes, and equally, an absolute minimum of sheet or plate in the brackets.

The bending performance for multi tube chassis is base on the diagonal member that used in the frame. The diagonal member will prevent whole chassis to occur deformation. The tube dimension and the total tube used in frame will influence the torsional performance. More the tubes used in the frame then better its torsion stiffness. Hence it will cause to increase the vehicle weight.

2.1.4 Space Frame

Space frame is a complexity frame. A true space frame has small tubes that are only in tension or compression with no bending or twisting loads. The chassis build from hundreds of separate tubes. It was difficult to build and a nightmare to fix. The space frame that is currently used for chassis simply uses smaller tubes, many carrying bending and torsional loads. If compare to ladder frame and multi tube frame, space frame able to provide a good performance in bending and torsional loads.

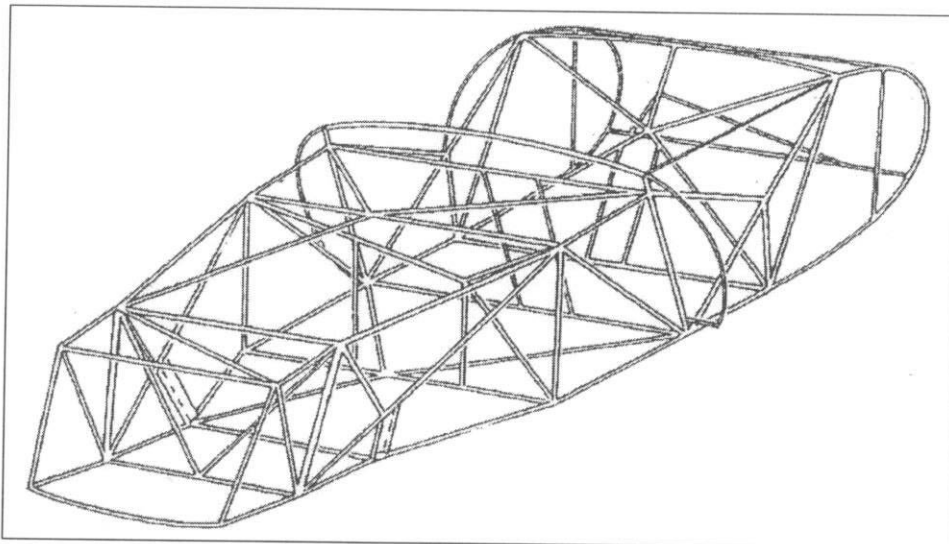


Figure 2.4: Space Frame [Source: *Automotive Engineering*, SAE].

Besides, space frame able to resist the impact forces. Space frame will absorb the momentum and arrange the momentum to whole body. Therefore, space frame can minimize the damage of passenger if the vehicles going to accident in high speed by reduce the load to passenger. Even through the space frame is the most efficient frame, but it is not effective in the cost. This is because it uses more tube and integrating work.

2.1.5 Choice

Having look and carefully examined the prospect of each of one of the possible concept. The multi-tube chassis was selected as it offers cost-effective for this project as the budget constrains heavily limits the choice available.

2.2 Suspension Systems

All dynamic vehicles have suspension systems. Commercial automobiles and trucks, motorcycles, road and mountain bikes and even shoes can be considered dynamic vehicles. By their nature, dynamic vehicles are concerned with motion and the generation of motion. With the motion, come forces, moments and accelerations that act on the vehicles, creating stresses, loads and moments on specific components and systems. The behaviour and response of the vehicle is dependent upon the forces imposed on that system from the external world. For wheeled and tired vehicles, the forces and moments generated by the tire's interaction with the ground are transmitted through the suspension system and create loads and moments at the chassis attachment points.

In the context of vibration theory, the suspension system is just a vibratory system with essential ingredients being inertial and elastic elements, and the central phenomenon is the cyclic interchange of kinetic and potential energies. Damping is essential for controlling the vibration. Damping is the

removal of energy from the oscillating system either by dissipating within the system or by transmission (radiation) away from the system. If the damping is light, the dynamical behaviour of the suspension system is principally determined by the relatively large elastic and inertial forces. The conventional suspension usually consists of springs as elastic elements, masses of various parts of the vehicle as inertial elements and shock absorber (dampers) as devices to provide damping. All of those elements are passive in the sense that no power is required from outside of the system. Such a suspension system is said to be a passive suspension system.

In the context of automatic control theory, the suspension system is a system that provides the desired control forces so that the vehicle body behaves in the desired manner. Optimal control theory has been used to determine the desired control forces of the suspension system. Unfortunately, the optimum suspension system cannot be implemented using only passive elements. The implementation of such a suspension system requires active force generators and thus power has to be supplied to the suspension system from an external source. For the reason that it requires an external power supply, it is called an active suspension system. Although, an active suspension shows better performance over a prescribed frequency band than that of the best possible passive system, or accomplishes a task that is not possible for a passive one, it must be admitted that active suspension, in general, are more costly, more complex and therefore, often less reliable than passive suspensions. To date, the use of the active suspension has been limited to cases of which performance gains outweigh the disadvantages of increased cost, complexity and weight.

A compromise between the active suspension and the passive one is called the 'semi-active' suspension system. In this type of suspension, some of the active suspension advantages are realized while using almost passive components in term of cost and complexity. Springs are still used as elastic elements as in the case of the passive suspension, but dampers are activated. The activated damper is a self-power, high-gain device which derives its control power from the disturbance of the roadway. In other words,

the damper force is generated totally passively as in a conventional damper. Only a small power source is required for instrumentation, signal-processing and low-power servos within the damper. For the fact that this suspension system uses only a small amount of externally supplied power, it is called a 'semi-active' suspension system. A significant advantage over fully active suspension is its fail-safe malfunction. Failure in the control circuitry cannot destabilize the system since the activated damper cannot supply power to the vehicle body. Most failures simply turn the semi-active damper back into a passive one which, however, may be stiffer or softer than desirable.

Several suspension systems will be discussed and outlined in this section, starting with a simple dependent configuration (solid axle, four link and De-Dion), progressing through more complicated independent systems (trailing arm suspensions) and finally discussing a more sophisticated suspension system like the McPherson Strut, multi link and double wishbone.

2.2.1 Solid Axle

In a solid axle configuration, the wheels are mounted on either side of a rigid beam. The motion of the wheels is therefore tied together and any motion experienced by one of the wheels is transmitted to the opposite wheel. The wheels act as like a coupled pair. It is a dependent suspension system, and consequently, the wheels must steer and track together. The advantage of a solid axle suspension is that the wheel camber is not affected by body roll. The disadvantages are that the sprung mass (mass of the axle, wheels and the suspension components) tends to be very high and that the volume required to package the suspension components (shock and leaf springs) tends to be significant.

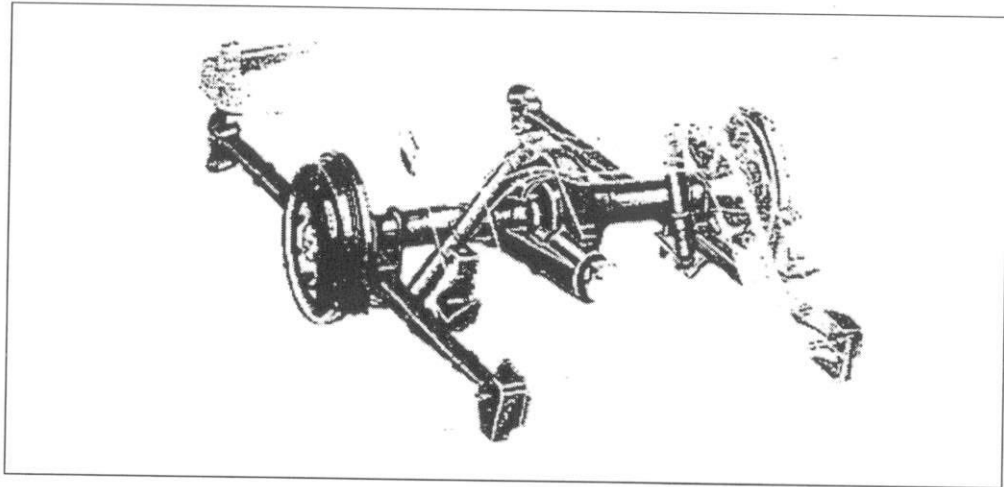


Figure 2.5: Solid Axle [Source: *Automotive Engineering*, SAE].

2.2.2 Four Link

Similar to the solid axle configuration, the wheels are mounted on either side of a rigid beam. The leaf springs are removed and replaced with coil springs and shocks absorbers. The rear differential is removed from the rear axle, thereby reducing the unsprung mass. The response of the axis is governed by the addition of linkages from the axle to the chassis. As is the case with the solid axle, the motions of the wheels are tied together.

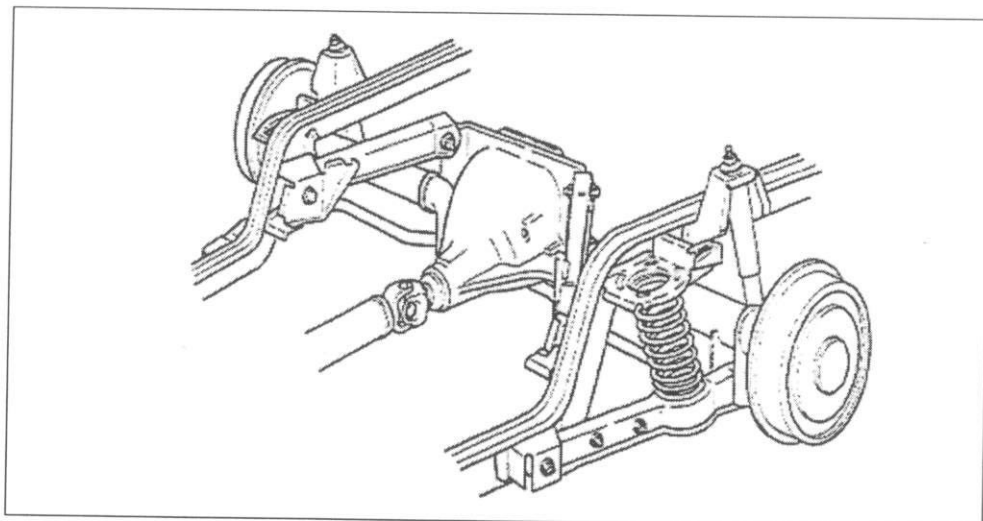


Figure 2.6: Four Link [Source: *Automotive Engineering*, SAE].

2.2.3 De-Dion

It consist of a cross tube between two driving wheels with a chassis mounted differential and half shaft. Trailing arm on each side supported the body by coil springs on it. The advantages are less interior space for rigid axle room and less differential weight for the gross vehicle weight. However, it needs sliding tube and half shaft as adding part of the suspension components. The main linkage components with its supporting axes are: trailing arm for x-axis; sliding tube and trailing arm for y-axis; leaf spring and damper for z-axis. The torque from acceleration and deceleration are by the semi elliptic leaf spring.

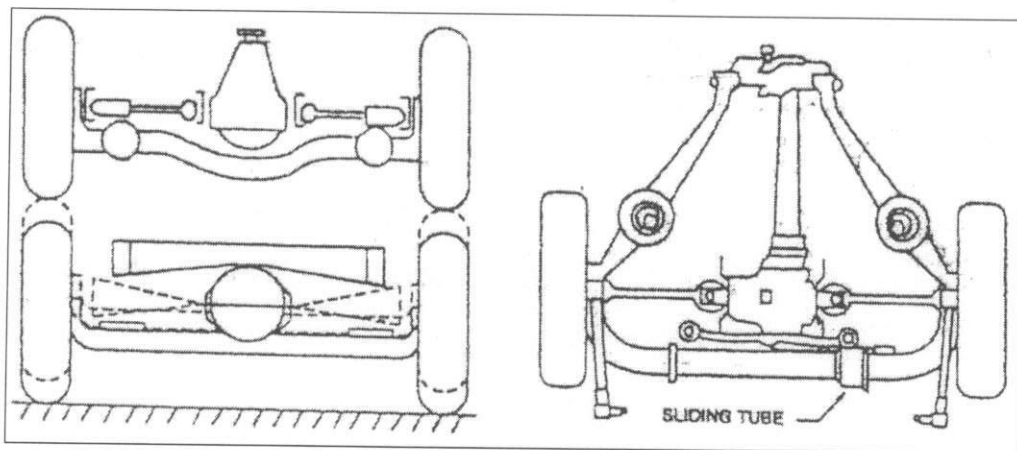


Figure 2.7: De-Dion [Source: *Automotive Engineering*, SAE].

2.2.4 Trailing Arm

The trailing arm suspension system is an independent suspension system. This suspension system allows for each wheel to move as a separate entity, without affecting the motion of the opposite wheel. By decoupling the wheels, the roll centre for each wheel is easier to control by geometrical design. Independent suspension systems allow for more efficient use of the packaging space restrictions of the automobile and provide a smoother passenger ride compared with the dependent suspension systems, with less overall vibration noise. Generally, independent suspension systems are less costly than alternative suspension systems.

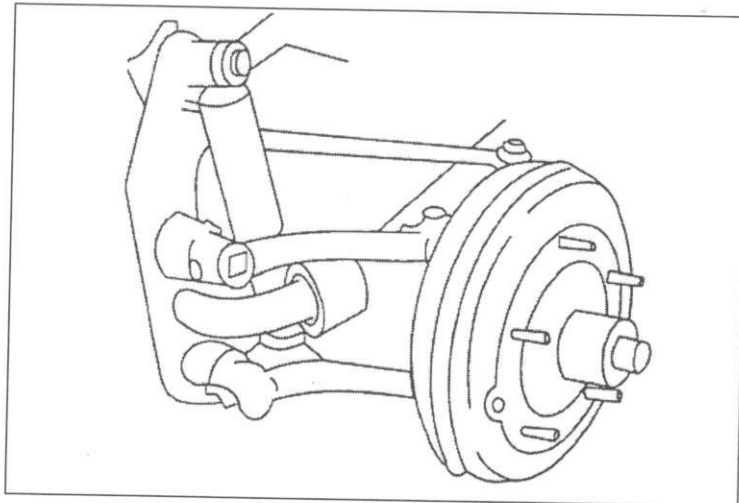


Figure 2.8: Trailing Arm [Source: *Automotive Engineering*, SAE]

The trailing arm suspension was developed as the first attempt at an independent suspension system. It uses parallel, equal length trailing arms connected to torsion bars. The torsion bars provide the springing action for the wheel. There is no coil spring or leaf spring.

2.2.5 McPherson Strut

The McPherson strut uses geometry with unequal arms. The primary advantage of the McPherson strut independent suspension system is that it is small and lightweight, with very little unsprung mass. It is also compact, but does tend to be large in the z-axis (tall). The McPherson strut suspension also has fewer total components compared to alternative rear suspension systems and is fairly straight forward to assemble and to repair. Another advantage of the McPherson suspension system is that the loads act as distributed loads over larger areas of the body structure.

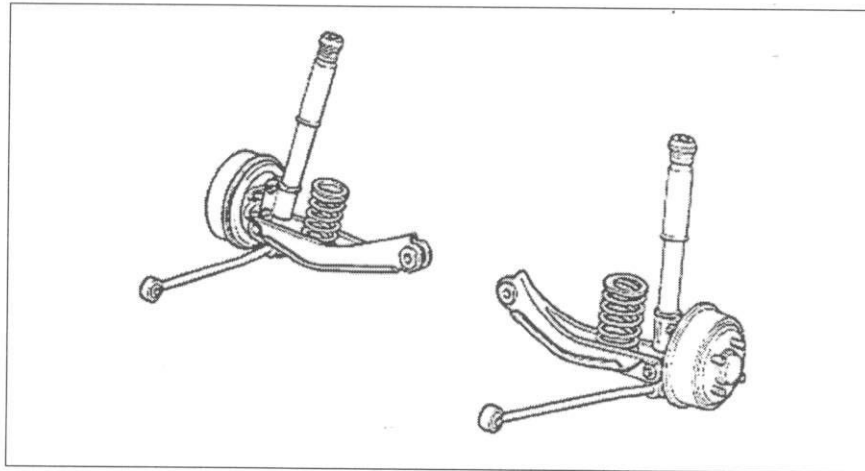


Figure 2.9: McPherson Strut [Source: *Automotive Engineering*, SAE]

2.2.6 Quadra Link

The Quadra link or multi link rear suspension utilizes the McPherson strut (shock absorber-coil spring) arrangement with three or four additional links. The suspension is positioned and controlled by use of the linkages. The multi-link rear suspension system is characterized by the use of radial bushings at the linkage ends, so that-plane bending moments are eliminated. The bushings are compliant, allowing for accurate control of the toe angle during cornering.

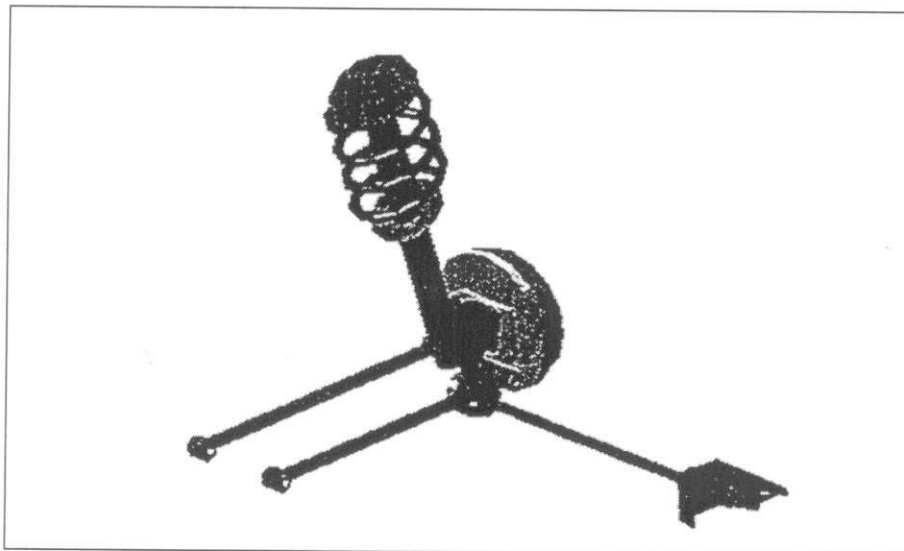


Figure 2.10: Quadra Link [Source: *Automotive Engineering*, SAE].

2.2.7 Double Wishbone

The double wishbone uses two 'A' shape lateral arms connected the wheel to the vehicle body. Usually the upper arm is shorter than the lower one. This unequal length characteristic will cause negative cambering during wheel vertical displacement. This suspension is suitable for front engine with rear wheel drives cars. There are few types recently for deferent suspension function design. The cambering effect will keep the outer turning wheel always straight to the road surface for good handling. Its geometry design required less space, able to assembly the rear deferential and driving shafts. The disadvantages are requiring careful refinement and accurate geometry design because of its kinematics abilities. Besides, cambering will cause track changing then increase tire wearing. The lower and upper control arm will support all the forces accept vertical forces, which acting on the coil spring and damper component.

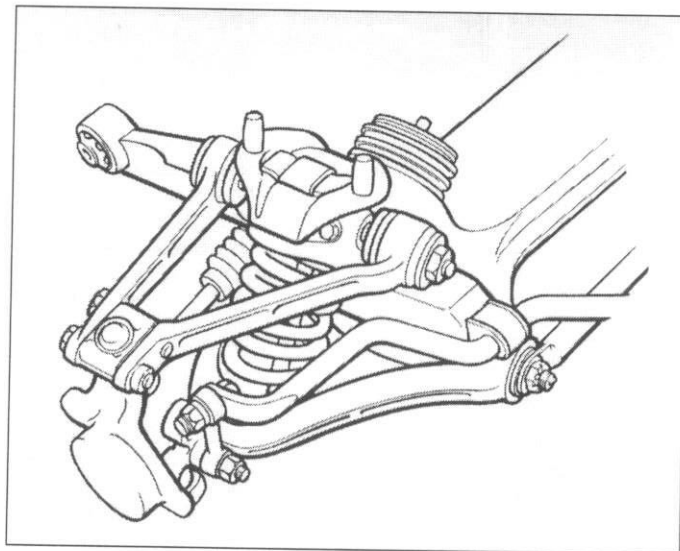


Figure 2.11: Double Wishbone [Source: *Automotive Engineering*, SAE].

CHAPTER 3

CHASSIS ANALYSIS

3.1 Introduction

Strength, rigidity and stiffness are the main concerns of constructing a supportive chassis for a vehicle. The chassis should be able to withstand the appropriate loads on and off the racetrack to ensure a high level of safety and performance. Chassis is frameworks that support the entire component in the car such as suspension system, seat, driver and engine. Even the framework of *Tramcar* is simple, but I need to know the maximum deformation of the chassis when all the loadings applied. Besides, I also need to know the torsional stiffness of the chassis when some cases occur, such as braking or one of the four wheels ride over a bump or into a hole.

In this thesis, all the deformation, stresses, contour and safety factor of the chassis analysed by using *visualNastran*. The drawing of chassis imported from *SolidWorks* into *VisualNastran* by ACIS file to make easier for analysis. Constraint fixed for each analysis. After the analysis in *VisualNastran*, we obtained the value of: -

- i. Maximum Von Mises stress/strain
- ii. Maximum shear stress/strain
- iii. Maximum principal stress/strain
- iv. Total displacement
- v. Safety Factor, n

3.2 Input Material Specifications

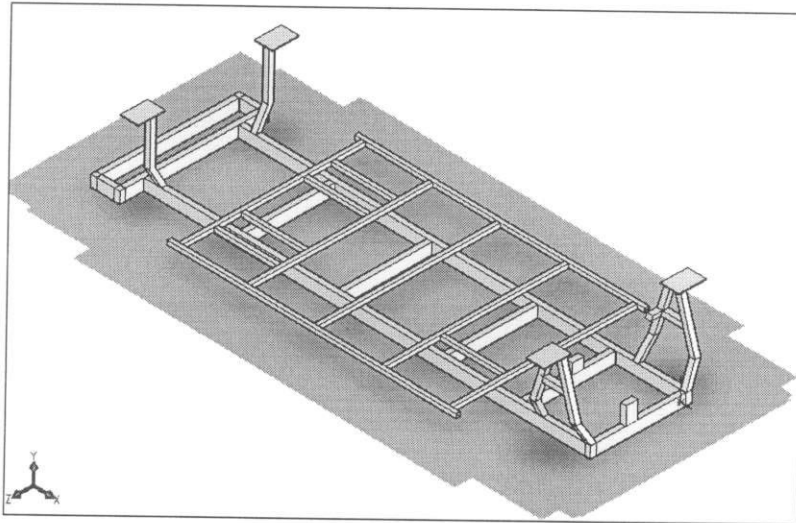
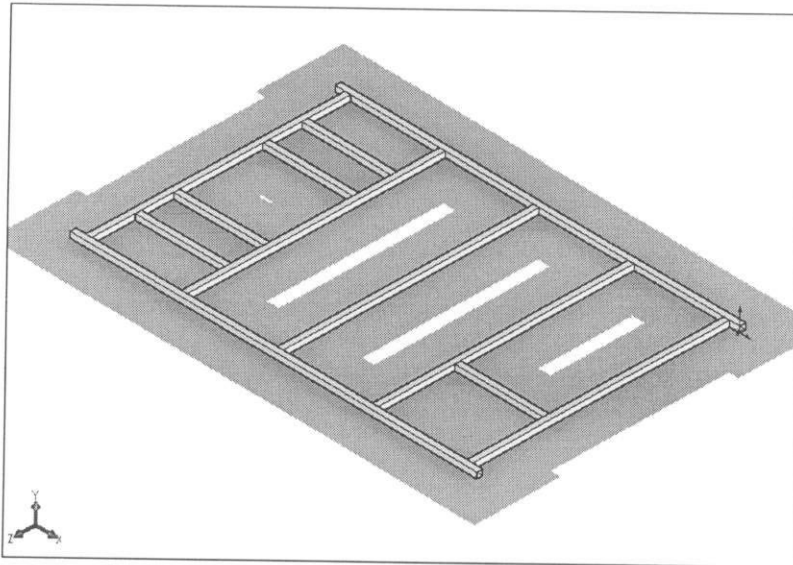


Figure 3.1: *Tramcar* chassis.

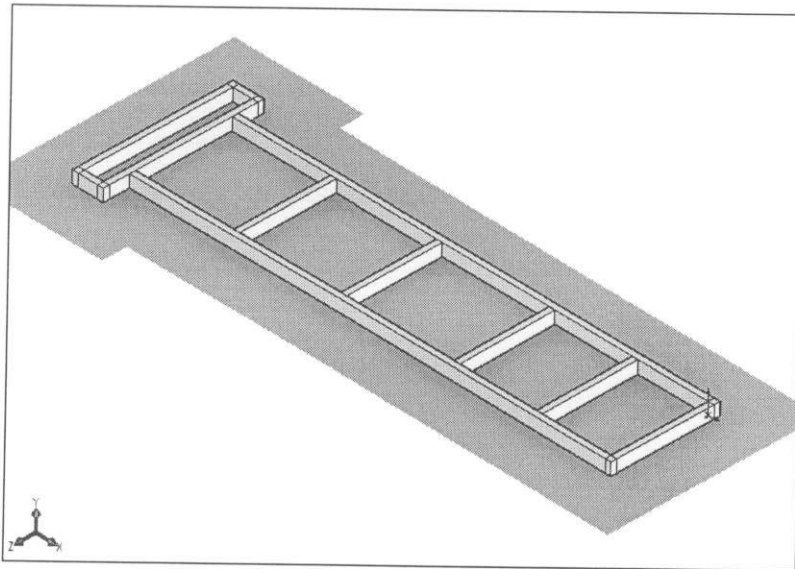
Figure 3.1 shows the isometric view of the *Tramcar* chassis design. Figure 3.2 and Figure 3.3 on the other hand show the upper and lower ladder frameworks associated with the chassis. The material selected is Structure Steel of ANSI i.e. the C1020 type. The material has the following properties: -

- Young's Modulus, E : 200GPa
- Yield stress, σ_{yield} : 331MPa
- Ultimate tensile stress, σ_{ultimate} : 448MPa
- Mass density, ρ : 7850kg/m³
- Poisson's ratio, ν : 0.29



Width : 38.10mm
Height : 38.10mm
Thickness: 2.50mm

Figure 3.2: The upper ladder frame



Width : 50.00mm
Height : 100.00mm
Thickness: 4.00mm

Figure 3.3: The lower ladder frame

3.3 Assumptions

The static and equivalent dynamic analyses were carried out with the assumption that material is of linear elastic. All joints were assumed to be perfectly welded or bonded. The structures were rested on a flat ground and fixed at the given bolting positions.

3.4 Loadings Applied

Before the analysis can be initiated, the boundary conditions were firstly set up. For this *Tramcar* chassis, the loads applied on it are estimated as given in the table below: -

Table 3.1: The loads applied on the chassis

Components	Estimated weight [kg]
Chassis	204.35
Seats and passengers	720.00
Engine	300.00
Tank with full petrol	30.80
Front cover body	23.00
Rear cover body	16.30
Cover roof	69.55
Others	300.00
Vehicle curb weight	984.00
Vehicle gross weight	1664.00

3.5 Static analysis

The static analysis was made to determine the safety factor of the chassis when the *Tramcar* was in a static condition. The loads due to passengers were taken in account in this analysis.

3.5.1 Boundary Conditions

For the static analysis, the boundary conditions were as follows: -

1. The entire load was applied to the chassis
2. Constraints are fixed onto the front and the rear suspension bars
3. 1g of force was applied on $-y$ direction.

3.5.2 Results

All the results of the contours are shown in Appendix B. The values can be summarized as follows: -

- | | |
|-------------------------------|-----------------------|
| i. Maximum Von Mises stress | (Figure B1): 101MPa |
| ii. Maximum shear stress | (Figure B2): 53.8MPa |
| iii. Maximum principal stress | (Figure B3): 113MPa |
| iv. Maximum Von Mises strain | (Figure B4): 0.000436 |
| v. Maximum shear strain | (Figure B5): 0.000694 |
| vi. Maximum principal strain | (Figure B6): 0.000531 |
| vii. Total displacement | (Figure B7): 4.23mm |
| viii. Safety Factor, n: | |

The safety factors are calculated as follows,

$$n = \frac{\sigma_{yield}}{\sigma_{principal}} = \frac{331 \times 10^6}{113 \times 10^6} = 2.93 \quad (\text{Normal stress}) \text{ --- (Eq 3.1)}$$

$$n = \frac{\sigma_{yield}}{2\tau_{max}} = \frac{331 \times 10^6}{2 \times 53.8 \times 10^6} = 3.08 \quad (\text{Shear stress}) \text{ --- (Eq 3.2)}$$

3.6 Bumping Analysis

The bumping analysis has been done to know the safety factor of chassis when the *Tramcar* rides over a bump.

3.6.1 Boundary Conditions

In bumping analysis, the boundary conditions were set as follows: -

1. The entire load was applied to the chassis.
2. Constraints fixed in front and rear suspension bar.
3. 2g of force was applied on the y -direction.

3.6.2 Results

All the results in the form of contour lines are shown in Appendix C. The values can conclude as below:-

- i. Maximum Von Mises stress (Figure C1): 114MPa

- ii. Maximum shear stress (Figure C2): 60.7MPa
- iii. Maximum principal stress (Figure C3): 128MPa
- iv. Maximum Von Mises strain (Figure C4): 0.000492
- v. Maximum shear strain (Figure C5): 0.000783
- vi. Maximum principal strain (Figure C6): 0.000599
- vii. Total displacement (Figure C7): 4.63mm
- viii. Safety Factor, n:

$$n = \frac{\sigma_{yield}}{\sigma_{principal}} = \frac{331 \times 10^6}{128 \times 10^6} = 2.59 \quad (\text{Normal stress})$$

$$n = \frac{\sigma_{yield}}{2\tau_{max}} = \frac{331 \times 10^6}{2 \times 60.7 \times 10^6} = 2.73 \quad (\text{Shear stress})$$

3.7 Braking Analyses

The braking analyses were made to identify the safety factor of the chassis when the *Tramcar* is subjected to a sudden braking.

3.7.1 Boundary Conditions

In undertaking the braking analyses, the boundary conditions were set with the following boundary conditions:-

1. The entire load was applied onto the chassis
2. Constraints fixed in front and rear suspension bars
3. 1g of force was applied in the x-direction

3.7.2 Results

All the results in the form of contours are shown in Appendix D. The values are summarised as below: -

- i. Maximum Von Mises stress (Figure D1): 76.5MPa
- ii. Maximum shear stress (Figure D2): 40.5MPa
- iii. Maximum principal stress (Figure D3): 85.4MPa
- iv. Maximum Von Mises strain (Figure D4): 0.000329
- v. Maximum shear strain (Figure D5): 0.000523
- vi. Maximum principal strain (Figure D6): 0.000400
- vii. Total displacement (Figure D7): 3.72mm
- viii. Safety Factor, n:

$$n = \frac{\sigma_{yield}}{\sigma_{principal}} = \frac{331 \times 10^6}{85.4 \times 10^6} = 3.88 \quad (\text{Normal stress})$$

$$n = \frac{\sigma_{yield}}{2\tau_{max}} = \frac{331 \times 10^6}{2 \times 40.5 \times 10^6} = 4.09 \quad (\text{Shear stress})$$

3.8 Chassis Torsional Stiffness Analysis

The torsional stiffness analysis was implemented to assess the chassis ability to withstand the torsional loading.

3.8.1 Boundary Conditions

In chassis torsional stiffness analysis, the boundary conditions set as follows:

1. Constraints fixed only in rear suspension bar.
2. 1.5kN, 3kN, 4.5kN, 6kN, 7.5kN and 9kN force applied in fore suspension bar on opposite direction.

3.8.2 Results

All the results in the form of contour lines are shown in Appendix E. Examples of calculation to obtain the torsional stiffness are show as follows:

$$\begin{aligned}\text{Torsion, } T &= \text{Applied force} \times \text{Distance (F} \times r) && \text{--- (Eq. 3.3)} \\ &= 9000 \times 0.6275 \\ &= 5647.50 \text{ Nm}\end{aligned}$$

$$\begin{aligned}\text{Twisting Angle, } \theta &= \tan^{-1} \frac{\delta}{r} && \text{--- (Eq. 3.4)} \\ &= \tan^{-1} \frac{0.0121}{0.6275} \\ &= 1.1047^\circ\end{aligned}$$

Here the twist angle is rather low indicating the rigidity of the chassis frame in its totality.

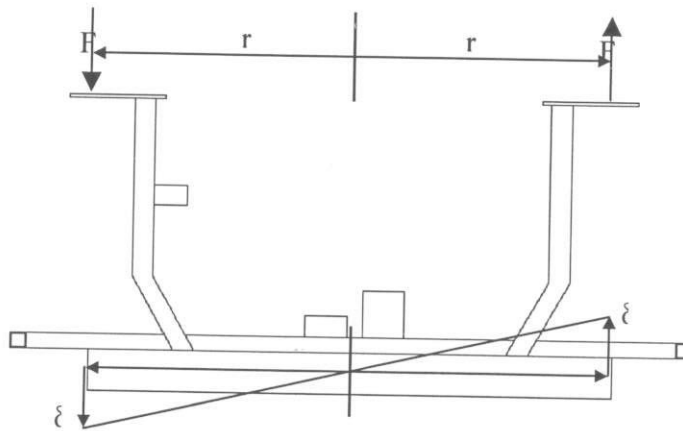


Figure 3.4: The chassis displacement

Table 3.2: Table of applied force, displacement, torsion and twisting angle during torsional stiffness analysis

Applied force, F [N]	Chassis displacement, δ [mm]	Torsion, T [Nm]	Twisting angle, θ [°]
0	0	0	0
1500	2.035	941.25	0.1858
3000	4.015	1882.50	0.3666
4500	6.050	2823.75	0.5524
6000	8.250	3765.00	0.7532
7500	9.900	4706.25	0.9039
9000	12.10	5647.50	1.1047

The values for torsion and twisting angle were used to plot a graph (Figure 3.5). The slope of the graph indicated the chassis torsional stiffness.

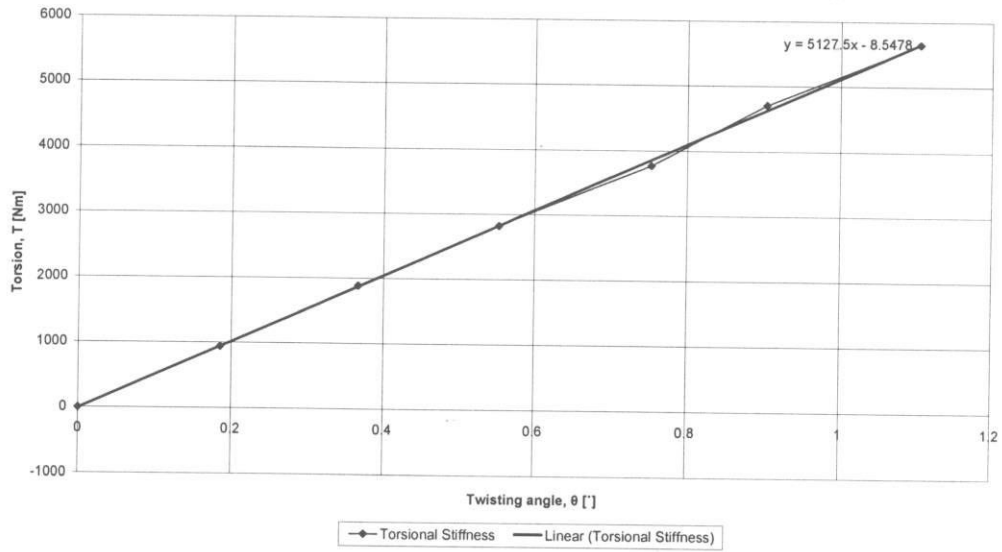


Figure 3.5: Graph torsion increasingly against twisting angle.

CHAPTER 4

SUSPENSION SYSTEM ANALYSIS

4.1 Introduction

Quarter car, half car and full car model can be created to determine the different characteristics of a vehicle under study, to determine for its ride and handling performance respectively. As for the vehicle ride aspect, the important parameters will include i) vehicle displacement, ii) yaw, iii) roll and iv) pitch response.

4.2 Quarter Car Model

The Figure 4.1 shows below the quarter car model representation. The quarter car model is a two degree-of-freedom type that emulates the vehicle body and axle dynamics with a single time respectively.

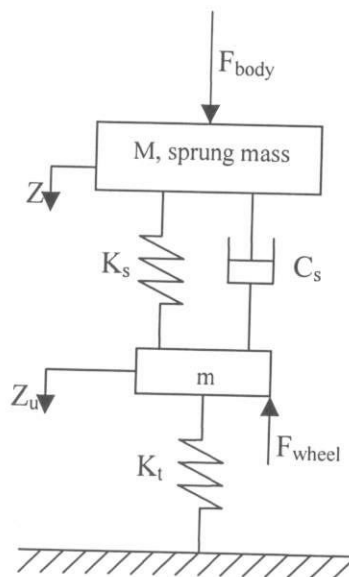


Figure 4.1: Quarter car model representation

For this model, the two degree-of-freedom that can be created is the heave displacement of the unsprung mass. However, model cannot be used to determine the roll and the pitching conditions. This study remains adequate and efficient to determine the many design issues but is not sufficient to warrant for the actual system design purposes.

As an example, the quarter car model is not able to study the influence of the wheelbase filtering mechanism on ride comfort. Half vehicle model is more convenient to design the passive as well as the active suspension systems and to study their influence on the interaction between the body bounce and pitch motions.

4.3 Half Car Model

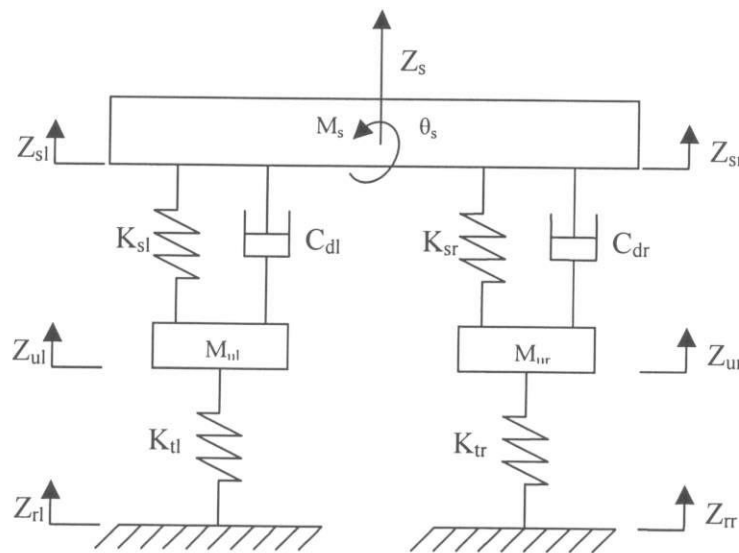


Figure 4.2: Half car model

The Figure 4.2 on the other hand illustrates a half car model of the Tramcar. The half car model is a four degree-of-freedom model that emulates the vehicle body and axle dynamics with a single time.

For a half car model, the four degree-of-freedom that can be created includes the roll or pitch model. The half-car model can either be the half car roll plane or the half car pitch plane.

An example for a half car pitch plane is whereby the vehicle is represented by a sprung mass supported by primary suspension system at each wheel. Here the lateral dynamics of the vehicle are ignored. As a result, only one front tire and one rear tire are considered in the model. The model consists of the sprung mass or car body supported on suspensions at the front and rear. The suspensions are connected to their respective tire axles, which are considered to be un-sprung masses. Additionally, the suspensions have stiffness and damping properties, the tire is represented as a simple spring.

As stated above, the half car model is convenience to determine either the passive susceptible system or active suspension system of their influence on the interaction the vehicle movement include the bounce, pitch or roll motion.

4.4 Full Car Model

Figure 4.3 shows a full car model. The full car model shown is a seven degree-of-freedom model that emulates the vehicle body and axle dynamics with a single time condition. Here the full car model was used to do the simulation since it was thought that the better overall result can be obtained through this technique.

The full vehicle suspension system is represented as a linearized seven degree-of-freedom system. It consists of a single sprung mass (car body) connected to four unsprung masses (front-left, front-right, rear left and rear-right wheels) at each corner.

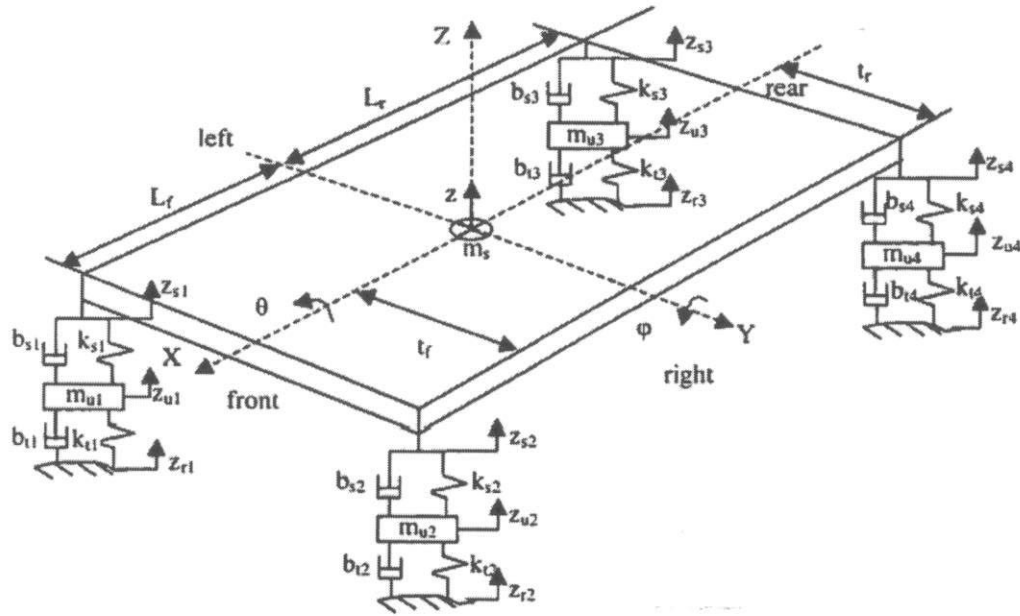


Figure 4.3: Full car model

The sprung mass is free to heave, pitch and roll while the unsprung masses are free to bounce vertically with respect to the sprung mass. The suspensions between the sprung mass and unsprung masses are modelled as linear viscous dampers and spring elements, while the tires are modelled as simple linear springs without damping. For simplicity, all pitch and roll angles are assumed to be small. The full car model can be used to predict more complexity of the vehicle ride and handling characteristic. The full car model can be used to determine the roll and pitch moment in one step compare to the half car model.

After applying a force-balance analysis to the model in Figure 4.3, the equations of motion are given as: -

$$\begin{aligned}
 m_s \ddot{z} = & -m_s g - (2K_{s_f} + 2K_{s_r})z - (2B_{s_f} + 2B_{s_r})\dot{z} + (2aK_{s_f} - 2bK_{s_r})\theta + (2aB_{s_f} - 2bB_{s_r})\dot{\theta} + \dots \\
 & + K_{s_f} z_{u_{fl}} + B_{s_f} \dot{z}_{u_{fl}} + K_{s_f} z_{u_{fr}} + B_{s_f} \dot{z}_{u_{fr}} + K_{s_r} z_{u_{rl}} + B_{s_r} \dot{z}_{u_{rl}} + K_{s_r} z_{u_{rr}} + B_{s_r} \dot{z}_{u_{rr}} + \dots \\
 & + f_{fl} + f_{fr} + f_{rl} + f_{rr}
 \end{aligned}$$

--- (Eq. 4.1)

$$\begin{aligned}
I_{xx}\ddot{\phi} = & -0.25w^2(2K_{s_f} + 2K_{s_r})\phi - 0.25w^2(2B_{s_f} + 2B_{s_r})\dot{\phi} + 0.5wK_{s_f}z_{u_{fl}} + 0.5wB_{s_f}\dot{z}_{u_{fl}} + \dots \\
& -0.5wK_{s_f}z_{u_{fr}} - 0.5wB_{s_f}\dot{z}_{u_{fr}} + 0.5wK_{s_r}z_{u_{rl}} + 0.5wB_{s_r}\dot{z}_{u_{rl}} - 0.5wK_{s_r}z_{u_{rr}} - 0.5wB_{s_r}\dot{z}_{u_{rr}} + \dots \\
& + 0.5wf_{fl} - 0.5wf_{fr} + 0.5wf_{rl} - 0.5wf_{rr}
\end{aligned}$$

--- (Eq. 4.2)

$$\begin{aligned}
m_u\ddot{z}_{u_{fl}} = & -m_u g + K_{s_f}z + B_{s_f}\dot{z} - aK_{s_f}\theta - aB_{s_f}\dot{\theta} + 0.5wK_{s_f}\phi + 0.5wB_{s_f}\dot{\phi} + \dots \\
& - (K_{s_f} + K_u)z_{u_{fl}} - B_{s_f}\dot{z}_{u_{fl}} + K_u z_{r_{fl}} - f_{fl}
\end{aligned}$$

--- (Eq. 4.3)

$$\begin{aligned}
m_u\ddot{z}_{u_{fr}} = & -m_u g + K_{s_f}z + B_{s_f}\dot{z} - aK_{s_f}\theta - aB_{s_f}\dot{\theta} - 0.5wK_{s_f}\phi - 0.5wB_{s_f}\dot{\phi} + \dots \\
& - (K_{s_f} + K_u)z_{u_{fr}} - B_{s_f}\dot{z}_{u_{fr}} + K_u z_{r_{fr}} - f_{fr}
\end{aligned}$$

--- (Eq. 4.4)

$$\begin{aligned}
m_u\ddot{z}_{u_{rl}} = & -m_u g + K_{s_r}z + B_{s_r}\dot{z} + bK_{s_r}\theta + bB_{s_r}\dot{\theta} + 0.5wK_{s_r}\phi + 0.5wB_{s_r}\dot{\phi} + \dots \\
& - (K_{s_r} + K_u)z_{u_{rl}} - B_{s_r}\dot{z}_{u_{rl}} + K_u z_{r_{rl}} - f_{rl}
\end{aligned}$$

--- (Eq. 4.5)

$$\begin{aligned}
m_u\ddot{z}_{u_{rr}} = & -m_u g + K_{s_r}z + B_{s_r}\dot{z} + bK_{s_r}\theta + bB_{s_r}\dot{\theta} - 0.5wK_{s_r}\phi - 0.5wB_{s_r}\dot{\phi} + \dots \\
& - (K_{s_r} + K_u)z_{u_{rr}} - B_{s_r}\dot{z}_{u_{rr}} + K_u z_{r_{rr}} - f_{rr}
\end{aligned}$$

--- (Eq. 4.6)

The system states are assigned as: -

$x_1 = z$	heave position (ride height of sprung mass)
$x_2 = \dot{z}$	heave velocity (payload velocity of sprung mass)
$x_3 = \theta$	roll angle
$x_4 = \dot{\theta}$	roll angular velocity
$x_5 = \phi$	pitch angle
$x_6 = \dot{\phi}$	pitch angular velocity
$x_7 = z_{u_{fl}}$	front-left wheel unsprung mass height
$x_8 = \dot{z}_{u_{fl}}$	front-left wheel unsprung mass velocity

- $x_9 = z_{u_{fr}}$ front-right wheel unsprung mass height
 $x_{10} = \dot{z}_{u_{fr}}$ front-right wheel unsprung mass velocity
 $x_{11} = z_{u_{rl}}$ rear-left wheel unsprung mass height
 $x_{12} = \dot{z}_{u_{rl}}$ rear-left wheel unsprung mass velocity
 $x_{13} = z_{u_{rr}}$ rear-right wheel unsprung mass height
 $x_{14} = \dot{z}_{u_{rr}}$ rear-right wheel unsprung mass velocity

The results of the system state equations analysis are as follows: -

$$\begin{aligned}
 \dot{x}_1 &= x_2 \\
 \dot{x}_2 &= -\frac{(2K_{sf}+2K_{sr})}{m_s}x_1 - \frac{(2B_{sf}+2B_{sr})}{m_s}x_2 + \frac{(2aK_{sf}+2bK_{sr})}{m_s}x_3 + \frac{(2aB_{sf}+2bB_{sr})}{m_s}x_4 + \frac{K_{sf}}{m_s}x_7 + \frac{B_{sf}}{m_s}x_8 + \dots \\
 &\quad + \frac{K_{sf}}{m_s}x_9 + \frac{B_{sf}}{m_s}x_{10} + \frac{K_{sr}}{m_s}x_{11} + \frac{B_{sr}}{m_s}x_{12} + \frac{K_{sr}}{m_s}x_{13} + \frac{B_{sr}}{m_s}x_{14} + \frac{1}{m_s}f_{fl} + \frac{1}{m_s}f_{rl} + \frac{1}{m_s}f_{rl} + \frac{1}{m_s}f_{rr}
 \end{aligned}$$

--- (Eq. 4.7)

$$\begin{aligned}
 \dot{x}_3 &= x_4 \\
 \dot{x}_4 &= \frac{(2aK_{sf}+2bK_{sr})}{I_{yy}}x_1 + \frac{(2aB_{sf}+2bB_{sr})}{I_{yy}}x_2 - \frac{(2a^2K_{sf}+2b^2K_{sr})}{I_{yy}}x_3 - \frac{(2a^2B_{sf}+2b^2B_{sr})}{I_{yy}}x_4 - \frac{aK_{sf}}{I_{yy}}x_7 + \dots \\
 &\quad - \frac{aB_{sf}}{I_{yy}}x_8 - \frac{aK_{sf}}{I_{yy}}x_9 - \frac{aB_{sf}}{I_{yy}}x_{10} + \frac{bK_{sf}}{I_{yy}}x_{11} + \frac{bB_{sf}}{I_{yy}}x_{12} + \frac{bK_{sf}}{I_{yy}}x_{13} + \frac{bB_{sf}}{I_{yy}}x_{14} - \frac{a}{I_{yy}}f_{fl} - \frac{a}{I_{yy}}f_{fr} + \dots \\
 &\quad + \frac{b}{I_{yy}}f_{rl} + \frac{b}{I_{yy}}f_{rr}
 \end{aligned}$$

--- (Eq. 4.8)

$$\begin{aligned}
 \dot{x}_5 &= x_6 \\
 \dot{x}_6 &= -\frac{w^2(2K_{sf}+2K_{sr})}{4I_{xx}}x_5 - \frac{w^2(2B_{sf}+2B_{sr})}{4I_{xx}}x_6 + \frac{wK_{sf}}{2I_{xx}}x_7 + \frac{wB_{sf}}{2I_{xx}}x_8 - \frac{wK_{sf}}{2I_{xx}}x_9 - \frac{wB_{sf}}{2I_{xx}}x_{10} + \dots \\
 &\quad + \frac{wK_{sr}}{2I_{xx}}x_{11} + \frac{wB_{sr}}{2I_{xx}}x_{12} - \frac{wK_{sr}}{2I_{xx}}x_{13} - \frac{wB_{sr}}{2I_{xx}}x_{14} + \frac{w}{2I_{xx}}f_{fl} - \frac{w}{2I_{xx}}f_{fr} + \frac{w}{2I_{xx}}f_{rl} - \frac{w}{2I_{xx}}f_{rr}
 \end{aligned}$$

--- (Eq. 4.9)

$$\begin{aligned}\dot{x}_7 &= x_8 \\ \dot{x}_8 &= \frac{K_{s_f}}{m_u} x_1 + \frac{B_{s_f}}{m_u} x_2 - \frac{aK_{s_f}}{m_u} x_3 - \frac{aB_{s_f}}{m_u} x_4 + \frac{wK_{s_f}}{2m_u} x_5 + \frac{wB_{s_f}}{2m_u} x_6 - \frac{(K_{s_f} + K_u)}{m_u} x_7 - \frac{B_{s_f}}{m_u} x_8 + \dots \\ &\quad - \frac{1}{m_u} f_{fl} - g + \frac{K_u}{m_u} z_{r_{fl}}\end{aligned}$$

--- (Eq. 4.10)

$$\begin{aligned}\dot{x}_9 &= x_{10} \\ \dot{x}_{10} &= \frac{K_{s_f}}{m_u} x_1 + \frac{B_{s_f}}{m_u} x_2 - \frac{aK_{s_f}}{m_u} x_3 - \frac{aB_{s_f}}{m_u} x_4 - \frac{wK_{s_f}}{2m_u} x_5 - \frac{wB_{s_f}}{2m_u} x_6 - \frac{(K_{s_f} + K_u)}{m_u} x_9 - \frac{B_{s_f}}{m_u} x_{10} + \dots \\ &\quad - \frac{1}{m_u} f_{fr} - g + \frac{K_u}{m_u} z_{r_{fr}}\end{aligned}$$

--- (Eq. 4.11)

$$\begin{aligned}\dot{x}_{11} &= x_{12} \\ \dot{x}_{12} &= \frac{K_{s_r}}{m_u} x_1 + \frac{B_{s_r}}{m_u} x_2 + \frac{bK_{s_r}}{m_u} x_3 + \frac{bB_{s_r}}{m_u} x_4 + \frac{wK_{s_r}}{2m_u} x_5 + \frac{wB_{s_r}}{2m_u} x_6 - \frac{(K_{s_r} + K_u)}{m_u} x_{11} - \frac{B_{s_r}}{m_u} x_{12} + \dots \\ &\quad - \frac{1}{m_u} f_{rl} - g + \frac{K_u}{m_u} z_{r_{rl}}\end{aligned}$$

--- (Eq. 4.12)

$$\begin{aligned}\dot{x}_{13} &= x_{14} \\ \dot{x}_{14} &= \frac{K_{s_r}}{m_u} x_1 + \frac{B_{s_r}}{m_u} x_2 + \frac{bK_{s_r}}{m_u} x_3 + \frac{bB_{s_r}}{m_u} x_4 + \frac{wK_{s_r}}{2m_u} x_5 - \frac{wB_{s_r}}{2m_u} x_6 - \frac{(K_{s_r} + K_u)}{m_u} x_{13} - \frac{B_{s_r}}{m_u} x_{14} + \dots \\ &\quad - \frac{1}{m_u} f_{rr} - g + \frac{K_u}{m_u} z_{r_{rr}}\end{aligned}$$

--- (Eq. 4.13)

All the equations stated above are then converted to simulate the performance using simulation tool i.e. *Matlab ver 6.5*. For easy reference the diagrams for models used are shown below.

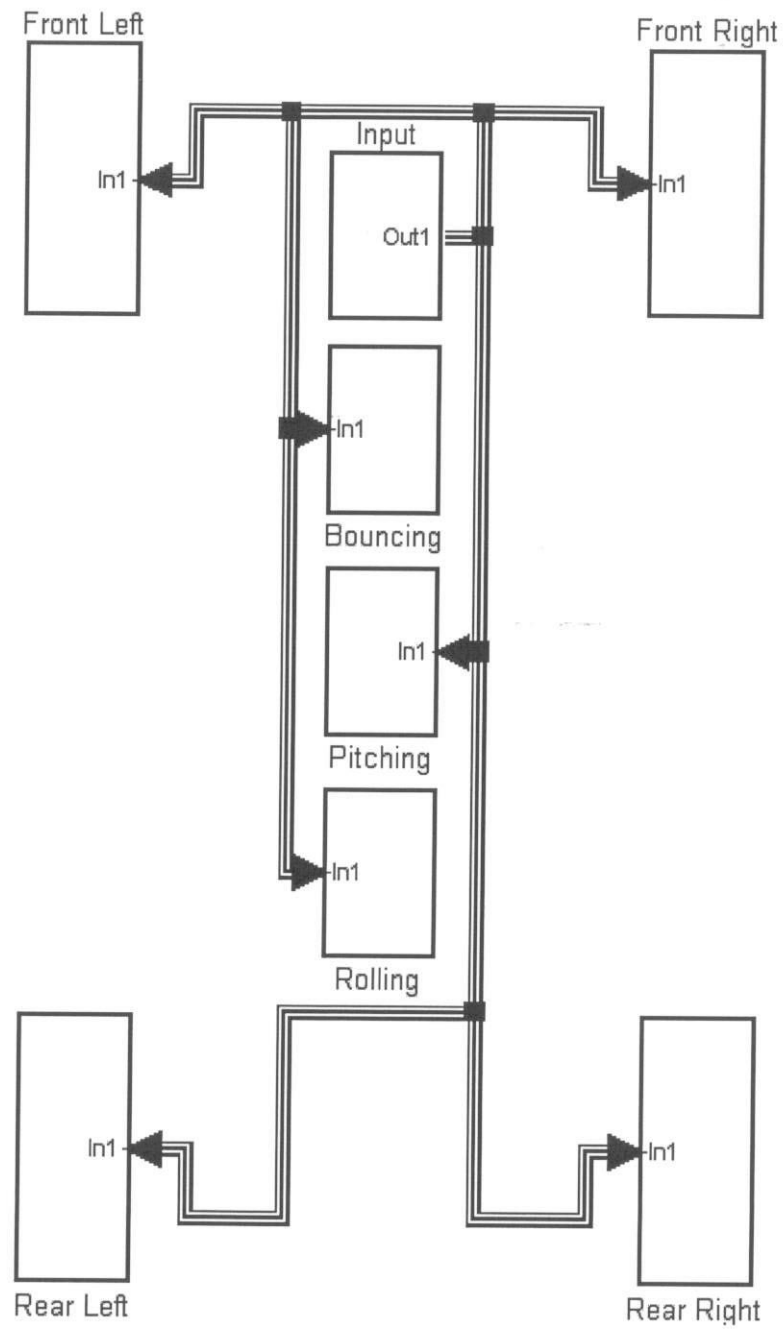


Figure 4.4: The full system of full car model

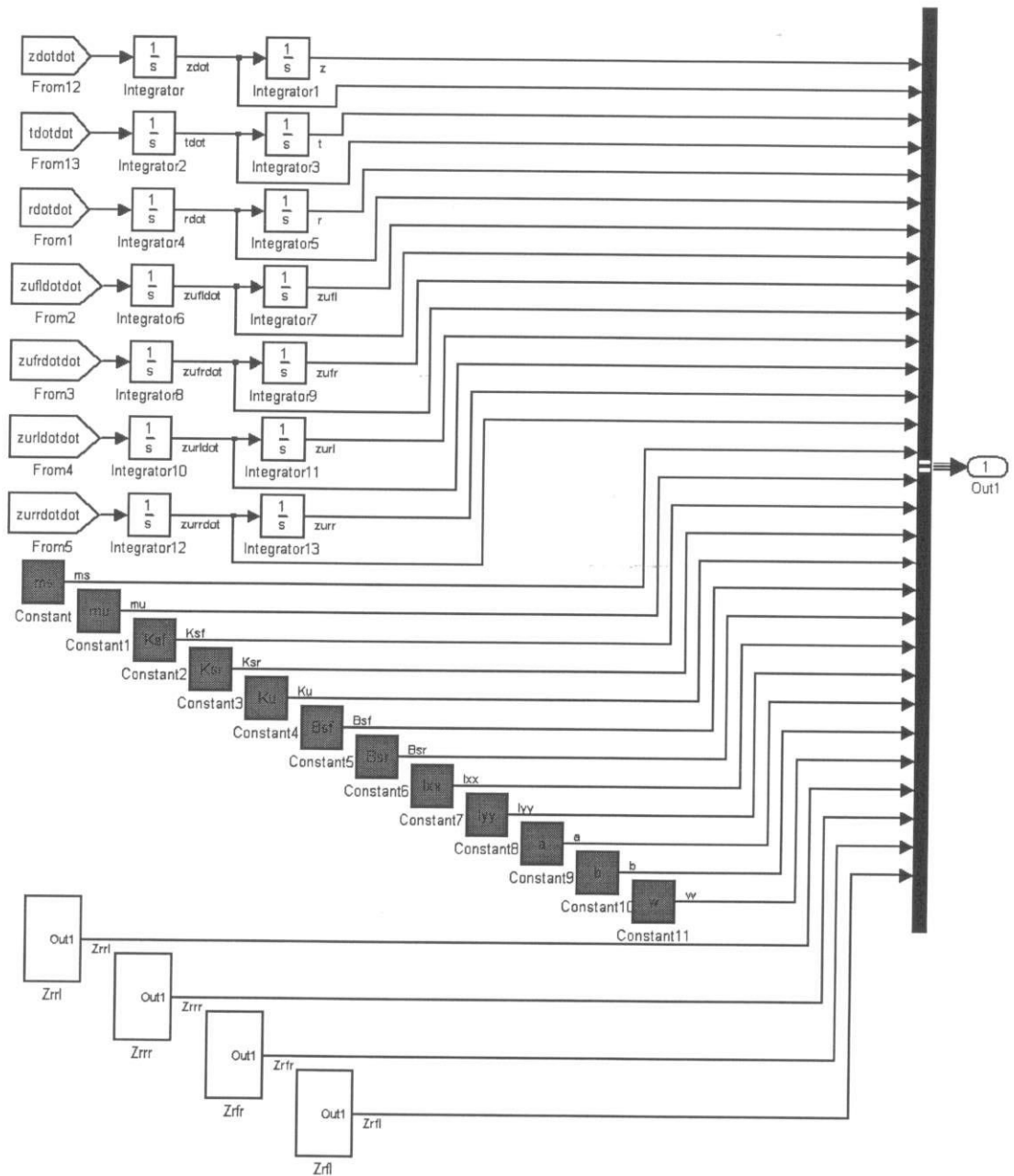


Figure 4.5: The inputs for the system

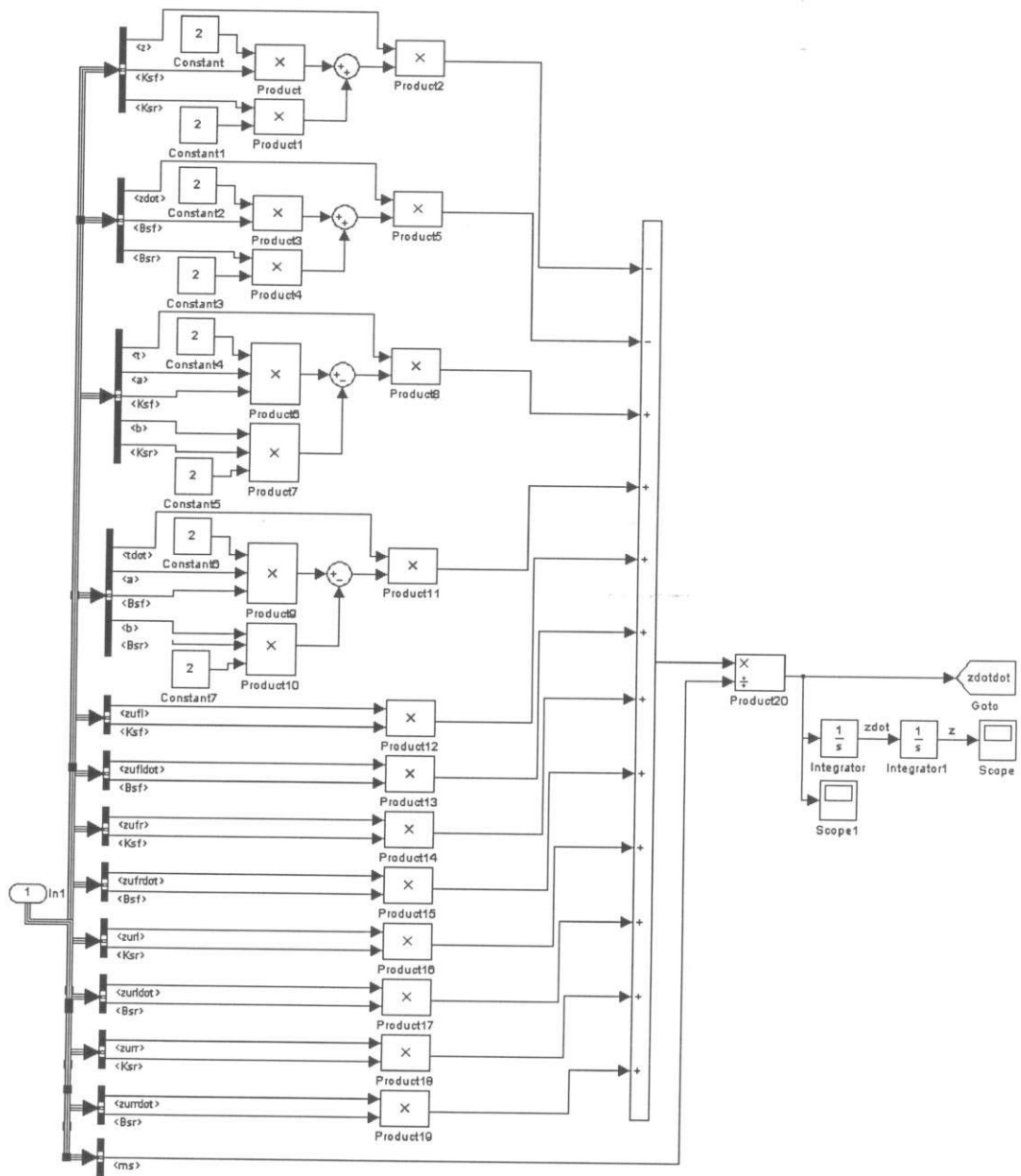


Figure 4.6: Subsystem for bouncing

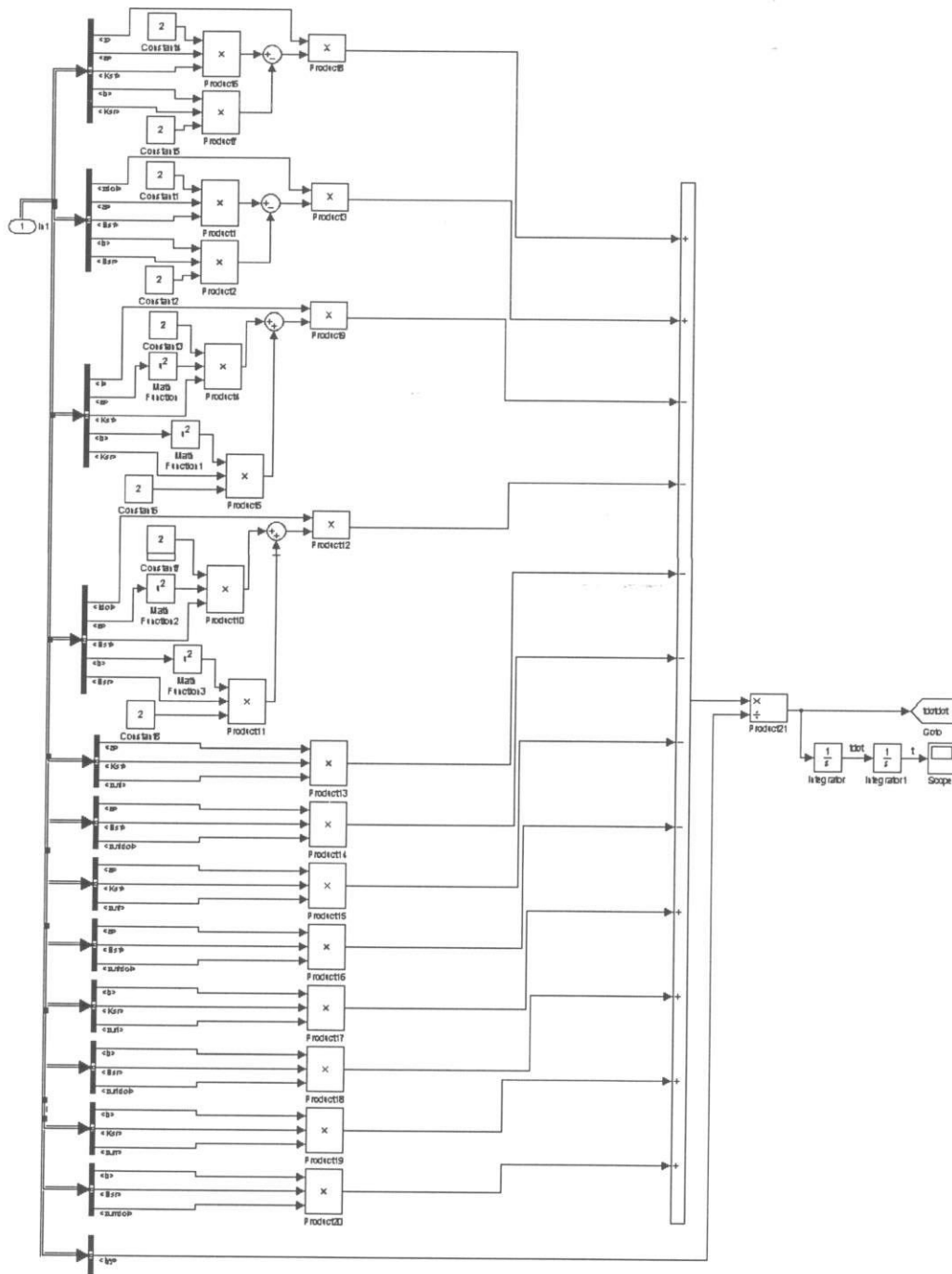


Figure 4.7: Subsystem for pitching

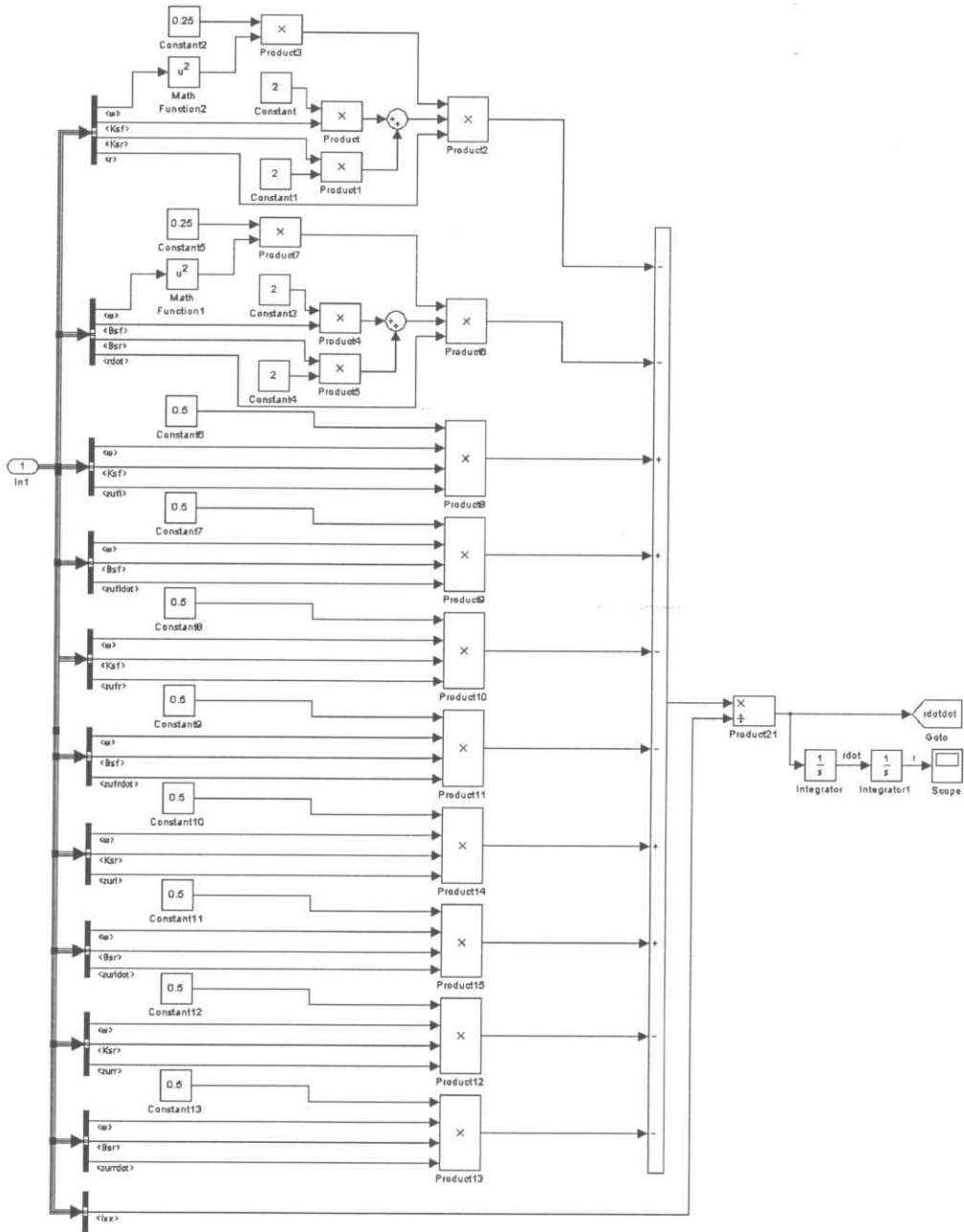


Figure 4.8: Subsystem for rolling

4.5 Conditions for Analysis

The conditions have been set up in the suspension analysis before we simulate in *Matlab 6.5*. There are: -

1. Vehicle driven over the bump at a constant speed of 20km/h.
2. The bump is 0.072m heights.
3. In bouncing and rolling analysis, only left hand side of vehicle driven over the bump (Figure 4.9) while both of the side driven over the bump in pitching analysis (Figure 4.10).
4. Two different suspensions stiffness are assumed to make a comparison suspension performance where the rest of input parameter remains constant.
5. To identify more clearly for the comfort of *Tramcar*, the result will compare with the result from *Proton Waja 1.6* which finish analyzed by ADC where the same analysis condition applied.

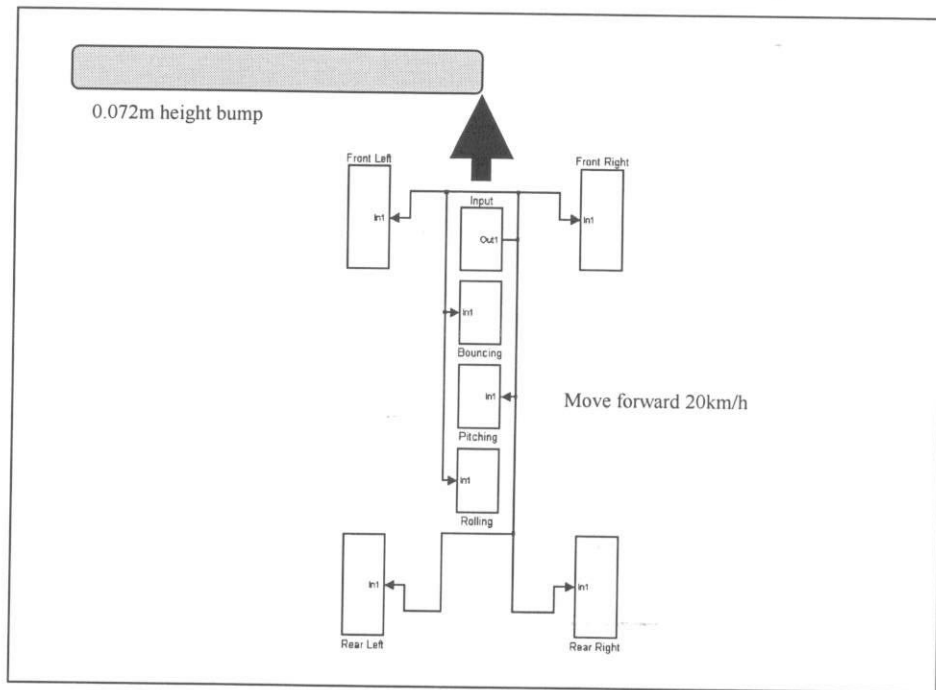


Figure 4.9: Condition for bouncing and rolling analysis

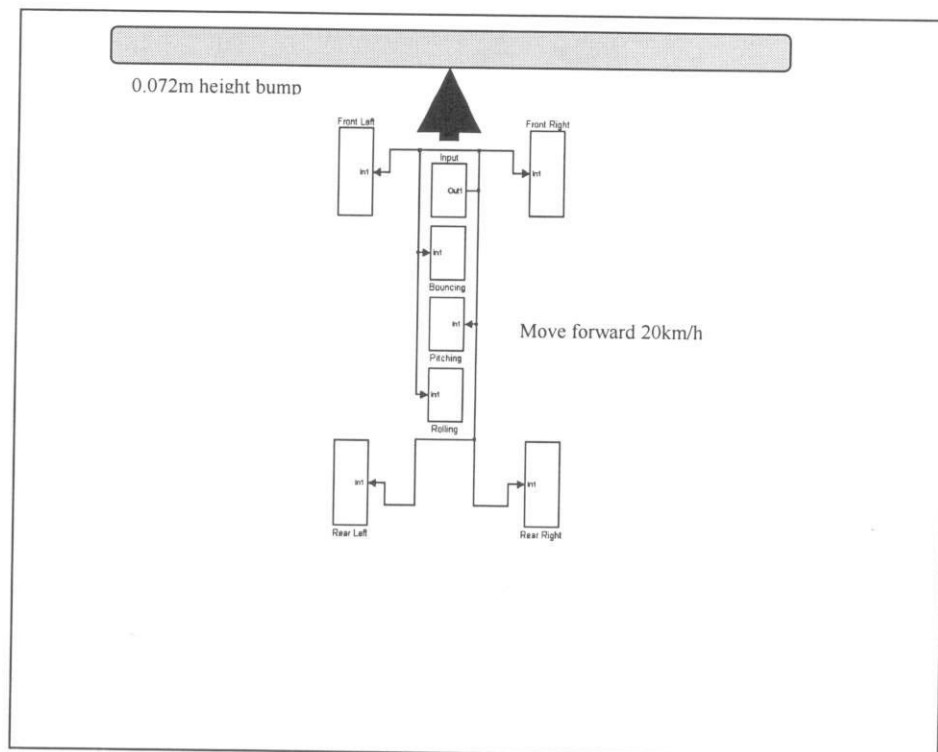


Figure 4.10: Condition for pitching analysis

4.6 The Input of Parameter

The following data are the input of parameter for *Tramcar* benchmarked to a reference i.e. *Proton Waja 1.6* using *Matlab* ver 6.5.

Table 4.1: Input parameters for *Tramcar* and *Proton Waja 1.6*.

Description [Units]	<i>Tramcar</i> parameter	<i>Proton Waja 1.6</i> parameter
Sprung mass [kg]	1664	1500
Unsprung mass [kg]	59*	59
Front suspension spring stiffness [N/m]	26500	35000
Rear suspension spring stiffness [N/m]	26500	38000
Tire spring stiffness [N/m]	190000*	190000
Front suspension damping [N/m/s]	1030.05	1000
Rear suspension damping [N/m/s]	1030.05	1100
Roll axis moment of inertia [kg-m ²]	729.67	460
Pitch axis moment of inertia [kg-m ²]	2813.79	2160
Length between front of vehicle and centre of gravity of sprung mass [m]	1.7085	1.4
Length between rear of vehicle and centre of gravity of sprung mass [m]	1.7085	1.7
Width of sprung mass [m]	3.417	3

* The value of unsprung mass and tire spring stiffness for *Tramcar* assumed same as the parameter with *Proton Waja 1.6*

4.7 Assumptions

The following are the assumptions made pertaining to the simulation outcomes:

1. The road profile has zero noise.
2. Air drag is neglected for a low speed (20km/hr).
3. The model is a passive suspension system where there is not control input.
4. The roll movement occurs around the vehicle's centre of mass but not around the roll centre.
5. All the chassis deformations were not taken into accounts as it was modelled as a rigid body.
6. Small angles for the slip angle of the tire, so the lateral forces always acts perpendicular to the vehicle axis.
7. The displacement of the suspension is only in the vertical direction, and geometry angles were not taken into account.
8. Small displacement for the masses so the displacement of the points where the forces applied was not needed to considerate.
9. The specified weight of the *Tramcar* is 984kg plus with 8 passengers' weight of 680kg includes the driver that gives a total of 1664kg of unsprung mass.
10. It is well known that motion of the sprung mass at the wheel frequency modes cannot be reduced if the only control input is a force applied between the sprung and unsprung masses.

11. The natural frequencies of heave, pitch and roll are determined from vehicle suspension dynamics and moments of inertia. Their damping is determined from the ride-dependent dynamics and moments.

4.8 Results

All the simulation results are shown in the form of graphical representations as follows: -

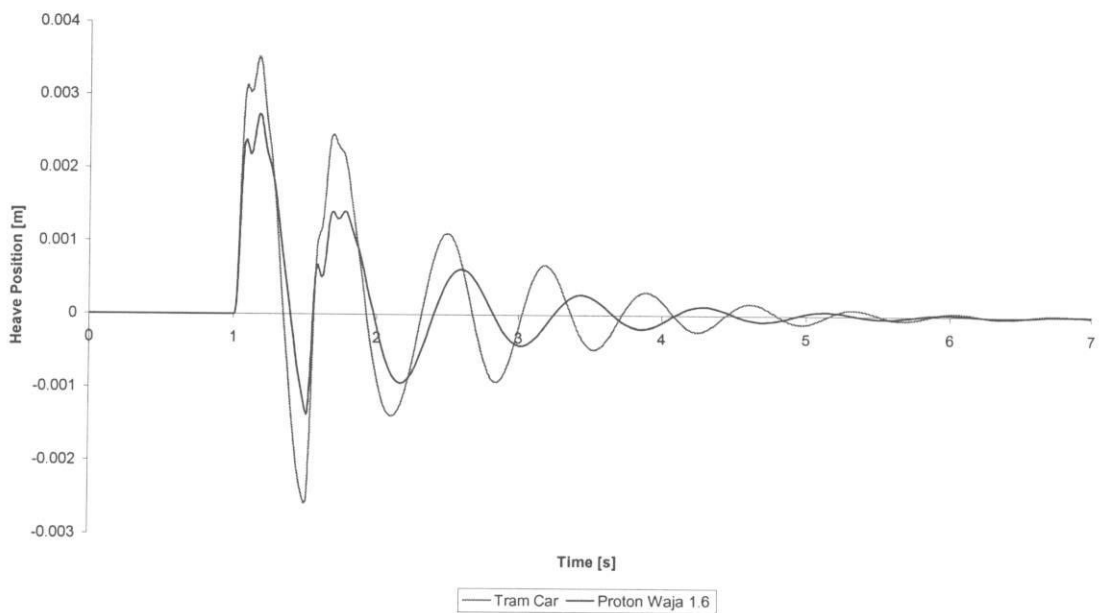


Figure 4.11: Bouncing Performance

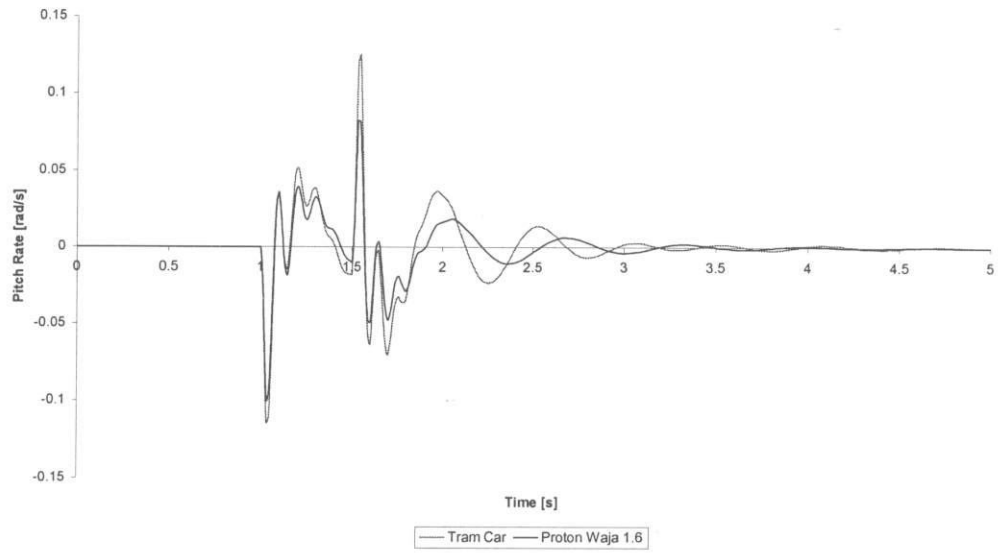


Figure 4.12: Pitching Performance

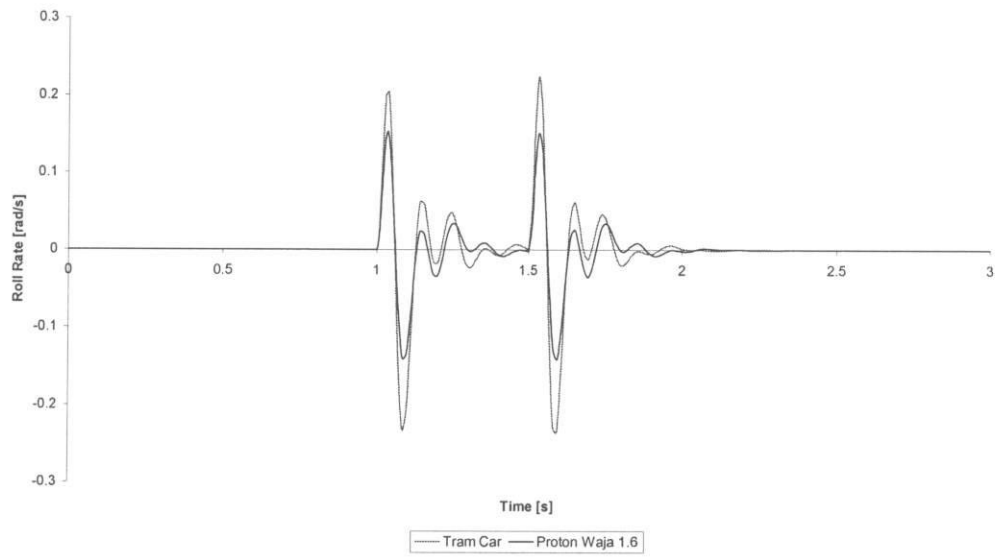


Figure 4.13: Rolling Performance

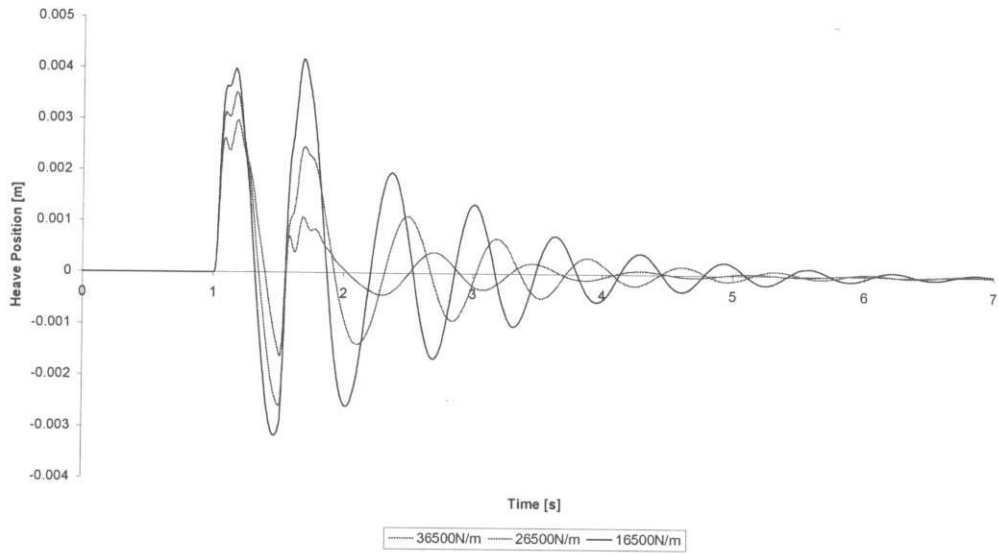


Figure 4.14: Comparison in bouncing performance for different stiffness

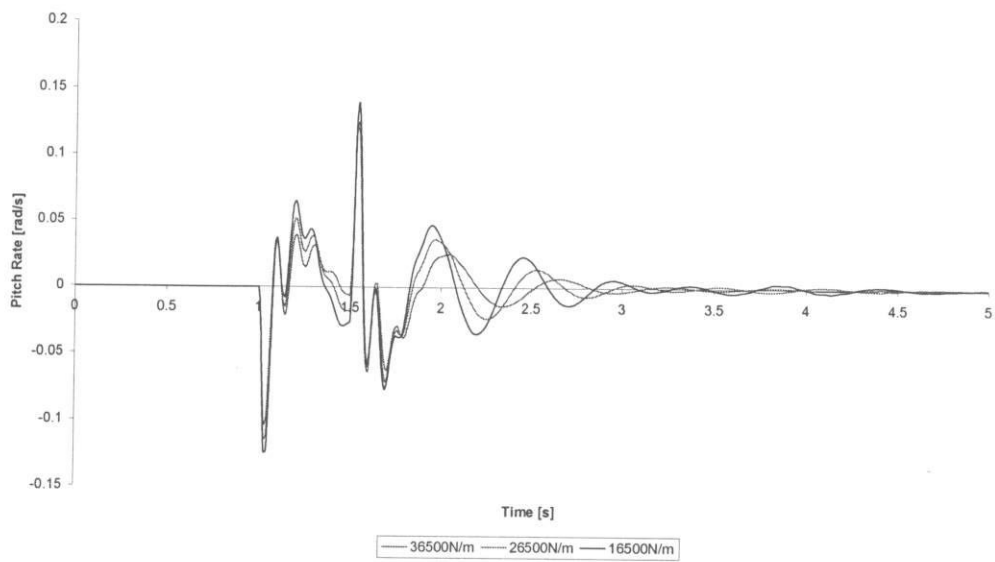


Figure 4.15: Comparison in pitching performance for different stiffness

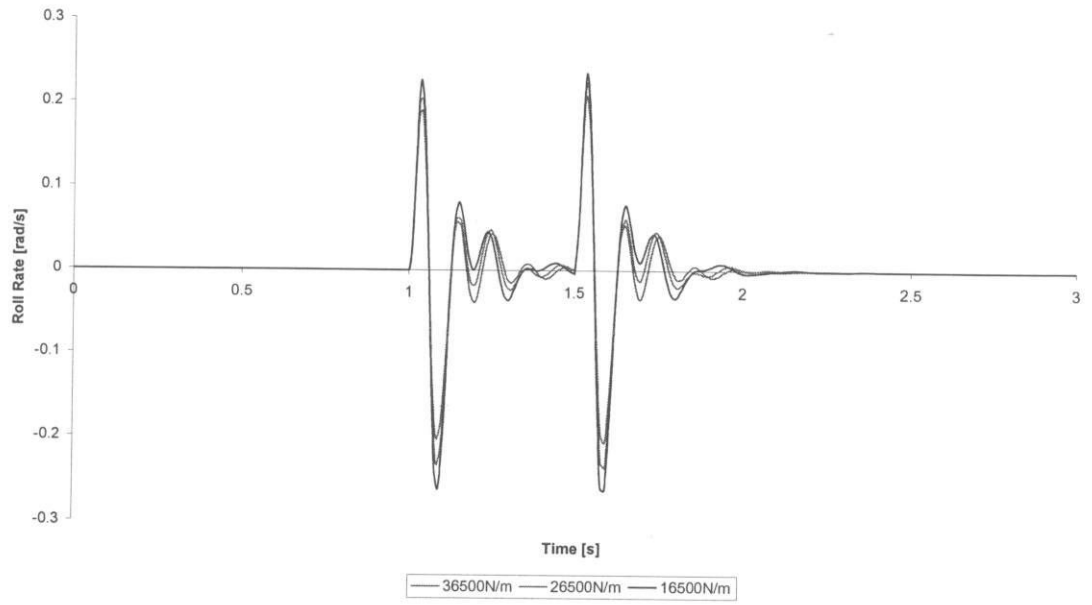


Figure 4.16: Comparison in rolling performance for different stiffness

CHAPTER 5

DISCUSSIONS

5.1 Chassis Analysis

From the chassis and suspension analyses of this project, the performance for both these parts in different situations can be obtained. Each of the results is discussed in the following sub-sections.

5.1.1 Static Analysis

In the first analysis, we got the maximum Von Mises Stress is 101MPa, the maximum shear stress is 53.8MPa, the maximum principal stress is 113MPa and the maximum displacement is 4.23mm. The safety factor for normal stress is 2.93 while in shear stress is 3.08.

From the safety factor, we can conclude that the framework is safe in static. The safety factor is satisfied for a vehicle. From literature review, we have known that a vehicle can be said 'safe' if the safety factor over 2.0. In the analysis we assumed all the joints are perfectly welded.

From the analysis, we obtained that the maximum stress occurred at the middle of chassis. The deformation is large here. The chassis will most probably fail at this place. Hence, we need to strengthen the cross bar. We can either use bigger diameter of steel bar or increase the thickness of the bar.

From the analysis, we can found out that the actual maximum stress occurred in the joint between the fore suspension bar and the lower ladder frame. In the contour of stress, we can see that the colour in orange-yellow. In this analysis, the fore suspension bar is assumed while the fore suspension bar is not appearing in the real *Tramcar*. This is because the entire fore of *Tramcar* is built from monoque. We can only analyze the chassis in this project. Although the maximum stress occurred in fore suspension bar, we did not take it as result.

The maximum Von Mises strain is 0.000436MPa, the maximum shear strain is 0.000694MPa and the maximum principal strain is 0.000531MPa. The value for strain is small which almost the zero, so we are neglected the effect of strain to the chassis.

In most vehicles applications, the static loading in normal condition would not create any problem or permanent distortion to the chassis. The torsion due to the unbalance support will bring more severe case.

5.1.2 Bumping Analysis

The second analysis is bumping analysis. In the analysis, we got the maximum Von Mises Stress is 114MPa, the maximum shear stress is 60.7MPa, the maximum principal stress is 128MPa and the maximum displacement is 4.63mm. The safety factor for normal stress is 2.59 while in shear stress is 2.73.

From the safety factor, we can conclude that the framework is safe when the *Tramcar* rode over a bump. The safety factor is satisfied for *Tramcar*. In the analysis we assume all the joints are perfectly welded.

From the result, we found out that the critical location for bumping analysis is almost the same for the static analysis. Referred to the contour, we obtained that the maximum displacement occurred at the middle of chassis. The chassis will most probably fail at this place. The maximum stress occurred at the fore suspension bar. As we mentioned before, we did not take it as result although the maximum stress occurred in fore suspension bar.

In bumping analysis, we assumed that 2g force applied to the whole chassis in $-y$ direction. This is equal to the force when *Tramcar* rode over a bump.

5.1.3 Braking Analysis

Based on the results of the bumping analysis, the chassis gives a better performance than the braking analysis. In the braking analysis, the maximum Von Mises Stress is 76.5MPa, the maximum shear stress is 40.5MPa, the maximum principal stress is 85.4MPa and the maximum displacement is 3.72mm respectively.

The chassis gives a more secure safety factor in braking analysis. The safety factor for normal stress has been determined as 3.88 while for shear stress is 4.09. From the safety factor, it can be concluded that the framework will safe when the *Tramcar* is subjected to sudden braking. Here, all the joints for the chassis are regarded as being perfectly welded.

As for the braking analysis, it was assumed that 1g force was applied to the whole chassis in $-x$ direction. This equals to the force when *Tramcar* brakes suddenly. This is the reason that caused for the maximum deformation to occur in y direction to be less than the maximum deformation due to bumping effect. When the *Tramcar* brakes suddenly, two directional forces will be applied to the chassis, i.e. the $-x$ direction and the $-y$ direction. In the bumping analysis, only $-y$ direction force was considered to be applied to the chassis.

5.1.4 Chassis Torsional Stiffness Analysis

It is apparent that torsion will be increase with the increase in the twisting angle. This was plotted for the purpose to getting the torsional stiffness value of the chassis, particularly so when there are extra forces applied on the fore suspension bar.

From the graph of torsion against the degree of torsion, it is found that the relationship is linear. As can be observed from the graph, the torsional stiffness of the chassis (from the slope of the graph), is 5127.5Nm/degree. This value is in range allowed for normal saloon car, which is from 3000Nm/degree to 9000Nm/degree.

When 10kN force is applied, the chassis lost its elasticity property. To maintain the elasticity property, the analysis only can be done until 9kN.

5.2 Suspension System Analysis

Base on the graph, the results for suspension system analysis are discussed as follows.

5.2.1 Bouncing Performance

Figure 4.11 shows the bouncing performance for the *Tramcar* and *Proton Waja 1.6* in 8 seconds simulation. We can clearly see that there were two different two curves plotted. The pink colour curve line indicated the simulation curve for *Tramcar*, we note that increment of the sprung mass heave position started at 1s which is the time when the front left wheel hit the bump. From the curve too, we note that there was a peak point around 3.522mm at 1.1711s. That means the *Tramcar* heaved the maximum value

3.522mm when the front wheel hit the bump. The second peak point occurred at 1.6943s where the rear wheel hit the bump. It is around 2.461mm heaved from the centre of gravity. Then the graph is damped off until more steady state. We noticed that the heave position was almost fully damped at around 7s.

On the other hand, the *Proton Waja 1.6* simulation curve was indicated in dark blue colour. The almost same orientation of behaviour as the *Tramcar* happened on the *Proton Waja 1.6* step up and down when compared to the simulation curve for *Tramcar*. What was different here, *Proton Waja 1.6* indicated the peak point around 2.727mm at 1.1706s. The second peak point occurred at 1.7712s where the rear wheel hit the bump. It is around 1.402mm heaved from the centre of gravity. Both the simulation graph shows that their heave position had a same pattern of length. They were being fully damped at almost the same time.

5.2.2 Pitching Performance

Graph 4.12 shows the pitching performance for the *Tramcar* and *Proton Waja 1.6* in 8 seconds simulation. Both of the graph indicated in much similarity started at 1s. The first negative slope shows that the vehicle pitched in the anti-clockwise direction. *Tramcar* shows the maximum pitch rate at 1.0358s about -0.11421rad/s . After the peak point, the curve was move to the positive value at 1.1001s about 0.036279rad/s and reached to 0.052034rad/s at 1.2040s. After that, the pitching motion is slowly damped before the rear wheel hit the bump. The curve was reach to the maximum positive value when the rear wheel hit the bump. The positive slope from the graph means that the *Tramcar* pitched in the clockwise direction. The *Tramcar* reached the maximum pitch rate at 1.5448s about 0.12485rad/s . The graph after that was almost the same with the performance for front wheel but in the negative value. All the pitching motion was being fully damped after 4s.

Meanwhile the fluctuation pattern was almost the same where the *Proton Waja 1.6* curve is a bit lower than the *Tramcar* curve. *Proton Waja 1.6* reached its maximum pitch rate at 1.0359s about -0.1002rad/s when the front wheel hit the bump and then reached the maximum value about 0.082056rad/s at 1.5327s after the rear wheels hit the bump.

5.2.3 Rolling Performance

Graph 4.13 shows the rolling performance for the *Tramcar* and *Proton Waja 1.6* for a period of 8 seconds simulation. Both of the cars set to hit the bump at 1 second. The first positive slope shows that the vehicle will roll in the clockwise direction. As for the *Tramcar*, the roll rate reached the maximum value at 1.0386s i.e. about 0.2038rad/s , which equals to $11.6769^\circ/\text{s}$. This happened when the car hit the bump and subsequently roll in the clockwise direction. It goes back to zero when it rode on the bump again. The roll rate then reached a negative value nearly i.e. -0.2320rad/s at 1.0871s. This occur when the front wheel slip down from the bump. The rolling effect then damped by the absorber slowly until it reached a more steady state at 1.5s before the rear wheel step on the bump. The graph then continued with the effect by the rear wheel when it step on the bump 0.5s after the front wheel. The almost same orientation of behaviour as the front wheel happened on the rear wheel step up and down. The roll rate reached the maximum at 1.5322s about 0.2234rad/s which equal to $12.7999^\circ/\text{s}$ for rear wheel. The rolling effect then damped by the absorber slowly as the front wheel until it reached a more steady state at 2 s.

For *Proton Waja 1.6*, the roll rate reached the first maximum at 1.0370s about 0.1527rad/s which equal to $8.7473^\circ/\text{s}$ while the negative value nearly -0.1399rad/s at 1.0857s for front wheel. The rolling effect then damped by the absorber slowly until it reached a more steady state at 1.5s before the rear wheel step on the bump. The graph then continued with the effect by the rear wheel when it step on the bump 0.5s after the front wheel. The almost same orientation of behaviour as the front wheel happened on the rear wheel step

up and down like the *Tramcar*. The roll rate reached the maximum at 1.5319s about 0.1505rad/s, which equals to 8.6230°/s for rear wheel. The rolling effect then damped by the absorber slowly as the front wheel until it reached a more steady state at 2 s.

5.2.4 Comparison Performance in Different Stiffness

The following graphs are the comparison for *Tramcar* suspension performance in different stiffness. Graph 4.14 shows the comparison in bouncing performance for different stiffness; graph 4.15 shows the comparison in pitching performance for different stiffness and graph 4.16 shows the comparison in rolling performance for different stiffness. From the graph, it is clearly indicated that the heave position, pitch rate and roll rate strongly dependent on the suspension stiffness when the other inputs are fix. If the softer suspension use on the *Tramcar*, then the heave position, pitch rate and roll rate is a bit higher if compared with the harder suspension. For example, in bouncing performance simulation, we can know that the heave position at 1.68s for 15600N/m stiffness is 4.18mm, for 25600N/m stiffness is 2.461mm and for 35600N/m stiffness is 1.074mm. The harder suspension gives the highest value of heave position. One more example we can look for the influenced of different stiffness at the rolling performance. If the 16500N/m stiffness use on the *Tramcar*, then the maximum roll rate is 0.23504rad/s while the 36500N/m stiffness give only the maximum roll rate at 0.20763rad/s. The same trend of results will be obtained when the pitching performance is examined for the *Tramcar* in different suspension stiffness.

CHAPTER 6

RETROFITTING OF CNG CONVERSION KIT

6.1 Why is the Need for Retrofitting?

This vehicle is not only to serve its purpose but also to showcase the ability of ADC in adapting new and relevant technologies pertaining to automotive engineering and able to demonstrate their applications in the creation of human wealth. With this in mind having to develop the vehicle is not enough but also to incorporate added value from the perspective of able to demonstrate its capability to use non conventional fuel.

In its early effort CNG in tandem with gasoline will be used. With the successful retrofitting of the tramcar with a commercially viable conversion kit, it is hope that this initiative can be expended to include hybrid and all-electric powertrain in the future.

6.2 CNG Conversion Vehicle Requirements

Suggested engine modifications are needed to assure engine reliability, optimized power, fuel consumption and emissions that include optimizing compression ratio, valve lift, valve timing, exhaust system and intake manifold. Special attention goes to the engine cooling, lubrication and the potential issue of excessive oil consumption. A properly modified and tuned engine can make the same power as the base engine.

Generally for gasoline conversion it calls for:

- i) improve cooling system
- ii) the need for engine oil cooler
- iii) the need for new valve seats
- iv) increase compression ratio

However, the key to the successful use of gaseous fuel is a sophisticated engine controller unit (ECU), i.e. the electronic engine management system which enables gasoline engines to operate on clean-burning CNG, LPG or Hydrogen.

ECU duty is to sense engine parameters in real time and instantly adjust to deliver the correct amount of fuel and the correct ignition timing. The system results in optimal engine performance, while always operating at the lowest emissions. The system and components can be installed in new vehicles, or retrofitted in existing fleets.

6.2.1 Bi-fuel System and Dual-fuel System

Bi-fuel systems use only one fuel at a time; they are particularly advantageous when alternative-fuel refueling stations are not always readily available. A switching system is added as part of the conversion so that the driver can switch from one fuel to the other.

Dual-fuel systems, on the other hand, run on a combination of an alternative fuel and diesel; they inject both fuels into the combustion chamber at the same time. Dual-fuel systems are used mostly in heavy-duty diesel engines, while bi-fuel systems are usually used in passenger cars or light- and medium-duty trucks.

Dedicated conversion systems run on only one fuel. These systems generally provide reduced emissions and better performance if they are tuned to optimize their operations on only one fuel, and they have no evaporative emissions because they use no gasoline. There are many types of pure CNG system vehicle in the market today and have been used quite successfully in many other countries such as Canada, Italy, New Zealand, India and the far east.

6.2.2 Optimize System

An optimize system is synonymous with a closed-loop system. A closed-loop system uses a feedback system to monitor and adjust engine performance continuously. An oxygen sensor in the exhaust system monitors the fuel/air mixture to the engine and compensates for changes, thereby optimizing emissions performance.

An open-loop system, in which carburetor is throttle-regulated does not provide optimum emission performance. This is because it does not compensate for changes in the fuel/air mixture. Such systems are generally used on older model vehicles that do not have computerized fuel control systems.

6.2.3 CNG Operation System

In CNG vehicles, the fuel is stored at a pressure range of 160 to 250 bar (2400-3600 psi) in one or more cylinders located under the body or in the trunk of the vehicle. The filling valve is placed near the tank or in the front grille. When the CNG leaves the cylinder tank, it travels through high-pressure fuel lines into one or more pressure regulators, where it is reduced to low atmospheric pressure prior entering the engine intake.

Unlike gasoline, which must be vaporized before ignition, CNG is already gaseous when it enters the combustion chamber. When the intake valve opens, the gas enters the combustion chamber, where it is ignited to power the vehicle.

6.2.4 Application of CNG in Vehicles

Natural gas is compressed to a high pressure and is stored on board the vehicle in cylinders installed in the rear, undercarriage, or atop the vehicle. When natural gas is required by the engine, it leaves the cylinders traveling through a high pressure pipe to a high pressure regulator (most often located in the engine compartment) where the pressure is reduced.

In carbureted engines, the fuel enters the carburetor (through a special fuel/air mixer) at close to atmospheric pressure through a specially designed natural gas mixer where it is properly mixed with air.

In fuel injected vehicles the natural gas enters the injectors at relatively low pressure (up to about 6 bars). In either case, natural gas then flows into the engine's combustion chamber and is ignited by spark, to create the power required to drive the vehicle. Special solenoid valves prevent the gas from entering the engine when it is shut off.

In bi-fuel vehicles, a fuel selector switch controls the flow of either natural gas or petrol. (In some systems the switchover is done automatically when the vehicle is out of natural gas). A fuel gauge is provided on the dashboard or it is incorporated into the normal fuel gauge so the driver can determine the amount of natural gas remaining in the fuel tanks.

The types of conversion kits are shown in Figure 6.1 and 6.2 respectively.

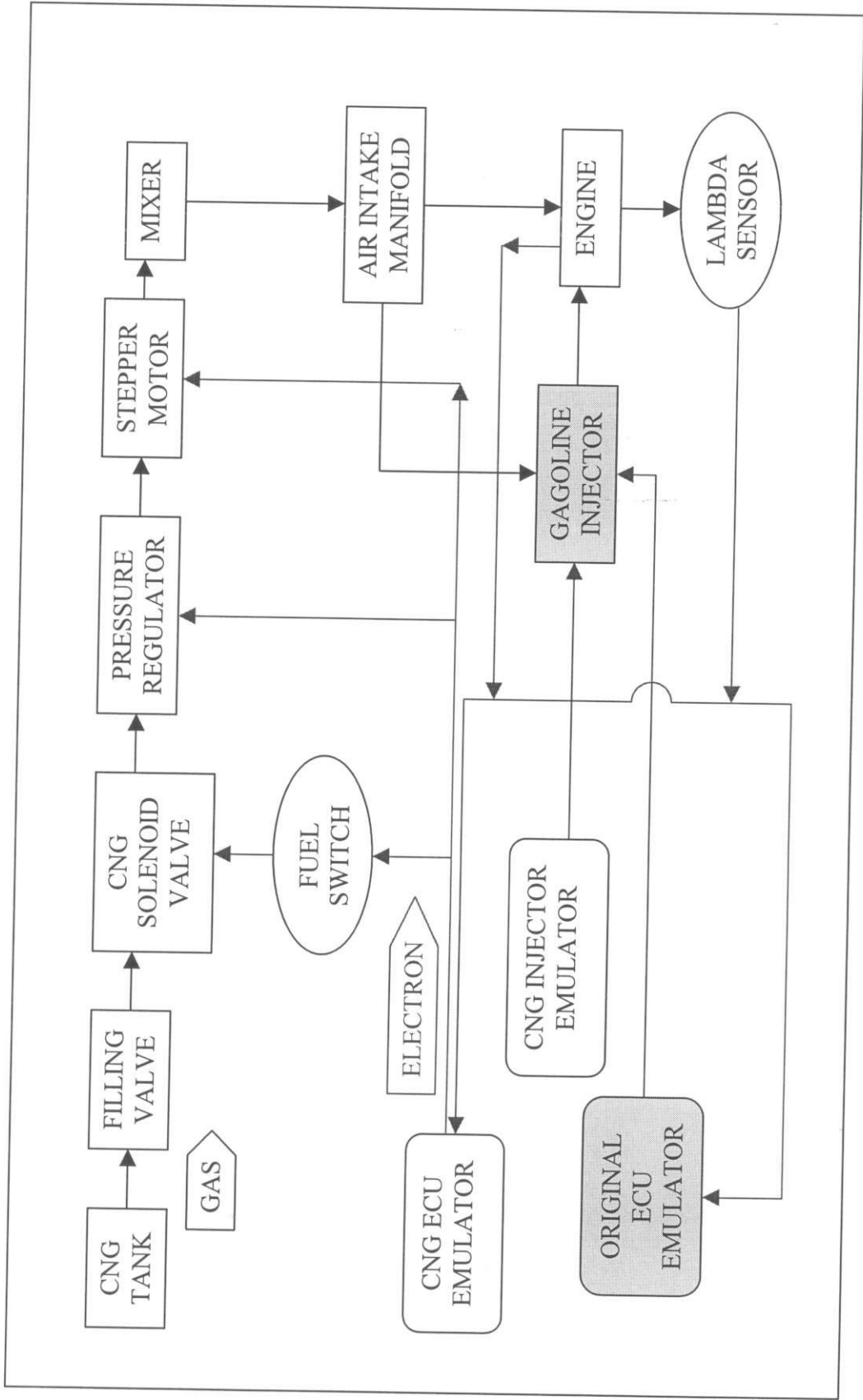


Figure 6. 1: Catalyst System

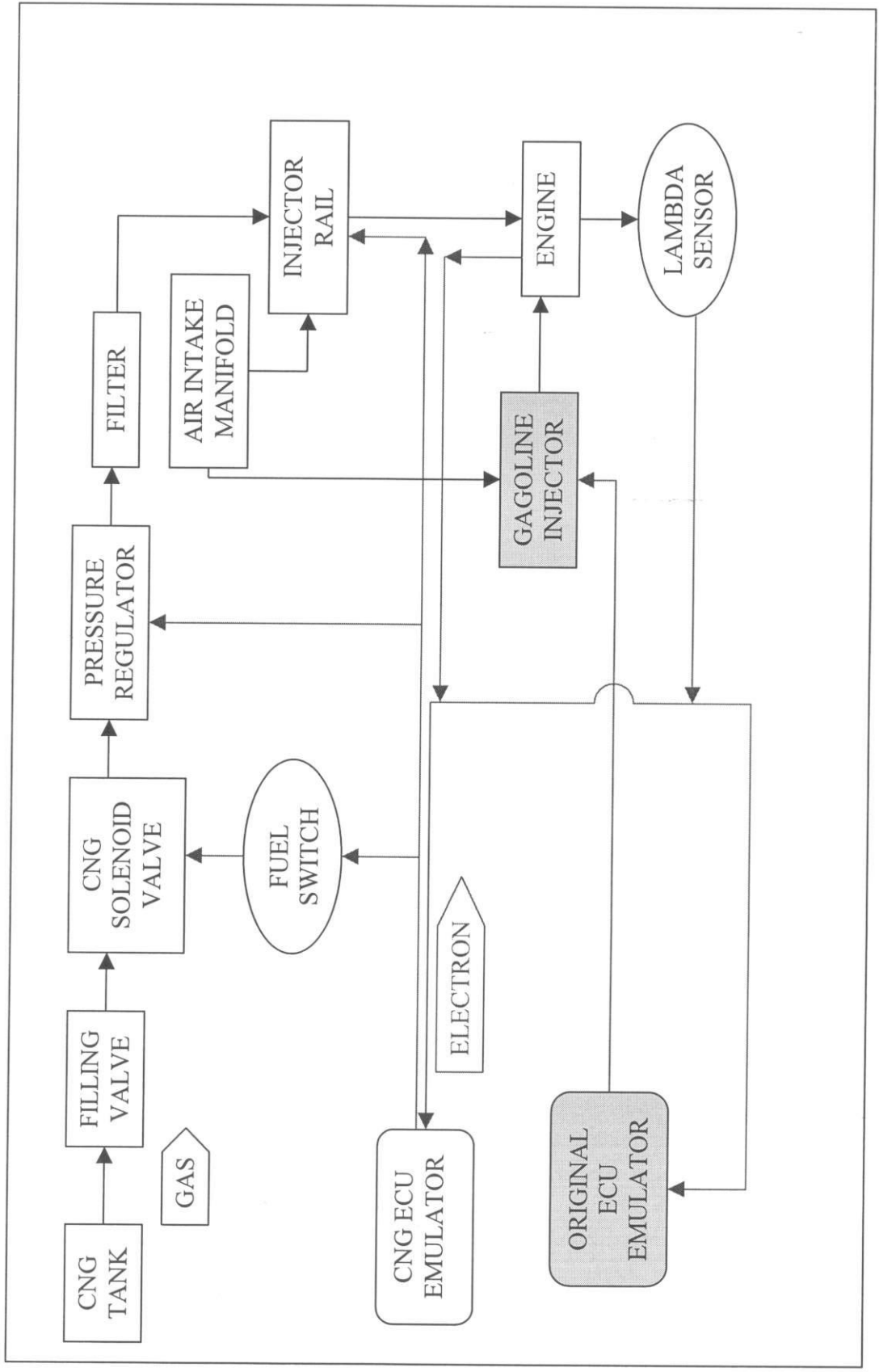


Figure 6.2: Sequential System

6.2.5 Sequential System (Multipoint Sequential Injection System)

One of the new technologies in natural gas vehicle, the multipoint sequential injection system, represents a new generation of bi-fuel CNG conversion system. The principle used by the CNG ECU to calculate the injection timing applied to the CNG injectors, is based on the acquisition of the gasoline injection timing by CNG ECU during CNG mode.

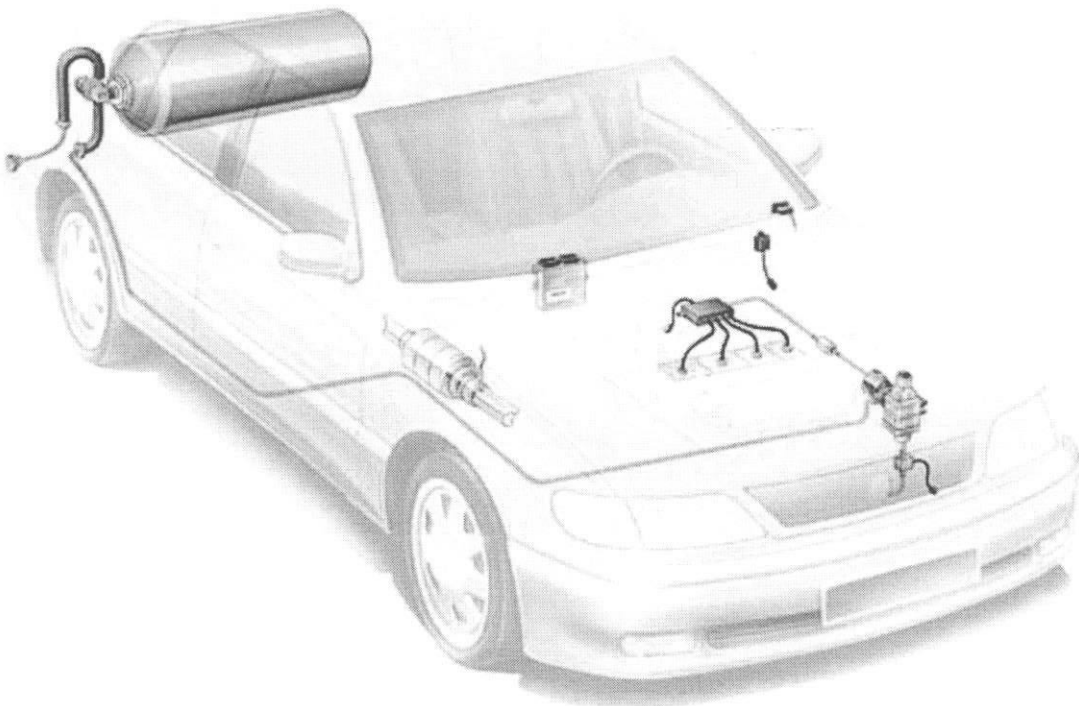


Figure 6.3: Sequential system illustrated

The engine management is, therefore, mainly left to the gasoline ECU whilst the CNG control unit translates gasoline actuations into an appropriate control for CNG injectors. In order to maintain the coherence with the gasoline system, the CNG ECU drives CNG injectors in the same sequence as gasoline injectors. Roughly, the CNG ECU converts an amount of energy that should be actuated

by the gasoline into an equivalent amount of energy that CNG has to release in order to compensate the differences between two fuels. This system can use different types of injectors according to the specifications of the application. In addition, it is minimally invasive with respect to the original gasoline engine management system. The CNG ECU is able to be easily integrated with the main engine management functions as mixture control, cut off, EGR, purge canister, etc and auxiliaries engine management functions as air-conditioning, power-steering, electric loads, etc.. The CNG ECU is able to calculate CNG injection timing using specific information as CNG injector rail pressure, CNG temperature, engine coolant temperature, and engine RPM and battery voltage, in addition to the inputs of the gasoline ECU [10].

6.2.6 Catalyst System (Natural Gas System with TN 1 Step Motor regulator and Lambda Control System/2)

Natural gas flows from the tank through the special valve and is conveyed to the engine compartment through high-pressure piping that is also connected to the refueling system.

The TN1/B step-motor reducer is installed in the engine compartment where the pressure of the incoming natural gas is reduced from 220 bars to the engine supply pressure. From the reducer, the natural gas flows to the air/fuel mixer (installed on the suction piping), which mixes the gas flow in proportion to engine demand represented by the vacuum generated in the mixing devices. The high-pressure solenoid valve allows the gas to flow only while the engine is running and with the switch in the gas position.

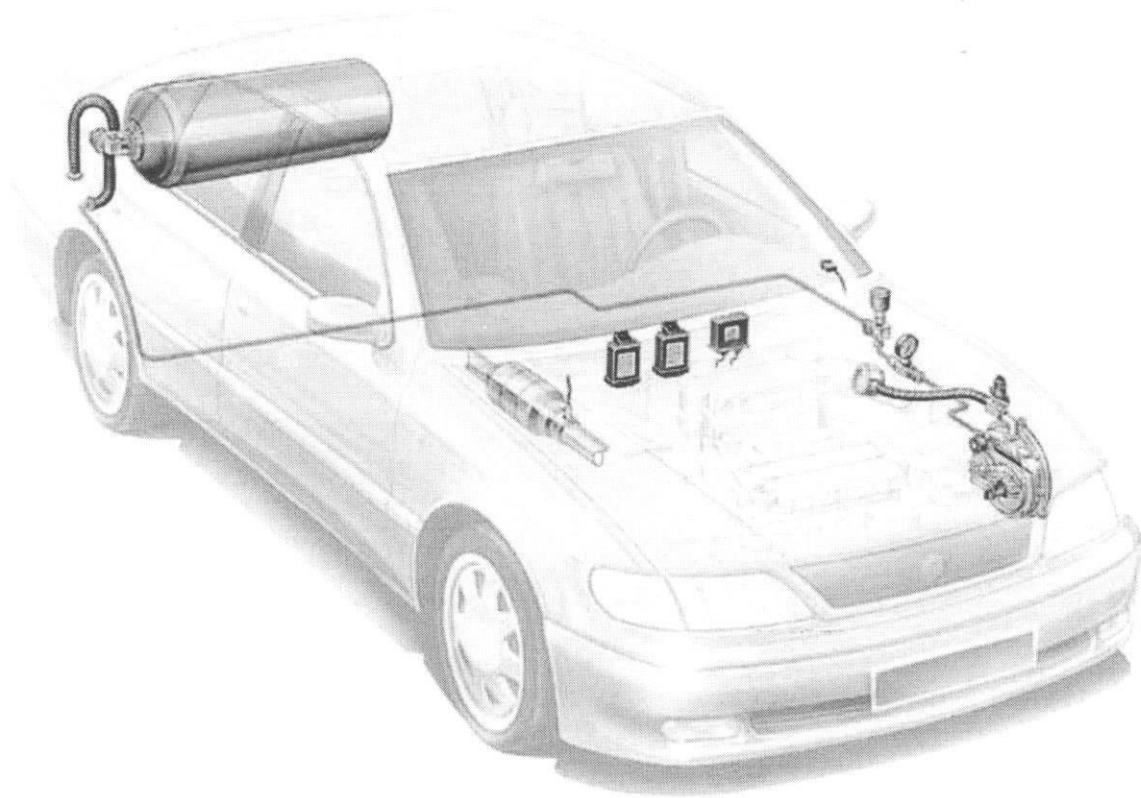


Figure 6.4: Catalyst System illustration

Lambda Control System/2 is a self-adjusting electronic system: no manual adjustments are required and it can adapt automatically to the different environmental and vehicle use conditions, ensuring efficient carburetion in terms of driving style, consumption and emissions. The Lambda Control System/2 computer electronically manages the gas flow adjustment, allowing the Lambda factor to reach the required value at all engine rpm thanks to 2 electromechanical actuators. One actuator is installed between the reducer and the mixer and doses the quantity of gas at medium and high rpm (maximum), while the second actuator of the pressure reducer adjusts the optimum gas flow for engine operation at idle (minimum), keeping it stable even when accessories such as an air conditioner or power steering system are operational.

Among its other functions, the LCS/2 computer can be used to start always with petrol, with automatic switchover to gas and, through the switch/indicator, allows the user, at any time, to select the fuel required, displaying the natural gas level in the tank. During gas operation, the electronic emulator (or the injector exclusion wiring) cuts off the petrol flow to the engine; while during petrol operation the natural gas flow to the engine is cut off by the high-pressure solenoid valve [10].

6.2.7 Carburetor System

The schematic arrangement of a simple gas assisted system is the carburetor system. This is shown in Figure 6.5 below.

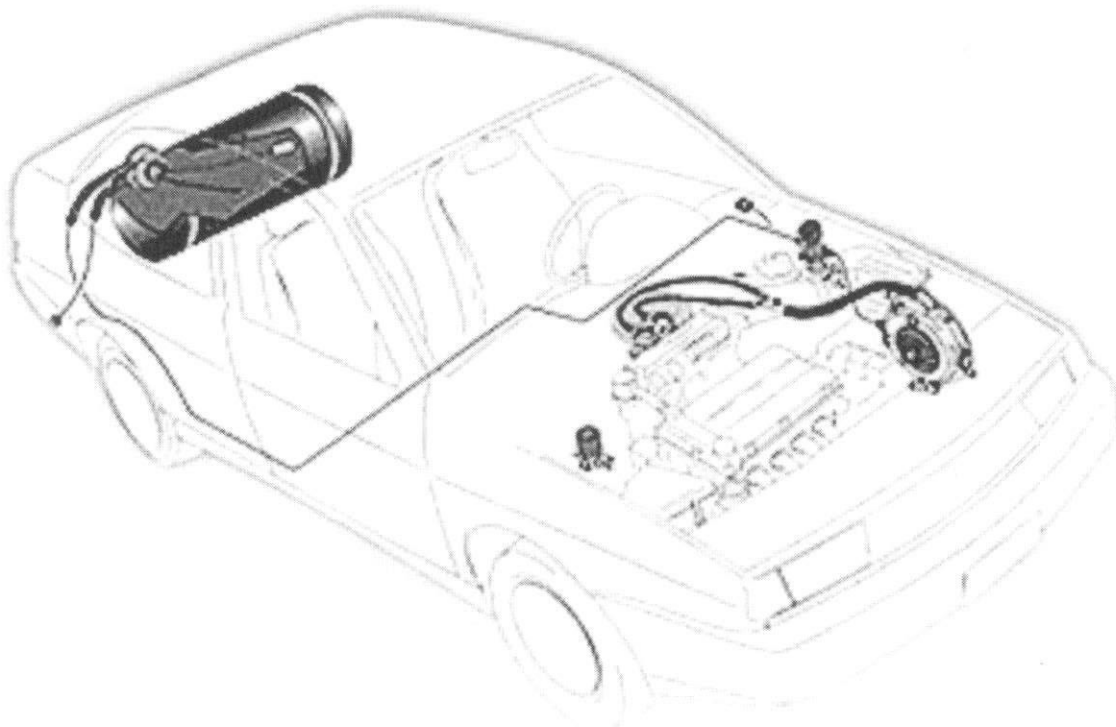


Figure 6.5: Carburetor system linking pressurized tank to engine

An example a CNG Minikit for retrofitting in a carburetor car is shown in Figure 6.6. This is suitable for use in engine from 20 to 90 kW.

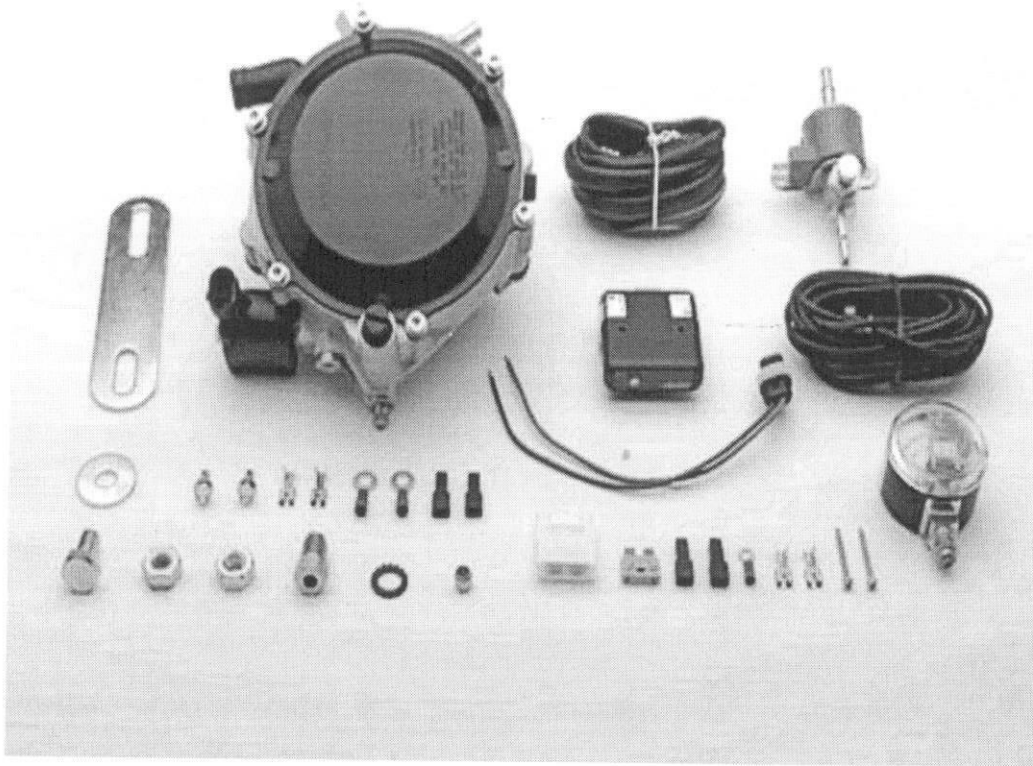


Figure 6.6: Conversions kit for carburetor car

The above system includes the following main components:

- CNG electronic reducer RME090
- AMP super seal harness for pressure reducer
- petrol solenoid valve
- fuel switch with level indicator M198 C
- pressure gauge complete with electronic pick-up for level indication
- reducer installation bracket
- accessory package for minikit installation

6.2.8 Economics of Vehicle Conversion to CNG

Converting a vehicle to CNG involves installing a natural gas fuel system and storage tanks. Dual fuel systems will retain the original conventional fuel system. On a dedicated NGV, the original conventional fuel system can be removed. Generally, dedicated NGV demonstrate better vehicle performance and lower emissions than dual-fuel NGV because the fuel system can be set to take advantage of the characteristics of only one fuel.

Prior to 1985, most gasoline vehicles had carbureted engines and NGV conversion systems were open-loop type - all controls are pre-set with no feed back and re-adjustment of air/fuel ratios, etc. Consequently, first generation and open-loop conversion systems do not provide a mechanism to allow the conversion system to adjust for optimum engine and emissions performance. However, with the advent of fuel-injected engines, computerized electronic engine and emissions controls allow adjustment of the air/fuel ratio and spark timing (on spark-ignition engines) to optimize engine and emissions performance. Monitoring and adjusting engine and emissions performance by computerized controls is carried out by the closed-loop feed back system for optimum engine and emissions performance [10].

The costs to convert a vehicle to operate on natural gas vary and depend on several factors such as the followings:

- A. First generation system
- B. Open-loop or closed-loop
- C. The type of vehicle to be converted and the ease of installation
- D. The quantity of on-board fuel storage desired
- E. The type of on-board fuel storage tanks selected
- F. Labor rates for conversion

6.3 Retrofitting of the Conversion Kit

The catalyst conversion system selected for the Tramcar can best be illustrated in the following Figure 6.7.

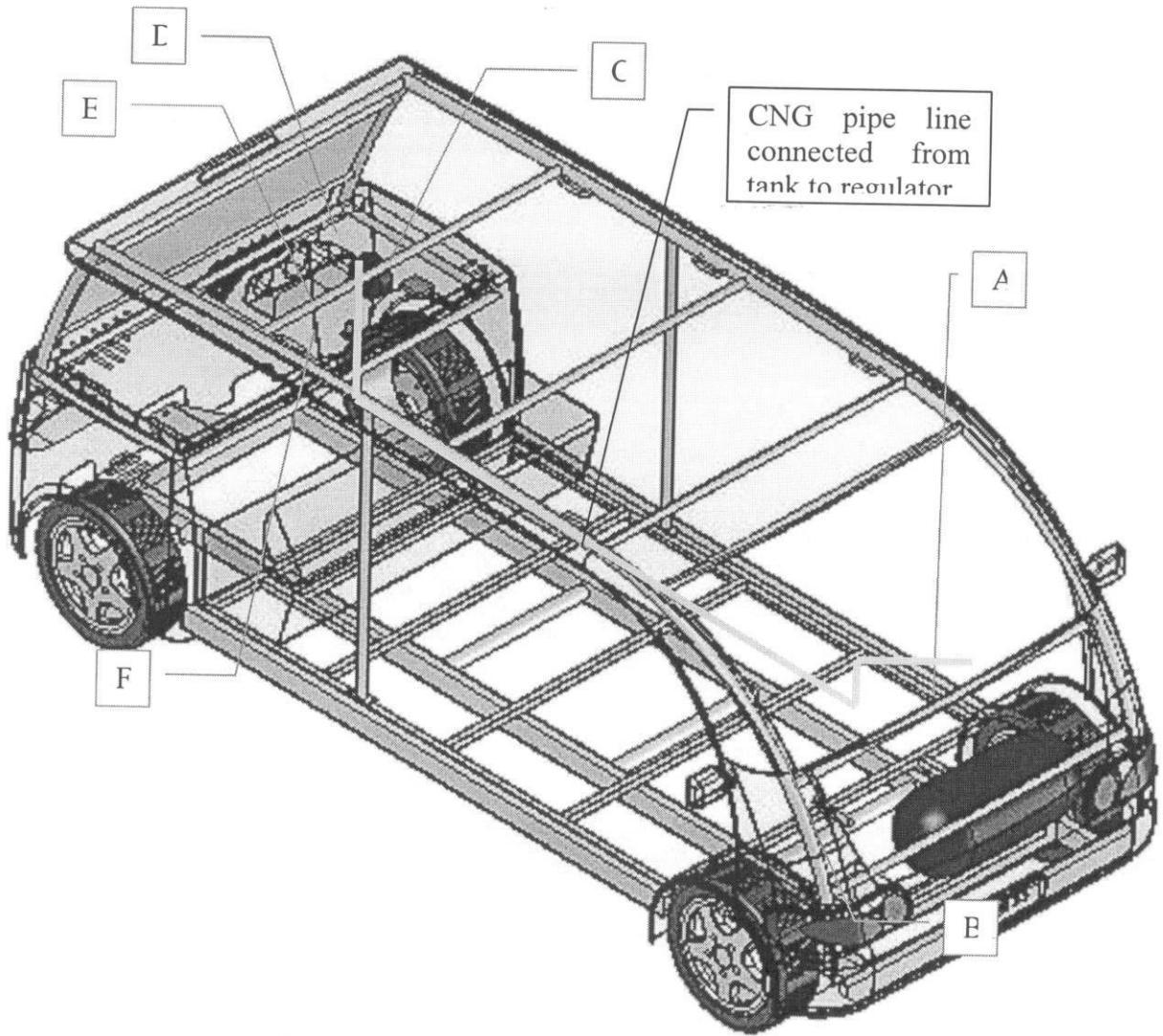


Figure 6.7: Schematic illustration about the Catalyst conversion system

The items labeled in the Figure are:

- A - CNG tank
- B - Filling valve
- C - CNG ECU
- D - Regulator
- E - Stepper motor
- F - Mixer

6.3.1 CNG Tank

The tank used is similar to the one shown here. It has a volume of 55 liter with a massive weight of 80 kg.

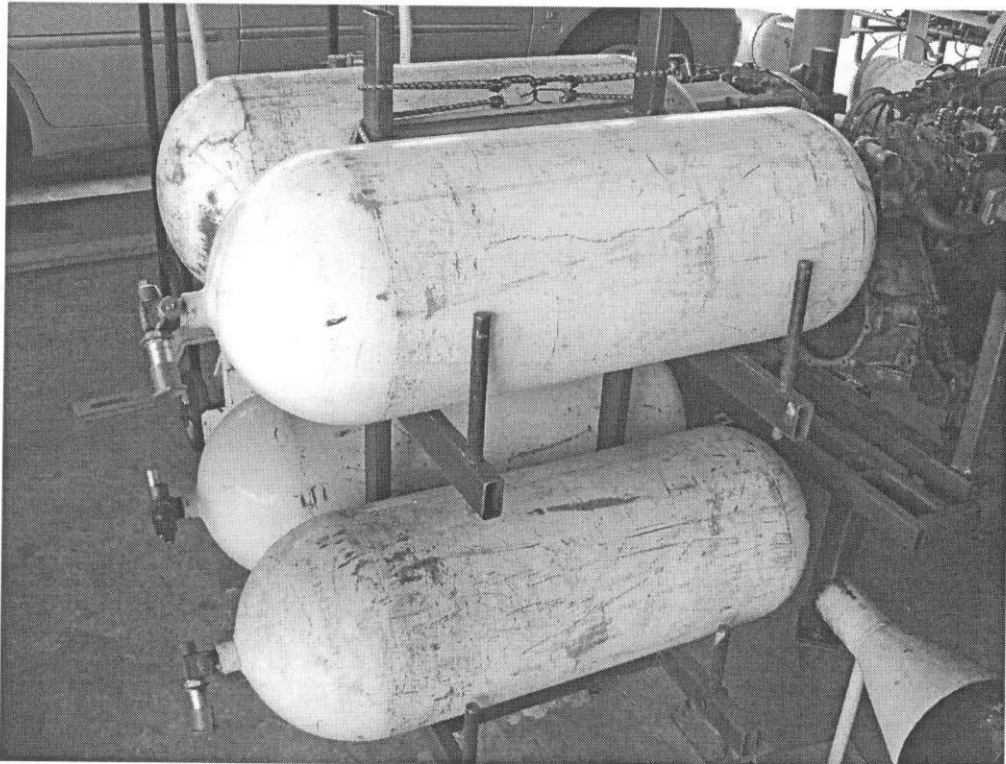


Figure 6.8: CNG steel tanks

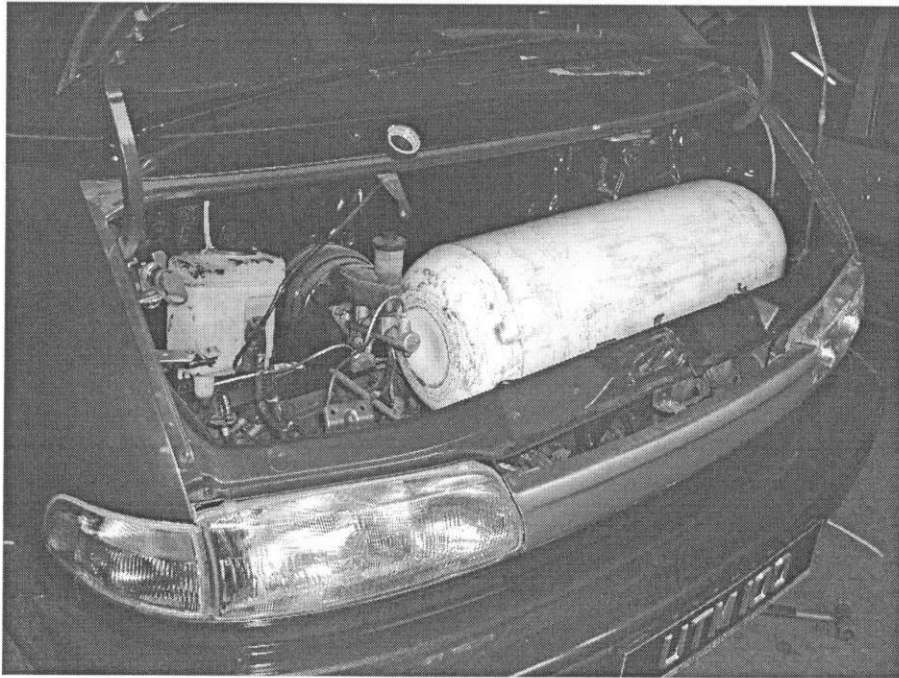


Figure 6.9: Location of CNG tank in the front compartment the *Tramcar*

6.3.2 Filling Valve

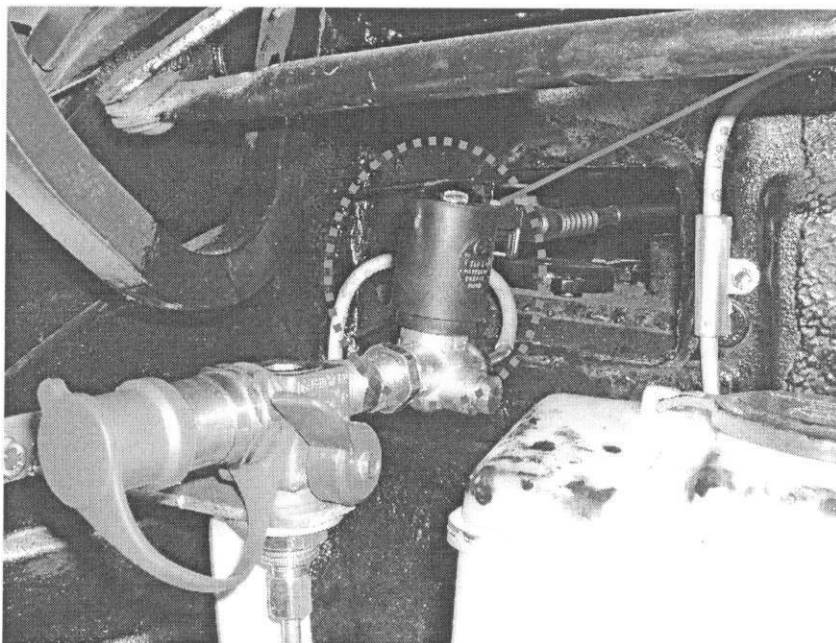


Figure 6.10: Filling valve location

Filling valve is a quick-coupling valve that allows fast charging of the gas during refilling. Figure 6.10 shows its close feature while Figure 6.11 shows how gas is being charged.

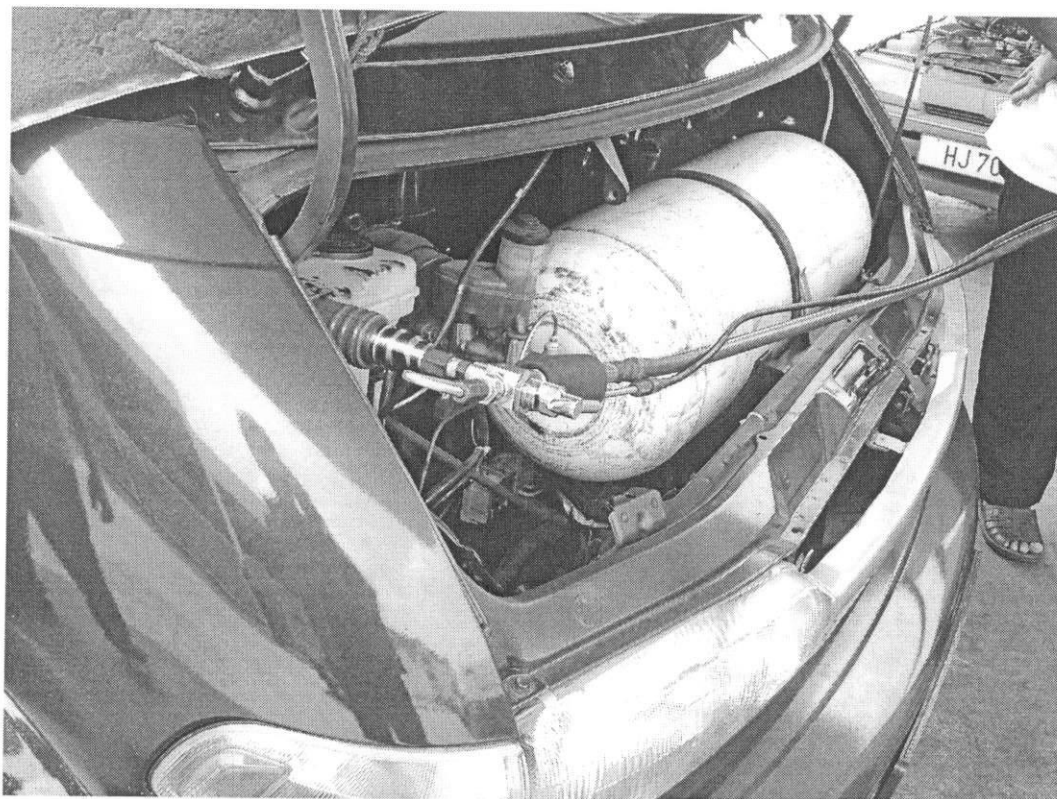


Figure 6.11: Charging of the gaseous fuel into the tank using the filling valve

6.3.3 CNG Cut-off Valves

In the event of emergency the gas is required to be isolated from the engine and its sub-system. In a CNG conversion kit an isolated valve, better known as the cut-off valve is incorporated in the system. There are two types of the cut-off valve used - a manual-operated and automatic. Figure 6.12 and 6.13 illustrates its physical features.

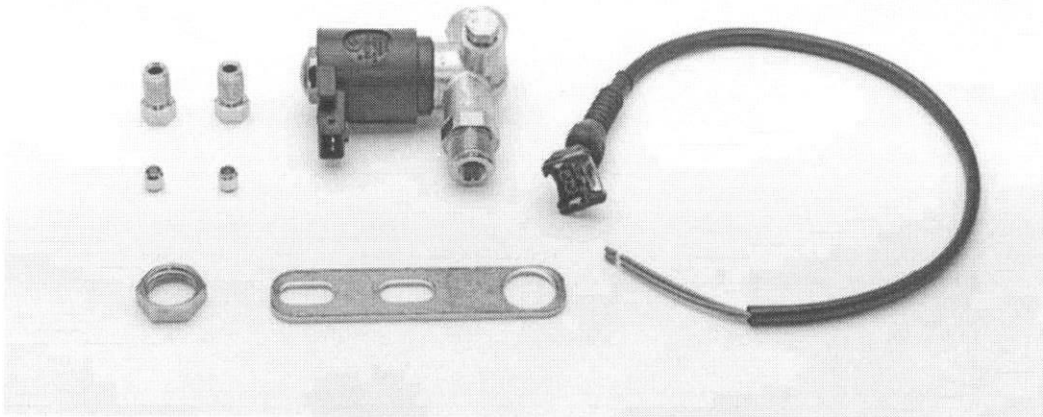


Figure 6.12: CNG cut-off valve 200 Bar, completed with wiring 500 mm attached to filling valve.



Figure 6.13: The emergency manual shut-off valve at the cylinder head

6.3.4 High Pressure Gas Piping

A high pressure pipework is required in dealing with pressurized gas. This is a steel pipe with a typical external diameter of 8 mm.

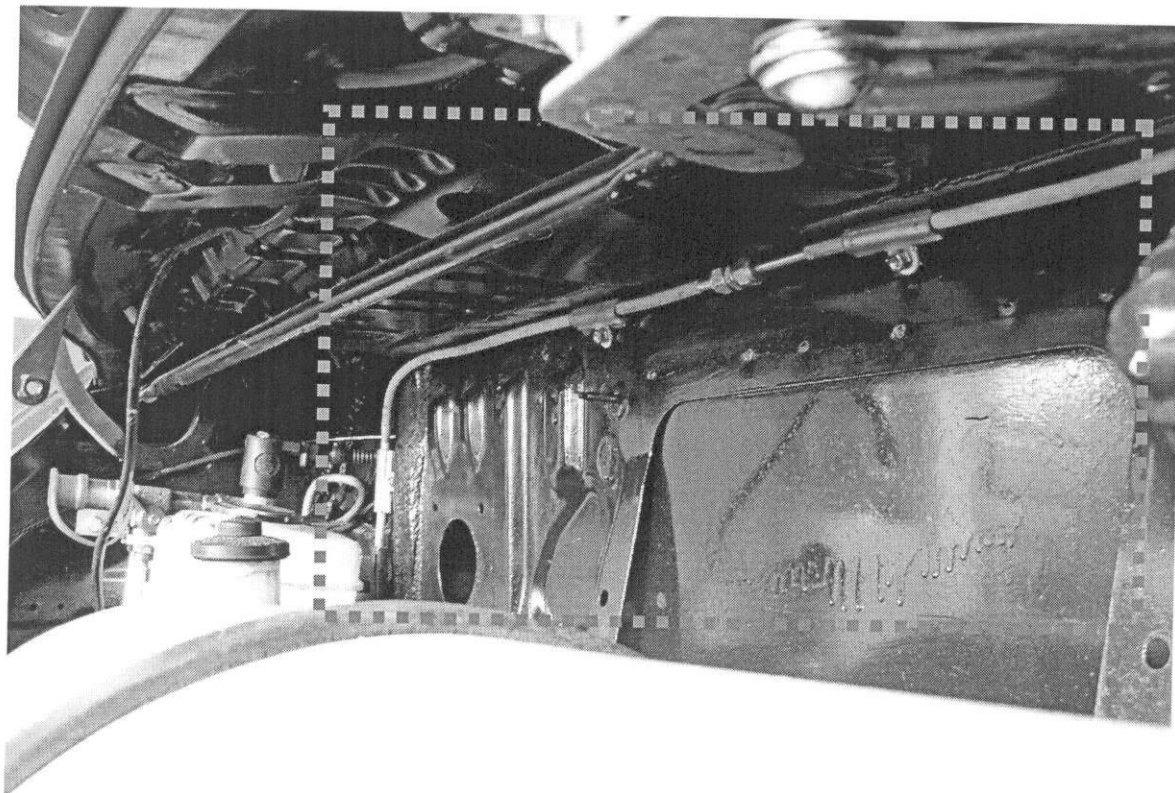


Figure 6.14: The gas pipe from CNG tank to the filling valve



The lowest chassis framework use as conduit and support for the gas pipe.

Figure 6.15: Connection of the gas pipe from the filling valve to the regulator

6.3.5 Pressure Regulator

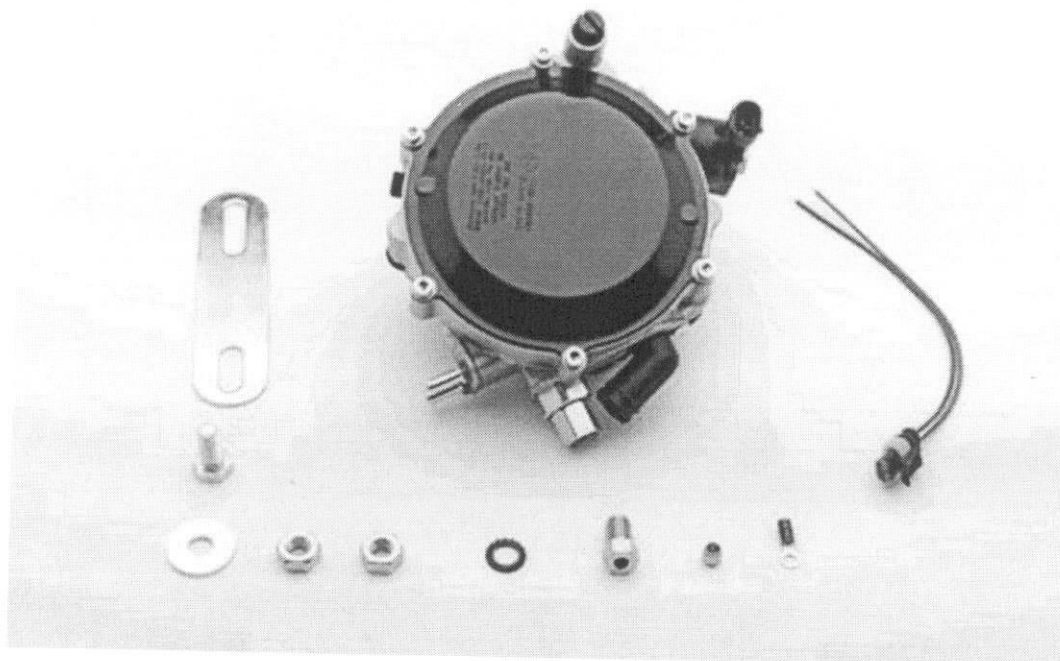


Figure 5.16: Lovato pressure regulator (RME090)

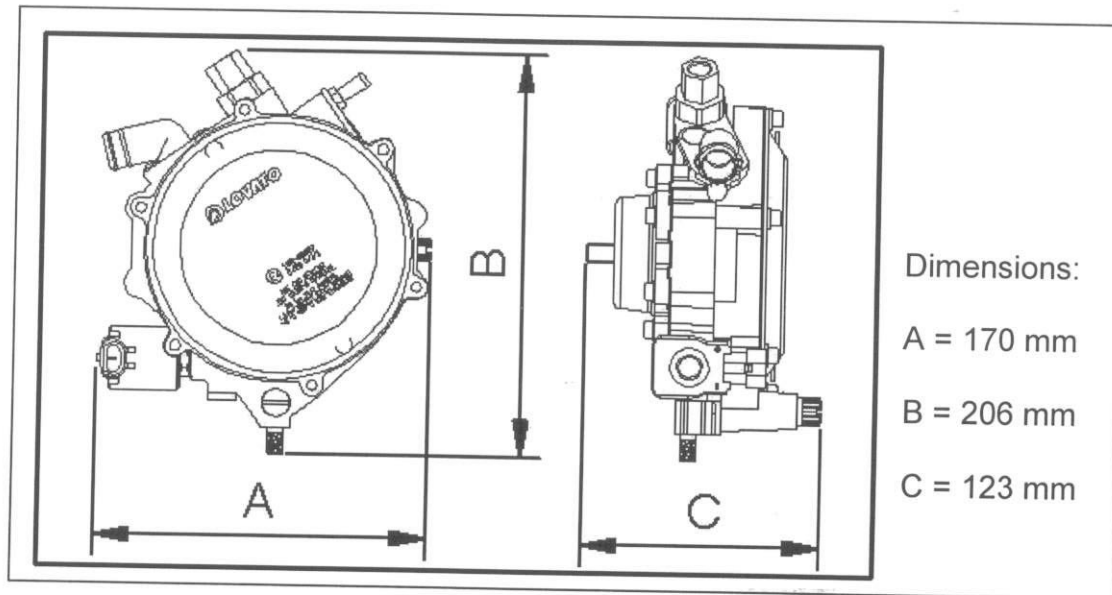


Figure 6.17: Dimension of the pressure regulator (RME090)

A CNG electronic reducer with dedicated fine idle tuning (for engine output of 20 to 90 kW) includes the following main components:

- 3-stage reducer with positive pressure idle device
- Vehicular application (suitable for vehicles with catalytic converter, fuel injection)
- Type of fluid: CNG (Compressed natural gas)
- Casing: GDALSI 13 UNI 5079
- Engine cooling circuit liquid heating
- Inlet pressure: 220 bar
- First stage adjustment pressure: 4 bar
- Second stage adjustment pressure: 1.5 bar
- Power supply: 12 V dc
- High-pressure solenoid valve coil power: 20 W
- Linear electromechanically actuator power: 2 W

The complete arrangement is shown in Figure 6.18.

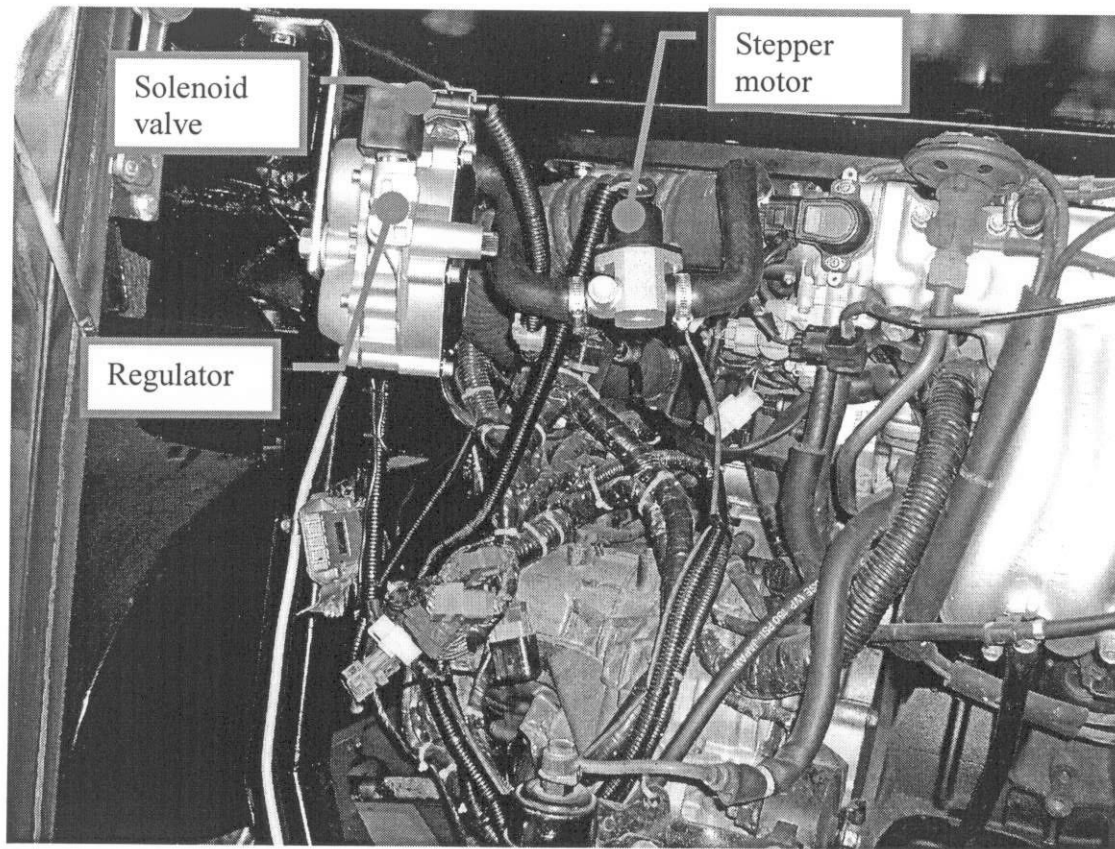


Figure 6.18: The regulator is installed in the engine compartment at the rear of *Tramcar*

The solenoid valve placed on the pressure regulator is switched on when the threshold of engine coolant temperature is reached. The system will switch to CNG mode when all the other conditions such as minimum RPM threshold and acceleration are reached.

6.3.6 Fuel Switch Injection

A fuel switch injection system allows the vehicle operator to switch fuel from gasoline to CNG and vice versa with ease. At a push of a button fuel switching is effortless and of fast response.

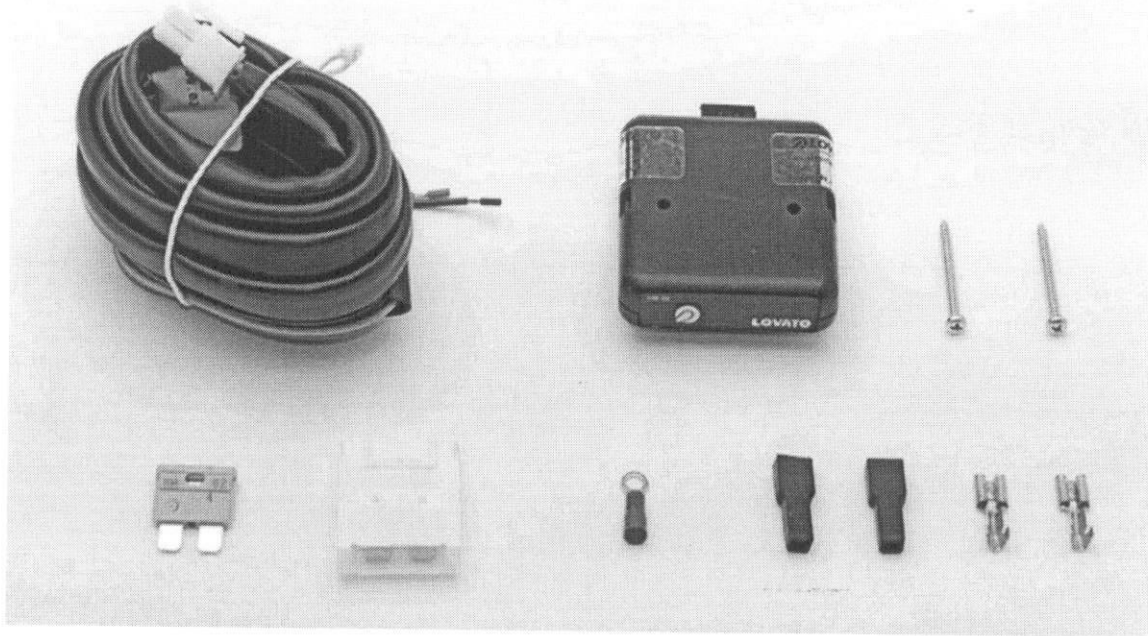


Figure 6.19: Fuel switch injection THERMOTRONIC M 198I with fuel level indicator, level indication is given by means of 4 green leds and 1 red led for reserve

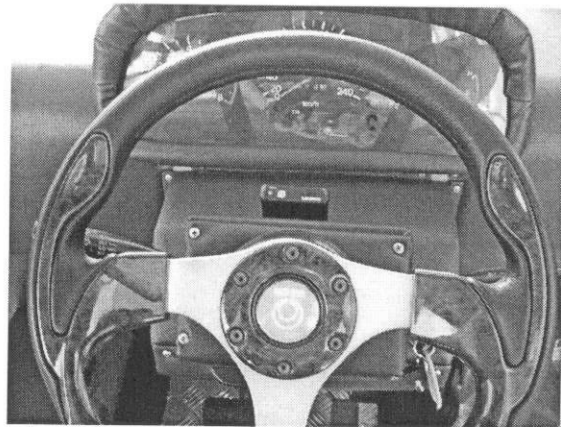
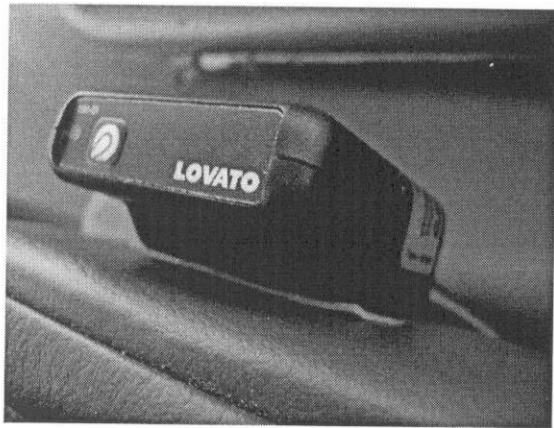


Figure 6.20: Location of the fuel switches that is convenience for the driver to observe the running system.

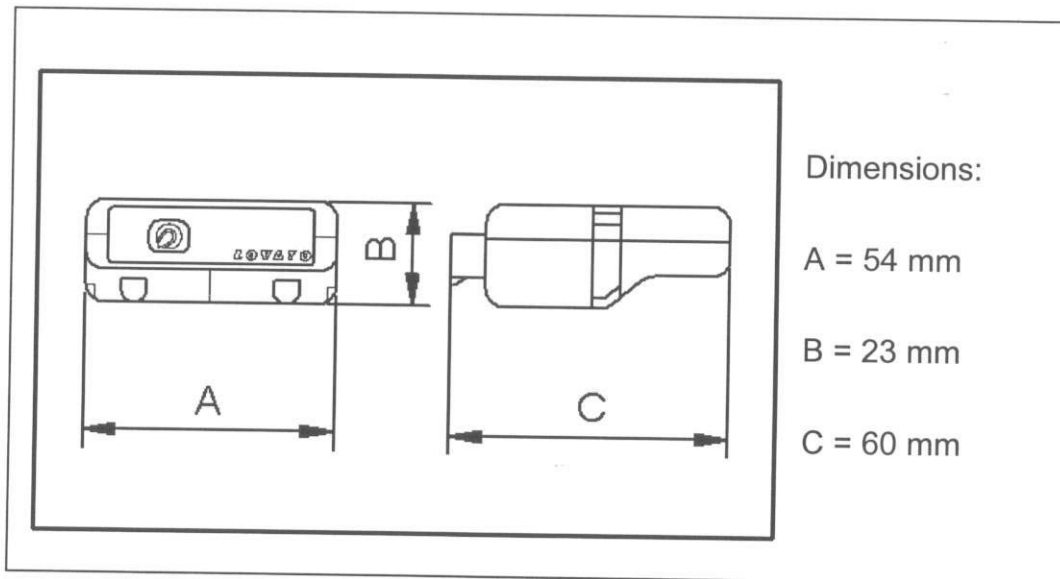


Figure 6.21: Dimension of the fuel switch

6.3.7 Gas Mixer

A gas mixer is a device that meters the proportionate amount of gas into the engine with the flow of air via the air filter assembly. Its internal geometrical structure resembles a venturi with fine holes embedded within the circumference of the venturi constriction. As the air flows through the constriction section, it will induce the gas thus allowing the more or less constant air-gas ratio to rush into the engine intake manifold at every engine cycle.

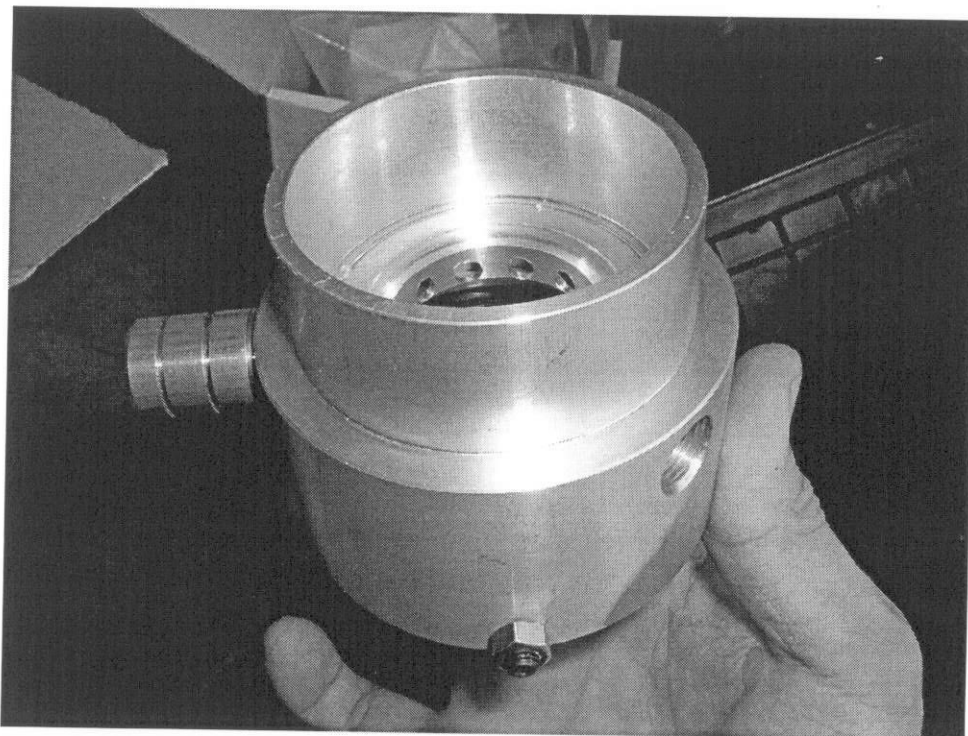


Figure 6.16: Prototype mixer use at the air intake manifold

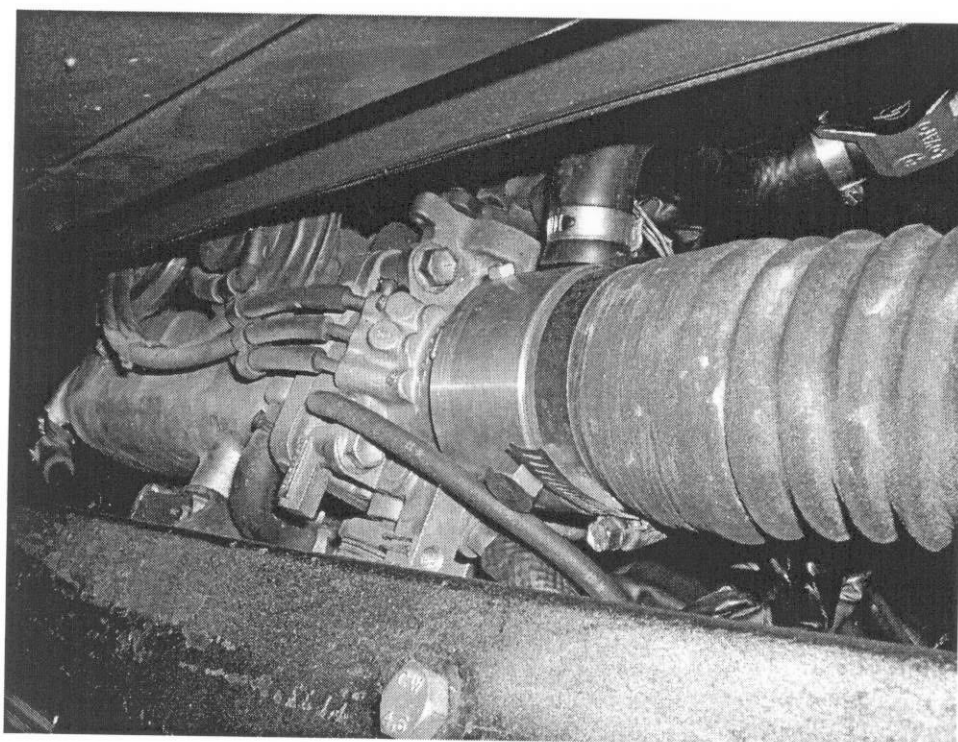


Figure 6.17: Installation of the mixer to the air intake manifold and the CNG supply line

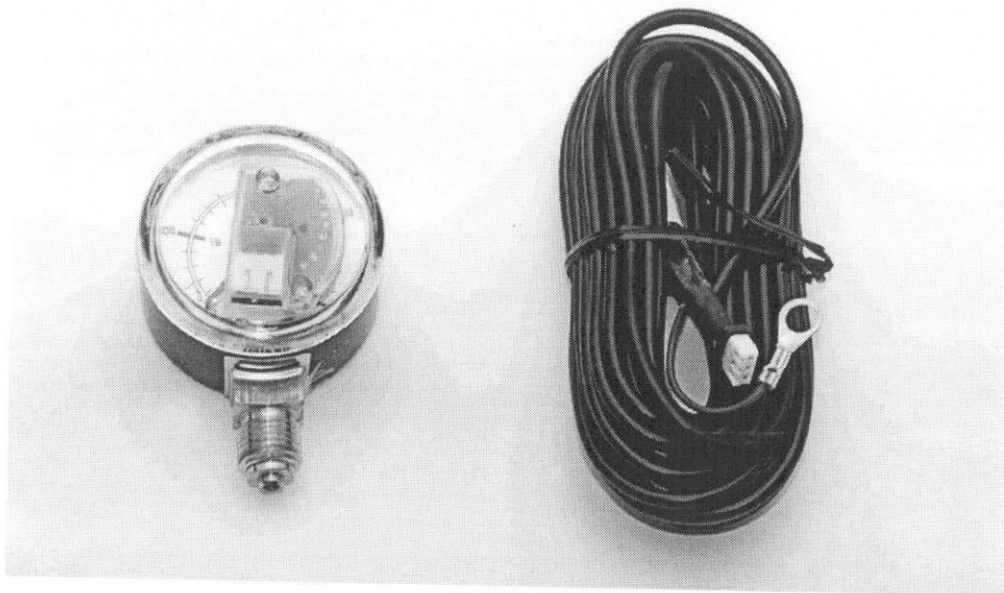


Figure 6.18: Pressure gauge completed with electronic pick-up for level indicator

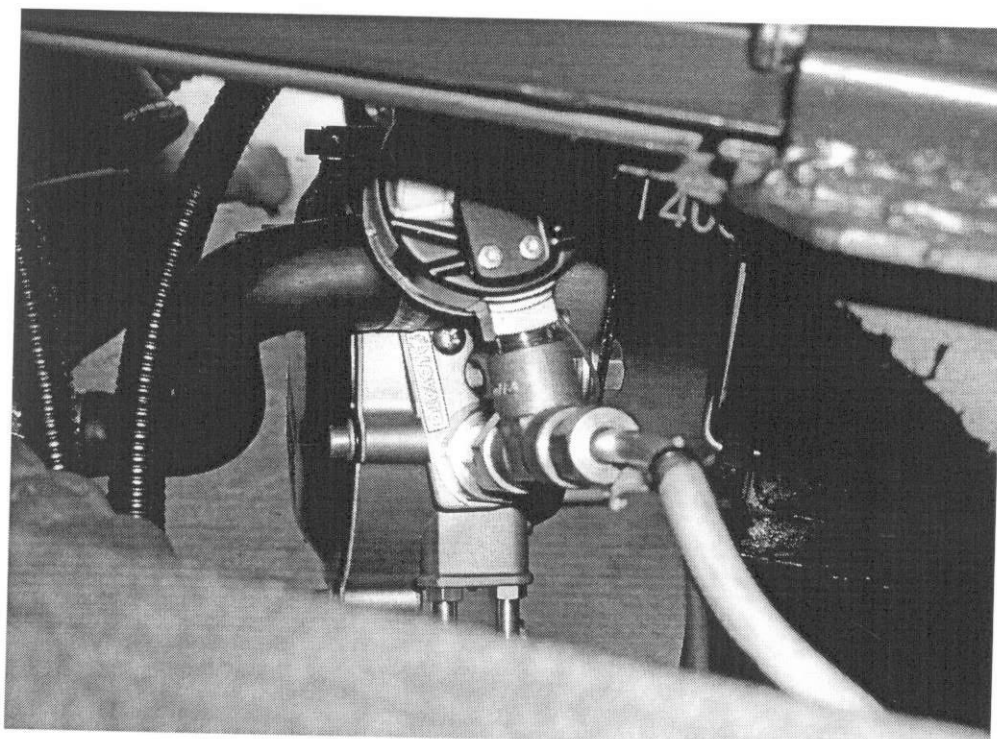


Figure 5.19: The pressure gauge connect to the high pressure pipe to monitor the pressure in the CNG tank

6.3.8 Injector Emulators

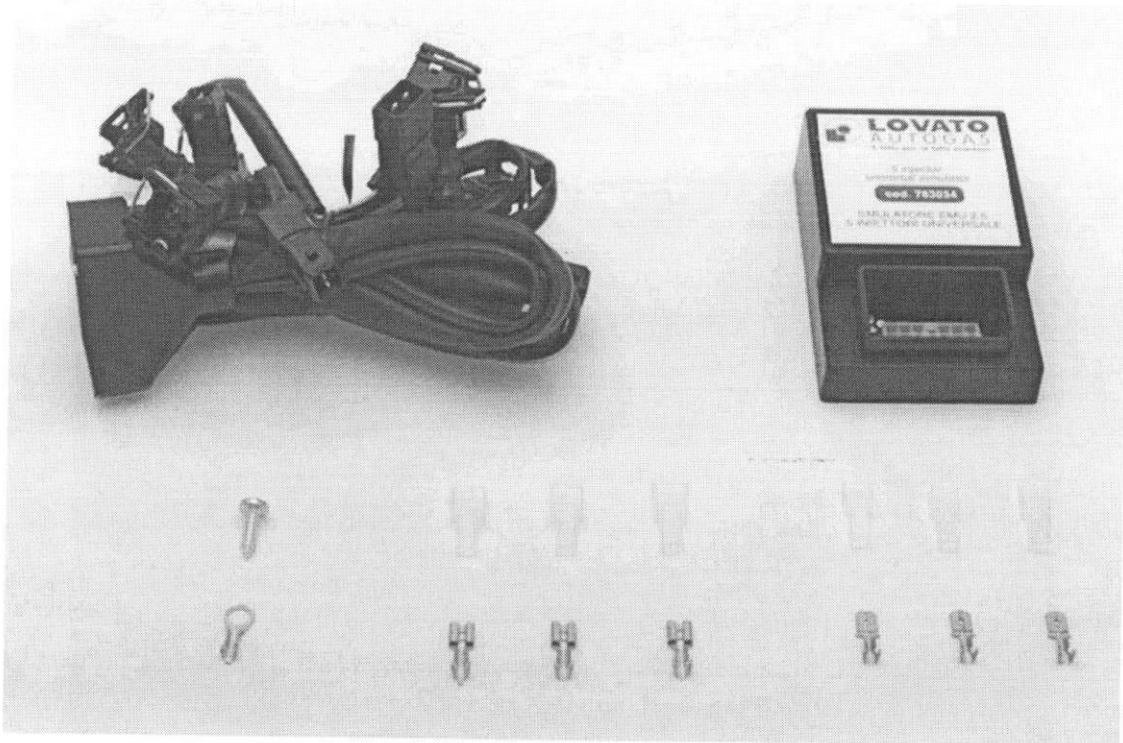


Figure 6.20: Emulator type 2, 5 - 5 cylinders with Europe standard harness

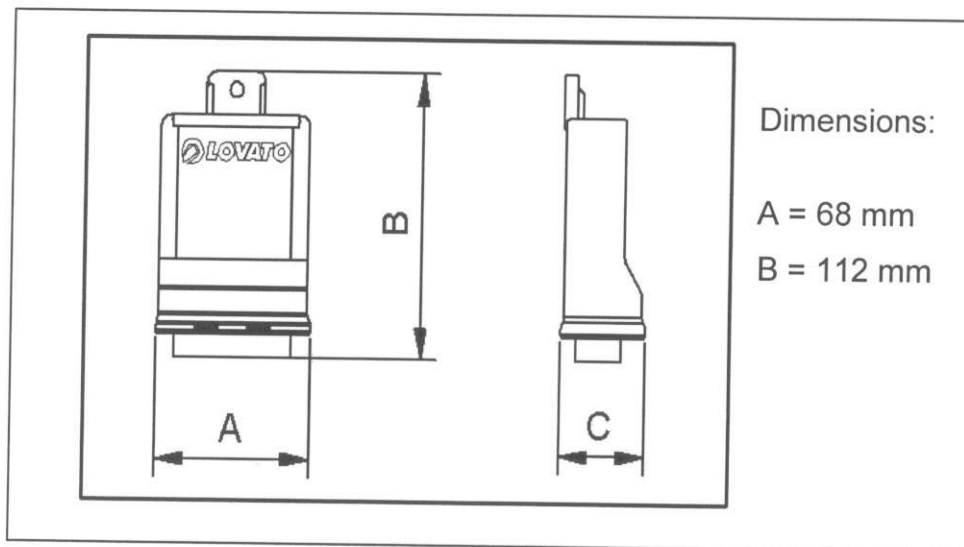


Figure 6.21: Dimension of the injector emulator

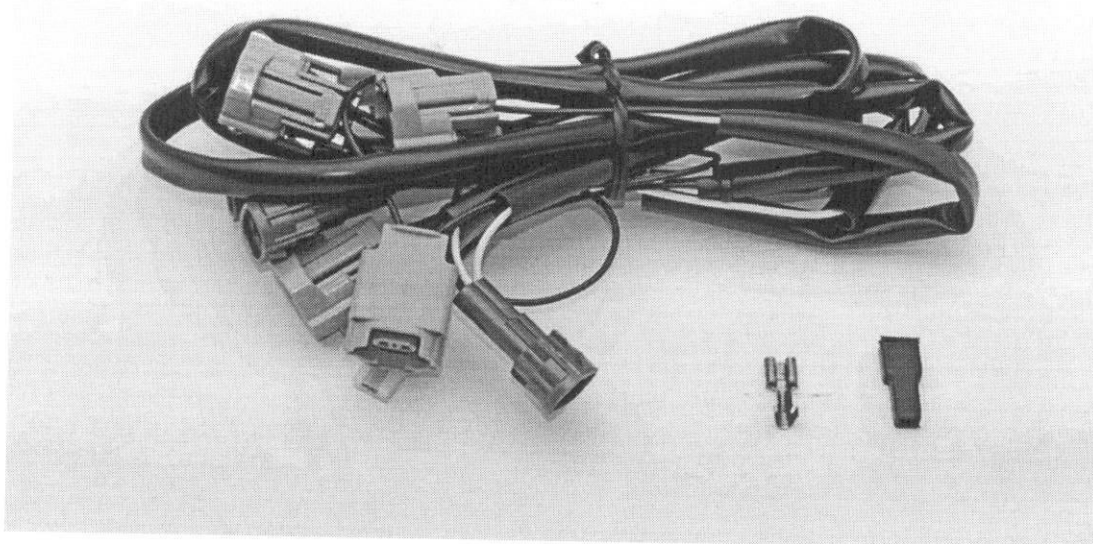


Figure 6.22: Injector cut-out Japan standard harness specified for Japanese engine

The LOVECO-PRO closed loop system is equipped with a level indicator fuel switch. It also includes the following main components:

- fuel switch MICRO LEVEL
- electronic ECU
- Flow actuator with step motor
- NTC temperature sensor
- wiring harness
- accessories package

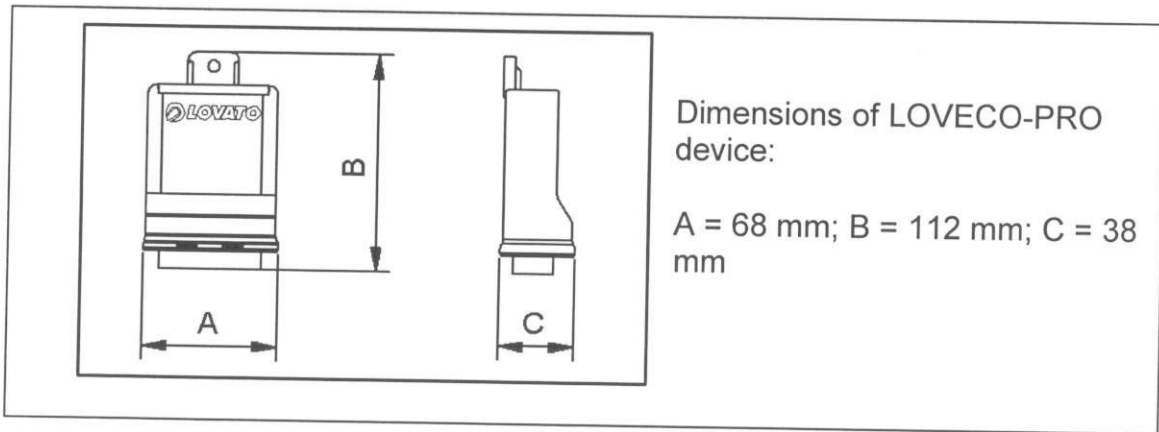
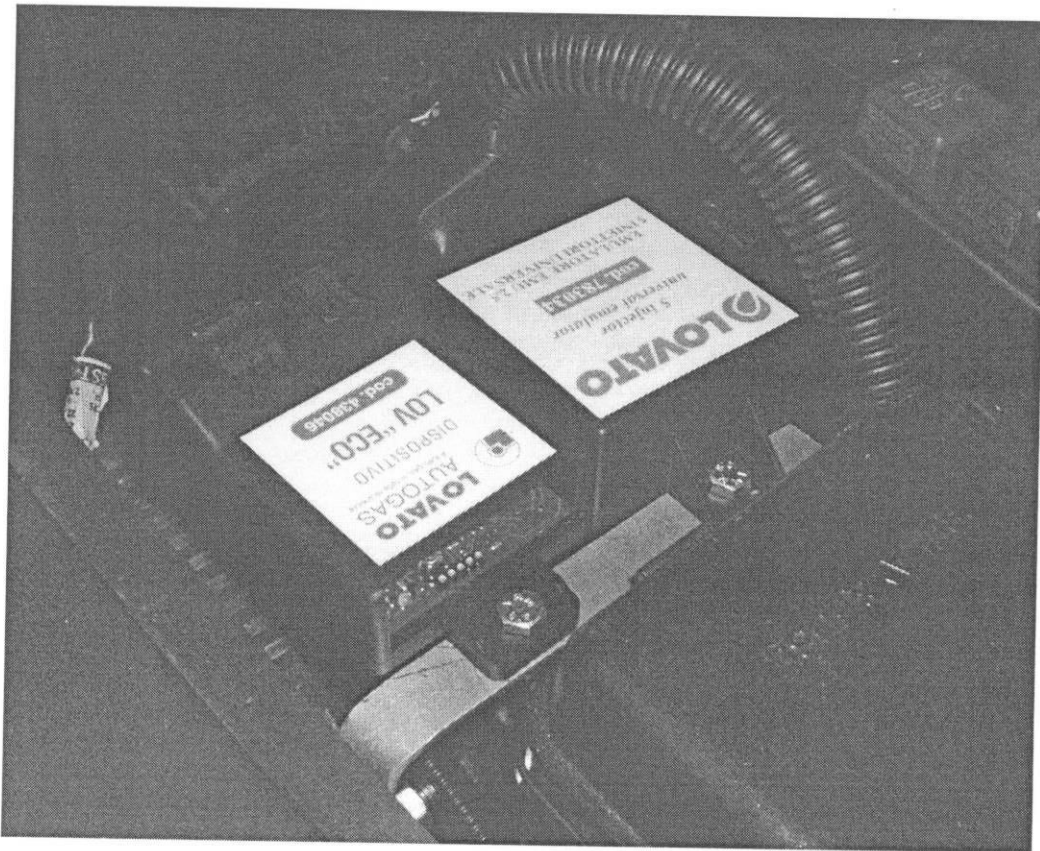


Figure 6.23: Photo and dimension of LOVECO-PRO.

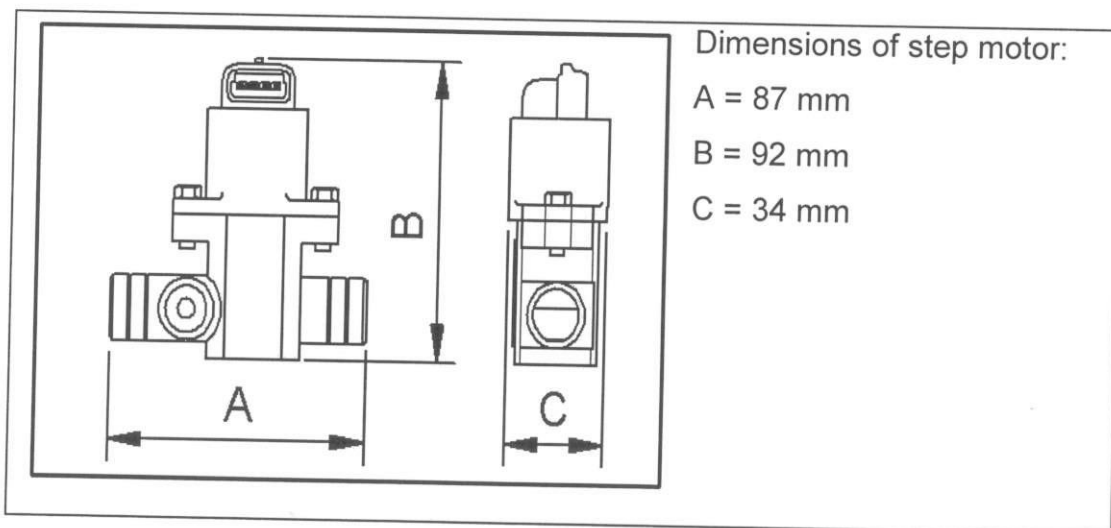
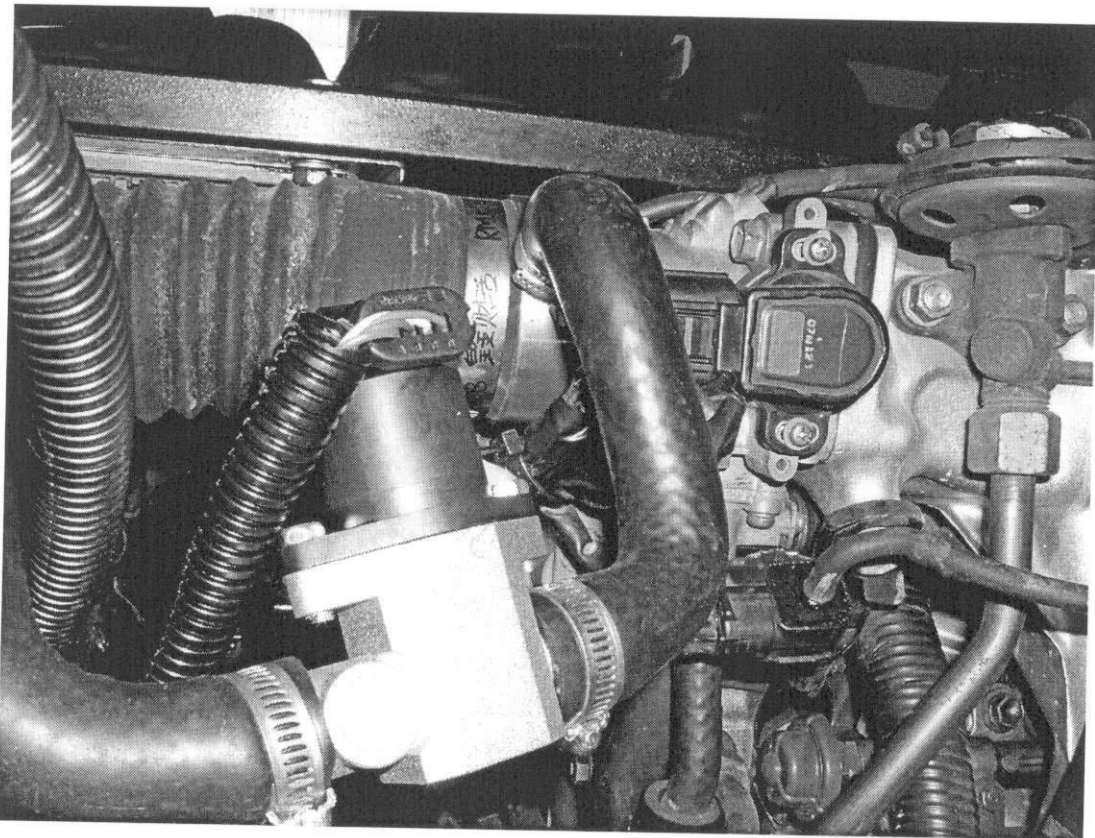


Figure 6.25: The photo of the stepper motor and its physical dimension

The gasoline injector during CNG mode is switched off with the control of injector emulator. The CNG ECU (LOVECO-PRO) starts to control the CNG system including the lambda sensor, throttle position sensor, RPM sensor, stepper motor and others relevant devices respectively.

6.4 Vehicle Test with CNG Conversion Kit

Having fitted the complete conversion kit with the assistance of the supplier, the *Tramcar* was tried extensively to assess its overall performance. It was noticed that after several trials and fine-tuning efforts, the vehicle now is fully a dual-fuel vehicle with a capability to demonstrate the gasoline-CNG operation.

CHAPTER 7

CONCLUSIONS AND RECOMMENDATIONS

7.1 Conclusions

The Tramcar was successfully designed, developed and tested for recreational purposes as part of the flagship project for ADC. To add an interesting feature to it is the incorporation of CNG conversion kit which has proven to be successful, in line with the theme of environmental-friendly people's mover within the UTM campus.

Proceeding all the analysis and computational results obtained on the *Tramcar*, the safety and comfort impart on the passengers due to its chassis and suspension system, subjected to various operating conditions were successfully identified.

The safety factor for a vehicle chassis has earlier been stressed to be beyond 2.0. The following table summarizes the safety factors for normal stress and shear stress and displacements of chassis for each of the analysis.

Table 7.1: Safety factors

	Safety factor		Displacement [mm]
	Normal stress	Shear stress	
Static analysis	2.93	3.08	4.23
Bumping analysis	2.59	2.73	4.63
Braking analysis	3.88	4.09	3.72

The maximum deformations in the three analyses have been proven to be less than 5mm. From the contour of deformation, it can be said that the maximum deformation will occur at the middle of chassis. However the deformation can be regarded as small and it can be concluded that the chassis is safe for use.

The magnitude of the chassis torsional stiffness was obtained from the slope of the graph of torsion against twisting angle. The value is 5127.5Nm/degree, which is in the range allowed for a normal saloon car i.e., 3000Nm/degree to 9000Nm/degree. As far as the torsional stiffness analysis is concern it has proven that the chassis is safe.

Also covered in the analysis was the comfort factor, which was only confined to the effect from the suspension system. Using the full car model and based on the response gain from the suspension design of *Proton Waja 1.6*, the *Tramcar* has performed badly in frequency isolation. For bouncing, pitching and rolling analysis, all the peak point in the graph for *Tramcar* were noted to be higher than the peak point for *Proton Waja 1.6*. This was due to *Tramcar's* suspension system was 'softer' than the *Proton Waja 1.6*. To support this argument, in rolling analysis, the *Tramcar* reached the maximum roll rate at 0.2234rad/s. However the *Proton Waja 1.6* reached the maximum roll rate at 0.1505rad/s. The different here is only 0.0719rad/s.

The results also indicate that both the suspension systems have almost taken the same time to damp their respective displacement. That clearly shows that the displacement absorption (for the suspension system) is almost the same with *Proton Waja 1.6*. Hence, it can be concluded that the *Tramcar* suspension performance does not differ much from *Proton Waja 1.6*.

7.2 Recommendations

Although the *Tramcar* can be classified as suitable for use, there are still some improvements to be made.

From the results of the contour of deformation analysis, the maximum stress will occur at the middle section of chassis. The maximum deformation is noted to occur at the same point. Since this is the weakest point, the chassis will most probably fail at this place. Hence, strengthening of the upper ladder frame cross bar must be made to avoid the failure occurrence. Two choices are available here, i.e. the use bigger diameter of steel bar or increase the thickness of bar.

For suspension system, the displacement is more on *Tramcar* than the reference vehicle, which is the *Proton Waja 1.6*. Here it is suggested that the *Tramcar* may consider the use of the higher suspension stiffness to mitigate the vibration level, and indirectly to increase the passengers' comfortable level. It is also suggested that to isolate the disturbance due to road irregularities, the increase the suspension damping rate must be made.

Below are some recommendations for future work with regard to safety and comfort factors: -

1. Analysis for other factor that influence the comfort level such as the position of seat, the view angle and the space for leg.
2. Design an external cover roof to protect passengers getting wet when raining.
3. The aerodynamic drag analysis.

BIBLIOGRAPHY

1. Gillespie, Thomas D. (1992). ***Fundamentals of Vehicle Dynamics***. Society of Automotive Engineers, Inc., Warrendale, Pennsylvania, USA.
2. Wild, R. (1978). ***A Practical Approach to Cab Suspension***. Society of Automotive Engineers, Warrendale, Pennsylvania, USA.
3. Brueck, Donald M. (1977). ***A Simplified Method for the Identification of Vehicle Suspension Parameters***, Society of Automotive Engineers (SAE), Warrendale, Pennsylvania, USA.
4. Ikenaga, S., Frank, L.L., Campos, J. and Leo, D. ***Active Suspension Control on Ground Vehicle Based on a Full Vehicle Model*** University of Texas, Arlington, USA.
5. Davis, L., Lewis, F.L., Scully, S. and Evans, M. ***Active Suspension Control of Ground Vehicle Heave and Pitch Motions***. University of Texas, Arlington, USA.
6. Zaid Hj. Mohd. Zin (1995). ***Pengenalan Kepada Pembuatan Kereta***. Kuala Lumpur: Dewan Bahasa dan Pustaka (DBP), Kementerian Pendidikan Malaysia.
7. Gibbs, H. G. and Richards, T. H. (1975). ***Stress, Vibration and Noise Analysis in Vehicles***, Applied Science Publication, London.
8. Fenton, John (1998). ***Handbook of Automotive Body and Systems Design***, Professional Engineering Publishing, London.
9. Howard, Geoffrey (1998). ***Chassis & Suspension Engineering***, Osprey Publication Ltd, London.
10. Campbell, Colin (1981). ***Automobile Suspensions***. London: Chapman and Hall Ltd., London, UK.
11. Bastow, Donald (1988). ***Car Suspension and Handling***, Pentech Press, London UK.
12. Reimpell, J. ***The Automotive Chassis***. Arnold Publisher.
13. L.Y. Chan, Doecke, M., Lalwani, H., H.W. Lau, T. Lau, C.C. Lee and C.C. Low. ***Design and Build of a Formula SAE Vehicle (Chassis, Shell and Instrumentation)***. Australia: Department of Mechanical Engineering, University of Adelaide, Adelaide, Australia.

14. Whitney, J.D. (1995). ***Experimental Characterize and Dynamic Simulation of a Quadra Link Independent Rear Automotive Suspension System***. University of Massachusetts, USA, M.Sc. Thesis.
15. Muhammad Hayat Bin Mohd Zamberi (2004). ***Relkabentuk Go-Kart***. Universiti Teknologi Malaysia (UTM), Final year project thesis.
16. Saiful Rahman Tarson (2003). ***Merekabentuk Cesis dan Pemilihan Roda untuk Go-Kart***. Universiti Teknologi Malaysia (UTM), Final-year project thesis.
17. Tam Wee Kong (2003). ***Study of Stress onto Car Body When Reached By Torsional and Bending Stiffness***. Universiti Teknologi Malaysia (UTM), Final-year project thesis.
18. Cheah Tat Wee (2001). ***Study and Analysis of a Passenger Car Suspension System***. Universiti Teknologi Malaysia (UTM), Final-year project thesis.
19. Kenneth J. Kelly (1998), ***The Effect of Fuels and Test Cycles on Light-Duty Vehicle Exhaust Emissions***, Ohio University Department of Mechanical Engineering.
20. Pulkrabek W.W. (1997), ***Engineering Fundamentals of the Internal Combustion Engines***. Prentice Hall International, inc.
21. www.lovatogas.com
22. www.iangv.org
23. www.angva2005.com
24. www.omnitekcorp.com
25. www.epa.gov
26. www.dieselgas.co.nz
27. www.mckenziecorp.com/dehydration.htm
28. www.brettandwolffllc.com/engines.html#Northport
29. www.baftechnologies.com/afs.htm
30. www.autogas.lv

APPENDIX A

OVERALL VEHICLE CHARACTERISTICS

Table A1: Engine characteristics

Engine type	Serial 4 Cylinder DOHC 16 Valve
Engine model	3S-FE
Displacement	1998 cc
Power density	8.71
Maximum power (net)	102.97 kW (140 PS)/6000 rpm
Maximum torque (net)	19.0 kgm (186.33 Nm)/4400 rpm
Fuel system	Electronic Fuel Injection
Fuel type	Unleaded Premium Gasoline
Compression ratio	9.5
Bore	86 mm
Stroke	86 mm

Table A2: Tramcar physical characteristics

Dimension [mm]	
Overall length	4700
Overall width	1851
Overall height	1763
Wheelbase	3417
Front track	1600
Rear track	1600
Unload ground clearance	190
Front overhang	970
Rear overhang	1090

Table A3: The vehicle estimation weight

Component	Estimated weight [kg]
Chassis	204.35
Seats and passengers	720.00
Engine	300.00
Full petrol tank	30.80
Front cover body	23.00
Rear cover body	16.30
Cover roof	69.55
Others	300.00
Vehicle curb weight	984.00
Vehicle gross weight	1664.00

Table A4: The suspension specifications

Suspension type	Independent McPherson Struts
Coil spring outer diameter	114 mm
Free length	351 mm
Fitted length	228 mm
Fitted load	5700 N
Spring constant	26.5 N/mm
Kingpin inclination	6°35' - 7°35'
Shock absorber type	Double Acting Tube
Stroke	120 mm
Damping forces (at 0.3 m/s):-	
Expansion	1030.05 N
Contraction	353.16 N

APPENDIX B

RESULTS OF STATIC ANALYSES

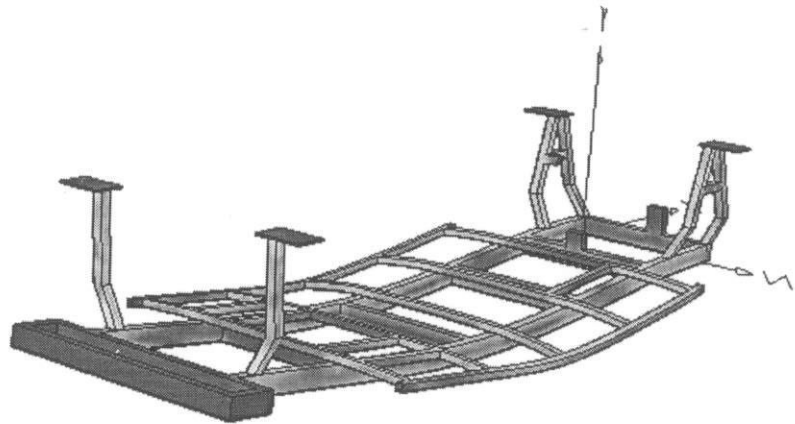
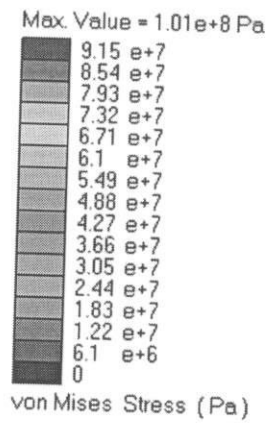


Figure B1: The contour of Von Mises stress

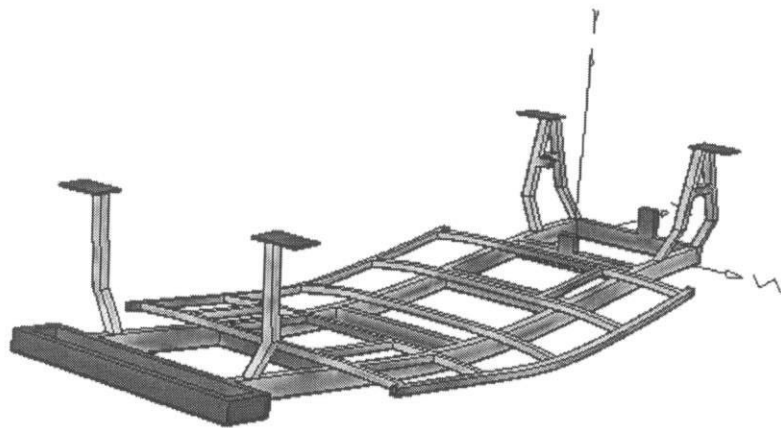
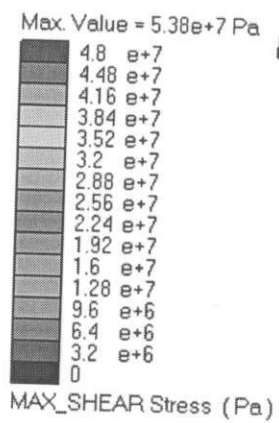


Figure B2: The contour of shear stress

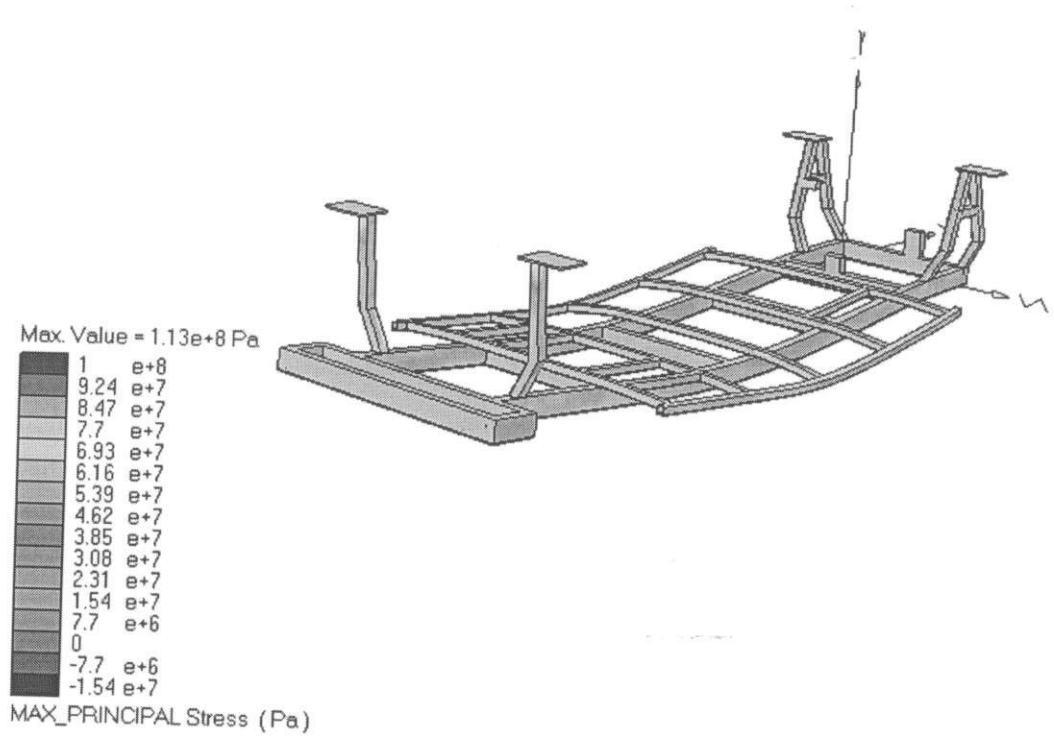


Figure B3: The contour of principal stress

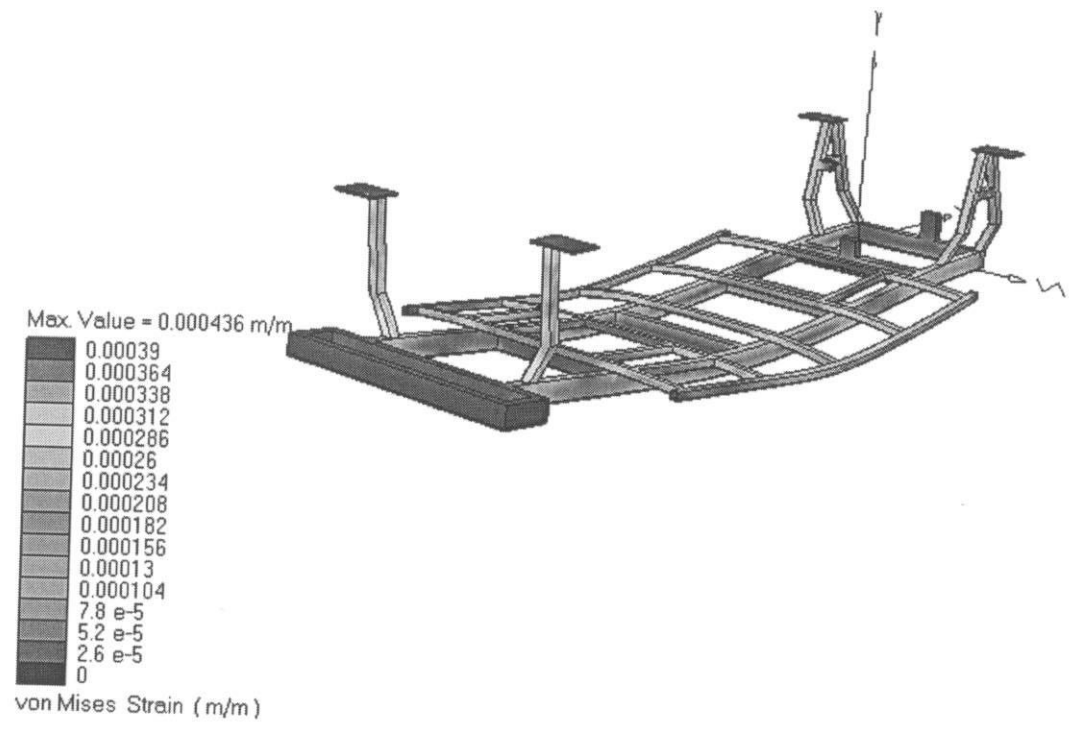


Figure B4: The contour of Von Mises strain

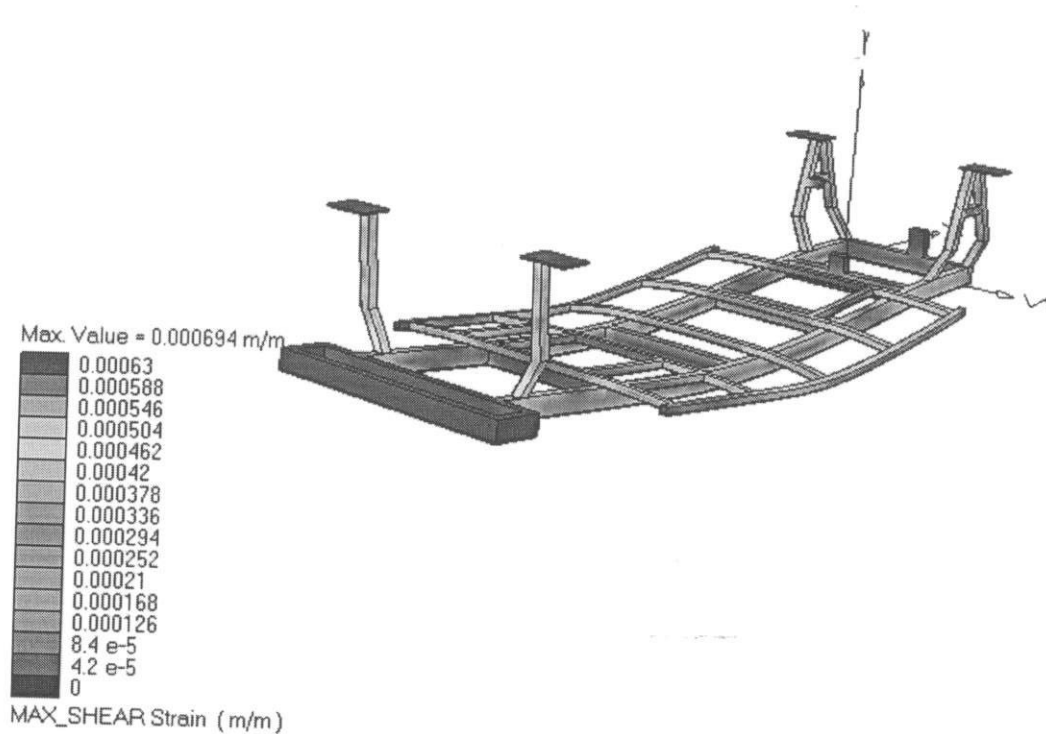


Figure B5: The contour of shear strain

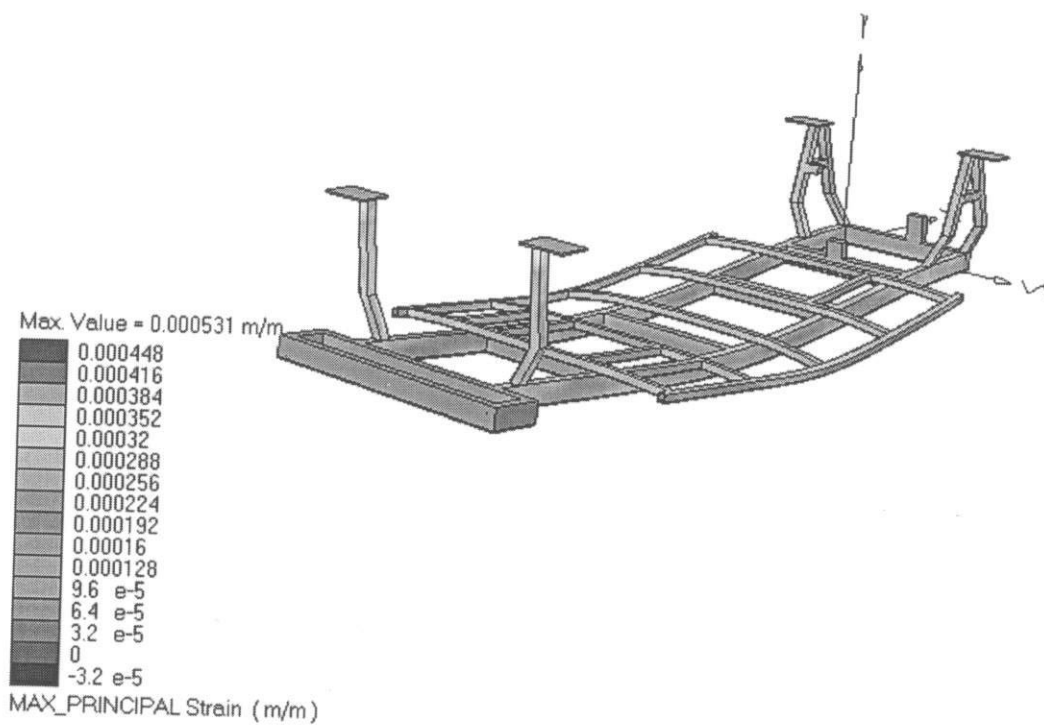
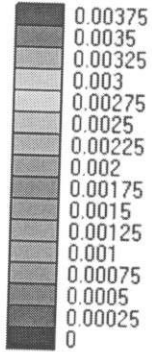


Figure B6: The contour of principal strain

Max. Value = 0.00423 m



Delta_MAG Displacement (m)

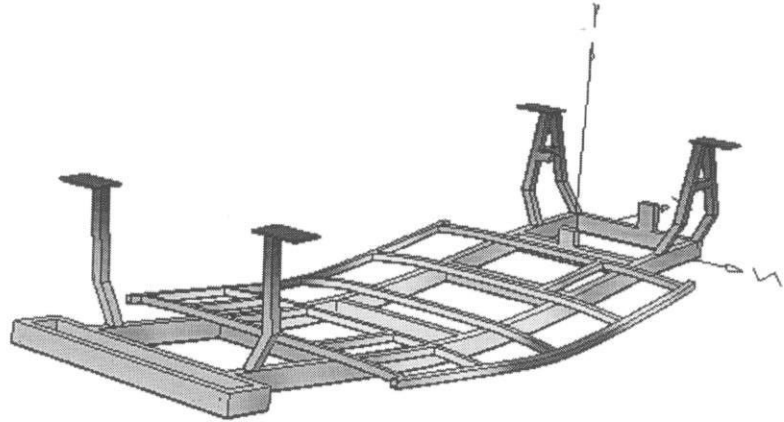
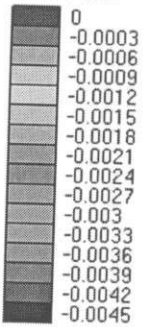


Figure B7: The contour of delta MAG displacement

Max. Value = -0.00421 m



Delta_y Displacement (m)

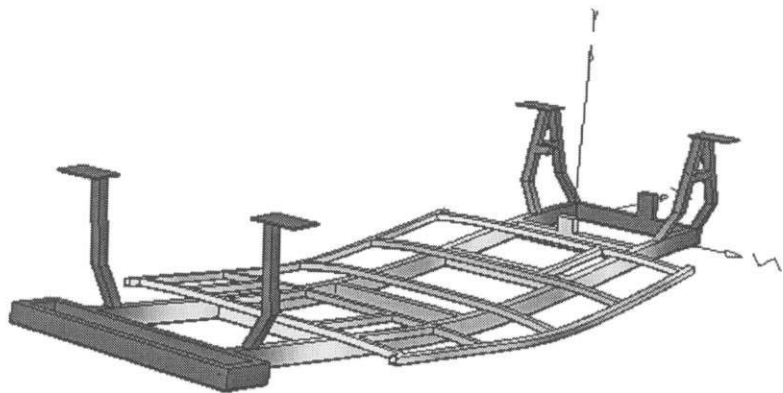


Figure B8: The contour of y-direction displacement

Note: All the deformation scaled by 48.5

APPENDIX C

RESULTS OF THE BUMPING ANALYSIS

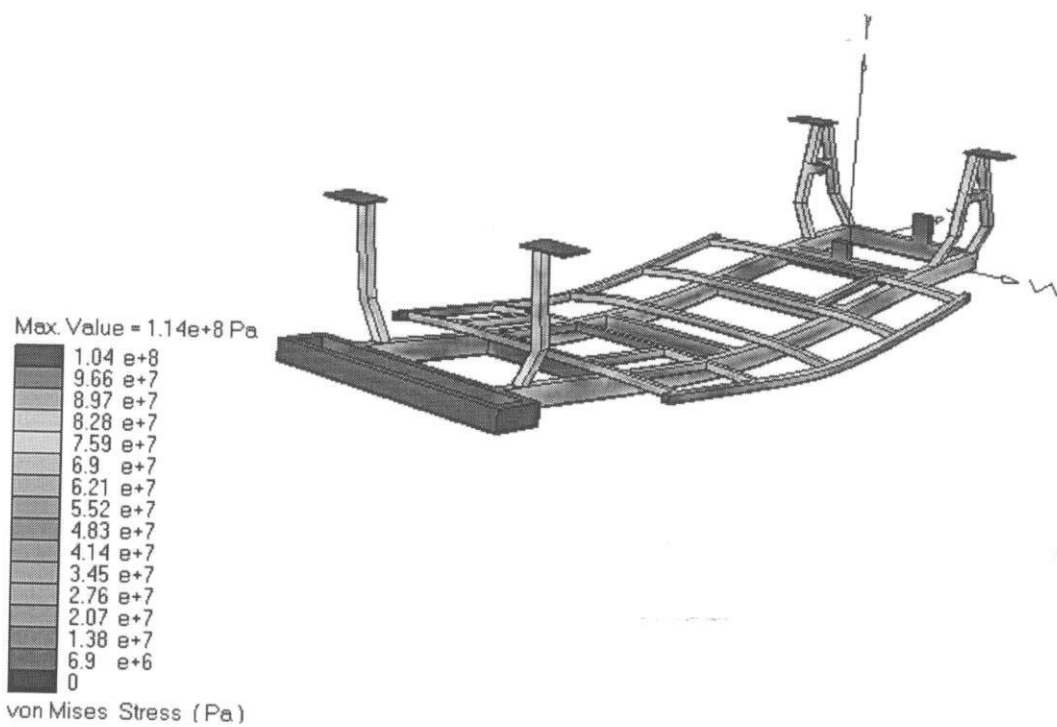


Figure C1: The contour of Von Mises stress

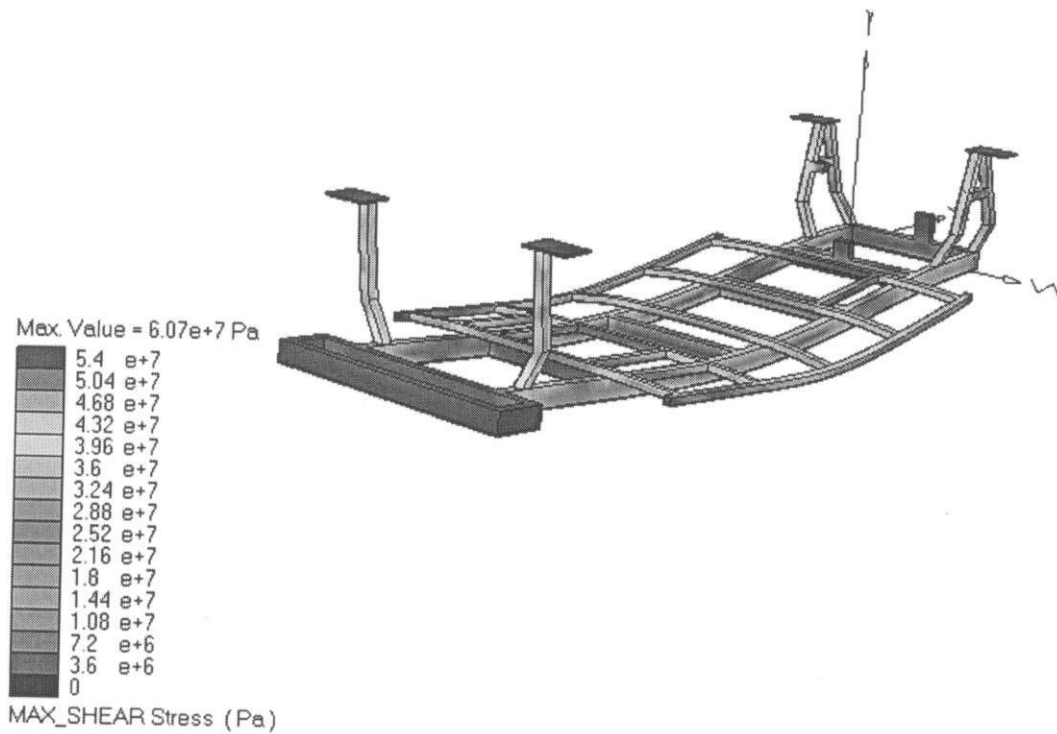
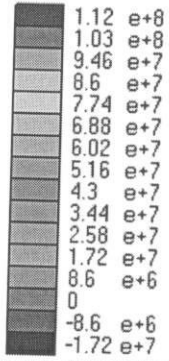


Figure C2: The contour of shear stress

Max. Value = 1.28e+8 Pa



MAX_PRINCIPAL Stress (Pa)

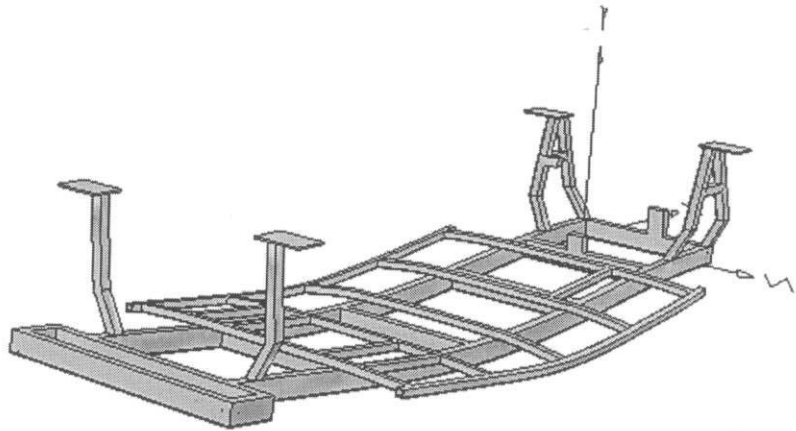
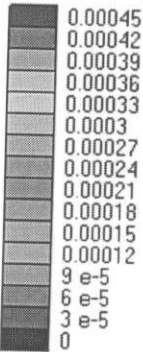


Figure C3: The contour of principal stress

Max. Value = 0.000492 m/m



von Mises Strain (m/m)

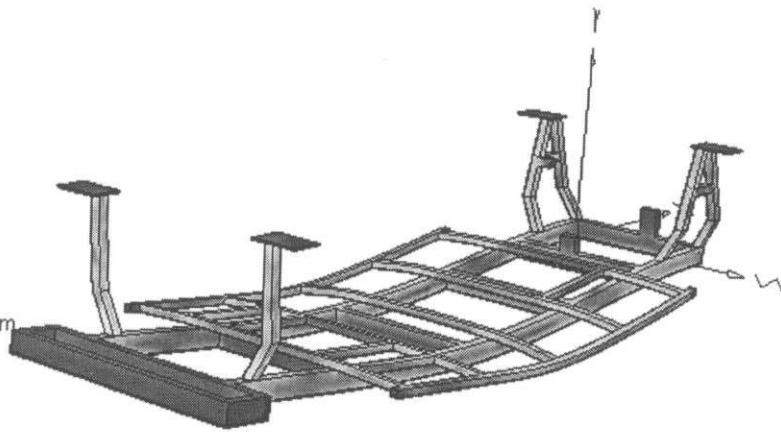


Figure C4: The contour of Von Mises strain

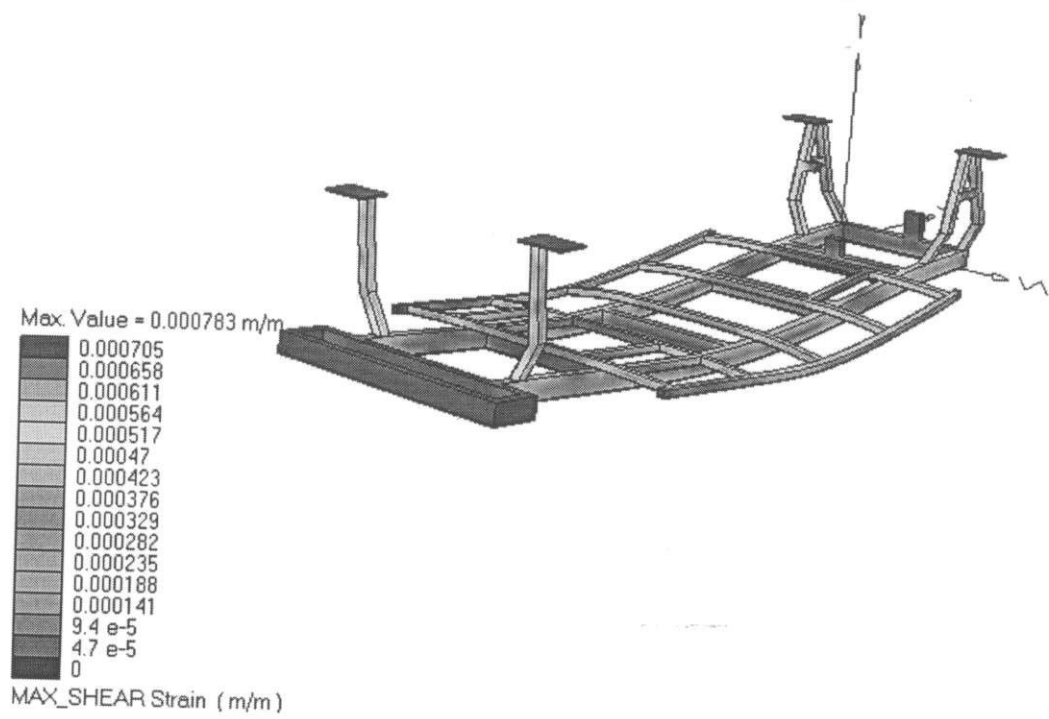


Figure C5: The contour of shear strain

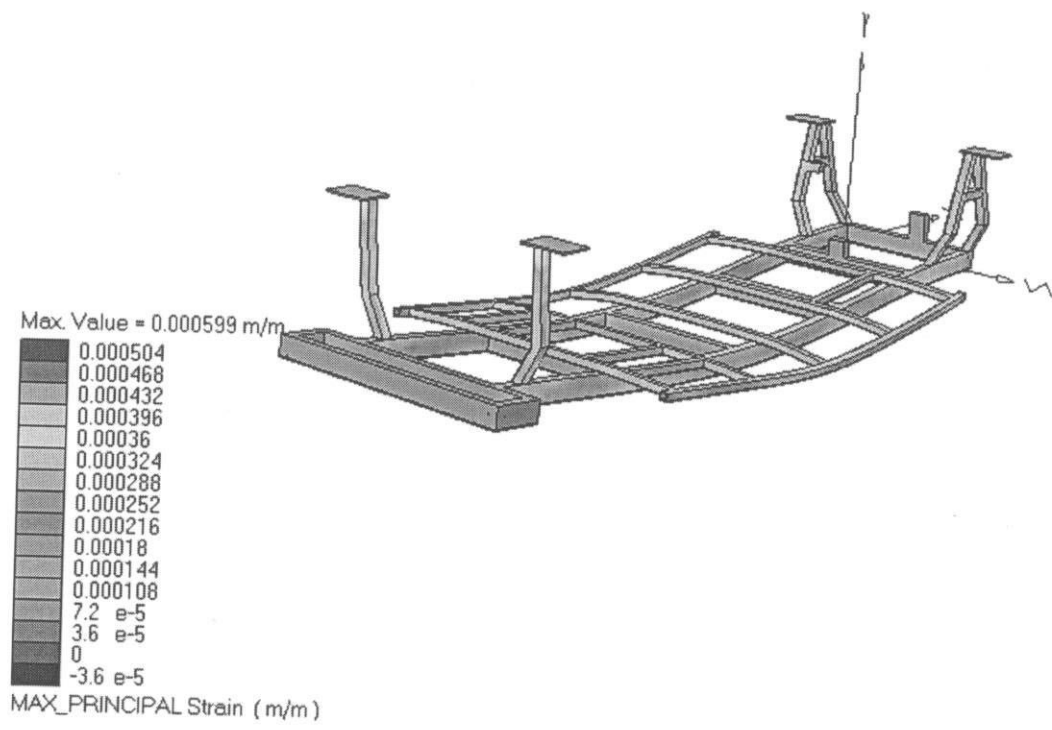


Figure C6: The contour of principal strain

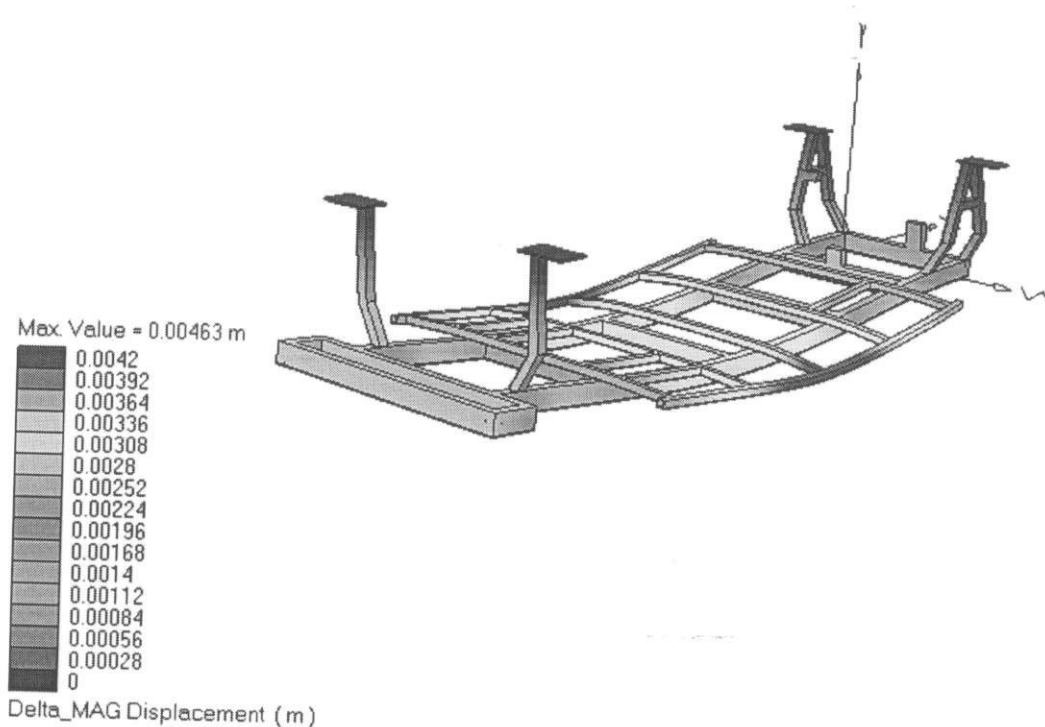


Figure C7: The contour of delta MAG displacement

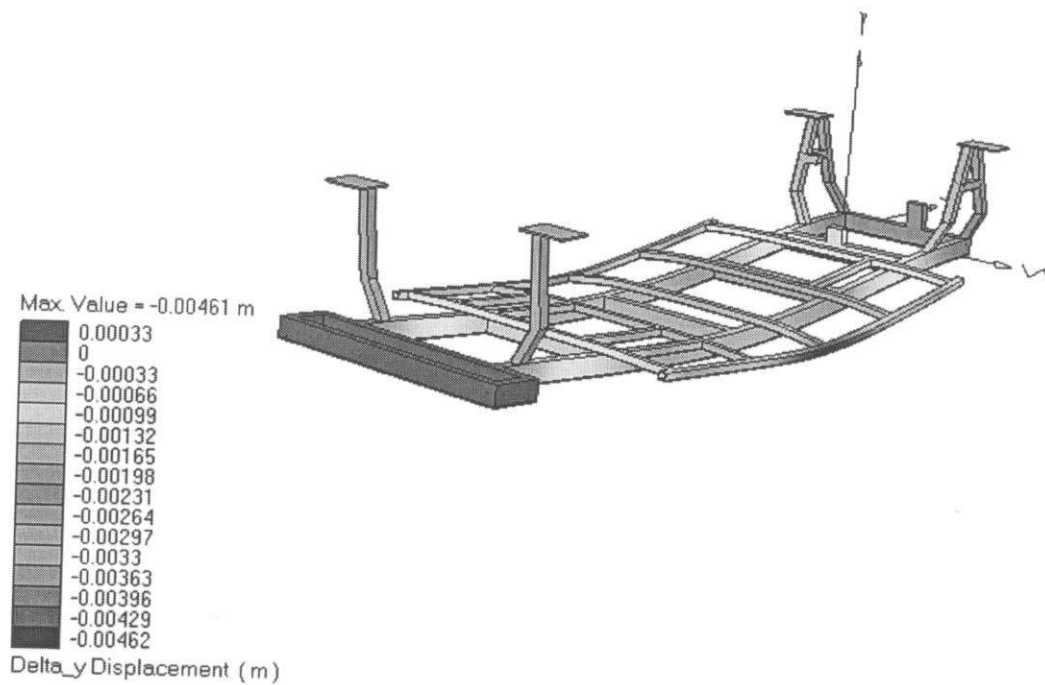


Figure C8: The contour of y-direction displacement

Note: All the deformation scaled by a factor of 44.3

APPENDIX D

RESULTS OF THE BRAKING ANALYSIS

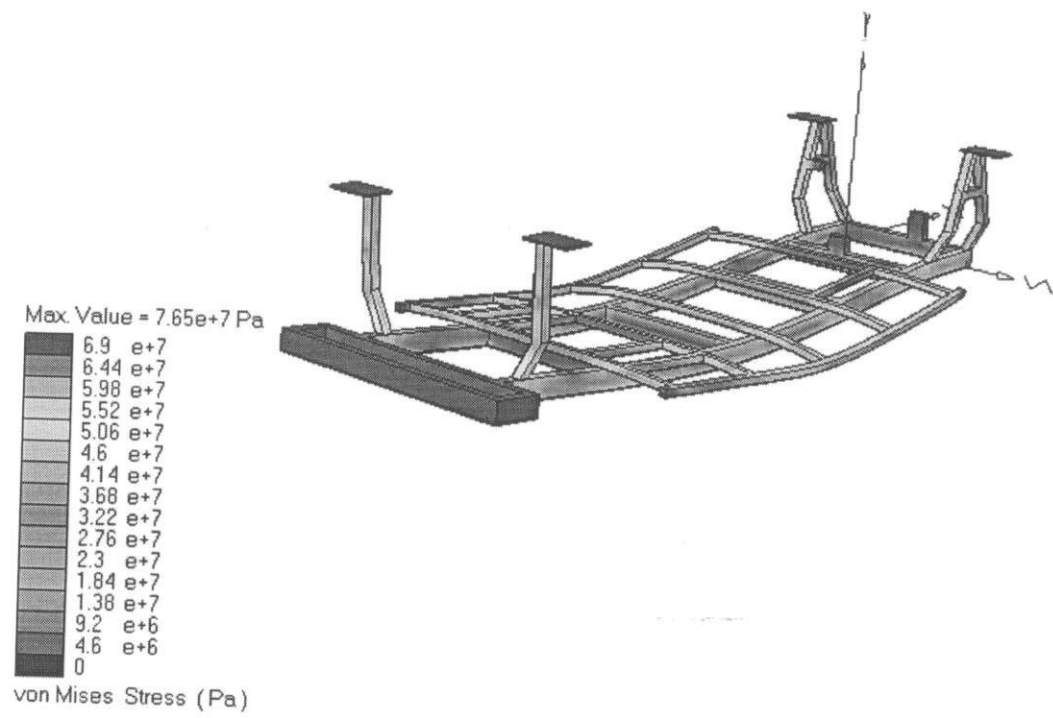


Figure D1: The contour of Von Mises stress

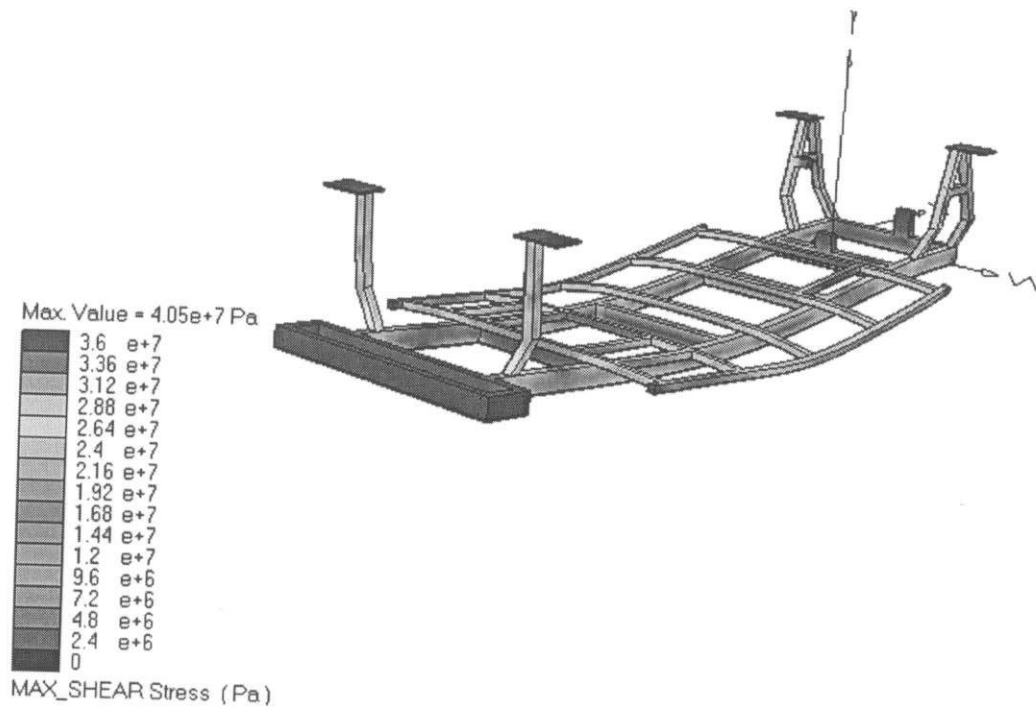


Figure D2: The contour of shear stress

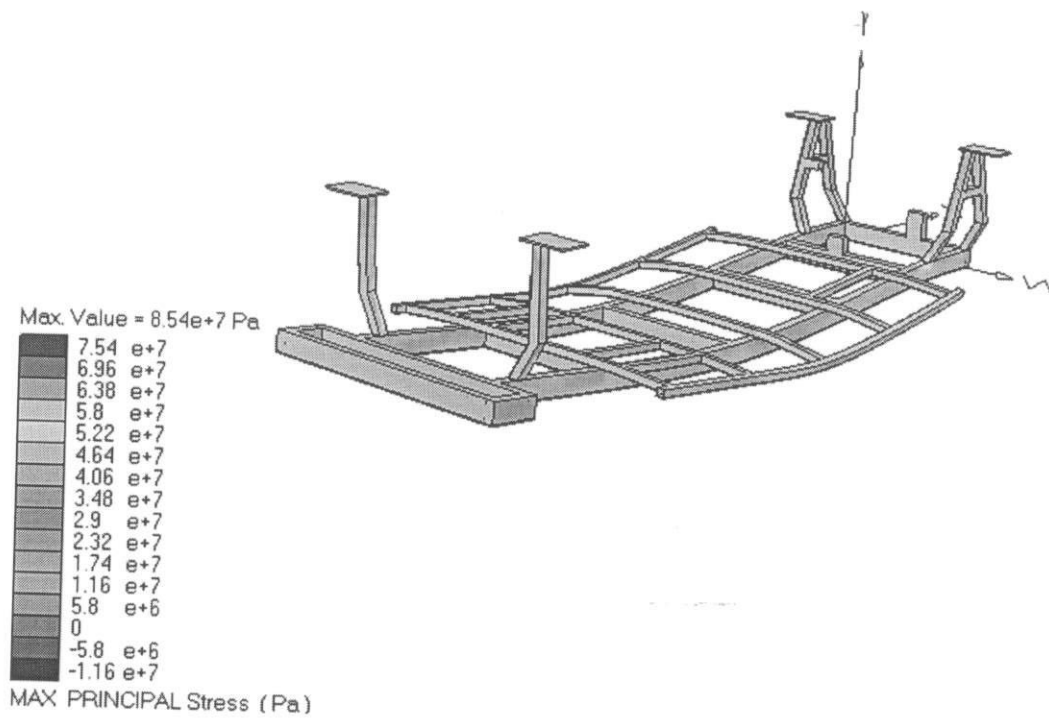


Figure D3: The contour of principal stress

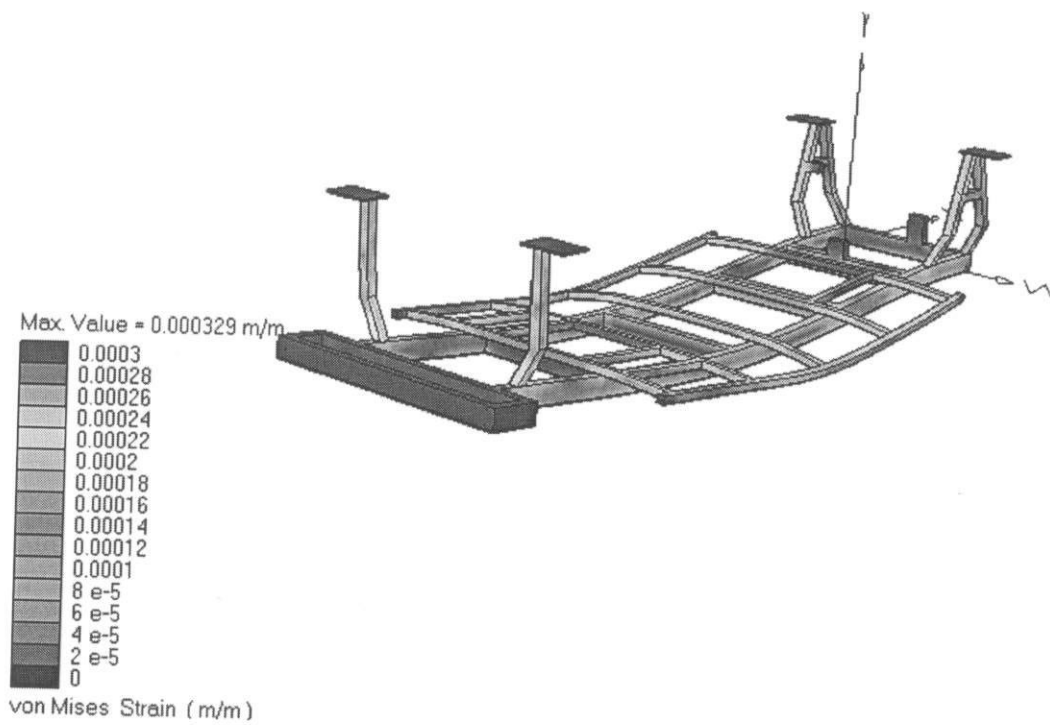


Figure D4: The contour of Von Mises strain

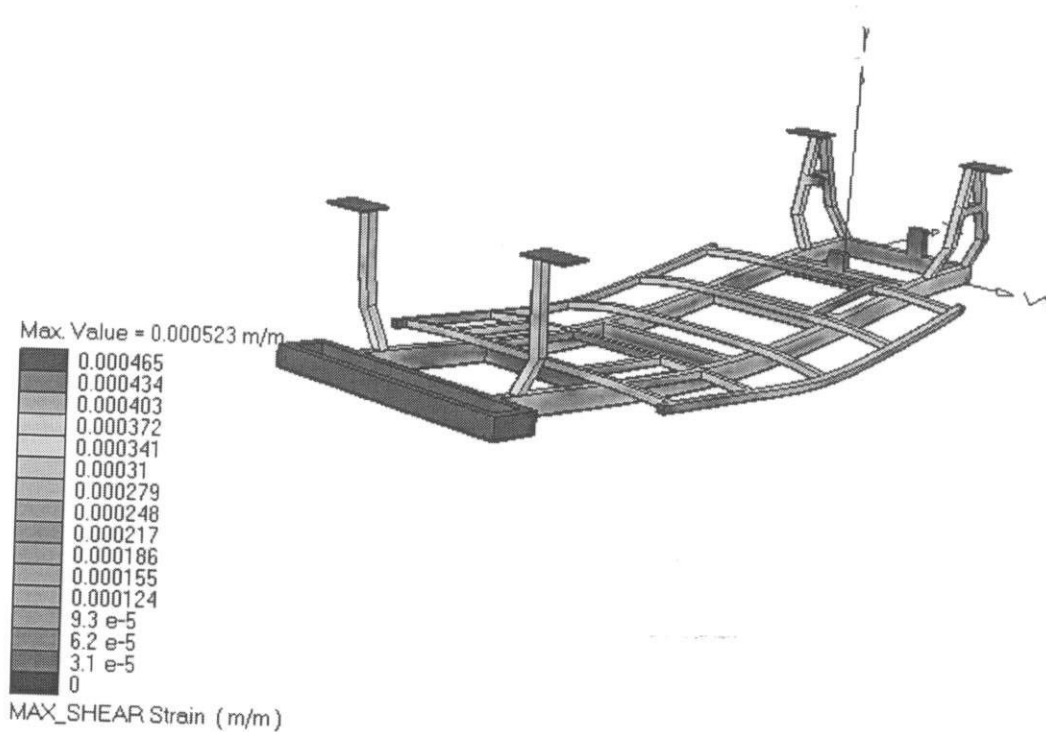


Figure D5: The contour of shear strain

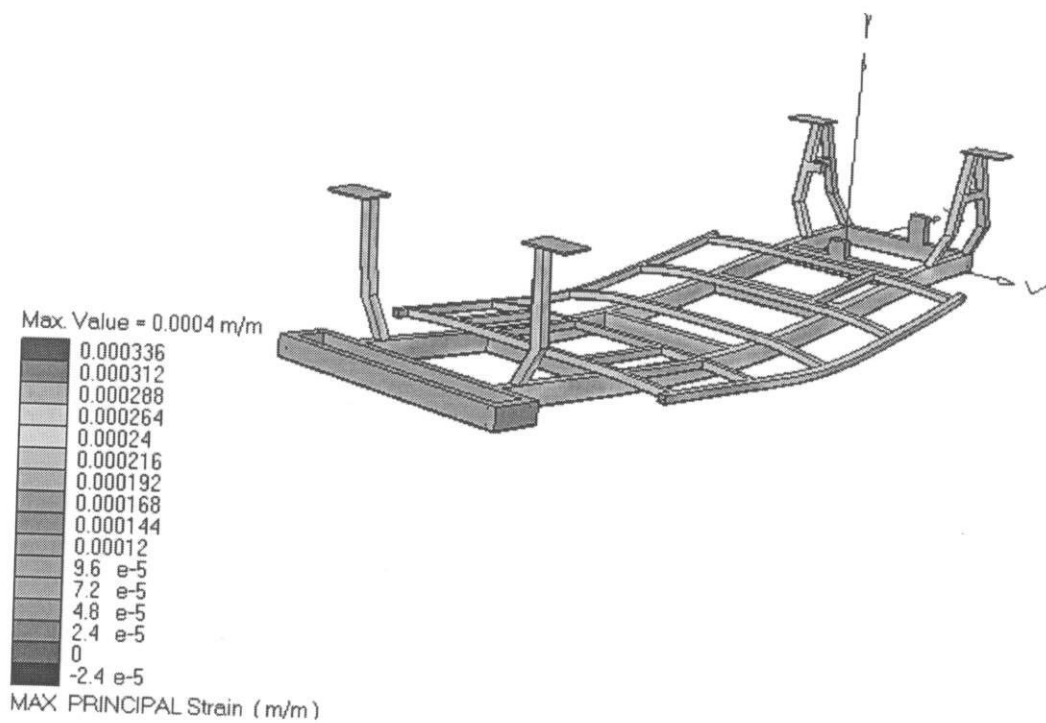


Figure D6: The contour of principal strain

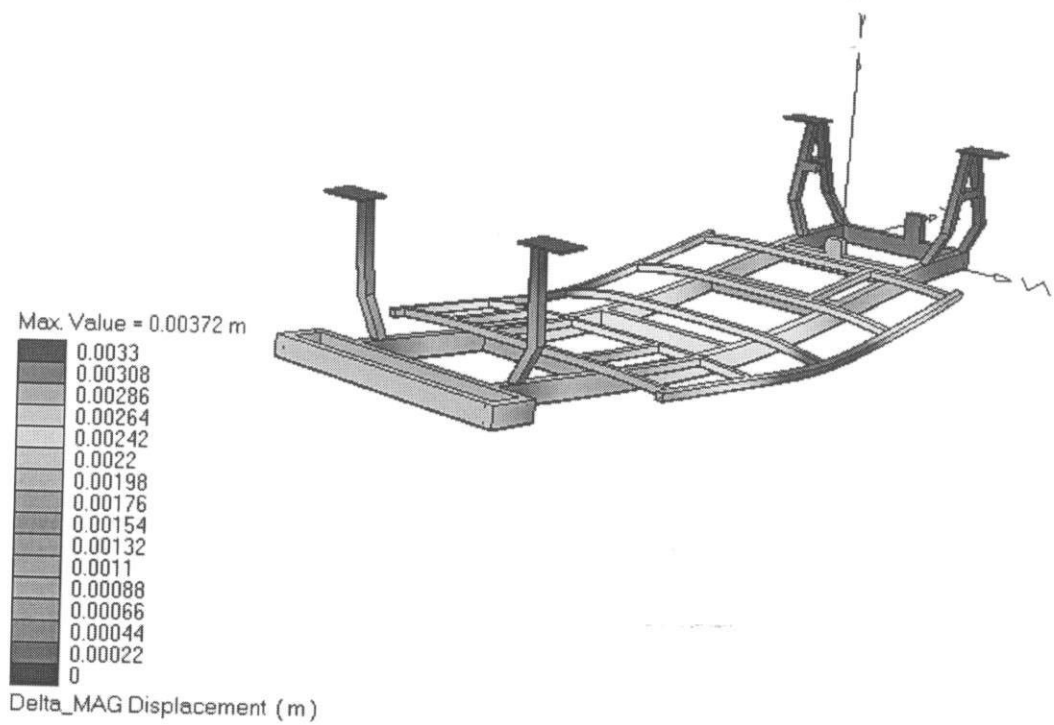


Figure D7: The contour of delta MAG displacement

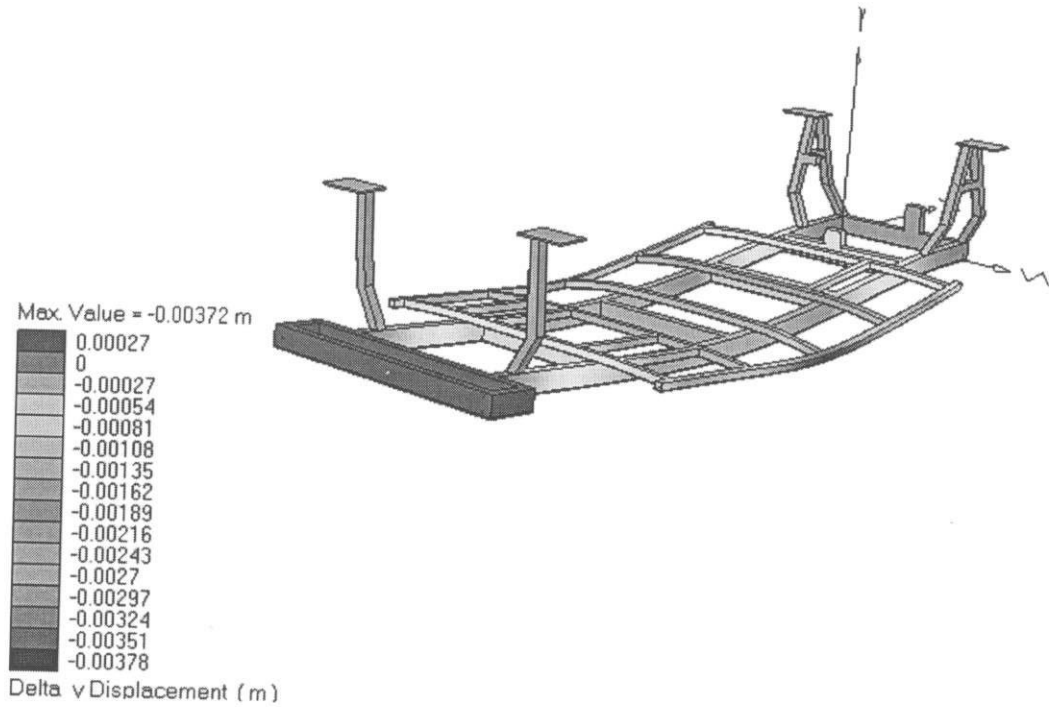


Figure D8: The contour of y-direction displacement

Note: All the deformation were scaled by a factor of 55.1

APPENDIX E

**RESULTS OF THE CHASSIS TORSIONAL
STIFFNESS ANALYSES**

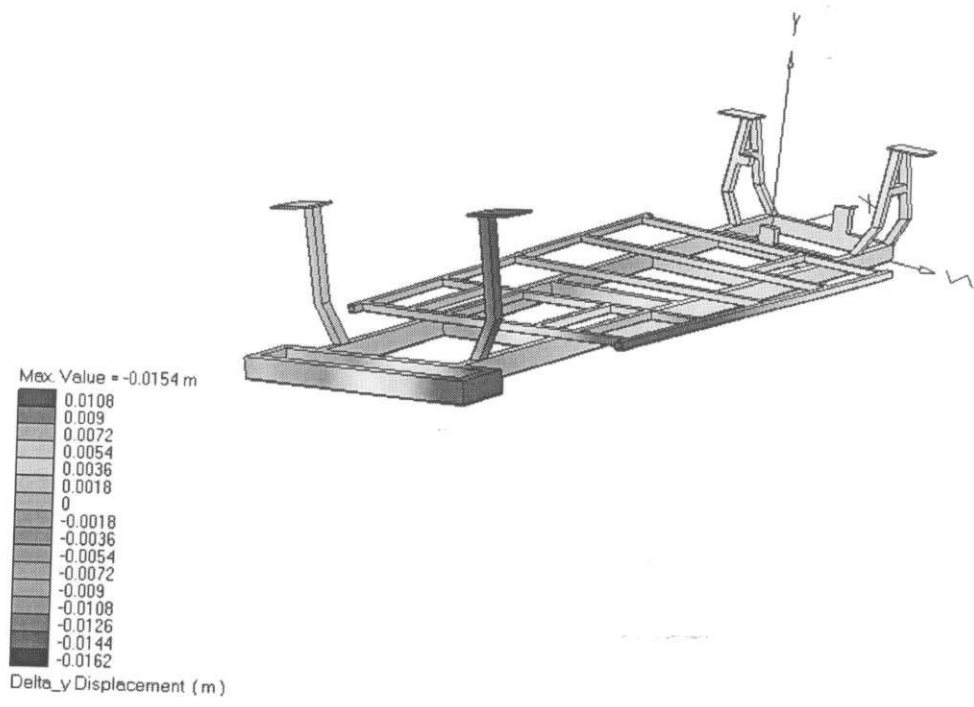


Figure E5: The contour and displacement due to 7500N
(The deformation was scaled by a factor of 8.44)

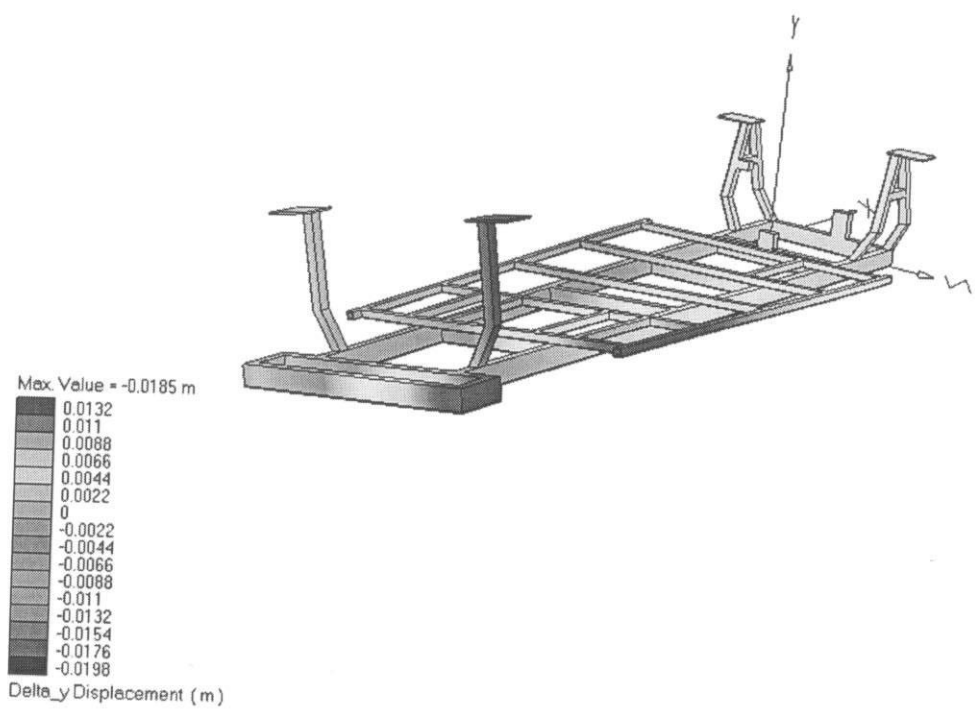


Figure E6: The contour and displacement due to 9000N
(The deformation was scaled by a factor of 7.04)

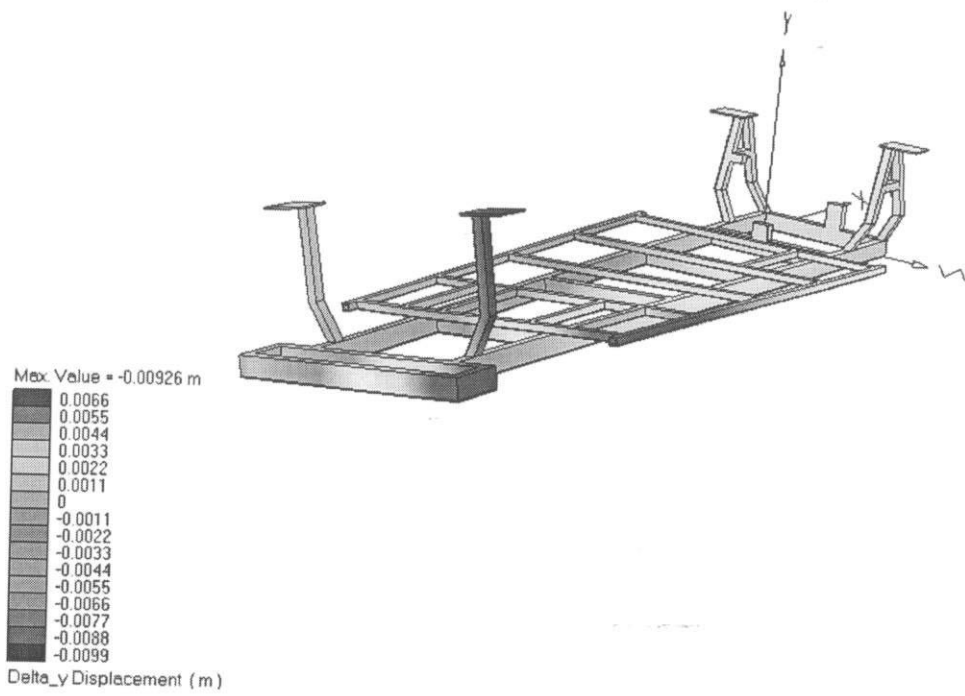


Figure E3: The contour and displacement due to 4500N
 (The deformation was scaled by a factor of 14.1)

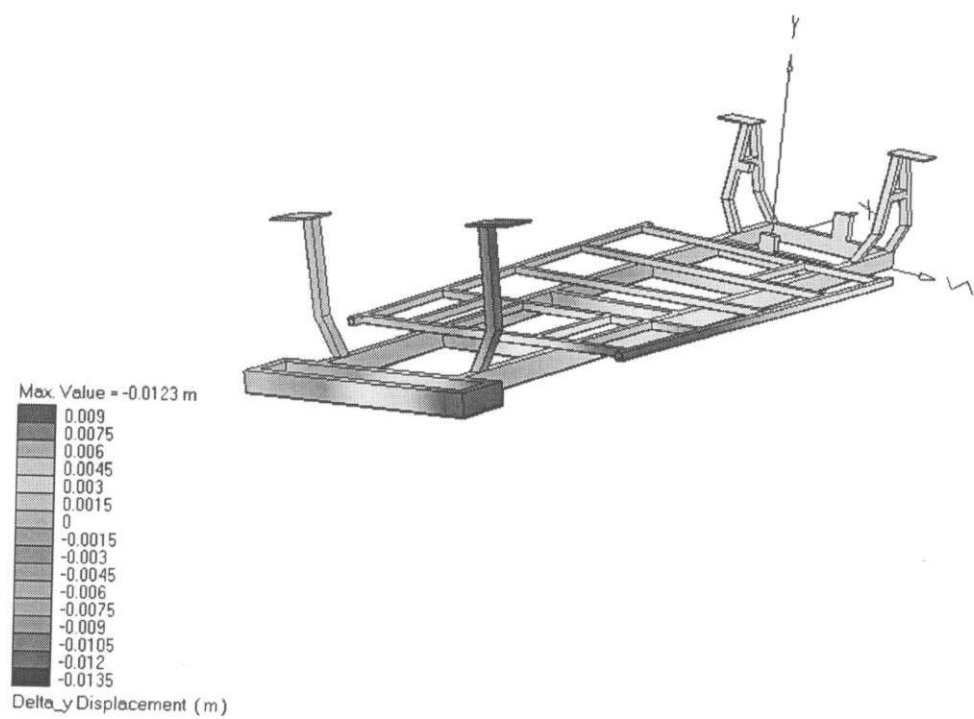


Figure E4: The contour and displacement due to 6000N
 (The deformation was scaled by a factor of 10.6)

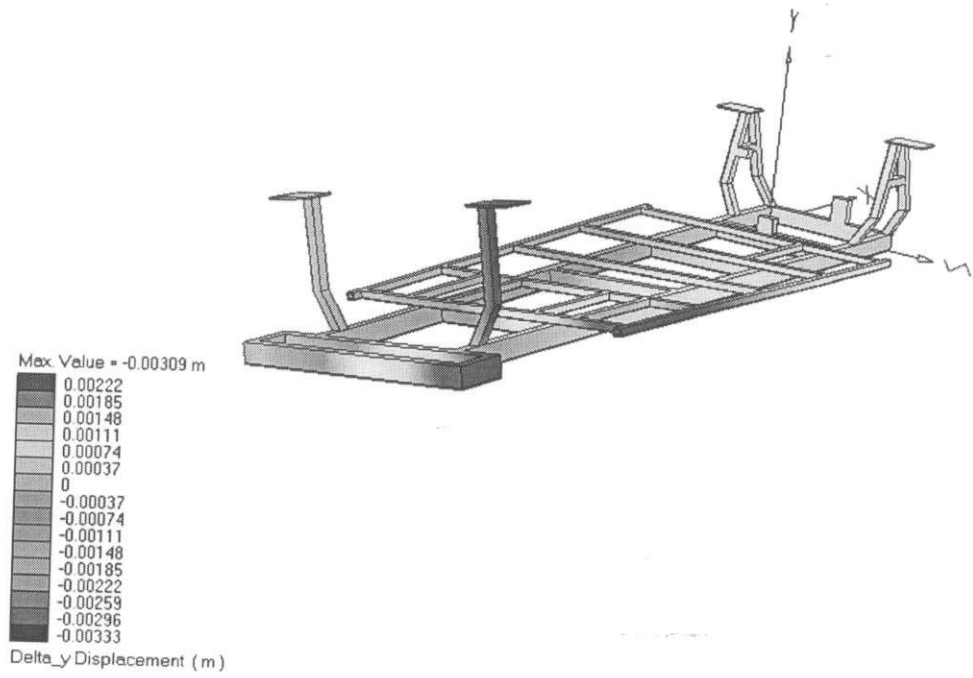


Figure E1: The contour and displacement due to 1500N
(The deformation scaled by 42.2)

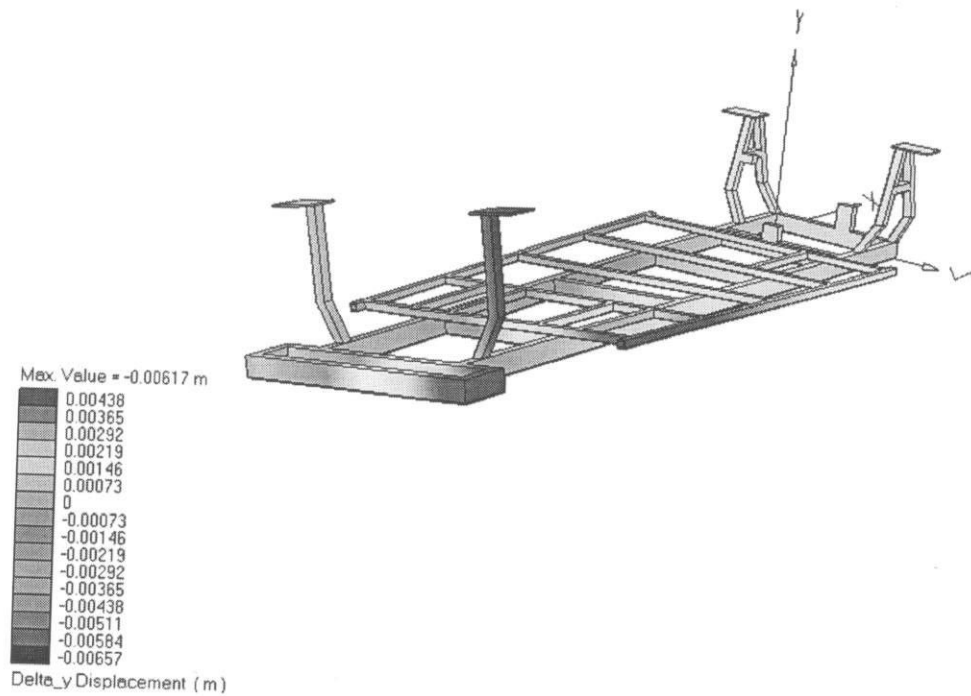
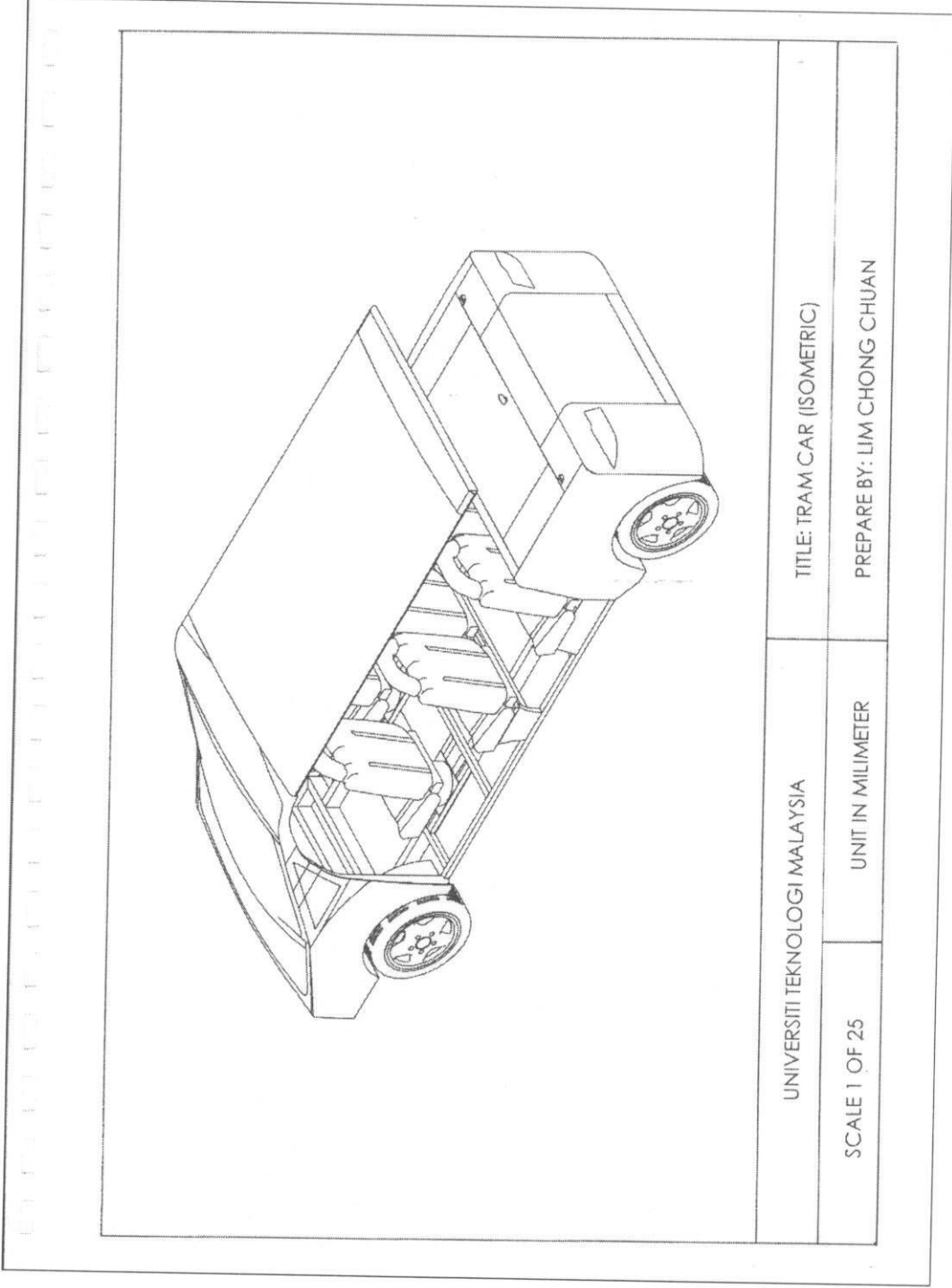


Figure E2: The contour and displacement due to 3000N
(The deformation scaled by a factor of 21.1)

APPENDIX F

**MANUFACTURING DRAWINGS OF THE
*TRAMCAR***



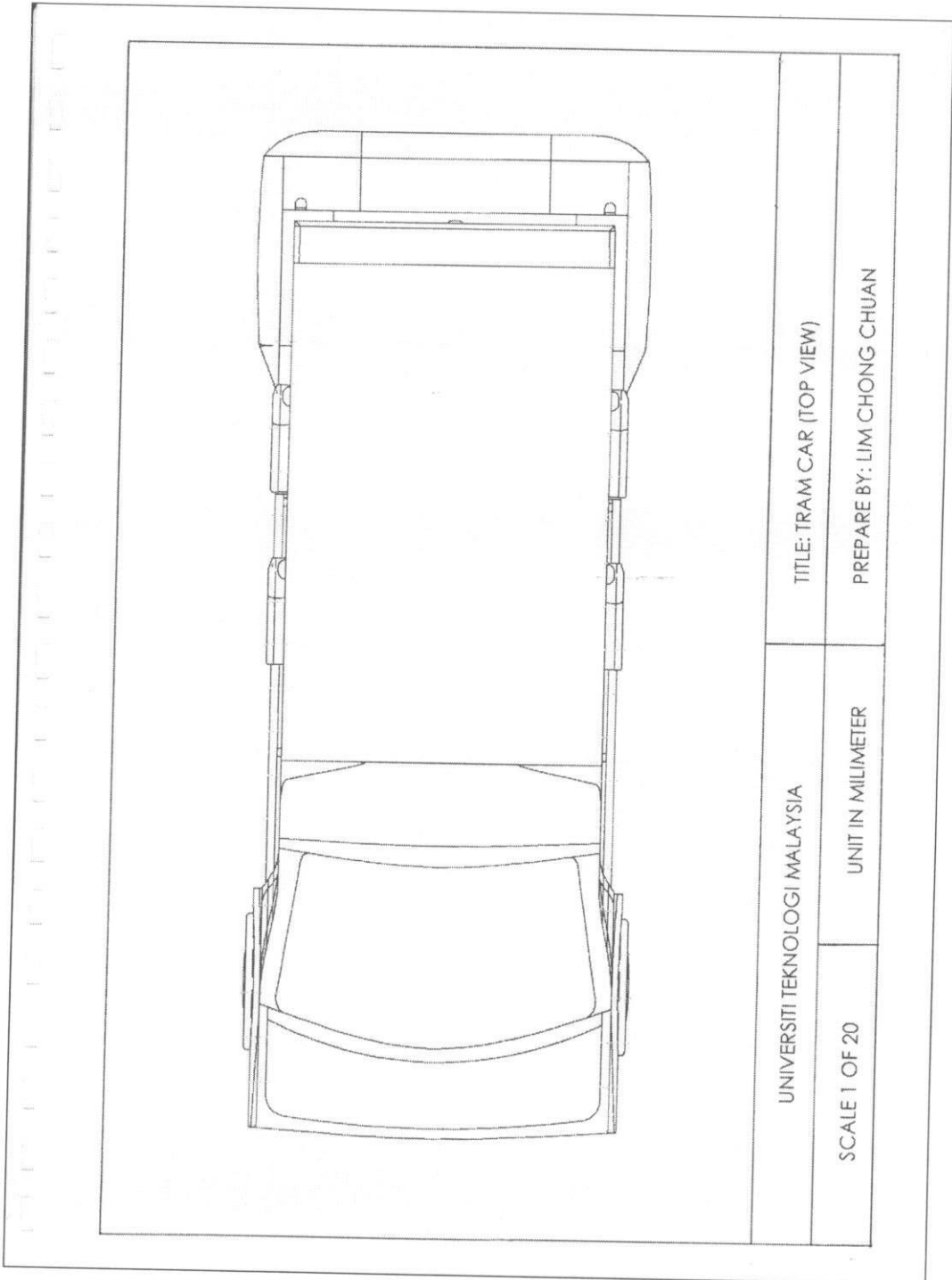
UNIVERSITI TEKNOLOGI MALAYSIA

TITLE: TRAM CAR (ISOMETRIC)

SCALE 1 OF 25

UNIT IN MILLIMETER

PREPARE BY: LIM CHONG CHUAN



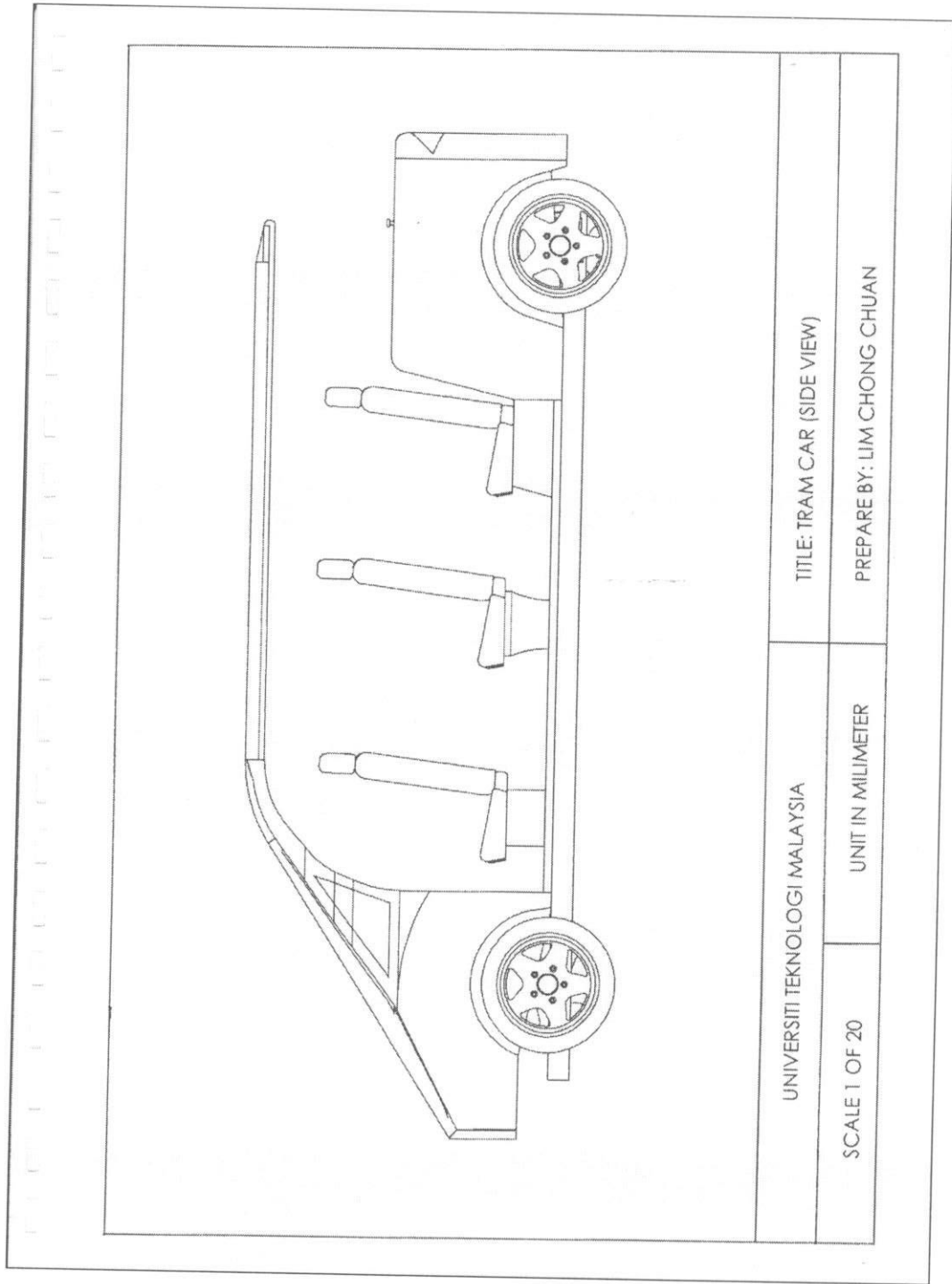
UNIVERSITI TEKNOLOGI MALAYSIA

TITLE: TRAM CAR (TOP VIEW)

SCALE 1 OF 20

UNIT IN MILLIMETER

PREPARE BY: LIM CHONG CHUAN



UNIVERSITI TEKNOLOGI MALAYSIA

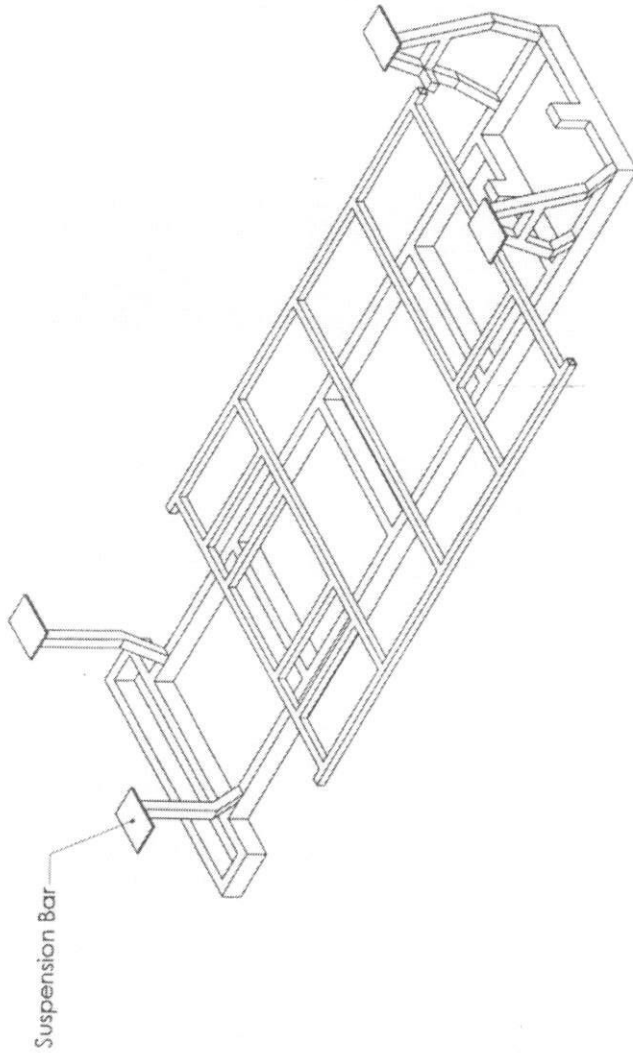
TITLE: TRAM CAR (SIDE VIEW)

SCALE 1 OF 20

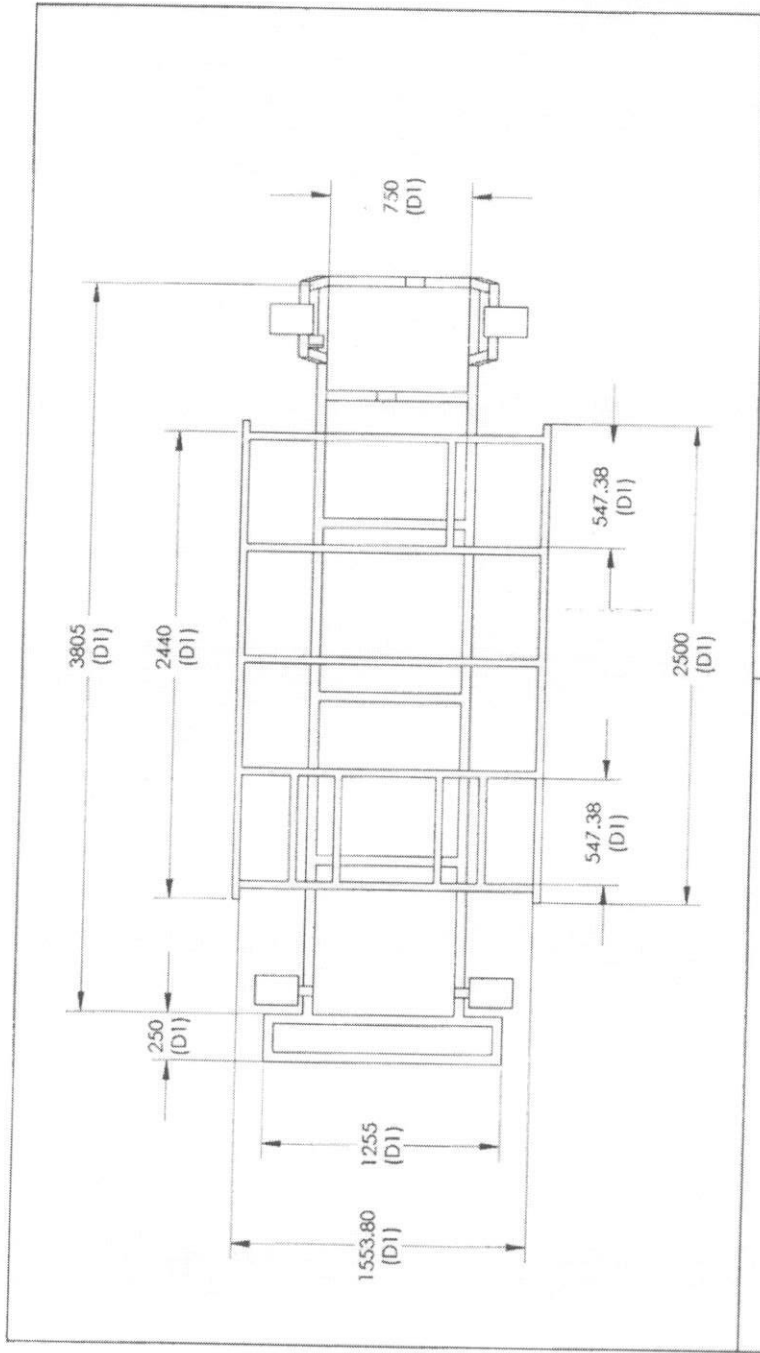
UNIT IN MILLIMETER

PREPARE BY: LIM CHONG CHUAN

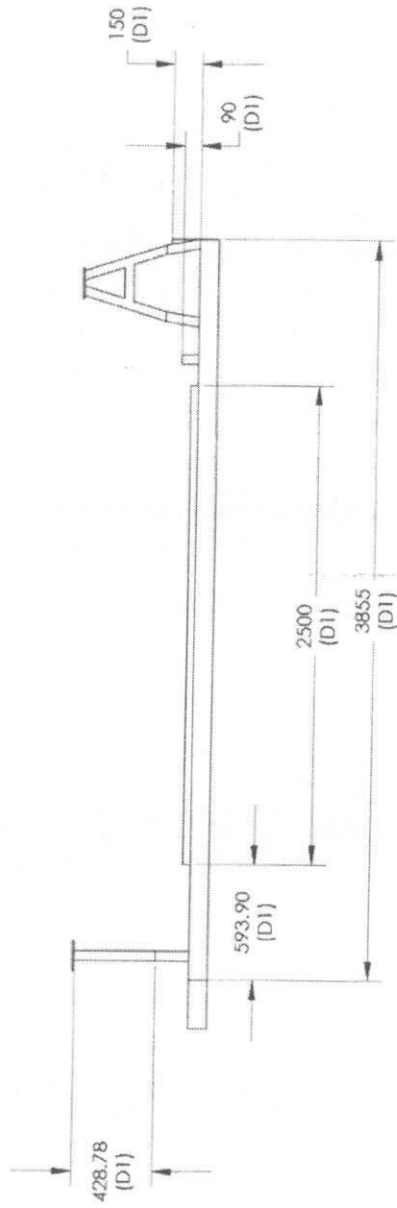
UNIVERSITI TEKNOLOGI MALAYSIA		TITLE: TRAM CAR (FRONT VIEW)	
SCALE 1 OF 15		PREPARE BY: LIM CHONG CHUAN	
UNIT IN MILLIMETER			



UNIVERSITI TEKNOLOGI MALAYSIA	TITLE: THE TRAM CAR FRAMEWORK (ISOMETRIC)	
SCALE 1 OF 20	UNIT IN MILLIMETER	PREPARE BY: LIM CHONG CHUAN



UNIVERSITI TEKNOLOGI MALAYSIA	TITLE: THE TRAM CAR FRAMEWORK (TOP VIEW)
SCALE 1 OF 25	UNIT IN MILLIMETER
PREPARE BY: LIM CHONG CHUAN	



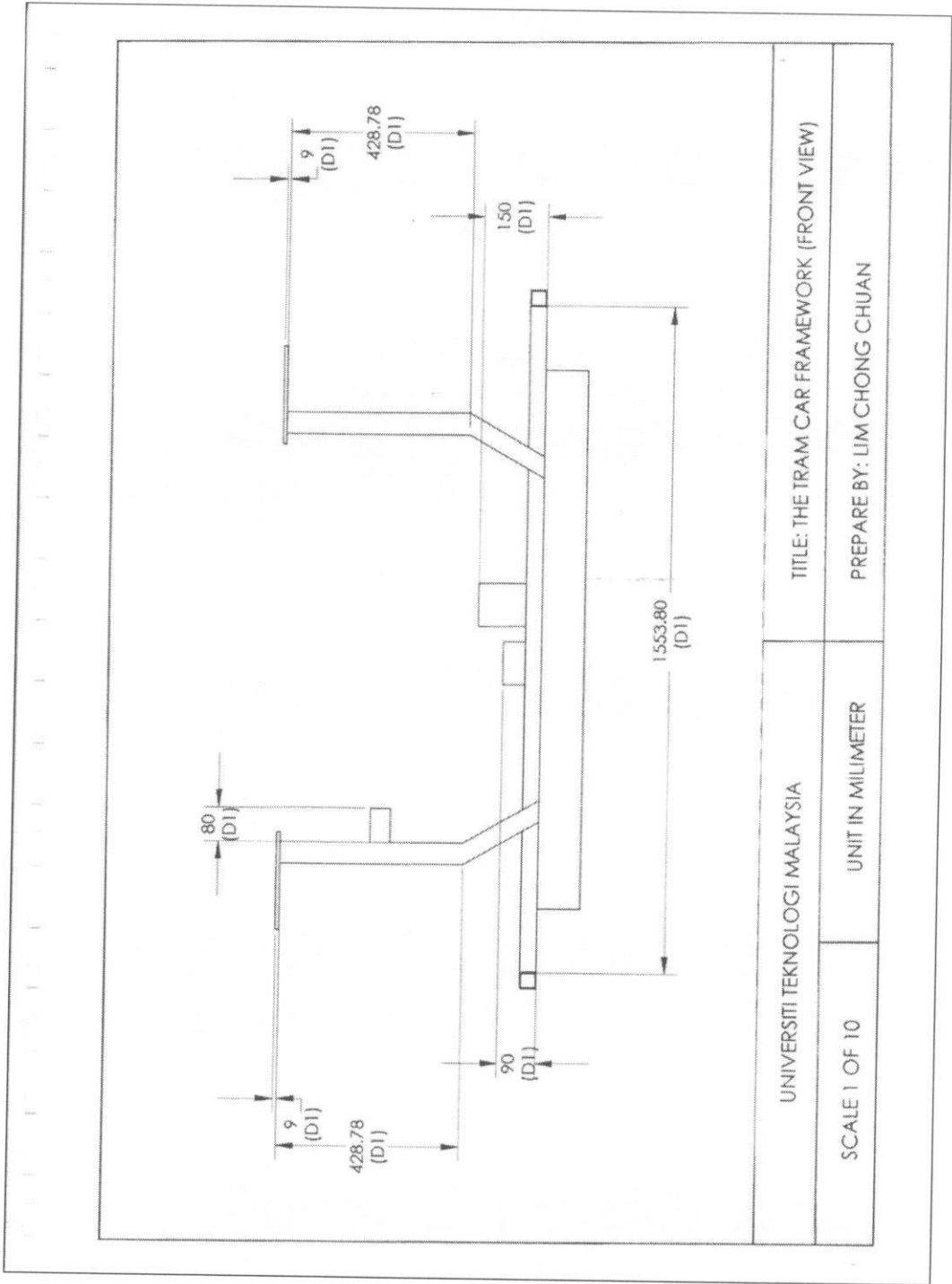
UNIVERSITI TEKNOLOGI MALAYSIA

TITLE: THE TRAM CAR FRAMEWORK (SIDE VIEW)

SCALE 1 OF 25

UNIT IN MILLIMETER

PREPARE BY: LIM CHONG CHUAN



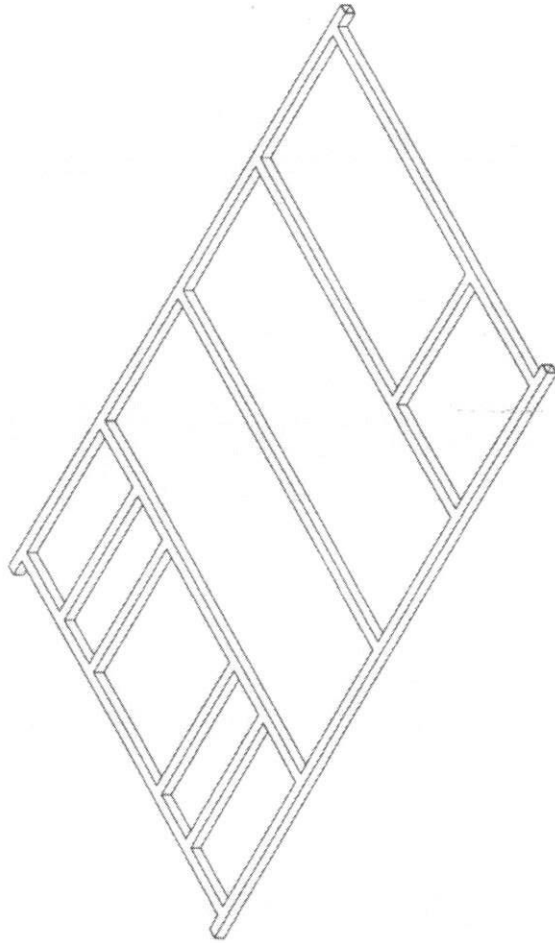
UNIVERSITI TEKNOLOGI MALAYSIA

TITLE: THE TRAM CAR FRAMEWORK (FRONT VIEW)

SCALE 1 OF 10

UNIT IN MILLIMETER

PREPARE BY: LIM CHONG CHUAN



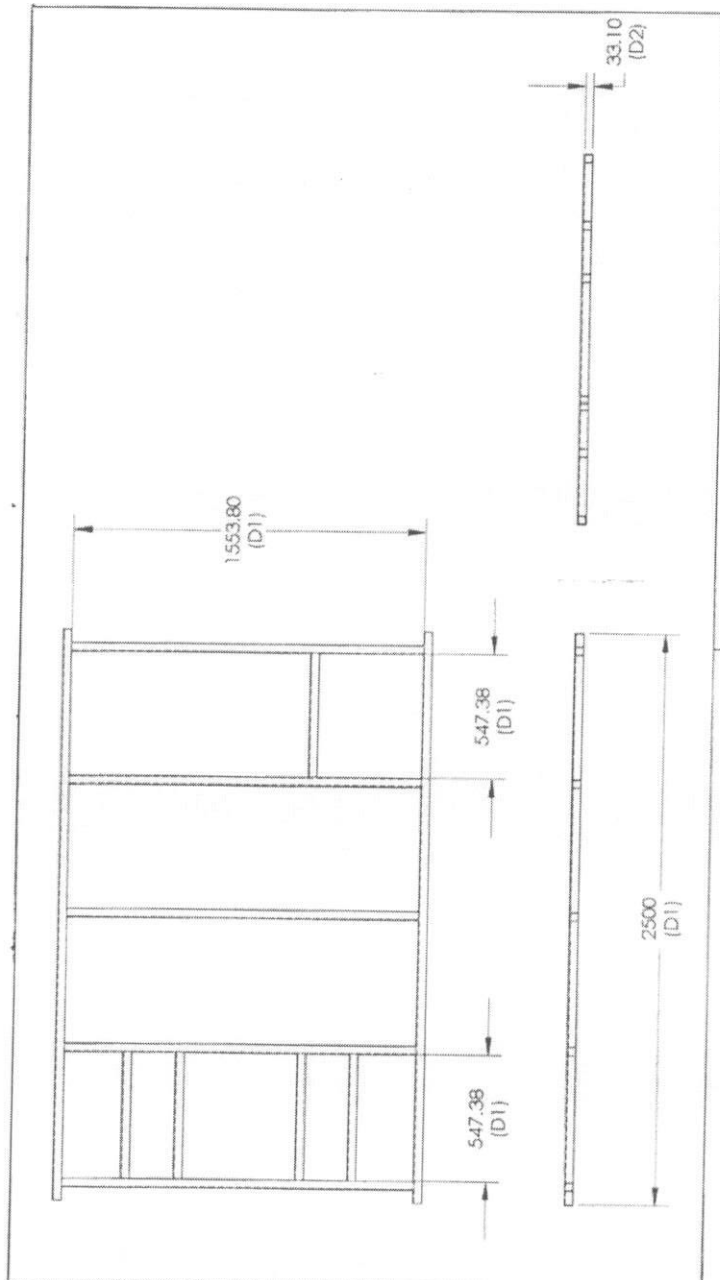
UNIVERSITI TEKNOLOGI MALAYSIA

TITLE: THE UPPER LADDER FRAMEWORK (ISOMETRIC)

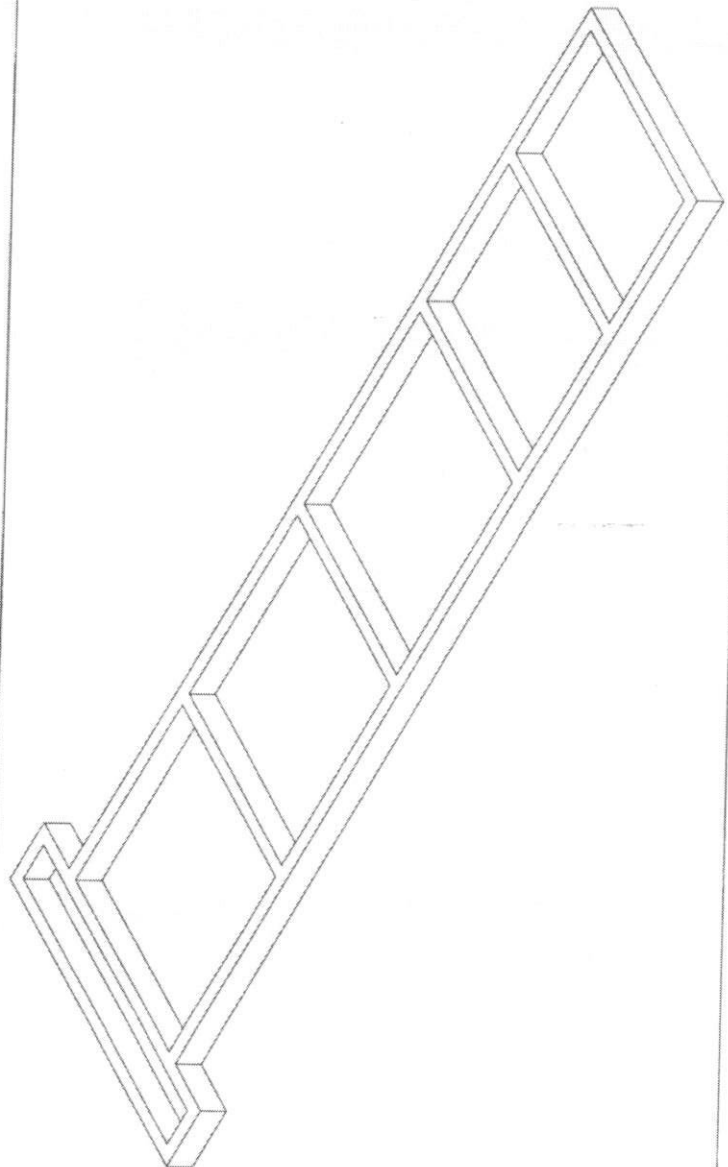
SCALE 1 OF 15

UNIT IN MILLIMETER

PREPARE BY: LIM CHONG CHUAN



UNIVERSITI TEKNOLOGI MALAYSIA	TITLE: THE UPPER LADDER FRAMEWORK (ORTHOGRAPHIC)
SCALE 1 OF 20	UNIT IN MILLIMETER
PREPARE BY: LIM CHONG CHUAN	



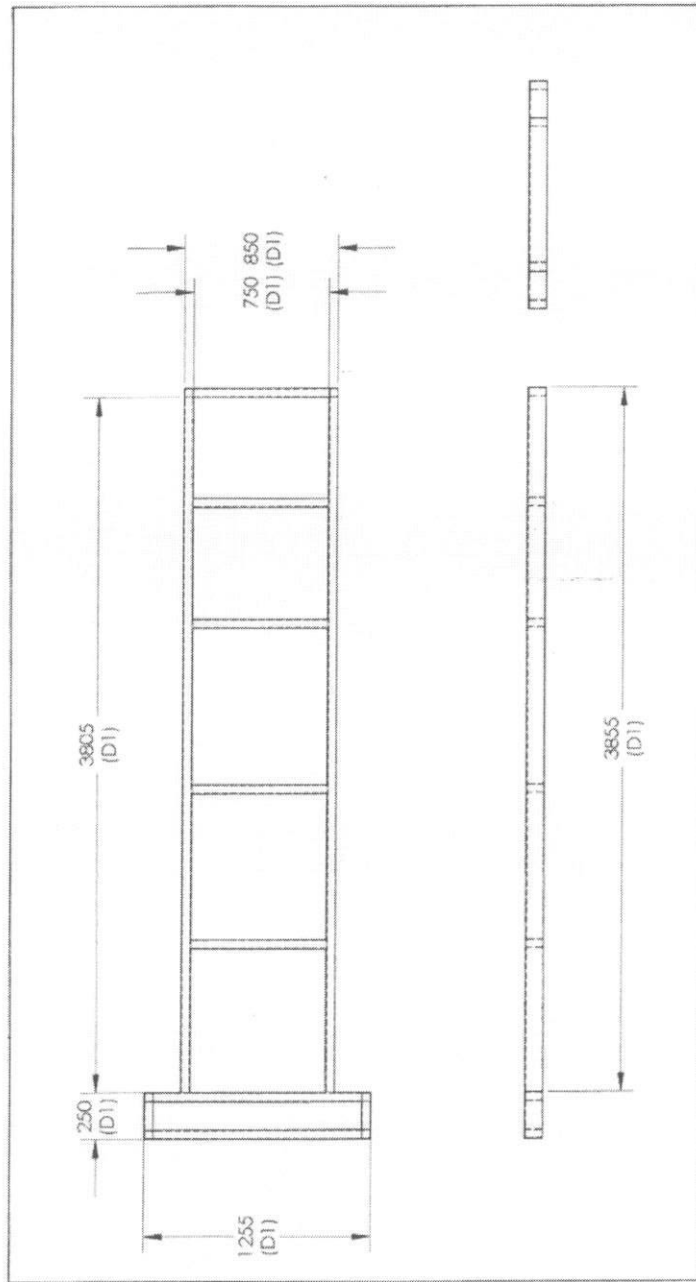
UNIVERSITI TEKNOLOGI MALAYSIA

TITLE: THE LOWER LADDER FRAMEWORK (ISOMETRIC)

SCALE 1 OF 15

UNIT IN MILLIMETER

PREPARE BY: LIM CHONG CHUAN



UNIVERSITI TEKNOLOGI MALAYSIA	TITLE: THE LOWER LADDER FRAMEWORK (ORTHOGRAPHIC)	
SCALE 1 OF 25	UNIT IN MILLIMETER	PREPARE BY: LIM CHONG CHUAN

APPENDIX G

PICTURES OF THE *TRAMCAR*



Figure G1: The exterior view of *tramcar*.



Figure G2: The front view of *tramcar*.



Figure G3: The rear view of *tramcar*.

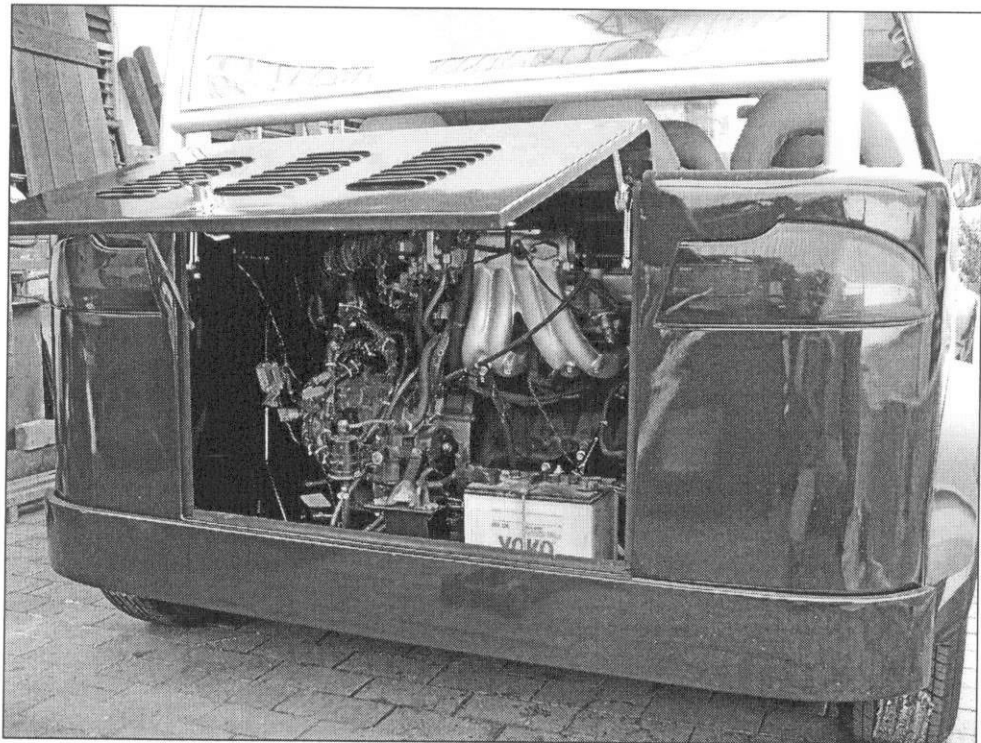


Figure G4: The engine location in *tramcar*.



Figure G5: The luxury seat in *tramcar*.



Figure G6: The interior view.

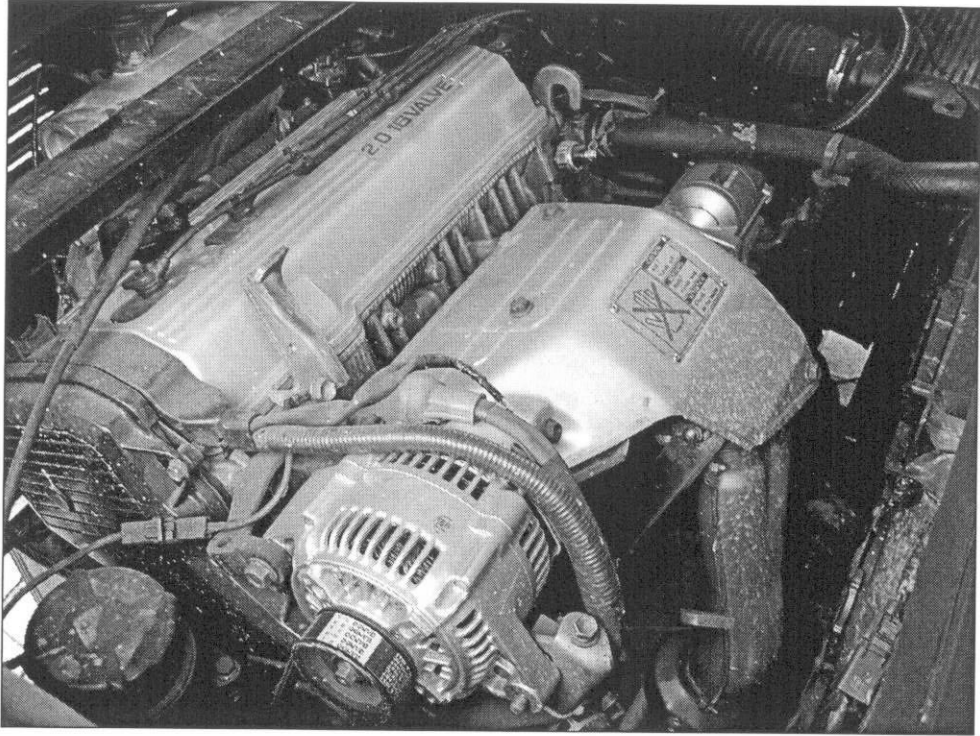


Figure G7: The Toyota Corona 16 valves engine.



Figure G8: The capacity of the engine used.